THE REQUIREMENT FOR COMPETENT ANTIGEN PRESENTING DENDRITIC CELLS AND POISED T CELLS FOR IMMUNE RESPONSES

by

Kyla Dione Omilusik

B.Sc., The University of British Columbia, 2002

A THESIS SUBMITTED IN PARTIAL FULFILLMENT OF
THE REQUIREMENTS FOR THE DEGREE OF

DOCTOR OF PHILOSOPHY

in

The Faculty of Graduate Studies

(Microbiology and Immunology)

THE UNIVERSITY OF BRITISH COLUMBIA
(Vancouver)

August 2011

ABSTRACT

Immune responses are initiated by dendritic cells (DCs) that cross present exogenous antigen to naïve T cells. DC cross presentation is essential for generating primary immune responses, yet the mechanistic details remain undefined. Using a CD74$^{-/-}$ mouse model, a CD74-MHC I association was shown to mediate trafficking of MHC I from the endoplasmic reticulum to endolysosomal compartments for antigenic loading. These studies describe a novel CD74-mediated cross presentation pathway in DCs that plays a major role in the generation of cytolytic T lymphocyte (CTL) responses against viral and cell-associated antigens. Viruses such as Human Immunodeficiency Virus (HIV) have evolved mechanisms to interfere with immune activation allowing persistence in the host. HIV can infect DCs so the HIV virulence factor, Nef, which interacts with MHC I, has the potential to interfere with MHC I trafficking in the cross presentation pathway. Using a Nef-expressing DC line, Nef was shown to downregulate surface MHC I by inhibiting Golgi-to-surface transport of newly synthesized MHC I and by increasing the recycling of surface MHC I. Coordinately, Nef was shown to inhibit both direct and cross presentation of viral and soluble antigen. Similarly, in a Nef transgenic mouse, Nef was shown to inhibit CTL responses to bacterial and viral infections. This unique immunosubversion mechanism likely contributes to immunodeficiency associated with Acquired Immunodeficiency Syndrome. Peripheral pools of naïve T cells capable of responding to DC stimulus are maintained through homeostatic cues including TCR signalling. Key to this is the second messenger calcium (Ca^{2+}); however, the identity of the components regulating intracellular Ca^{2+} concentrations is unclear. Through examination of a knock-out mouse model, the Ca^{2+} channel, $Ca_V1.4$, was shown to play a

cell-intrinsic role in naïve T cell development and survival. $Ca_V1.4$ is critical for regulation of intracellular Ca^{2+} stores and for TCR-induced increases in cytosolic Ca^{2+}, which impacts Ras/ERK and NFAT activation. The $Ca_V1.4$ deficiency causes a loss of naïve T cells and results in immunodeficiency. These studies reveal a critical function for $Ca_V1.4$ in naïve T cell homeostasis. Collectively, this thesis demonstrates the importance of cross presenting DCs and maintenance of T cells for functional immunity.

PREFACE

During my PhD, I had the opportunity to work with and learn from two talented Research Associates, Dr. Genc Basha and Dr. John Priatel. The first section of my thesis, Chapter 3, was performed with Dr. Basha. He made the initial observation regarding CD74-deficiency and impaired cross presentation (**Figure 3.1 and Figure 3.7**). In addition, he performed the confocal experiments (**Figure 3.8 and Figure 3.9**). The remainder of the work, with the exception of **Figure 3.10D** that I performed on my own, was performed in collaboration. A version of chapter 3 is prepared as a manuscript for submission: Genc Basha*, Kyla Omilusik*, Anna T. Reinicke, Nathan Lack, Kyung Bok Choi, and Wilfred A. Jefferies. (2011). Identification of a CD74-Dependent MHC Class I Cross-Presentation Pathway (* denotes co-first authorship).

The experiments in the second section of my thesis, chapter 4 and 5 were performed by me. Chapter 4 is prepared as a manuscript for submission (Kyla Omilusik, Anna T. Reinicke, and Wilfred A. Jefferies. (2011). HIV-1Nef Impairs Dendritic Cell MHC I Cross-Presentation.).

Chapter 6, the final section of my thesis, was predominantly performed in collaboration with Dr. Priatel. Ms. Teresa Wang and Dr. Xiaoxi (Brook) Chen made the initial observation. I conducted the expression studies (**Figure 6.1**), the T cell receptor signalling analysis (**Figure 6.6A,B,D**), the bone marrow transfer experiment (**Figure 6.7**) and infection analysis (**Figure 6.13A,B,F,G,H**). Together, Dr. Priatel, Dr. Chen and I performed cell subset assessment (**Figure 6.2, Figure 6.3 and Figure 6.9**) and homeostatic proliferation analysis (**Figure 6.12**). In collaboration, Dr. Chen and I completed cytokine analysis following infection (**Figure 6.13C,D,E**). Dr. Priatel and Dr.

Chen analyzed peripheral T cell apoptosis (**Figure 6.8 and Figure 6.10**). Dr. Priatel performed intracellular calcium analysis (**Figure 6.4 and Figure 6.5**), phosho-Erk signalling (**Figure 6.6C**) and survival signalling (**Figure 6.11**). This chapter is prepared as a manuscript that is currently accepted for publication at *Immunity*: Omilusik KD*, Priatel JJ*, Chen X*, Wang, YT*, Xu H, Choi KB, Gopaul R, McIntyre-Smith A, Teh HS, Tan R, Bech-Hansen NT, Waterfield D, Fedida D, Hunt SV, Jefferies WA, (2011), The $Ca_V1.4$ Calcium Channel Is a Critical Regulator of T Cell Receptor Signaling and Naive T Cell Homeostasis, Immunity, doi:10.1016/j.immuni.2011.07.011. (* denotes co-first authorship).

All studies were performed following the guidelines set by both the University of British Columbia's Animal Care Committee and the Canadian Council on Animal Care. The animal care breeding protocols are: A07-0373, and A09-0824. The animal care protocols for these studies are: A07-0270, A04-0267, A06-0346, and A05-1109. The biosafety protocols are: B06-0040 and B04-0179.

TABLE OF CONTENTS

LIST OF TABLES

LIST OF FIGURES

LIST OF SYMBOLS AND ABBREVIATIONS

AIDS	Acquired Immunodeficiency Syndrome
AIHA	Coombs-positive autoimmune hemolytic anemia
AP	adaptor protein
AP-1	activator protein-1
APC	antigen presenting cell
ARF6	ADP-ribosylation factor 6
ADP	adenosine diphosphate
ADPR	ADP-ribose
ATP	adenosine triphosphate
BAD	BCL-2 antagonist of cell death
BAFT3	basic leucine zipper transcriptional factor ATF-like 3
BAK	Bcl-2 homologous antagonist/killer
BAX	Bcl-2–associated X protein
BCL-2	B cell lymphoma 2
BID	BH3-interacting domain death agonist
BIM	BCL-2 interacting mediator of cell death
Bp	base pair
β2m	beta-2-microglobulin
BSA	bovine serum albumin
bmDC	bone marrow-derived dendrtic cell
Ca^{2+}	calcium
CaMK	Ca^{2+}-calmodulin-dependent kinase
CAPRI	Ca^{2+}-promoted Ras inactivator
CARMA1	caspase recruitment domain and membrane-associated guanylate kinase-containing scaffold protein
CK1	casein kinase 1
cDNA	complementary deoxyribonucleic acid
CLIP	MHC Class II-associated invariant chain peptide
CRAC	Ca^{2+} release-activated Ca^{2+} channels
CREB	cyclic AMP-responsive element-binding protein
CTL	cytotoxic T lymphocyte
DC	dendritic cell
DCIR2	dendritic cell inhibitory receptor–2
DC-SIGN	DC-specific intercellular adhesion 3-grabbing non-integrin
ΔY	MHC I (H-2K^b) lacking a cytoplasmic tyrosine motif
DHP	dihydropyridine
DOCK180	dedicator of cytokinesis 180
DMEM	Dulbecco's Modified Eagle Medium
DNA	deoxyribonucleic acid
DNase	deoxyribonuclease
DYRK1A	dual specificity tyrosine-phosphorylation regulated kinase 1A
EC	elite controllers
ELC	endolysosomal compartment

Endo H	endoglycosidase H
ER	endoplasmic reticulum
ERK	extracellular signal-regulated kinase
FACS	fluorescent-activated cell sorting
FBS	fetal bovine serum
FRC	fibroblastic reticular cell
Gads	GRB2-realted adaptor downstream of shc
GAPs	GTPase activating proteins
GEF	GTP-exchange factor
GFP	green fluorescent protein
GSK3	glycogen synthase kinase 3
gp120	HIV glycoprotein 120
GRB2	growth factor receptor-bound protein 2
HBSS	Hank's balanced salt solution
HEPES	4-(2-hydroxyethyl)piperazine-1-ethanesulfonic acid
HIV	Human Immunodeficiency Virus
HSC	heat shock protein
HVA	high voltage activated
ICAM	intracellular adhesion molecule-1
ICM	immunofluorescent confocal microscopy
IFN	interferon
IFNγ	interferon-gamma
IκB	inhibitor of NF-κB
IKK	IκB kinase
IL	interleukin
ip	intraperitoneally
IP_3	inositol-1,4,5-trisphosphate
IP_3R	inositol-1,4,5-trisphosphate phosphate receptor
IRAP	insulin-regulated animopeptidase
IRES	internal ribosomal entry site
ITAM	immune receptor Tyrosine-based Activation Motif
ITK	IL-2 induced tyrosine kinase
iv	intravenously
JAK-STAT	Janus kinase signal transducer and activator of transcription
JNK	jun NH2-terminal kinase
K^bWT	wild type H-2K^b (MHC I)
LAMP	lysosome-associated membrane protein
LAT	the linker for the activation of T cells
LC	langerhan cell
LFA-1	leukocyte function-associated molecule-1
LLO	listeriolysin O
LTTC	L-type Ca^{2+} channels
LTNP	long term non-progressors
LTR	long terminal repeats
LVA	low voltage activated

MALT1	mucosa-associated lymphoid tissue lymphoma translocation gene 1
MAPK	mitogen-activated protein kinase
MCL1	myeloid cell leukemia sequence 1
MCS	multiple cloning site
MFU	mean fluorescent unit
MHC	major histocompatibility complex
Min	minute
MOI	multiplicity of infection
NAD^+	nicotinamide adenine dinucleotide
NEAA	nonessential amino acids
Nef	negative factor
NFAT	nuclear factor of activated T-cells
NK cell	natural killer cell
NP-40	Nonidet P-40
OPC	oropharyngeal candidiasis
ORF	open reading frame
OVA	ovalbumin
PAGE	polyacrylamide gel electrophoresis
PAK2	p21 activated kinase 2
PAMPs	pathogen associated molecular patterns
PBS	phosphate buffered saline
PCR	polymerase chain reaction
PD-1	programmed death 1 receptor
pDC	plasmacytoid dendritic cell
PDL-1/2	programmed death ligand 1/2
PE	phycoerythrin
PI3K	Phosphatidylinositol 3-kinases
PIP_2	phosphoinositol 4,5-bisphosphate
PIP_3	phosphatidylinositol 3,4,5-trisphosphate
P-Loop	pore-forming loop
PM	plasma membrane
PMA	phorbol 12-myristate 13-acetate
PKC θ	Protein kinase C θ
PRR	Proline rich region
PRRs	Pattern-recognition receptors
Rac1	Ras-related C3 botulinum toxin substrate 1
RasGRP1	ras guanyl nucleotide-releasing protein
rLMOVA	recombinant *Listeria monocytogenes* expressing ovalbumin
RPMI	Roswell Park Memorial Institute
RT-PC	reverse transcriptase-polymerase chain reaction
RNA	ribonucleic acid
SAM	sterile α –motif
SAPK	stress-activated protein kinase
SBBC	Sydney Blood Bank Cohort
SD	standard deviation

Sec	second
SEM	standard error of the mean
SH2/3	Src homology 2/3
SLO	secondary lymphoid organs
SLP-76	SH2 domain-containing leukocyte phosphoprotein of 76 kDa
STIM1	stromal interaction molecule 1
TAP	transporter associated with antigen processing
TCA	trichloroacetic acid
TCR	T cell receptor
TFR	transferrin receptor
Tg	transgenic
TGN	trans Golgi Network
Treg cell	T regulatory cell
TRPC	transient receptor potential channels
VA	vector alone
VSV	Vesicular Stomatitis Virus
VV	Vaccinia Virus
VV-OVA	Vaccinia Virus expressing ovalbumin
WCL	whole cell lysate
ZAP-70	ζ-chain associated protein of 70 kDa

ACKNOWLEDGEMENTS

First and foremost, I would like to acknowledge my supervisor, Dr. Wilf Jefferies, for his unending creativity, patience, and support. His great humour and drive in good times and bad have pushed me to work and achieve far beyond my expectations. His expert scientific training has led me to develop many essential skills that will stay with me for my career. I am indebted to Dr. John Priatel and Dr. Genc Basha for their guidance and scientific training. I am a better scientist for having had the opportunity to learn from them. I am also grateful to my committee members, Dr. Michael Gold, Dr. Pauline Johnson and Dr. Douglas Waterfield, for their support and advice over the years. I would like to thank the Jefferies' lab members past and present, including Dr. Robyn Seipp, Dr. Francesca Setiadi, Dr. Cheryl Pfeifer, Dr. Jason Grant, Dr. Mei Mei Tian, Lonna Munro, KB Choi, Lisa Murphy and Ana Chávez Steenbock, for creating a collaborative and caring work environment. In particular, I am grateful to Dr. Anna Reinicke for her great scientific discussion, her help with experiments, editing manuscripts and my thesis and mostly for her kindness, optimistic spirit and friendship. Also, from the Jefferies' lab, I would like to thank my bench-mate Dr. Kaan Biron for his endless humour, support and email forwards. I would like to acknowledge Dr. Greg Lizée and Matt Finlay for generating the Nef transgenic founders, Ray Gopaul and Andy Jefferies for their expert assistance with animal breeding and care, and Taka Murakami for his genotyping skills. A special thanks to Adam McIntyre-Smith for the long hours spent helping me with experiments and Andy Johnson and Justin Wong at the UBC FACS Facility for their expert assistance. Thanks to the Microbiology and Immunology Department, the Michael Smith Laboratories (MSL), and the Biomedical Research Centre

(BRC) where most of the work for this thesis was completed. Specifically, I appreciate the 2nd floor of the BRC who brought endless humour to science. This work was partially funded by Translational Research in Infectious Disease (TRID) Scholarship and Canadian Institute of Health Research (CIHR) scholarship.

Finally, I have to thank my family and friends who stayed by me through my graduate studies and never failed to wonder when I would be done being a student. I especially appreciate my parents, Lee and Wynone Omilusik, my twin sister, Dacia Omilusik, and my husband, Rob Rempel for all their love and encouragement over the years and their patience when I talked to no end about science. It is with their support and inspiration, I am able to take on and achieve my goals as a scientist.

CHAPTER 1. GENERAL INTRODUCTION

When the body mounts a response against an invading pathogen, there are many elements of the immune system that must work in concert for a successful outcome. Two components that are highlighted in this thesis are the dendritic cell (DC) and the T cell. First, DCs, localized at key sites of pathogen entry, must be able to effectively take up and present antigen to naïve T cells [1]. Second, naïve T cells must be present and poised to respond to their cognate antigen on DCs.

1.1 Innate and adaptive immunity

Our immune system reflects the history of pathogen engagements in the drive towards ensuring the survival of our species. The immune system is complex and multilayered consisting of three major components: external barriers, innate responses and adaptive responses. Upon encounter with a pathogen, the physical (such as skin, ciliated epithelia, and mucosal membranes) and chemical barriers (such as enzymes in secretions, stomach acids) of the body constitute an initial line of defence [2]. If these barriers are breached and the pathogen evades the body, the innate immune response provides almost immediate protection. The innate system lacks memory and the cells respond through set germ-line encoded receptors termed pattern-recognition receptors (PRRs), which recognize common molecular structures or pathogen-associated molecular patterns (PAMPs) [2]. PRRs in the Toll-like receptor and NOD-related receptor families have recently emerged as important components of innate recognition [2]. Upon pathogen contact, innate cells use phagocytosis as a key effector mechanism. Engulfed pathogens

are destroyed by digestive enzymes or reactive oxygen species produced by the cell [3]. In addition, these cells secrete chemokines and cytokines to attract and activate additional immune cells and anti-microbial peptides to destroy pathogens [2, 4, 5]. The second line of defence, the adaptive immune response, takes days to develop but is highly specialized to recognize and respond to specific antigens [2]. Antigen-specific receptors expressed on lymphocytes are generated through gene rearrangement events, creating a vast pool of lymphocytes expressing diverse antigen receptors able to respond to a nearly infinite number of different antigens [2]. In this way, the adaptive immune system has the ability to specifically respond to virtually any pathogen that has invaded the body by inducing antibody production and effector T cell function. In addition, after successful elimination of the pathogen, the adaptive system establishes memory allowing quick and efficient generation of adaptive responses upon re-infection with the same pathogen [2]. It is through effective interplay between the individual components that the immune system is able to successfully protect the body from infection.

1.2 Dendritic cells

DCs provide a link between the innate and adaptive immune components and are critical to initiating immune responses [1, 5]. DCs are localized to areas of pathogen entry as well as in lymphoid organs and express a large array of PRRs so are able to detect a pathogen invasion [1]. DCs can internalize antigen very efficiently, can present this antigen on both major histocompatability complex (MHC) I and II molecules and express high levels of costimulatory molecules. Therefore, DCs effectively prime T cell responses. In fact, DCs seem to be the only cell type that is proficient at activating naïve

T cells [1, 6-8]. Taken together, DCs are potent antigen presenting cells that are essential for initiating strong T cell responses.

1.2.1 DC subsets

DCs are a heterogeneous population consisting of several phenotypically and functionally distinct subsets [reviewed in [9]]. DCs are divided into two major categories: conventional DCs (cDC) and plasmacytotd DCs (pDC) [1, 9]. Conventional DCs can be further separated into three subgroups. These are: migratory DCs, lymphoid-organ DCs, and monocyte-derived or inflammatory DCs [1, 9].

The cDC class known as migratory DCs develop from early precursors in the peripheral tissues, such as skin and mucosal tissues. Here the DCs remain immature forming a surveillance network, continually and efficiently sampling antigens [1, 9]. These cells travel through afferent lymphatics to draining lymph nodes and make up about fifty percent of total lymph node DCs [10, 11]. During this migration, DCs acquire a mature phenotype characterized by high levels of MHC and co-stimulatory molecule expression and an ability to present captured antigen to T cells [1, 12]. In this way, migratory DCs provide information to the immune system about the tissue environment [1]. Several groups have attempted to classify the migratory DCs into smaller subsets. The skin contains at least three populations of migratory DCs [13]. Langerhan cells (LC) are a specialized migratory DC type migrating from the skin epithelium while classic dermal ($CD11b^+$) and $CD103^+$ DCs migrate from the dermis [1, 13]. In the lung, $CD103^+$ DCs as well as a $CD11b^+$ DC subtype that is likely equivalent to the classic dermal DC in the skin have been identified [13, 14]. The gut contains typical $CD103^+$ DCs as well as a

unique $CD11b^{+}CD103^{+}$ DC subset that appears to be similar to LCs or classic dermal DCs. Further to this, the $CD103^{+}$ migratory DC equivalents have been identified in lymph nodes draining several organs including the liver and kidney [13].

Lymphoid-organ DCs, the second category of cDCs, originate from bone marrow precursors that are seeded from the blood in lymphoid tissues and develop here without prior trafficking through the peripheral tissues [15]. These resident cells comprise the other half of the lymph node DCs and all of the spleen and thymus DCs as these organs lack connections to the lymphatic system [9, 11]. Lymphoid-organ DCs are identified based on their expression of the T cell co-receptors, CD4 and CD8, and can be grouped into three smaller populations: $CD8^{+}CD4^{-}$ ($CD8^{+}$ DCs), $CD8^{-}CD4^{+}$ ($CD4^{+}$ DCs) and $CD4^{-}CD8^{-}$ (double negative DCs). Without infection, these DCs can remain in an immature state for their entire lifespan [16]. However, maturation can be induced by stimuli such as infection or multiple traumas [16-20].

The final grouping of cDCs is the monocyte-derived or inflammatory DCs. Monocytes circulate in the blood and in conditions of inflammation appear to differentiate into ‘emergency DCs’ [1, 9]. In mouse models of *Leishmania major* infection, monocyte-derived DCs can be found in the skin and take on antigen presenting function [21, 22]. Further to this, monocyte-derived DCs appear to accumulate in the skin of some leprosy patients [23]. It has been suggested these monocyte-derived DCs are precursors of migratory DCs and infection leads to an increase in the recruitment and differentiation of this cell type [24, 25]. However, following, *Listeria monocytogenes* or systemic inflammation, monocyte-derived DCs can also be found in the spleen that lacks

migratory DCs [15, 26]. Therefore, it remains unclear if these cells are related to any DCs found in the body in a steady-state.

Distinct from cDCs, pDCs develop from precursors in the bone marrow before entering the blood [24]. Under steady-state conditions, pDCs are found in the lymph node, spleen, mucosal-associated lymphoid tissue, thymus and liver [27, 28]. During inflammatory conditions or infection, pDCs become activated and accumulate in afflicted tissue and respective draining lymph nodes [27, 28]. Their main role appears to be in secreting large amounts of type I interferons (IFN) to enhance both innate and adaptive immune responses [1]. However, pDCs express MHC and costimulatory molecules and when in a mature state can activate T cells [27, 29, 30]. pDCs have been shown to efficiently present endogenous antigens on both MHC I and II. On the other hand, pDCs appear to be less endocytic than cDCs and their ability to present exogenous antigen is not yet clearly defined [27].

1.2.2 Mechanisms of antigen presentation

All DCs are capable of capturing, processing and presenting antigen on both MHC I and II for activation of T cells. Traditionally, it was believed that MHC I molecules present peptides from endogenously-derived proteins while MHC II molecules are specialized for presentation of exogenously-acquired antigen. Bevan [31, 32] was the first to show cross-talk between these pathways by demonstrating that CTL responses can be generated against an exogenous antigen, minor histocompatibility antigens from transplanted donor cells. Since then, the clear antigenic distinction between the MHC I and MHC II pathways has faded and an obvious interplay has emerged (**Figure 1.1**).

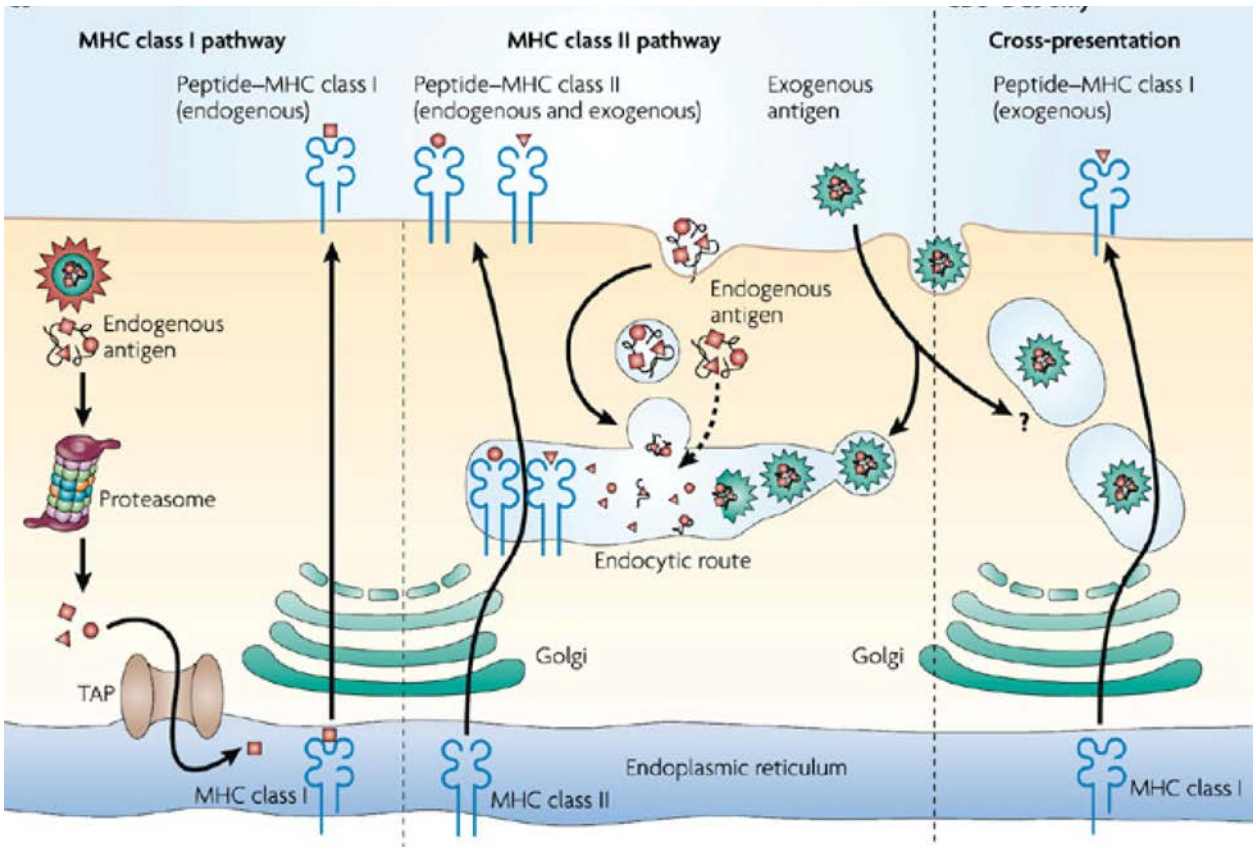

Figure 1.1 DC antigen presentation pathways.
DCs have the capacity to load endogenous antigen that has been processed via the proteasome on MHC I and exogenous antigen that has been degraded in endolysosomes on MHC II. In DCs, cross presentation or intersection between these two pathways occurs. Endogenous antigen such as endocytic pathway proteins or plasma membrane components or cytosolic proteins processed by autophagy can enter the endolysosomal pathway for subsequent loading on MHC II. Exogenous antigen internalized through endo/phagocytosis can be presented by MHC I. Reprinted by permission from Macmillan Publishers Ltd: [Nature Reviews Immunology] ([9]), Copyright (2007).

1.2.2.1 Classical MHC I antigen presentation

DCs are capable of processing and presenting antigens on MHC I to activate $CD8^+$ T cells which can then differentiate into cytotoxic T lymphocytes (CTLs). Once activated, CTLs have the ability to recognize and kill virally-infected or malignant cells, serving to remove the risk of infection or tumour spread. In the traditional or classical pathway of MHC I antigen presentation, DCs process and present endogenous antigen to $CD8^+$ T cells (**Figure 1.2**) [33, 34]. Intracellular proteins in the cytosol including defective ribosomal products and viral proteins are cleaved into short amino acid peptide fragments by a multicatalytic proteinase complex, the proteasome [9, 35, 36]. These peptides are transported into the endoplasmic reticulum (ER) lumen via the transporter associated with antigen presentation (TAP) [36]. In the ER, the assembly of the MHC I–peptide complex occurs with the assistance of several chaperone proteins, including calnexin, calreticulin and tapasin [36, 37]. The final stable MHC complex is dependent on the oligomerization of the MHC I heavy chain, β2–microglobulin (β2m) and the antigenic peptide [36]. The stable MHC trimeric complex exits the ER and traffics to the cell surface via the secretory pathway [36]. Once on the cell surface, the MHC I-peptide complex can be recognized by $CD8^+$ T cells and subsequently cause proliferation and differentiation of these cells into armed effector T cells [36].

1.2.2.2 Classical MHC II antigen presentation

$CD4^+$ T cell responses are critical for the generation of antibody responses against pathogens as well as play a role in controlling CTL activation [38]. DCs can internalize,

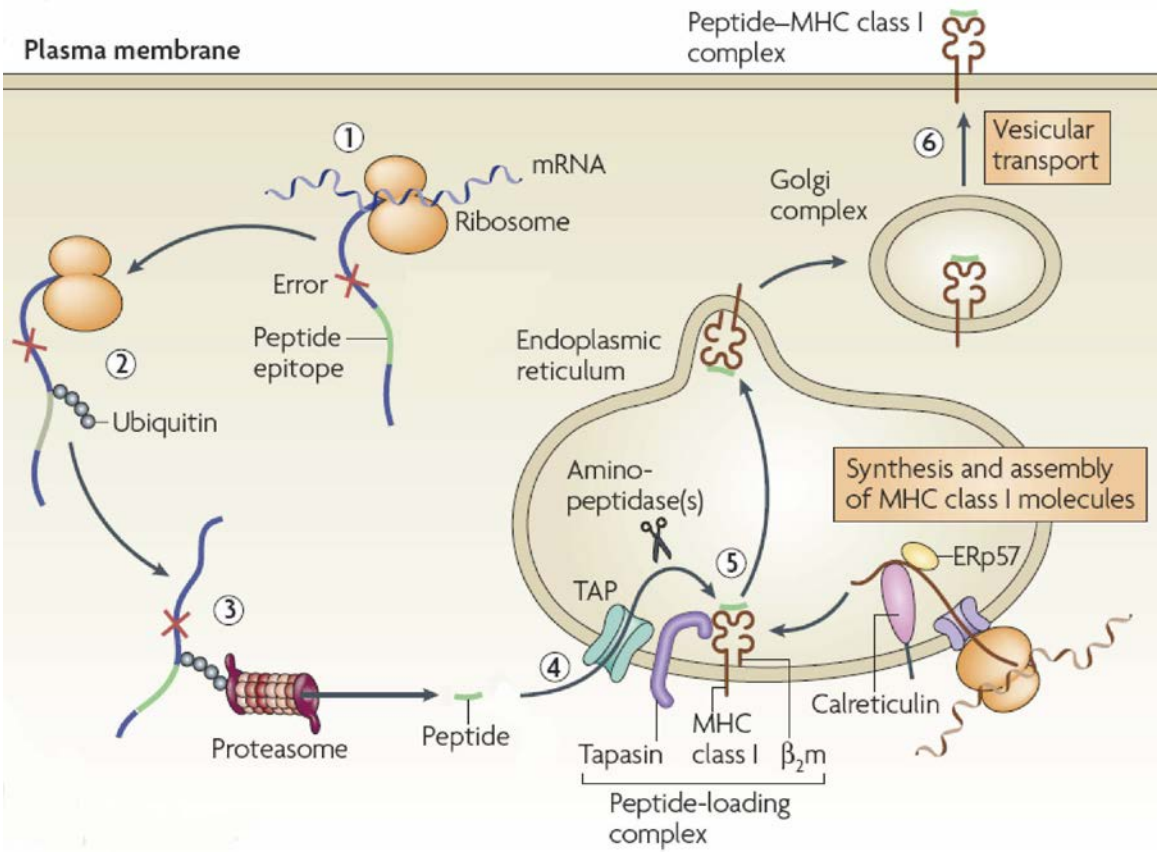

Figure 1.2. Classical MHC I antigen presentation.
Endogenous antigen is loaded onto MHC I in 6 steps. **(1)** Protein translated endogenously is acquired. This may be misfolded or erroneous self protein or protein derived from an intracellular pathogen. **(2)** Ubiquitination marks the antigen protein for degradation. **(3)** The proteasome degrades the ubiquitinated protein into peptides. **(4)** Peptides are delivered to the endoplasmic reticulum (ER) through the TAP transporter. In the ER, peptides may be further trimmed by amino peptidases. **(5)** The processed antigenic peptides are loaded into the binding groove of nascent MHC I. **(6)** MHC I is trafficked to the cell surface for recognition by $CD8^+$ T cells. Adapted by permission from Macmillan Publishers Ltd: [Nature Reviews Immunology] ([34]), Copyright (2008)

process and present exogenous proteins via the MHC II pathway for activation of $CD4^+$ T cells (**Figure 1.3**) [38]. In this pathway, the antigenic proteins are internalized and degraded via the endolysosomal pathway [39]. During the biosynthesis of the MHC II an ER chaperone known as CD74 (invariant chain) becomes associated with the complex to prevent premature binding of endogenous peptides. The CD74 cytoplasmic tail also contains a di-leucine motif that directs the MHC II complex through the endocytic pathway and into a specialized compartment termed the MIIC that contains internalized exogenous antigen [39]. Proteolytic enzymes, such as cathepsin S and L, process the antigen and degrade Ii to CLIP [38]. Finally, as a result of low pH, proteolytic trimming and a chaperone protein, HLA-DM, the CLIP is removed from the MHC class II complex to allow binding of exogenous antigenic peptide [38]. More specifically, HLA-DM functions as a peptide editor that allows peptide exchange that facilitates binding of a high affinity peptide [38]. The peptide-loaded MHC II is then trafficked to the cell surface for $CD4^+$ T cell sampling [39].

1.2.2.3 MHC I cross presentation

Antigen presenting cells (APCs) must be alerted to intracellular changes such as malignant transformations or viral or intracellular bacteria infections in order to activate CTLs to kill the affected cell. Therefore, when a tumour or infection is not APC-derived or impairs the classical MHC I pathway, alternate mechanisms must be employed [40]. DCs are distinct from other cell types in that they are specialized to take up dead cells and cellular debris containing antigenic proteins and process these exogenously-derived antigens for presentation on MHC I [6]. This unique antigen processing pathway is

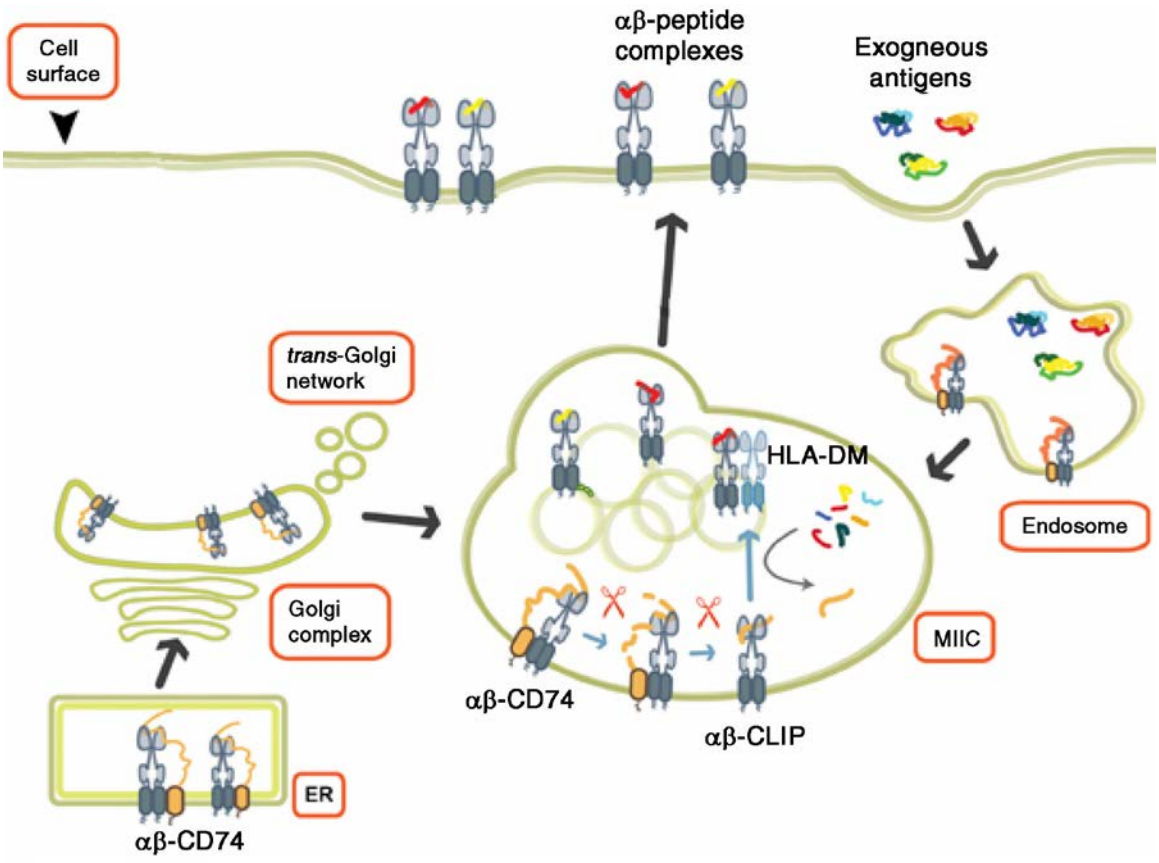

Figure 1.3. Classical MHC II antigen presentation pathway.
As MHC II αβ heterodimers are assembled in the endoplasmic reticulum (ER), CD74 associates with the peptide binding groove to prevent premature binding of endogenous antigen. CD74 chaperones MHC II to the MIIC compartment that contains endocytosed exogenous antigen. Endosomal proteases degrade the exogenous antigen as well as CD74 to CLIP (orange) that remains associated with the binding groove of MHC II. HLA-DM aids in exchanging CLIP for relevant exogenous antigenic peptides (red or yellow). Upon loading, MHC II traffics to the cell surface for recognition by $CD4^+$ T cells. Adapted by permission from Macmillan Publishers Ltd: [The EMBO Journal]([38]) Copyright (2008).

termed the MHC I cross presentation pathway [reviewed in [40]]. Although the cross presentation pathway is essential for $CD8^+$ T cell-mediated responses against viruses, tumours, self antigens and allografts, the mechanistic details remain unclear [41]. Three major models (**Figure 1.4**) exist to explain exogenous antigen presentation by MHC I in DCs: the cytosolic pathway model, the phago-ER model and the vacuolar model [reviewed in [41]].

The cytosolic pathway model proposes that exogenous antigen is transported from an endosome or phagosome to the cytosol [42]. The mechanism by which the antigen enters the cytosol is unclear. The existence of a size-specific channel that permits movement of antigen to the cytosol has been investigated [41, 43, 44]. Components of the ER-associated degradation (ERAD) pathway such as Sec61 and Derlin 1 have been suggested as candidate channels [45-48]. Once the antigen has gained access to the cytosol, it can then be degraded by the proteasome and enter the classical MHC I pathway [41, 44, 49]. In this way, MHC I molecules loaded with exogenous antigenic peptides can activate $CD8^+$ T cells.

The phago-ER model has arisen from the notion that ER recruitment occurs during phagosome formation [50, 51]. This allows the MHC I presentation machinery and the ERAD system to be incorporated into the phagosome [52-54]. This novel mixed ER-phagosome vesicle, the ‘ergosome’, may be a specialized organelle involved in loading of peptide onto MHC I during cross presentation [52, 53]. An ERAD protein translocation channel, Sec 61, was identified in the ergosome compartment [52, 53]. This channel may export antigen to the cytosol for processing by proteasomes [53]. Once processed, peptides may enter the ER and the classical MHC I pathway or may be transported back

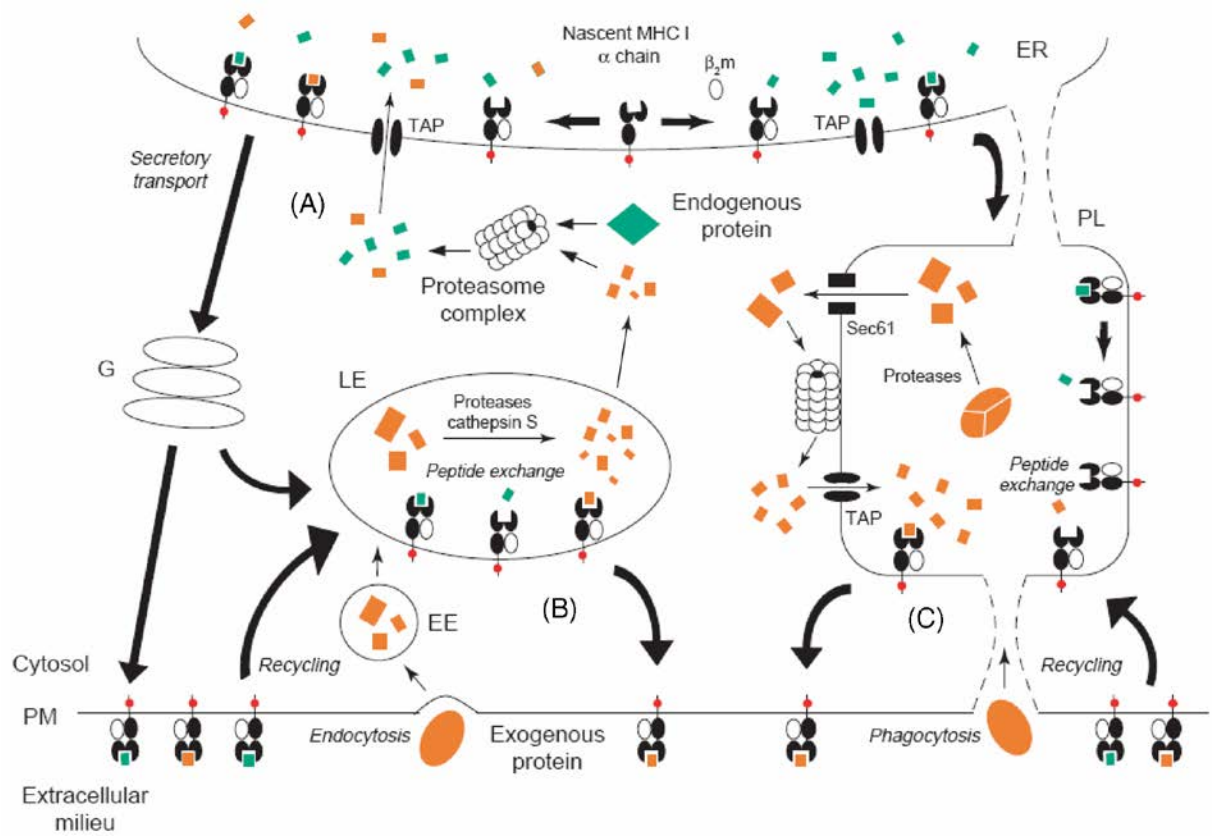

Figure 1.4. Models of MHC I cross presentation.
(A) Cytosolic Model: Exogenous protein (orange) is internalized into the endolysosomal pathway through early endosomes (EE) to late endosome compartments (LE), where proteolytic processing may occur. The exogenous peptide is transported from this compartment to the cytosol where it can enter the classical MHC I pathway along with endogenous antigen (green). **(B)** Vacuolar Model: Extracellular protein antigens are internalized into an LE compartment, where they are degraded into antigenic peptides by proteases such as cathepsin S. MHC I can access the LEs by recycling from the cell surface directed by a tyrosine motif found in the cytoplasmic tail (red) or potentially directly from the trans-Golgi network. Peptide exchange, facilitated by low pH, occurs enabling MHC I to be loaded with exogenous antigens before being transported to the cell surface**. (C)** Phago-ER model: Phagocytosis of exogenous protein involves the fusion of endoplasmic reticulum (ER) membrane with plasma membrane (PM) to form a novel organelle termed the phagolysosome (PL). This compartment contains ER components such as TAP, tapasin and Sec 61, making it self-sufficient for cross presentation. Phagocytosed exogenous protein is partially degraded, transported into the cytosol (perhaps by the Sec61 transporter), then further degraded by the proteosome which has been proposed to be associated with the cytosolic face of the PL compartment. The exogenous peptides are transported back into the same PL compartment by TAP, where they loaded onto MHC I. Adapted from Trends in Immunology, Volume 26, Issue 3, Gregory Lizée, Genc Basha and Wilfred A. Jefferies, Tails of wonder: endocytic-sorting motifs key for exogenous antigen presentation, 141-149 Copyright (2005), with permission from Elsevier.

into the ergosome by TAP, which is also present in the membrane of this compartment. Subsequently, MHC I molecules can be loaded with exogenous antigenic peptides and be directed to the cell surface to present the antigen to $CD8^+$ T cells [52, 53]. Despite providing a novel mechanistic view of cross presentation, this model has been questioned [50]. The recruitment of ER components to the phagosome has been refuted [41, 50, 55], and the ER has been shown to contribute very little to the phagosome formation [50]. Also, electron microscopy studies could not confirm fusion of the ER lumen and phagosomes [50]. Furthermore, through mathematical calculations, the ER-phagosome fusion as a model of cross presentation was predicted to be highly inefficient [41, 55].

The third non-mutually exclusive model, the vacuolar model, parallels the MHC II pathway. Exogenous antigen is taken up by endocytosis or phagocytosis, and is subsequently degraded through the endolysosomal or phagolysosomal pathways. Cathepsin S, a protease resident in endocytic compartments, has been proposed to play a key role in generating peptides in the vacuolar pathway [56, 57]. In addition, a trimming peptidase, insulin-regulated animopeptidase (IRAP) found in the endosomal compartments, may also process peptides [58]. Recycling MHC I may encounter the antigenic peptides in a post-Golgi, phagolysosomal or endolysosomal compartment and peptide exchange on the MHC I molecule may occur [59]. Alternatively, newly synthesized MHC I may traffic directly from the ER perhaps directed by chaperone proteins such as CD74 [56, 60, 61]. The loaded complex is then targeted back to the cell surface for presentation to $CD8^+$ T cells [59]. This model has been shown to be important for several antigens including proteins associated with bacteria, viruses and soluble antigen alone [59, 62-66].

Recent data from the Jefferies lab [59, 65, 66] provide evidence for the vacuolar model of cross presentation and addresses the issue of MHC I trafficking [59, 65]. Splenic DCs incubated with the well-characterized soluble antigen, ovalbumin (OVA), were seen to form H-2K^b-OVA complexes that primarily colocalized with LAMP1, a marker for endolysosomes. These results indicate that LAMP1-positive endolysosomal compartments of DCs are the main sites of MHC I loading of cross presented exogenous OVA peptide. Further to this, a tyrosine-based targeting signal within the MHC I cytoplasmic domain was identified as a requirement for MHC I routing through the LAMP1 positive antigenic loading compartments [59]. Within exon 6 of the MHC I cytoplasmic tail, a notable evolutionary conservation of one tyrosine residue was observed. To investigate the importance of this conservation, transgenic mice were created expressing MHC I (H-2K^b) containing a single substitution of phenylalanine for tyrosine in the conserved targeting signal (ΔY mice). These mice mounted inferior antiviral CTL responses when challenged with Vesticular Stomatitis Virus (VSV) and Sendai Virus [59]. DCs from ΔY mice were directly examined for cross presentation ability. Through confocal microscopy analysis, it was shown that surface MHC I is targeted through the endolysosomal pathway to a LAMP1 antigenic loading compartment [65]. However, in the absence of the Y-based targeting sequence, only a fraction of the MHC I molecules were actually being directed to endolysosomal compartments within DCs [59]. When incubated with soluble OVA, the ΔY splenic DCs had few H-2K^b-OVA complexes in LAMP1 positive compartments [59]. These results support a model (**Figure 1.5**) in which the tyrosine-based signal serves to target surface MHC I molecules to the appropriate endocytic compartment for loading of antigenic peptides [59, 65].

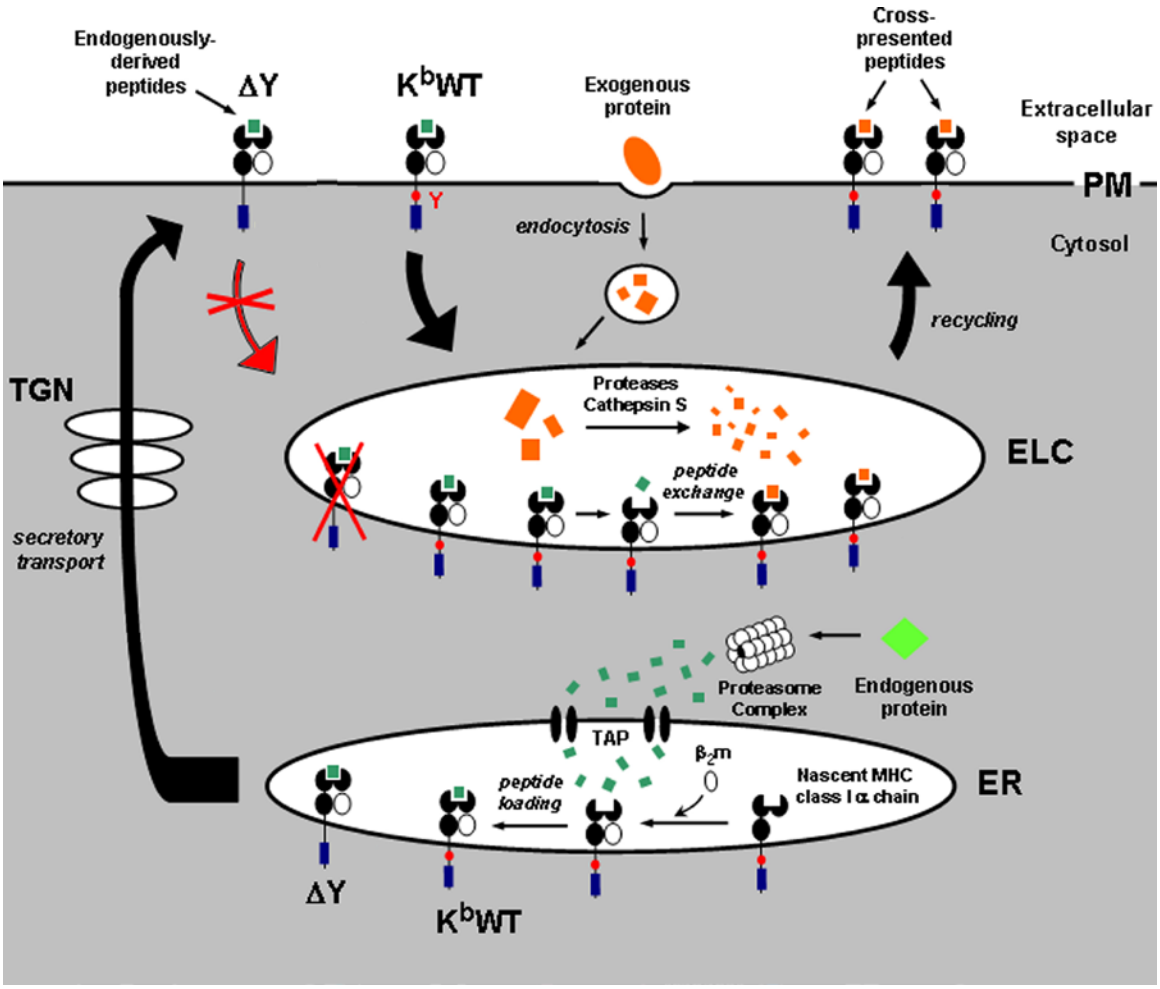

Figure 1.5. MHC I trafficking in the vacuolar model of cross presentation.
During Classical MHC I antigen presentation (bottom), endogenously-synthesized proteins (green) are degraded by the proteosome complexes then transported into the endoplasmic reticulum (ER) by TAP for binding to nascent MHC Iα/β2-microglobulin dimers. MHC I loaded in the ER is then transported via the secretory pathway to the cell surface. During cross presentation, endocytosed exogenous protein (orange) can be transported into endolysosomal compartments (ELC) and degraded by resident proteases such as Cathepsin S. Surface MHC I is constitutively internalized into the endocytic pathway by a mechanism that requires a MHC I cytoplasmic tyrosine (Y) motif (K^bWT= wild type MHC I). MHC I directed to the ELCs can exchange endogenous peptides acquired in the ER with exogenous antigens then recycle back to the plasma membrane (PM). If this tyrosine motif is missing (ΔY), the MHC I will not be able to be internalized to the ELC and will remain at the PM. Adapted from [65].

1.2.2.4 MHC II cross presentation

Although less has been described about MHC II cross presentation, endogenous peptides including those derived from nuclear, mitochondrial and cytosolic proteins have been isolated from the MHC II complex [34, 67-69]. Endocytic pathway proteins and membrane proteins that are recycled into the endosomal pathway have access to the MHC II pathway [69]. Alternatively, endogenous antigen can enter the lysosomal pathway for interaction with the MHC II antigen presentation machinery by way of autophagy (**Figure 1.6**) [70]. Autophagy has long been known to function to control the homeostasis of the intracellular environment by removing damaged or surplus organelles, eliminating aggregate or misfolded proteins and redirecting nutrients in times of stress [71]. Now, autophagy is recognized as a means of immune surveillance [71]. In fact, autophagy-driven MHC II antigen presentation has been demonstrated for not only self antigens but also tumour, viral, and ectopically-expressed bacterial proteins, as well as model antigens [71-75].

During the initiation of autophagy, the phagophore, a double membrane structure, sequesters the cytoplasmic components to be engulfed. New membrane is added to enlarge and seal the contents into an autophagosome [71, 76]. There may be several mechanisms the autophagic machinery uses to recognize cytosolic pathogens. First, signalling through pattern recognition receptors such as TLRs, Nod-like receptors and RIG-I-like receptors as well as cytokine receptors such as IFN-γ, activate autophagy [71, 77]. Reactive oxygen species produced in response to the pathogen's presence also increase autophagy [78, 79]. Alternatively, microbial products may be marked for autophagy, for example by ubiquitination [76, 77]. Furthermore, specific proteins may be

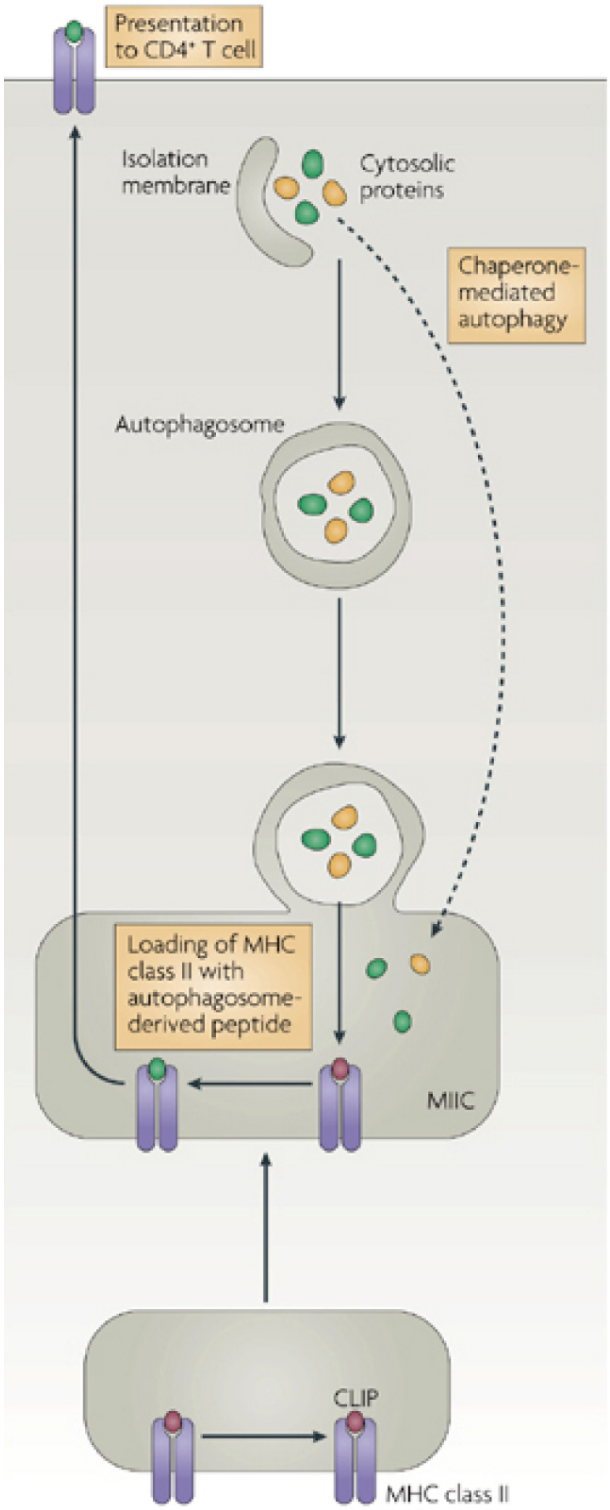
Presentation to CD4+ T cell
Isolation membrane
Cytosolic proteins
Chaperone-mediated autophagy
Autophagosome
Loading of MHC class II with autophagosome-derived peptide
MIIC
CLIP
MHC class II

Figure 1.6. Model of MHC II cross presentation.
Endogenously synthesized proteins such as self or intracellular microbial or viral antigens are engulfed into autophagosomes that can fuse with late endosomes containing MHC II (MIICs). Here, antigen can be degraded, loaded onto MHC II and trafficked to the cell surface for presentation to $CD4^+$ T cells. Reprinted by permission from Macmillan Publishers Ltd: [Nature Reviews Immunology] ([76])Copyright (2008).

targeted to the autophagosome through chaperone-mediated autophagy [71, 76]. In this pathway, proteins containing specific pentapeptide motifs are imported by a molecular chaperone complex that includes the lysosome-associated membrane protein 2 (LAMP2a) and heat shock protein (HSC70) [71]. Autophagosomes can fuse with MHC II containing late endosomes [76]. Here, proteolytic cleavage of antigens occurs and resultant peptides are subsequently loaded onto MHC II [71, 76]. The loaded complex traffics to the cell surface for presentation to $CD4^+$ T cells [34].

1.2.3 DC subsets and antigen presentation

Although all DCs can present antigen on MHC I and II, the different subsets may have distinct roles in the initiation of immune responses [9, 40]. DCs appear to present endogenous self or viral antigen on MHC I and II with equal ability [17, 75, 80-83]. However, the capacity to present exogenous antigens may be varied [9, 40]. Several studies indicate that $CD8^+$ lymphoid-organ DCs and $CD103^+$ migratory DCs are the most efficient at cross presentation [13, 40, 84]. In support of this, mice deficient for the transcription factor BATF3 lack these DCs and are unable to cross present; however, these mice are able to present exogenous antigen on MHC II and can mount $CD4^+$ T cells responses [85]. During inflammation, monocyte-derived DCs may be able to cross present as well [40]. The ability to present exogenous antigen on MHC II appears to be more wide-spread. However, $CD8^-$ lymphoid-organ DCs and $CD11b^+$ migratory DCs have been suggested to be specialized for MHC II presentation of exogenous antigen [13, 86-90]. pDCs are generally considered to be poor presenters of exogenous antigen and their role in an infection setting is yet to be fully described [27]. Migratory DCs have

been suggested to play an additional role in antigen presentation. These cells may function as carriers delivering antigen to resident DCs in the lymphoid organs [13, 84].

Several explanations have been provided for the difference in exogenous antigen presentation ability between different DC subsets [9, 40]. First, DC subsets may express specialized antigen presentation machinery [87, 91]. Variable expression of MHC I and II pathway components have been described in DC subsets [86, 91]. Also in support of this, Savina *et al* have described differential assembly of NOX2, a NADPH oxidase that allows production of reactive oxygen species for proton consumption and maintenance of an alkaline environment [92, 93]. In $CD8^+$ but not $CD8^-$ DCs, Rac2 drives NOX2 assembly on enodocytic compartments creating a less acidic environment favouring antigen preservation for cross presentation [92]. Second, presentation of exogenous antigen though the MHC I or MHC II pathway may depend on the mechanism of uptake [40, 94]. The endocytosis mechanisms utilized may introduce antigen into distinct organelles for antigen presentation [9, 40]. It has been suggested that pinocytosed antigen can reach both MHC I and MHC II pathways while antigens taken up by phagocytosis preferentially enter the cross presentation pathway [9, 94]. Following this, DC expression of endocytic receptors such as Fc receptors and C-type lectin receptors is subset-specific [40]. While subset differences are only beginning to be elucidated, it is clear that the heterogeneity of the DC population allows for the generation of immune responses to a diverse range of infections.

1.2.4 Viral inhibition of antigen presentation

As outlined above, DCs are indispensable for the generation of protective immunity against viruses [95]. They are positioned in the body at key points of viral entry including the skin, mucosal surfaces and blood [40]. Here, they can recognize viruses early and activate the adaptive immune system to mediate viral clearance [95]. Many viruses, including Human Immunodeficiency Virus (HIV), have evolved mechanisms to manipulate DC function in order to evade host recognition [96].

1.2.4.1 HIV

HIV was first isolated in 1983 and was soon recognized to be the causative agent of acquired immune deficiency syndrome (AIDS) [97]. Two types of HIV, HIV-1 and HIV-2, have been identified; however, these viruses are distinct from each other with HIV-2 exhibiting lower transmission rates and a less pathogenicity [98]. In fact, many HIV-2 infections result in a nonprogressive disease [99]. On the other hand, HIV-1 is responsible for the majority of the infection leading to the AIDS pandemic and has been the focus of much of the ongoing research [100]. Recent reports from 2008 estimated that 33.4 million people were infected with HIV world-wide and 2 million AIDS-related deaths occurred that year [101]. Despite advances in understanding HIV and AIDS, many elements of disease pathogenesis remain unclear, including the mechanisms HIV uses to evade host immune responses which allow the disease to progress.

1.2.4.1.1 Immune responses to HIV

HIV (HIV-1 referred to as HIV from this point) establishes itself as a persistent infection in the host. Left untreated, HIV will usually progress to AIDS within 10 years [102]. However, this rate varies between individuals and a rare population termed elite controllers' (ECs) can control viremia levels remaining asymptomatic indefinitely [103]. This indicates that the immune system is capable of mounting a response against HIV and to some degree can function to control the infection [104].

During viral infections, CTLs have the ability to recognize and kill virally-infected cells. This serves to prevent the risk of infection of surrounding tissues and reduces pathogen load leading to the eradication of the infectious organism [40]. Expectedly, this holds true for HIV infections as well [102]. Studies have demonstrated that increased CTL levels correlate with low plasma levels of HIV [105-107] and good CTL responses are found in HIV-infected individuals who are not progressing to AIDS [105, 108]. Furthermore, depletion of $CD8^+$ CTLs from a rhesus monkey model of SIV (simian immunodeficiency virus) results in high viremia and rapid progression to an AIDS-like syndrome [109, 110]. These studies highlight the importance of CTL responses in controlling HIV infections.

$CD4^+$ T cell responses are critical in generating antibody responses against pathogens as well as play a role in controlling cytotoxic T cell activation [111]. Further to this, $CD4^+$ T cells may take on cytotoxic properties and function to directly kill HIV-infected cells [104, 112]. In HIV patients, a correlation between the generation of efficient $CD4^+$ T cell responses and the ability to control initial stages of an HIV infection to allow maintenance of low viral loads was observed [113-115]. In addition, ECs exhibit HIV-

specific $CD4^+$ T cells with strong proliferative potential [103]. Loss of these proliferating $CD4^+$ T cells leads to disease progression [103]. Furthermore, analysis of patients infected with non-pathogenic HIV-2 revealed that in comparison to pathogenic HIV-1 infected individuals, a strong, polyclonal, anti-HIV $CD4^+$ T cell response is maintained [99]. In all, the generation of $CD4^+$ T cell responses is required for HIV immunity [116].

1.2.4.1.2 HIV interaction with DCs

Efficient activation of antiviral $CD8^+$ and $CD4^+$ T cell responses for control of HIV infection needs to be initiated by DCs. However, HIV interacts with DCs to facilitate viral transmission while impairing immune activation to escape surveillance [96, 117]. At infection sites, immature DCs residing in the skin and mucosal surfaces have been proposed to be the first cells to encounter HIV [117, 118]. From here, DCs can migrate to lymphoid tissues and may function to mediate viral spread to $CD4^+$ T cells, the main cellular target of HIV [117]. It has long been observed *in vitro* that HIV-pulsed DCs can enhance infection of T cells [119]. Recently, several mechanisms have been proposed to explain this phenomenon [117].

DCs can be directly infected by HIV and the progeny produced may be transferred to $CD4^+$ T cells though *cis*-infection. Both cDCs and pDCs are targets of HIV infection [118]. They express the HIV receptor CD4 and co-receptors including CXCR4, CCR5, required for HIV infection; therefore, direct infection of DCs can occur [117 , 120]. Infected cDCs and pDCs have been isolated from the blood of HIV-positive individuals [95, 117, 118]. However, the frequency of HIV infection in DCs *in vivo* appears to be 10-100 times lower than in $CD4^+$ T cells [121] and only 1-3% of DCs can be productively

infected *in vitro* [122]. Interestingly, susceptibility to HIV infection has been shown to increase when DCs are co-infected with sexually transmitted pathogens such as *Neisseria gonorrhoeae* and *Candida albacans* [123, 124]. Furthermore, exposure of DCs to the recreational drug, methamphetamine, led to increased HIV infection that correlated with increased expression of HIV co-receptors CCR5 and CXCR4 [125]. Despite reduced frequency and productivity of infection, direct infection of DCs likely plays a role in viral pathogenesis. HIV-2 is much less proficient at infecting DCs and this has been proposed as one factor leading to its reduced virulence compared to HIV-1[124, 126].

DCs can also capture HIV and transfer whole virus to $CD4^+$ T cells by *trans*-infection [reviewed in [117]]. DCs can capture and internalize HIV through several receptors including the C-type lectins, DC-SIGN, mannose receptor and langerin, and heparin sulfates [117, 127]. DC-SIGN is the best studied receptor for mediation of *trans*-infection. DC-SIGN interaction with the HIV surface glycoprotein, gp120, leads to rapid internalization of HIV into a low-pH, non-lysosomal compartment where it can remain infectious for several days [95, 117]. However, DC-mediated *trans*- infection can occur independently of DC-SIGN [117, 118]. When DC-SIGN was blocked with a specific antibody or DC-SIGN expression was inhibited with small interfering RNA, DCs could still mediate *trans*- infection [128]. Langerin, a LC-specific C-type lectin, was originally hypothesized to support *trans*- infection and could compensate in the absence of DC-SIGN; however, further studies suggested that Langerin not only mediates HIV internalization but also subsequent degradation thereby inhibiting transmission [118, 129]. Recently, syndecan-3, a DC-specific heparin sulfate proteoglycan, has been shown to bind HIV and mediate efficient transmission [130].

Upon uptake of HIV, DCs migrate to secondary lymphoid organs where the virus is transferred to interacting $CD4^+$ T cells via c*is*- or *trans*- infection [95, 117]. For efficient *trans*-infection, DC and $CD4^+$ T cell contact must occur [131]. DCs and T cell conjugates are thought to form an infectious synapse that is structurally similar to the immunological synapse [117]. Interaction between ICAM-1 on DCs and LFA-1 on T cells supports the transmission of HIV and may be important for infectious synapse formation [132]. Close contact mediated by the infectious synapse allows transfer of internalized HIV [117]. This has been suggested to occur through DCs release of virus within exosomes [133, 134]. Alternatively, HIV may travel along membrane nanotubules or filopodia that have been shown to connect infected cells to uninfected cells [124, 135]. Infected DCs can also release HIV progeny for *cis*-infection of T cells. In fact, long-term HIV transmission has been proposed to involve *de novo* replication of virus in DCs. A model by Wu *et al*. proposes a scenario in which DC transfer captured HIV to $CD4^+$ T cells within the first 24 hours following infection. At this point, HIV internalized into the DCs' endolysosomal pathway is degraded; therefore, productively infected DCs become HIV reservoirs and replicate virus for dissemination for several days [117, 124]. In essence, HIV has evolved efficient mechanisms to "hijack" DCs to advance infection.

HIV not only uses DCs as viral reservoirs, it also appears to manipulate DC function to control immune responses. HIV manipulates host innate and adaptive immune responses causing a progressive immune suppression leaving the HIV-infected host susceptible to secondary infections [95]. Gradual loss of $CD4^+$ T cells, $CD8^+$ T cell dysfunction and decreased NK cell numbers and function have all been noted [136]. As DCs are essential regulators of immune responses, these observed deficiencies may be a

result of impaired DC number and function [136]. More specifically, DC numbers in the blood of HIV-infected individuals progressing to AIDS are significantly decreased when compared to non-progressing HIV-infected patients [137, 138]. The DCs that are present in HIV-infected individuals have low allogeneic or autologous immunostimulatory function demonstrating an HIV-directed functional impairment [136, 139-141]. In support of this, DCs infected *in vitro* have an impaired ability to mature and DCs from infected individuals have reduced surface levels of co-stimulatory molecules, CD80 and CD86 [140, 142, 143]. Immature DCs induce tolerance rather than immunity suggesting that HIV infected DCs may have difficulty generating immune responses following infection [136]. Taken together, HIV's ability to infect, deplete and impair DCs is likely an important factor leading to immunosuppressive characteristic of AIDS.

1.2.4.1.3 HIV-Nef

The HIV genome consists of 9 open reading frames. Like all retroviruses, HIV encodes for three standard retroviral polyproteins: Gag, Pol and Env. Gag and Env polyproteins are cleaved to form the structural proteins that make up the viral core and outer membrane. The cleaved Pol polyprotein products are enzymes needed for viral integration and replication [144]. HIV also encodes six additional proteins: Tat, Rev, Vif, Vpr, Vpu and Nef. Tat and Rev provide gene regulatory function and are essential for the viral lifecycle [144]. The remaining four are accessory proteins that allow for efficient production of virus *in vivo* [144]. Nef is of particular interest to this thesis as it central for HIV pathogenesis and replication *in vivo* and for the development of AIDS [reviewed in [145]].

Nef (**Ne**gative **F**actor) was originally identified as a factor negatively influencing HIV replication [146]; however, it is now recognized as an important virulence factor [145]. The role of Nef *in vivo* was first observed in 1991 when Kestler *et al*. noted that an SIV-*nef* deletion severely reduced pathogenicity of SIV in rhesus macaques [147]. SIV viral loads remained low and AIDS rarely developed in contrast to wild type SIV infections [147]. Also, infections performed with SIV containing a premature stop codon inserted in the *nef* gene resulted in a quick restoration of the *nef* ORF [147]. Further *in vivo* SIV infection studies demonstrated that small deletions in the *nef* sequence were rapidly repaired by duplication events restoring the virus to its virulent form [148]. These studies point to an evolutionary drive for the maintenance of a functional Nef protein.

Also in the early 1990s, live-attenuated vaccines were being evaluated. One vaccine candidate was SIV (SIVmac239Δnef) with a 182 bp deletion in the *nef* gene [149]. In adult rhesus macaques, vaccination with SIVmac239Δnef was shown to protect against SIV challenge [149]. Further studies with an alternate *nef* mutant live-attenuated SIV vaccine candidates corroborated these initial observations [150]. Protection was seen against mucosal and intravenous challenges as early as 3 weeks and as late as 2.25 years post-vaccination [150]. It appeared that by simply mutating the *nef* gene a pathogenic virus was converted into a live-attenuated vaccine and hopes were high that a safe and effective AIDS vaccine could be developed [150]. However, this optimism was short lived. Vaccine trials in neonate macaques began as part of a project to prevent mother-to-child transmission. Unexpectedly, oral vaccination of newborn monkeys resulted in high viral loads and rapid progression to AIDS [151, 152]. Although a vaccine was not

developed from these studies, the importance of Nef as a virulence factor was reinforced further.

Deletions of *nef* have been associated with cases of non-progression to AIDS in humans [153]. The best studied long term non-progressors (LTNP) are the Sydney Blood Bank Cohort (SBBC). In the early 1980's, prior to HIV-1 blood testing in Australia, eight individuals became infected with *nef*-deleted HIV when administered contaminated blood products originating from a common donor [154]. To date, there have been no AIDS-related deaths observed in the SBBC [153]. Three patients are "elite" LTNPs and have lived over 20 years without symptoms of AIDS [153]. However, the others did eventually present with declining $CD4^+$ T cells and detectable viral loads after 17 years and are now considered slow progressors [153]. From the SBBC, it is evident that Nef is an important factor for *in vivo* pathogenicity.

1.2.4.1.4 Immune evasion mechanisms of HIV-Nef

Nef is a 27 kDa myristoylated protein expressed early in the viral replication cycle. While the N- and C-terminus ends of the protein can be quite variable, the core domains of Nef remain relatively conserved [145]. Nef has no enzymatic function but does act as an adaptor protein, sequestering host proteins resulting in their aberrant function allowing viral immune evasion and efficient viral replication [153]. Relevant to this thesis, Nef has been shown to downregulate cell surface expression of both MHC I and MHC II molecules [136].

Nef mediated downregulation of surface MHC I is a key element of HIV immune-evasion. The importance of this mechanism was revealed in a study examining an SIV-

nef allele with a point mutation disrupting MHC I downmodulation [155, 156]. This mutation was strongly selected against *in vivo* and a rapid reversion to the wild type form capable of downregulating MHC I occurred [155, 157]. Further *in vivo* studies demonstrated that *nef* alleles with the ability to downregulate MHC I are selected for early in HIV infection; however, in late stage infection when the immune system is almost non-existent, the selection for this Nef characteristic is reduced [157, 158]. This evolutionary drive for Nef to maintain the ability to downregulate MHC I implies this is important for Nef's function.

The decrease in surface MHC I was attributed to Nef fifteen years ago; however, the details of the cellular pathway still remain uncertain [159]. Two non-mutually exclusive pathways have been proposed (**Figure 1.7**). First, MHC I downregulation results from a Nef-mediated increase in MHC I internalization from the cell surface [160]. Alternatively, Nef blocks newly synthesized MHC I trafficking through the Golgi to the cell surface [156]. The net result of either model is an accumulation of MHC I in the trans Golgi Network (TGN) and the eventual transfer of MHC I to lysosomes for degradation [160].

In the first model, Nef has been proposed to internalize surface MHC I through a multi-step pathway (**Figure 1.8**) [160-163]. Initially, Nef interacts with PACS-2 (phosphofurin acidic cluster sorting protein-2), a sorting protein known to localize proteins to the secretory pathway. PACS-2 directs Nef to the TGN where Nef recruits a srk family kinase (SFK). The SFK binds and phosporylates ZAP70/syk which subsequently binds and activates phosphatidylinositide-3 kinase (PI3K). PACS-1 localizes this complex (Nef-SFK-Zap-70/syk-PI3K) to the plasma membrane where

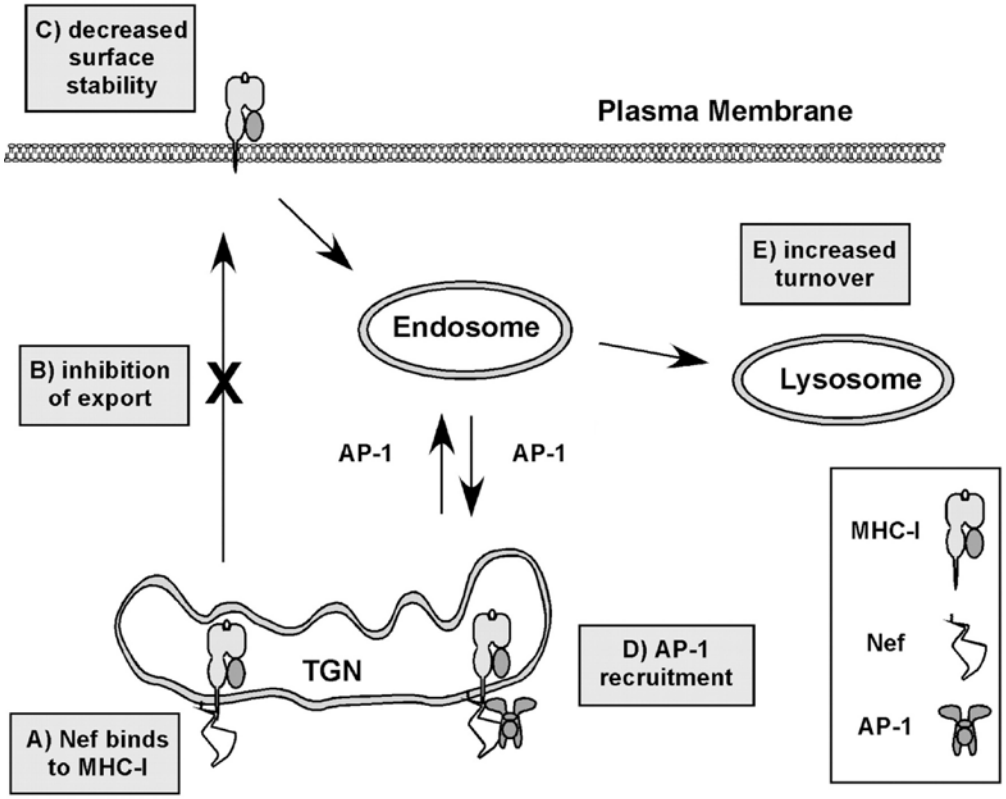

Figure 1.7. Proposed models of Nef-mediated MHC I downregulation.
(A) Nef can interact with MHC I at the *trans* Golgi Network (TGN). **(B)** This may inhibit MHC I export to the plasma membrane. **(C)** MHC I that escapes Nef's initial effects and traffics to the cell surface may experience decreased surface stability. **(D)** This is due to a Nef-mediated increase in MHC I turnover and mis-trafficking of MHC I to the TGN. **(E)** The MHC I accumulating in the TGN may eventually be directed to lysosomes for degradation. Amended from Microbiology and Molecular Biology Reviews, 2006, volume 70, 548-563, doi:10.1128/MMBR.00042-05 with permission from American Society for Microbiology [156].

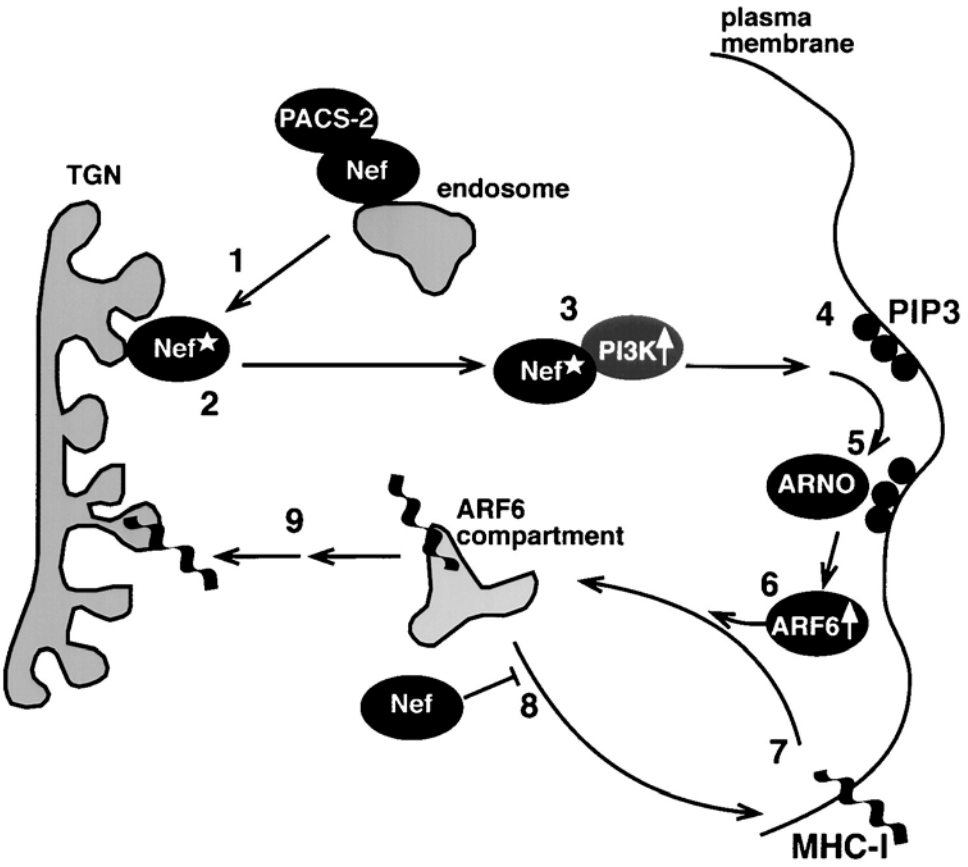

Figure 1.8. Model of Nef-mediated increase in MHC I internalization.
(1) PACS-2 binds and localizes Nef to the *trans* Golgi Network (TGN**). (2)** Here, Nef recruits and activates SFK and Zap-70/syk (indicated by star). **(3)** The Nef- SFK-Zap-70/syk complex binds and activates PI3K (as shown by arrow). **(4)** The Nef-SFK-Zap-70/syk-PI3K localizes to the plasma membrane and generates PIP_3. **(5)** ARNO is recruited to PIP_3-containing membrane. **(6)** ARNO activates ARF6 (as shown by arrow). **(7)** The result is an increase in ARF6-dependent MHC I endocytosis from the cell surface. **(8)** Nef further block the recycling of internalized MHC I from the ARF6 compartment to the cell surface, **(9)** and mediates delivery of internalized MHC I molecules to the TGN. Altered from: Cell, Vol 111, Issue 6, Anastassia D. Blagoveshchenskaya, Laurel Thomas, Sylvain F. Feliciangeli, Chien-Hui Hung, Gary Thomas, HIV-1 Nef Downregulates MHC-I by a PACS-1- and PI3K-Regulated ARF6 Endocytic Pathway, 853-866., Copyright (2002), with permission from Elsevier.

phosphatidylinositol 3,4,5-trisphosphate (PIP_3)-containing lipids are generated. Increased PIP_3 at the plasma membrane recruits the guanine nucleotide exchange factor, ARNO, to the cell surface allowing GTP loading of ARF6. The end result is an acceleration of ARF6 mediated MHC I endocytosis and removal of MHC I from the cell surface. MHC I recycling back to the cell surface is blocked by Nef and internalized MHC I subsequently traffics to the TGN either by Nef linking MHC I to PACS-1 or directly to AP-1[163-165]. Despite much work defining this model, details are still disputed and independent results have been presented opposing Nef's dependency on PACS-1 and ARF6 for MHC I downregulation [166, 167]. This leaves open the possibility that Nef uses an alternative method to increase MHC I recycling from the cell surface.

Additional studies support a second model explaining the impediment of MHC I trafficking. Nef has been shown to affect the transport of newly synthesized MHC I to the cell surface [156]. Nef appears to stop MHC I trafficking within the TGN. Here, Nef has been proposed to directly interact with the cytoplasmic tail of MHC I and link MHC I to the adaptor protein, AP-1, known to sort proteins at the TGN [156, 164, 165]. The interaction with AP-1 eventually leads to the delivery of MHC I to lysosomes for degradation. This model does not take into account the observations that Nef increases MHC I internalization; therefore, both proposed mechanism likely function accounting for the dramatic perturbations observed in MHC I trafficking patterns that contribute to reduced CTL activity.

Although considerably less work has been done to describe Nef's interaction with MHC II, Nef has also been reported to interfere with MHC II trafficking and antigen presentation [160, 168]. Nef appears to cause increased immature CD74 associated MHC

II and decreased mature antigen-bound MHC II on the cell surface [169-171]. Further to this, Nef expression has been shown to reduce the movement of immature MHC II to lysosomes for degradation of CD74 while increasing the amount of mature MHC II in lysosomes [171]. Similar to the MHC I downregulation pathway, Nef may decrease the amount of mature MHC II on the cell surface by retarding delivery of newly synthesized MHC II to the cell surface [170] or by increasing endocytosis of surface MHC II and targeting it to lysosomal compartments [168, 170, 171]. As a consequence, reduced surface MHC II likely favours HIV survival by interfering with the ability of the host to generate $CD4^+$ T cell responses.

1.3 T cells

In the body's steady-state, a pool of T cells that express a diverse T cell receptor (TCR) repertoire is maintained in the periphery [172]. In the event of an infection, T cells can recognize the infectious antigen presented by DCs through their TCR and are induced to proliferate and differentiate into effector cells capable of clearing the pathogen. Effector T cells are usually maintained for a few weeks before they die most likely from neglect allowing the T cell population to be restored to its steady-state levels [173]. A few of the antigen-specific cells will survive indefinitely as memory T cells [174].

1.3.1 T cell activation

1.3.1.1 Proximal events in T cell activation

A T cell becomes activated when its TCR recognizes cognate antigen presented on MHC by a DC. A series of signalling events ensue following ligation of the TCR. Depending on the strength of the TCR stimulus and the presence of costimulatory and cytokine signals, the T cell will be induced to survive or establish effector function [173]. The TCR is a complex of several proteins specialized for either ligand recognition or signalling [175]. The predominate αβ TCR contains the clonotypic αβ chains in a heterodimer that can recognize and bind MHC/peptide complexes. However, this heterodimer lacks signalling ability so for this purpose is linked noncovalently to nonpolymorphic TCR-ζ chain homodimer and CD3-γ,-δ,-ε chains [176]. It is generally thought that the total TCR complex is assembled as TCRαβ, CD3 γε, CD3δε and ζζ (**Figure 1.9**) [176].

The TCR complex recognizes and binds peptide-bound MHC on the surface of APCs. The CD4 coreceptor expressed on T helper cells or CD8 coreceptor on cytotoxic T cells helps in recognition by binding to MHC II or MHC I, respectively. The coreceptors bind to membrane-proximal sites of the MHC/peptide complex leaving the surface free to interact with the TCR [177]. Upon TCR ligation, the TCR-ζ chain and CD3-γ,-δ,-ε chains transduce signals through Immune receptor Tyrosine-based Activation Motifs (ITAMs) present in their cytoplasmic domains. ITAMs consist of two tyrosine residues in a consensus sequence, YXXL/I-X_{6-8}-YXXL/I, where Y is tyrosine, L is leucine, I is isoleucine and x can be any amino acid [178]. The TCR complex contains at total of 10 ITAMS with one on each CD3 chain and 3 in tandem on each ζ chain [175]. Two Src

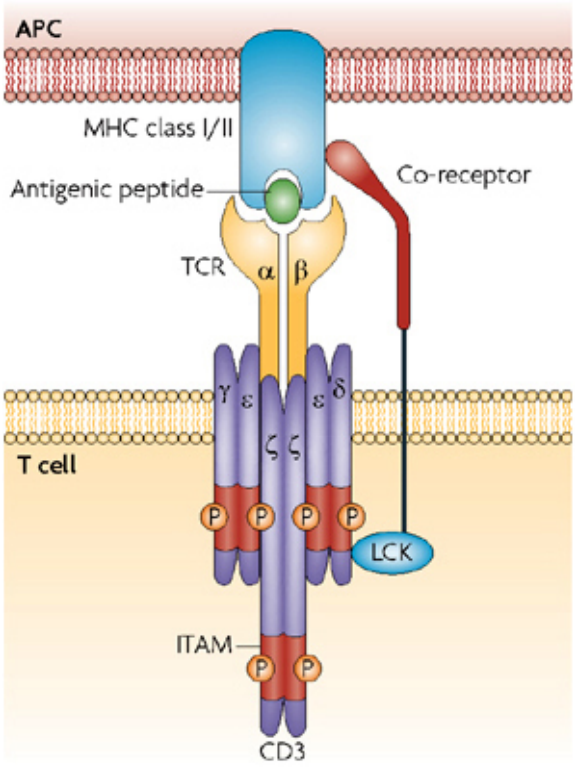

Figure 1.9. The TCR complex.
The TCR complex assembled as TCRαβ, CD3 γε, CD3δε and ζζ interacts with MHC in complex with antigenic peptide. The CD4 or CD8 co-receptor stabilizes this interaction and brings the associated kinase, LCK, into proximity. LCK phosphorylates the Immunoreceptor Tyrosine-based Activation Motifs (ITAMs) present in the TCR complex to initiate signalling. Reprinted by permission from Macmillan Publishers Ltd: [Nature Reviews Immunology] ([179]), Copyright (2008).

family kinases, Lck and Fyn, are responsible for the phosphorylation of the ITAMs that serve as the initial signal that the TCR has recognized its MHC/antigen complex [176]. Lck and Fyn are localized to the membrane through myristoylate/palmitoylate posttranslational modifications [180]. Lck is further associated with the CD4 and CD8 coreceptors through a di-cystiene motif [180]. Src-family kinases are regulated by conformational changes caused by the phosphorylation and dephosphorylation of inhibitory and activating tyrosine residues. In the inactive state, the inhibitory tyrosine is phosphorylated allowing an interaction with its Src homology (SH)2 domain and creating a non-functional protein conformation that is further stabilized by SH3 domain interactions [180]. Upon dephosphorylation by CD45, the Src kinase shifts to an 'open' conformation allowing transphosphorylation of the activating tyrosine in the catalytic domain and protein activation [180]

Although it is clear that the initial step involves the phosphorylation of ITAMS by Lck and Fyn, it is still unclear how the engagement of the TCR complex leads to this phosphorylation event [176]. Several models have been presented as an explanation and it is likely that they are not mutually exclusive [176, 181]. TCR clustering has been a long standing model that proposes cross-linking of receptors allows transphosphorylation of CD3 and ζ chains by associated kinases [176]. Adhesion and accessory molecules may mediate close contact between the T cell and APC concentrating the TCR complex, co-receptors and signalling molecules and excluding inhibitory phosphatases [176]. As antigenic peptide/MHC may be in minority compared to self-peptide/MHC on the surface of a presenting cell, cross-linking of antigen/MHC may not always be realistic. A pseudodimer or a dimerization between a self-peptide/MHC and an antigen/MHC may

initiate TCR signalling allowing for amplification of the TCR signalling cascade [176, 182] Alternatively, a conformational change may be responsible for signal transduction [176]. In resting cells, the ζ or CD3-ε tails may be closely associated with the plasma membrane leaving Lck unable to access them for phosphorylation; however, upon TCR engagement, the tails may be released into a conformation favourable for Lck activity [183, 184]. Furthermore, the observation that TCR activation exposes a proline-rich region (PRR) on the CD3ε chain that allows recruitment of the adaptor protein, noncatalytic tyrosine kinase (Nck) before ITAM phosphorylation suggests that Nck may be responsible for the recruitment of kinases to mediate ITAM phosphorylation [176, 185]. However, experiments with mice deficient for the CD3ε PRR domain eliminating the Nck/CD3 association maintained normal T cell development and function [186]. Therefore, further investigation is required for a clear understanding.

Upon TCR engagement, the formation of the proximal signalling complex is initiated allowing the activation of downstream signalling pathways to occur (**Figure 1.10**). Phosphorylated ITAMs recruits ζ-chain associated protein of 70 kDa (ZAP-70) kinase which becomes phosphorylated and activated by the Src family kinase, Lck [180]. ZAP-70, in turn phosphorylates the scaffold proteins linker for the activation of T cells (LAT) and SH2 domain-containing leukocyte phosphoprotein of 76 kDa (SLP-76). These two proteins function together to recruit and organize effector molecules for multiple signalling pathways [176]. LAT contains nine tyrosines that are phosphorylated and bind PLCγ1, PI3K, growth factor receptor-bound protein 2 (GRB2), and GRB2-realted adaptor downstream of shc (Gads) [176]. SLP-76 is constitutively bound to Gads and attaches to the signalling complex when Gads binds LAT. SLP-76 has three tyrosines that become

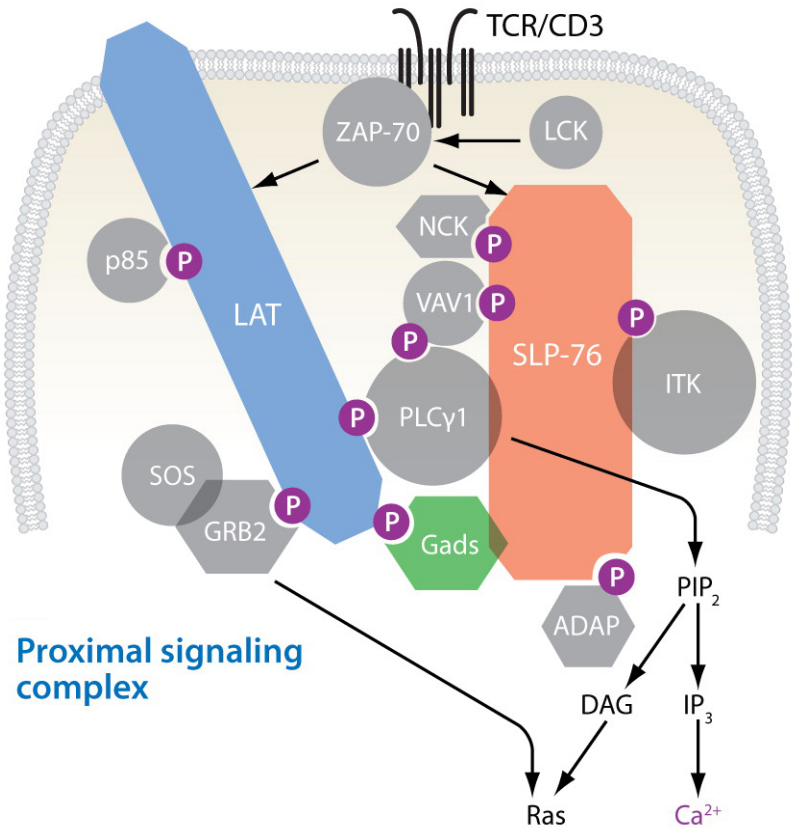

Figure 1.10. The proximal signalling events at the TCR complex.
The formation of the proximal signalling complex is initiated when LCK phosphorylates (P) and activates ZAP-70. ZAP-70 in turn phosphorylates LAT recruiting Gads and its binding partner SLP-76. Here, ZAP-70 further phosphorylates SLP76. Together, LAT and SLP76 form a scaffold that recruits additional effector molecules (circles) and adapter proteins (octagons). These initial signalling events lead to the production of the second messengers inositol 1,4,5-trisphosphate (IP_3) and diacylglycerol (DAG) that initiate Ca^{2+} and RAS/PKCθ signalling, respectively. Used with permission of ANNUAL REVIEWS, INC., from T Cell Activation, Jennifer E. Smith-Garvin, Gary A. Koretzky, Martha S. Jordan, 27, 2009; permission conveyed through Copyright Clearance Center, Inc.

phosphorylated and interact with Vav1, Nck and IL-2 induced tyrosine kinase (Itk). SLP-76 further interacts with PLCγ1 through a PRR domain and with adhesion and degranulation-promoting adapter protein (ADAP) and hematopoietic progenitor kinase 1 (HPK1) through a SH2 domain [176].

PLCγ1 is an important molecules leading to several downstream effects of TCR activation. PLCγ1 is activated by the kinase, Itk [176]. Itk associates with the cell membrane via an interaction between its PH domain and PIP_3 that is generated by PI3K activity [187]. Here Itk interacts with the LAT/SLP-76 scaffold through its SH2/SH3 domain and becomes phosphorylated by Lck [187]. Once activated, Itk phosphorylates itself and PLCγ1 [187]. The active phospholipase hydrolyzes the membrane lipid phosphoinositol 4,5-bisphosphate (PIP_2) generating the second messengers inositol 1,4,5-trisphosphate (IP_3) and diacylglycerol (DAG) [176]. These second messengers have several downstream effects. IP_3 initiates an increase in intracellular calcium (Ca^{2+}) while DAG activates two major pathways through Ras and Protein kinase C **(**PKC) θ [176, 187].

1.3.1.2 Calcium-mediated signalling

Ca^{2+} is a universal second messenger important for T cell quiescence, differentiation and effector function [188, 189]. An increase in intracellular Ca^{2+} levels is initiated by IP_3 produced by PLCγ1. IP_3 binds to IP_3 receptors (IP_3R) in the ER causing release of ER Ca^{2+} stores into the cytoplasm. In a mechanism termed store-operated Ca^{2+} entry (SOCE), depletion of ER Ca^{2+} stores triggers a sustained influx of extracellular Ca^{2+} through Ca^{2+}

release-activated Ca^{2+} (CRAC) channels in the plasma membrane [189]. The electrophysiological characteristics of the CRAC channel are well defined; however the identity and the mechanism of activation are not clear. There are several families of channels expressed on the plasma membrane of T cells [190]. Recently, using high-throughput RNA interference screens, an ER Ca^{2+} sensing molecule stromal interaction molecule 1 (STIM1) and a pore-forming plasma membrane protein, ORAI1, have been identified as the CRAC channel. Transient receptor potential (TRP) channels have also been the focus of much attention and have been reported to activate by store depletion. IP_3R, similar to the ER-associated Ca^{2+} channels, have been shown to be expressed at the plasma membrane. As well, the adenosine triphosphate (ATP) responsive purinergic P2 receptors (P2X) have shown significant Ca^{2+} permeability. Finally, voltage-dependent Ca^{2+} channels (Ca_V), the focus of this thesis, have been identified in T cells [189-191].

1.3.1.2.1 Calcium channels in T cells

1.3.1.2.1.1 ORAI1 and STIM1

A recent discovery of STIM1 and a pore-forming plasma membrane protein ORAI1 has led to the development of a popular model (**Figure 1.11**) [reviewed in [192]]. In this model, the ER transmembrane protein, STIM1, senses the depletion of Ca^{2+} stores. STIM1 exists as a monomer when Ca^{2+} is present, stabilized through an interaction between its luminal EF hand domain and sterile α –motif (SAM). When ER Ca^{2+} stores are depleted, the EF-SAM domain interaction in STIM1 becomes unstable resulting in the oligomerization of STIM1 molecules [193, 194]. STIM1 oligomers accumulate in puncta

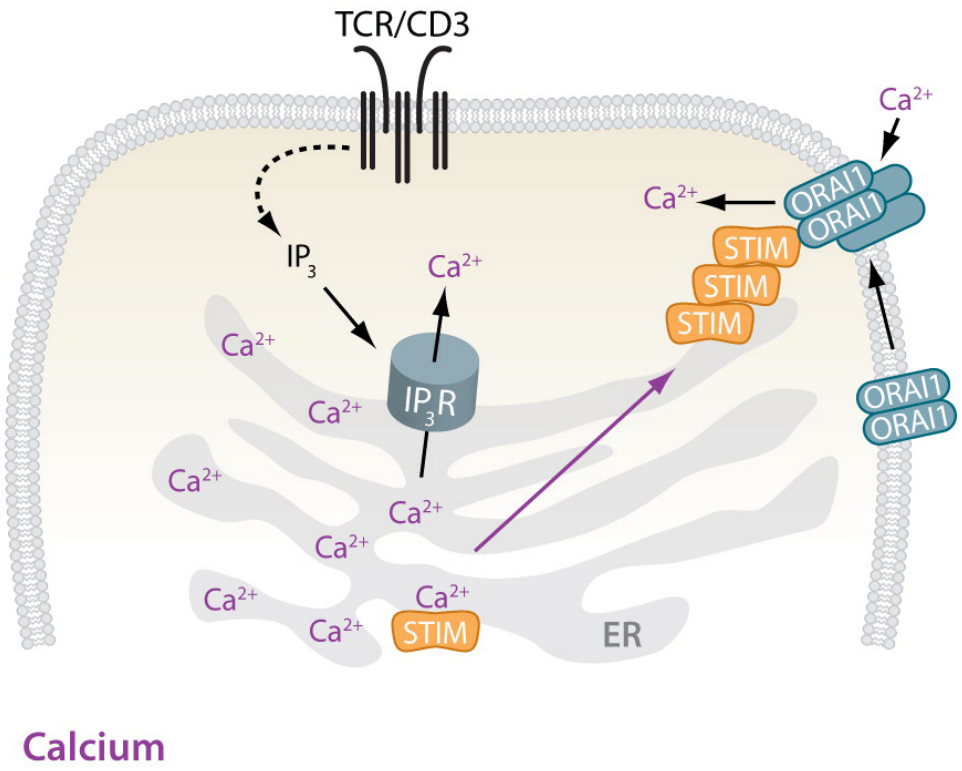

Figure 1.11. CRAC channel activation.
The 1,4,5-trisphosphate (IP_3) produced by TCR engagement activates IP_3 receptors (IP_3R) in the endoplasmic reticulum (ER) to release Ca^{2+} into the cytoplasm. STIM can sense the depletion in ER Ca^{2+} stores through EF hand motifs that bind Ca^{2+}. Without bound Ca^{2+}, STIM molecules cluster and move to areas of the ER in close proximity to the plasma membrane. Here, STIM co-localizes with ORAI1 channels inducing their activation and the subsequent influx of extracellular Ca^{2+}. Used with permission of ANNUAL REVIEWS, INC., from T Cell Activation, Jennifer E. Smith-Garvin, Gary A. Koretzky, Martha S. Jordan, 27, 2009; permission conveyed through Copyright Clearance Center, Inc.

in regions of ER 10-25 nm beneath the plasma membrane [195-197]. Here, ORAI1 at the plasma membrane can interact with STIM1 [198, 199]. ORAI1 has been suggested to exist as a dimer in the plasma membrane and upon STIM1 interaction forms tetramers that can function to import Ca^{2+} [200].

ORAI and STIM function has been analyzed in immunodeficient patients [reviewed in [192]]. Linkage mapping lead to the discovery of *ORAI1* mutations in individuals experiencing symptoms similar to those associated with severe combined immunodeficiency (SCID) characterized by severe infections early in life [201-204]. Lymphocyte numbers were normal in these patients indicating normal development and peripheral maturation [192]. However, the lymphocytes had impaired SOCE and I_{crac}, the Ca^{2+} current gated by the CRAC channel [192]. As well, the peripheral T cells were unable to be activated as demonstrated *in vivo* by minimal responses in skin delayed-type hypersensitivity reactions and *ex vivo* by reduced proliferation upon stimulation [203-205]. Further to this, these patients had no antigen-specific antibody responses following infection or vaccination [192]. Recently, a homozygous nonsense mutation in *STIM1* was identified in three members of a family that suffer from severe immunodeficiency [206]. The clinical condition was reminiscent of the ORAI1 patients in that normal lymphocyte numbers and TCR repertoire could be seen; however, severe proliferation defects were observed in lymphocytes examined *ex vivo* [206]. Dissimilar to the ORAI1-deficiency, these patients also experienced lymphoproliferative and autoimmune disease [206]. This was seen as lymphadenopathy (enlarged lymph nodes) and hepatosplenomegaly (enlarged liver and spleen). Two patients suffered from Coombs-positive autoimmune hemolytic anemia (AIHA). In addition, all three presented with thrombocytopenia resulting from

autoimmunity towards platelets that were coated with autoantibodies against platelet glycoprotein Ib/IX [206]. It has been suggested that this autoimmunity observed in STIM1-deficient patients is a consequence of the reduced T regulatory (Treg) cell numbers found in the periphery [192, 206].

ORAI1 and STIM1 knock-out mouse models have also been developed. In contrast to the human patients, these mice die early postnatally for reasons that are still unclear [192, 207-211]; however, defects in skeletal muscle that contribute to a severely runted phenotype may play a role [192]. In mouse models lacking ORAI1, CRAC current measured in T cells is reduced; however, residual currents do remain [209]. ORAI1-deficient mice have been shown to have impaired cytokine secretion [209]. However, a subsequent study found no defect in T cell proliferation [207]. Like the human studies, murine T cell development was found to be normal in the absence of *ORAI1* [209]. *STIM1*$^{-/-}$ mice, similar to *ORAI1*$^{-/-}$ mice, have no CRAC channel function or SOCE and no subsequent activation of the nuclear factor of activated T cells (NFAT) transcription factor [212]. In addition, T cells from these mice have impaired cytokine secretion [212]. T and B cell development appears normal; however, CD4^{+}Foxp3^{+} Treg cells are severely reduced. This presumably results from reduced Ca^{2+}/NFAT dependent induction of Foxp3 expression and the subsequent impairment in Foxp3/NFAT DNA-binding complex formation [212-214]. The impaired Treg development and function in these mice results in autoimmune and lympho-myeloprolifertaive syndromes similar to those observed in *STIM1*-deficient human patients [212].

1.3.1.2.1.2 Transient receptor potential (TRP) channels

The role of TRP channels in lymphocyte Ca^{2+} signalling has also been investigated. The first TRP family member was discovered in *Drosophila* and was found to have a role in visual transduction [215]. Subsequently, twenty-eight mammalian TRP channel proteins have been identified [215]. These are grouped into six subfamilies based on amino acid sequence similarities: the classical TRPs (TRPCs) that are most similar to *Drosophila* TRP; the vanilloid receptor TRPs (TRPVs); the melastatin TRPs (TRPMs); the mucolipins (TRPMLs); the polycystins (TRPPs); and ankyrin transmembrane protein 1 (TRPA1) [215]. The 6 transmembrane domain TRP channels form pores that are permeable to cations including Ca^{2+} [215]. TRPC1, TRPC3, TRPC6, TRPM2, TRPM4, TRPM7, TRPV5 and TRPV6 have been shown to be expressed in cultured or primary T cells [189, 216].

TRP channels have been investigated as candidates for the CRAC channel. TRPV6 channel is highly permeable to Ca^{2+} and has been shown to be activated by store-depletion [217]. In addition, when a dominant-negative pore-region mutant of TRPV6 was expressed in Jurkat T cells, the I_{crac} was diminished [217]. However, subsequent studies could not confirm TRPV6 role as a CRAC-like channel [218, 219] and the CRAC channel inhibitor, BTP2, had no effect on the TRPV6 channel activity [220, 221]. TRPC3 channels have also been under consideration as CRAC channels following the discovery that Jurkat T cell lines with mutated TRPC3 channels had reduced Ca^{2+} influx following TCR stimulation. This impairment could be overcome by overexpression of a wild type TRPC3 [222, 223]. TRPC3 has been shown to be activated in response to store-depletion

[224]; however, the major stimuli gating TRPC3 seems to be DAG [225]. The current role of TRP receptors in SOCE is still under investigation.

The TRPM2 channel in T cells has also been extensively examined. TRMP2 is a non-selective Ca^{2+} channel that is activated by intracellular second messengers ADP-ribose (ADPR), nicotinamide adenine dinucleotide (NAD^+), H_2O_2 and cyclic ADPR [226-228]. TRPM2 has been proposed to be associated with cell death in that activation of T cells can increase endogenous ADPR levels in T cells activating TRPM2 and cell death [229]. In addition, it has been proposed that H_2O_2 activation of TRPM2 links reactive oxygen species production with cell death [230]. Taken together, TRPM2 can contribute to some degree to Ca^{2+} signalling in T cells.

1.3.1.2.1.3 IP_3 receptors (IP_3R)

The IP_3Rs, similar to those found in the ER, have been suggested to function as Ca^{2+} channels at the plasma membrane [190, 231]. IP_3 dissipates rapidly after TCR engagement; therefore, IP_3 induced activation of plasma membrane receptors would only contribute to short-term Ca^{2+} signalling [190]. Alternatively, it was suggested that IP_3Rs in the ER, known to bind IP_3 to deplete ER Ca^{2+} stores, change conformation upon ER store depletion and signal to surface IP_3Rs to open [232]. IP_3R have been detected on the cell surface of cultured T cells [231, 233]. However, IP_3 induced Ca^{2+} currents across the plasma membrane could not be detected [234]. As an alternate function based on the numerous protein binding sites present in the modulatory domain of the channel, IP_3Rs have been proposed to operate at the plasma membrane as scaffolds [235]. Further work is required to clearly fit the IP_3R into the Ca^{2+} signalling network in T cells.

1.3.1.2.1.4 P2X receptors

Seven ATP-gated Ca^{2+} permeable channels have been identified: $P2X_1$-$P2X_7$. These channels were found to form homo- or heterodimers [236]. Four P2X channels ($P2X_1$, $P2X_2$, $P2X_6$ and $P2X_7$) were found to be expressed in thymocytes [236] These channels allow thymocytes to increase intracellular Ca^{2+} levels in response to extracellular ATP [236]. As well, ATP generated through TCR stimulation has been shown to activate the $P2X_7$ channel [237]. Analysis of P2X receptor deficient mice revealed no major defects in T cell development or function [189, 238]. Therefore, the role of P2X channels in T cell Ca^{2+} signalling and function remains to be determined.

1.3.1.2.1.5 Ca_V channels

Ca_V channels function in excitable cells such as nerve, muscle and endocrine cells where they open in response to membrane depolarization to allow Ca^{2+} entry [239]. However, pharmacological and molecular genetic studies have demonstrated the existence of Ca_V in T cells [240-245]. The Ca_V channels were initially classified based on the voltage required for activation into the subgroups high-voltage activated (HVA) and low-voltage activated (LVA) channels. Further analysis of the Ca^{2+} channels allowed for additional classification of the channels into groups with distinct biophysical and pharmacological properties: T (tiny/transient) - , N (neuronal) - , P/Q (Purkinje) - , R (toxin-resistant) - , L (long-lasting) -type channels [239, 246].

The Ca_V channels are heteromultimeric protein complexes composed of 5 subunits: α_1, α_2, β, δ and γ (**Figure 1.12A**). The α_2 and δ subunits are linked together though disulfide bonds to form a single unit referred to as $\alpha_2\delta$. The α_1 subunit of the channel is

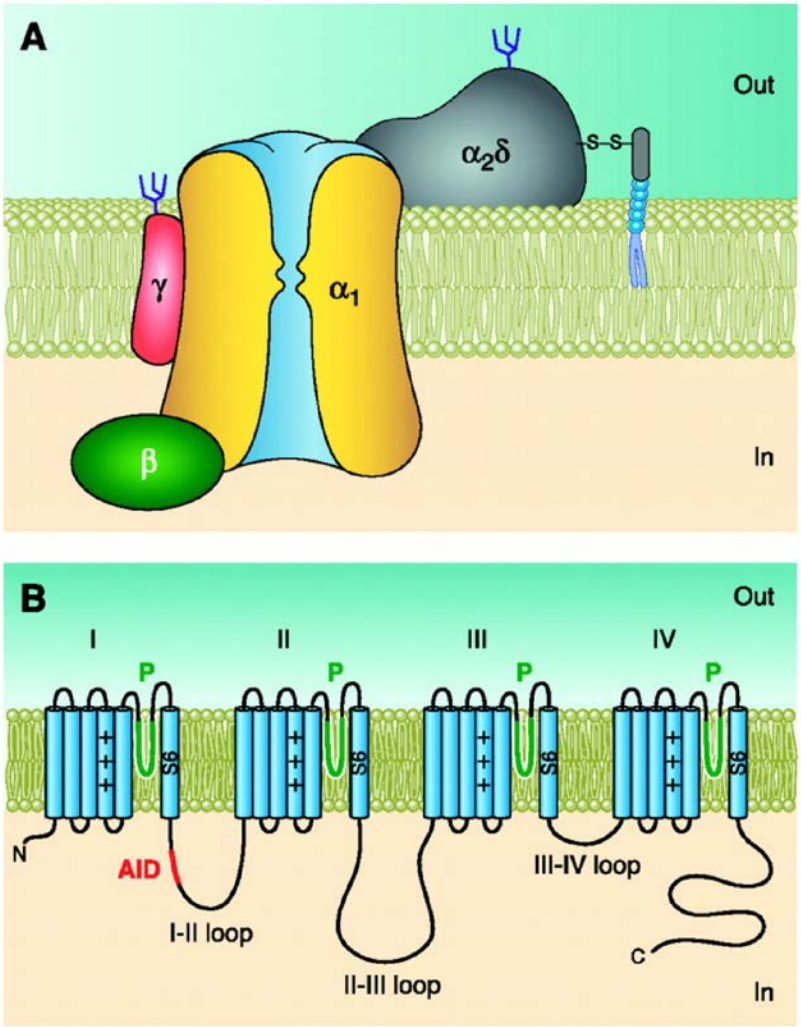

Figure 1.12. Structure of Ca_V1 Ca^{2+} channels.
(A) The Ca_V1 Ca^{2+} channels are composed of 5 subunits: α_1, α_2, β, δ and γ. The α_2 and δ subunits are linked by disulfide bonds into a single unit. The α_1 subunit forms the pore structure and is responsible for the channel's properties. The additional subunits regulate the location and activation of the $\alpha_1$subunit. **(B)** The α_1 subunit is composed of 4 motifs (I-IV) that consist of 6 transmembrane domains (S1-S6). The pore-forming (P) loop is located between S5 and S6. The positively charged (+) S4 domain makes up the channel's voltage sensor. The high-affinity β subunit interaction site or α interaction domain (AID) is located in the loop between motif I and II. Used from with Zafir Buraei and Jian Yang, Physiological Reviews, 2010, with permission from Am Physiol Soc.

the pore forming component responsible for the channel's unique properties while the $\alpha_2\delta$, β and γ subunits regulate the structure and activity of α_1 [239]. The α_1 subunit consists of four homologous repeated motifs (I-IV) each composed of six transmembrane segments (S1-S6) with a reentrant pore-forming loop (P-loop) between S5 and S6 (**Figure 1.12B**). The P-loop contains four highly conserved negatively charged amino acids responsible for selecting and conducting Ca^{2+} while the S6 segments form the inner pore [239]. The S4 segments are positively charged and constitute the voltage sensor. The pore opens and closes through voltage mediated movement of this sensor [246].

Ten mammalian α_1 genes subunits are divided into three subfamilies based on similarities in amino acid sequence. The Ca_V1 family contains L-type channels; the Ca_V2 family consists of N- P/Q-and R-type channels; and the Ca_V3 family are T-type channels (**Table 1.1**) [239]. Pharmacological and genetic studies have demonstrated the existence of Ca_V1 or L-type channels in T cells (**Table 1.2**) [190]. The Ca_V1 channels exist as four isoforms: $Ca_V1.1$, $Ca_V1.2$, $Ca_V1.3$, and $Ca_V1.4$. In excitable cells, L-type Ca^{2+} channels require high voltage activation and have slow current decay kinetics. They have a unique sensitivity to 1,4-dihydropyridines (DHPs), a wide drug class that can either activate (for example: Bay K 8644) or inhibit (for example: nifedipine) the activity of the channel [246]. Ca_V1 in T cells share elements of molecular structure and drug sensitivity in the classically defined L-type channel; however, the T cell channels are thought not to be gated by membrane depolarization [190].

Recently, in the Jefferies lab, analysis of $Ca_V1.4$ in T cells was performed [240, 241]. The $Ca_V1.4$ α_1 is encoded by the *CACNA1F* gene. This gene was originally cloned from human retina [247]. Here, $Ca_V1.4$ mediates Ca^{2+} entry into the photoreceptors promoting

Channel family	Current type	Contributing α_1 subunit
Ca_v1	L-type	α1.1, α1.2, α1.3, α1.4
Ca_v2	P/Q-type	α2.1
	N-type	α2.2
	R-type	α2.3
Ca_v3	T-type	α3.1, α3.2, α3.3

Table 1.1. Ca_V1 Ca^{2+} channel family members.
The Ca_V1 Ca^{2+} channel family consists of 3 members each with characteristic currents and corresponding α1 subunits that contribute the channels unique characteristics. Used from Zafir Buraei and Jian Yang, Physiological Reviews, 2010, with permission from Am Physiol Soc.

Ca_V subtype	Cell type and tissue distribution	Expression	Refs
$Ca_V1.1$	Human Jurkat T cell line	mRNA	[248]
	Mouse effector $CD8^+$ T cells	mRNA/Protein	[249]
	Mouse $CD4^+$ T cells	mRNA/Protein	[250]
$Ca_V1.2$	Human Jurkat T cell Line	mRNA	[251]
	Human peripheral blood T cells		
	Human Jurkat T cell line	mRNA/Protein	[244]
	MOLT-4 and CEM T cell lines		
	Mouse $CD8^+$ T cells	mRNA	[249]
	Mouse $CD4^+$ T cells	mRNA/Protein	[250]
$Ca_V1.3$	Human Jurkat T cell line	mRNA/Protein	[244]
	Mouse $CD8^+$ T cells	mRNA	[249]
	Human Jurkat T cell line		
$Ca_V1.4$	Human spleen		[240, 241]
	Human peripheral blood $CD4^+$/ $CD8^+$ T cells		
	Human spleen and thymus	mRNA/Protein	[251]
	Rat spleen and thymus		
	Mouse naïve $CD8^+$ T cells	mRNA/Protein	[249]
	Mouse $CD4^+$ T cells	mRNA	[250]
Ca_V1	Mouse 2G12.1 T cell hybridoma	mRNA	[242]
(unspecified)	Mouse $CD4^+$ Th2 cells	mRNA	[252]

Table 1.2. Ca_V1 Ca^{2+} channels identified in T cells.
T cell specific Ca_V1 Ca^{2+} channel expression has been demonstrated through analysis of mRNA and protein in various rat, mouse and human cell lines and primary tissue and cell populations. Adapted from Trends Pharmacol Sci, 27/7, Kotturi, M. F.Hunt, S. V., Jefferies, W. A. Roles of CRAC and Cav-like channels in T cells: more than one gatekeeper?, 360-7., Copyright (2006), with permission from Elsevier.

tonic neurotransmitter release [253]. Kotturi *et al.* identified the $Ca_V1.4$ α_1 subunit mRNA and protein in Jurkat T cells as well as in human peripheral blood T cells [240, 241]. Pharmaceutical analysis was further performed to demonstrate the contribution of L-type Ca^{2+} channels to T cells Ca^{2+} signalling [240]. Treatment of Jurkat T cells and human peripheral blood T cells with the DHP agonist Bay K 8644 increased intracellular Ca^{2+} and induced ERK 1/2 phosphorylation while treatment with the DHP antagonist nifedipine blocked Ca^{2+} influx, ERK 1/2 phosphorylation, NFAT activation and IL-2 production. In addition, nifedipine blocked T cell proliferation [240]. Sequence analysis revealed that the $Ca_V1.4$ expressed in T cells exists as two novel splice variants (termed $Ca_V1.4a$ and $Ca_V1.4b$) distinct from the retina [241]. $Ca_V1.4a$ lacks exons 31, 32, 33, 34 and 37 which results in a deletion of transmembrane segments S3, S4, S5 and half of S6 in motif IV (**Figure 1.13A,B**). As a result, the voltage sensor domain and part of the DHP binding site and EF-hand Ca^{2+} binding motif are deleted from the channel. Removal of the voltage sensor may alter the voltage-gated activation of this channel. Instead, gating in T cells may be through alternate mechanisms such as ER store-depletion or TCR signalling [254]. Partial deletion of the DHP binding site may decrease the sensitivity of T cell-specific $Ca_V1.4$ channels providing an explanation why large doses of DHP antagonists are required to completely block Ca^{2+} influx through Ca_V channels in T cells [255]. Furthermore, the splice event caused a frameshift that changed the carboxy-terminus to a sequence that resembles (40% identity) the $Ca_V1.1$ channel found in skeletal muscle [241]. The second splice variant, $Ca_V1.4b$, lacks exons 32 and 36 causing a deletion of the extracellular loop between S3 and S4 in motif IV (**Figure 1.13C,D**). The voltage sensing motif is not spliced out; however, it has been proposed that removal of

$Ca_V1.4a$ Precursor Pre-mRNA (Motif IV)

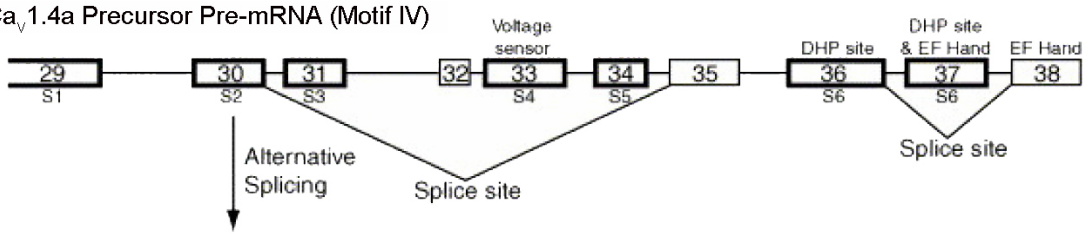

$Ca_V1.4a$ Mature mRNA (Motif IV)

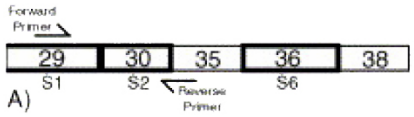

$Ca_V1.4a$ Protein

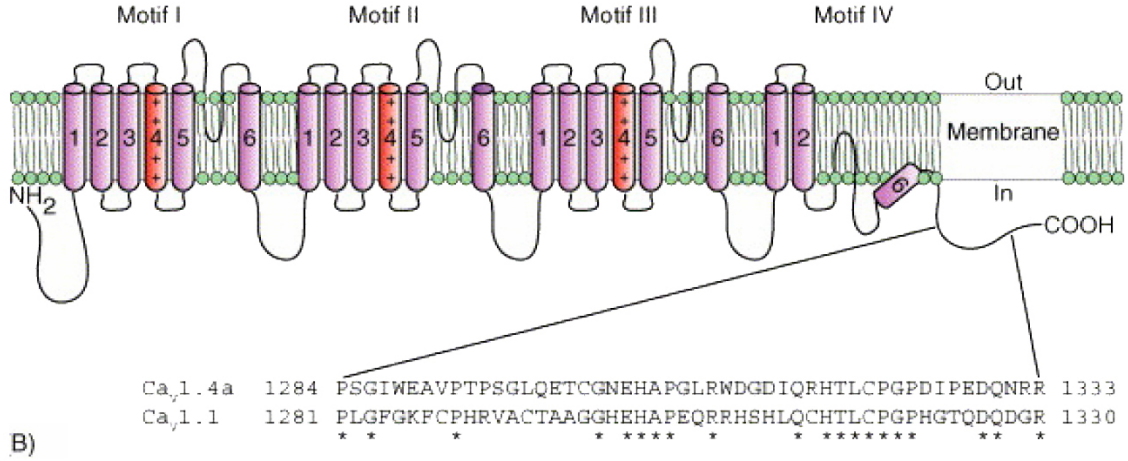

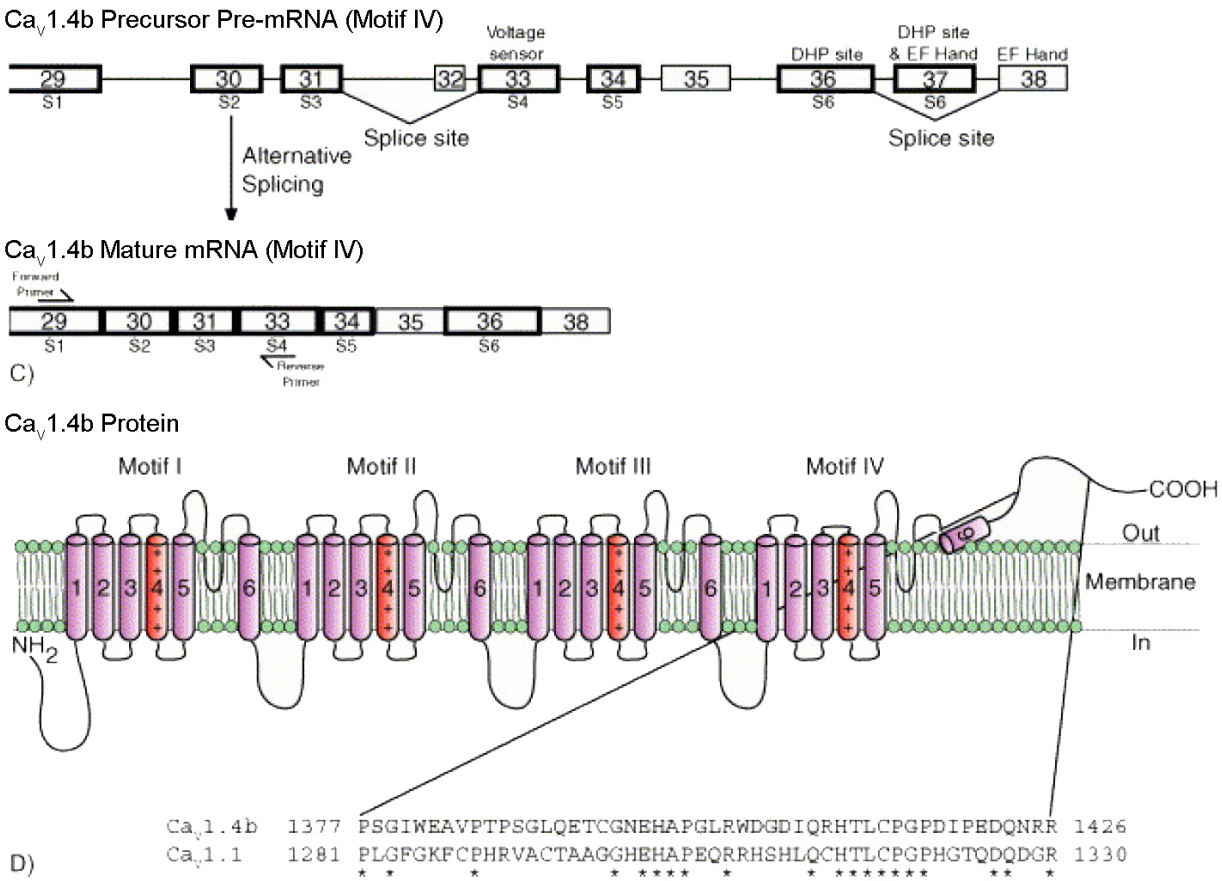

Figure 1.13. Ca$_V$1.4 mRNA splice sites and putative protein topology.
(A) Ca$_V$1.4a mRNA is alternatively spliced eliminating exons 31–34 and 37. This leads to the deletion of exons in Motif IV that encode S3, S4, S5 and half of S6. **(B)** The putative Ca$_V$1.4a channel topology is shown. **(C)** Ca$_V$1.4b mRNA is alternatively spliced eliminating exons 32 and 37. This leads to the deletion of a portion of motif IV that encodes the extracellular loop linking segments S3 and S4 and half of the transmembrane segment S6, respectively. **(D)** The putative Ca$_V$1.4b channel topology is shown. Bolded boxes represent exons encoding transmembrane segments. The segment number is written below the respective box. Lines connecting exon boxes represent introns. Transmembrane segments are purple except for the S4 voltage sensor domain which is red. Reprinted from Mol Immunol., 42/12, MF Kotturi and WA Jefferies. Molecular characterization of L-type calcium channel splice variants expressed in human T lymphocytes, 1461-74, Copyright (2005), with permission from Elsevier.

the extracellular loop may alter the voltage sensing function of this channel [241]. Upon membrane depolarization, the S4 voltage sensor domain moves and this splicing event may leave the domain in a conformation that prevents S4 movement [256, 257]. Like $Ca_V1.4a$, the carboxy-terminus of $Ca_V1.4b$ also shares 40% amino acid identity with the $Ca_V1.1$ due to a frameshift. In addition, an early stop codon prematurely truncates the channel [241].

Although the expression of Ca_V1 channels in T cells has been established, the functional role they play is less clear. Recently, the regulatory β subunits that mediate Ca_V channel assembly, plasma membrane targeting and activation were assessed in T cells [239]. The β3 and β4 family members have been shown to be expressed in $CD4^+$ T cells. Upon TCR cross-linking $CD4^+$ T cells from β3 or β4-deficient mice showed impaired Ca^{2+} influx, NFAT nuclear translocation and cytokine secretion [250]. Cav1.1 expression was found to be reduced in the β4-deficient T cells providing a possible role for Ca_V1 in lymphocyte function [250]. β3-deficiency has also been analyzed in $CD8^+$ T cell populations [249]. $\beta 3^{-/-}$ mice have reduced numbers of $CD8^+$ T cells possibly due to increased spontaneous apoptosis induced by higher expression of Fas. Upon activation, these $CD8^+$ T cells have decreased Ca^{2+} entry, proliferation and NFAT nuclear translocation. β3 was found to associate with $Ca_V1.4$ and several TCR signalling proteins suggesting its role in TCR gated Ca^{2+} signalling [249]. Ca_V1 channels have also been suggested to play a role in survival [254]. $Ca_V1.2$ expressed in mast cells has been reported to protect against antigen-induced cell death by maintaining mitochondria integrity and inhibiting the mitochondrial cell death pathway [258]. It has been proposed that Ca^{2+} influx through $Ca_V1.2$ at the plasma membrane is important for maintenance of

the mitochondrial Ca^{2+} concentration $[Ca^{2+}]_m$ thereby providing the cell with prosurvival signals [254]. Although Ca_V1 function is vital for T cell Ca^{2+} signalling, the exact function they play is still unclear. Further work is required to clarify the role each Ca^{2+} channel family plays in shaping the Ca^{2+} signal.

1.3.1.2.2 Downstream effects of calcium

The sustained entry of Ca^{2+} into the cell results in the activation of signalling molecules and transcription factors that induce expression of genes required for T cell activation, proliferation, differentiation and effector function [191, 259]. In T cells, Ca^{2+} can activate a variety of targets including the serine/threonine phosphatase calcineruin and its transcription factor target NFAT, Ca^{2+}-calmodulin-dependent kinase (CaMK) and its target cyclic AMP-responsive element-binding protein (CREB), myocyte enhancer factor 2 (MEF2) targeted by both calcineruin and CaMK, and NFκB [189, 259].

The best studied downstream effect of Ca^{2+} is the calcineruin- NFAT pathway [189, 259]. Increased Ca^{2+} levels promote the binding of Ca^{2+} to calmodulin inducing a conformation change that allows calmodulin to bind and activate the serine/threonine phosphatase calcineurin [259]. Calcineurin dephosphorylates serines in the amino-terminus of NFAT exposing a nuclear localization signal. This results in the transport of NFAT into the nucleus. Here, NFAT can interact with other transcription factors, integrating signalling pathways and inducing gene expression patterns dependent on the context of the TCR signalling [176]. In particular, NFAT can complex with AP-1 induced through Ras signalling (see below) to initiate transcription of genes such as IL-2 important for T cell activation [260]. NFAT can also interact with FOXP3 in Treg cells

and has been shown to cooperate with STAT proteins to induce Th1 or Th2 differentiation through T-bet or GATA3 transcription factor expression [259]. NFAT-dependent transcription appears to be highly dependent on sustained Ca^{2+} levels [189]. A drop in intracellular Ca^{2+} levels immediately results in NFAT rephosphorylation by NFAT kinases such as glycogen synthase kinase 3 (GSK3), casein kinase 1 (Ck1) and dual specificity tyrosine-phosphorylation regulated kinase 1A (DYRK1A) [261-263]. This masks the nuclear localization signal leading to export of NFAT from the nucleus and termination of NFAT-dependent transcription. The importance of Ca^{2+}/NFAT signalling is emphasized in studies using T cells treated with pharmaceutical inhibitors of calcineurin or using T cells with genetic defects in Ca^{2+} influx. These studies showed impaired expression of cytokines as well as hundreds of other genes [222, 264-266]

Ca^{2+} influx can also activate the kinase, CaMK. In T cells, two CaMK family members, CaMKII and CaMKIV have been shown to function in TCR signalling. [267]. CaMKII acts to inhibit TCR signalling through a mechanism that has yet to be completely defined. It has been proposed that CaMKII may function to compete against calcineurin by phosphorylating NFAT. [268]. Alternatively, CaMKII may directly phosphorylate calcineurin inhibiting its activity [267]. On the other hand, CaMKIV functions as a positive regulator of TCR signalling. CaMKIV is thought to function by phosphorylating the transcription factor CREB. CREB in turn induces expression of immediate early genes including *Jun* and *Fos*, which cooperate with NFAT to drive expression of genes important for activation such as IL-2 [269].

The transcription factor Mef2, has also been identified to play a role in Ca^{2+} signalling. Binding sites for Mef2 are located in the promoter regions of several cytokines

including IL-2. In an unstimulated state, Mef2 is constitutively bound to these sites and interacts with Cabin1 along with its associated class I histone deacetylases (HDACs) and a histone methyltransferase or class II HDACs forming a complex that functions to silence promoter activity [270, 271]. Upon an increase in intracellular Ca^{2+}, a nuclear subset of calmodulin becomes activated and binds Cabin1 and class II HDACs inducing them to disassociate from Mef2 [272, 273]. The transcriptional coactivator p300 can then bind Mef2 allowing cytokine expression [272, 273]. Additionally, in the presence of increased Ca^{2+}, HDACs associated with Mef2 may directly bind calmodulin and be induced to dissociate from Mef2. Alternatively, HDACs and Cabin1 may be directly phosphorylated by CaMK and other kinases inducing dissociation from Mef2 [267, 274]. To increase the transactivation function of Mef2 and induce robust gene expression, additional transcription factors are also recruited. Through Ca^{2+}-induced calcineurin activation, NFAT enters the nucleus and binds to the Mef2-p300 complex increasing stabilization and upregulating transcription [267].

NFκB activation has also been shown to depend on Ca^{2+} levels [275]. Studies using pharmaceuticals to inhibit calcineurin activity have reported an inhibition of NFκB activation [276-280]. In addition, SKF96365, a chemical inhibitor of Ca^{2+} channels blocking Ca^{2+} entry into T cells leads to reduced NFκB activity [280]. It has been proposed that calcineurin might function to dephosphorylate inhibitor of NF-κB (IκB) at its PEST domain promoting its instability and degradation. IκB is found associated with NF-κB localizing in the cytosol. Upon IκB degradation, NFκB is released and can enter the nucleus to activate gene transcription [281].

Taken together, Ca^{2+} plays a vital role in many aspects of T cells signalling through the TCR receptor. It is clear that the TCR signal transduction pathways are not linear but function as an intricate network with extensive cross-talk between Ca^{2+} signal transducers.

1.3.1.3 DAG-mediated signalling

DAG production leads to the recruitment of cellular proteins and the propagation of the TCR signalling pathway (**Figure 1.14**) [282]. One protein recruited to the membrane is the GTP-exchange factor (GEF), Ras guanyl nucleotide-releasing protein (RasGRP). Here, RasGRP can activate Ras by inducing the release of GDP and the binding of GTP [282]. A second GEF, son of sevenless (SOS), is also expressed in T cells. SOS is associated with GRB2 and is recruited to the TCR signalling complex through this adaptor protein [176]. RasGRP and SOS have been proposed to function together for Ras activation. In a positive feedback mechanism, RasGFP created by RasGRP catalyzes SOS activity, increases Ras activation and amplifies the TCR signal [283]. Ras is required for the activation of Raf-1, a MAPK kinase kinase (MAPKKK), that in turn activates the MAPK kinase (MAPKK) and then the MAPK, extracellular signal-regulated kinase (ERK) 1 and 2 [176]. Activated ERK can phosphorylate a transcription factor Elk-1 leading to the transcription of Fos. Fos combines with Jun to form the transcription factor, activator protein-1 (AP-1), to induce gene expression required for proliferation and differentiation [284]. ERK can also target and activate STAT3 that contributes to increased transcriptional activity [284].

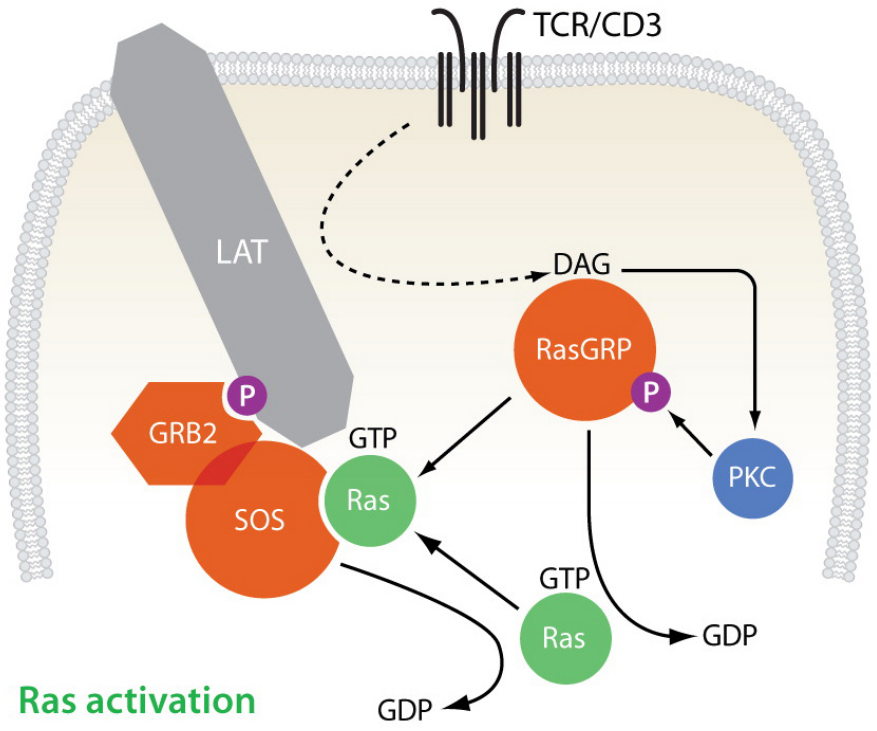

Figure 1.14. TCR-induced Ras activation.
DAG produced by TCR engagement recruits RasGRP to the membrane where it is phosphorylated and activated by PKC. RasGRP induces Ras to exchange GDP for GTP and so become activated. RasGTP can then bind SOS catalyzing its GEF activity and increasing Ras activity and the propagation of the TCR signal. Used with permission of ANNUAL REVIEWS, INC., from T Cell Activation, Jennifer E. Smith-Garvin, Gary A. Koretzky, Martha S. Jordan, 27, 2009; permission conveyed through Copyright Clearance Center, Inc.

Ca^{2+} has been proposed to regulate the Ras/MAPK pathway in T cells [260]. RasGRP that activates Ras activity not only has a DAG binding domain but also has a pair of EF hand motifs that can directly bind Ca^{2+} [285]. Through this interaction, Ca^{2+} and DAG can control activation and membrane localization of RasGRP. One model proposes that upon weak TCR stimulation, cytosolic Ca^{2+} and DAG is generated slowly resulting in the localization of RasGRP to the DAG-rich Golgi membrane [286]. However, strong TCR signalling results in a robust rise in intracellular Ca^{2+} leading to the generation of large quantities of DAG at the plasma membrane allowing RasGRP recruitment to this location [286]. The site of activation may play a role in what ERK can target downstream thereby contributing to differential signalling dependent on the stimulus [286]. Ca^{2+} also contributes to ERK/MAPK deactivation. Ras is inactivated by GTPase activating proteins (GAPs) including CAPRI (Ca^{2+}-promoted Ras inactivator). CAPRI is recruited to the plasma membrane and activated in a calcium dependent manner, reducing RasGTP levels and subsequent signalling through the ERK/MAPK pathway [285].

DAG production also recruits PKCθ to the plasma membrane to initiate a pathway leading to NF-κB activation. At the membrane, PKCθ phosphorylates a scaffold protein called CARMA1 (caspase recruitment domain and membrane-associated guanylate kinase-containing scaffold protein), which subsequently binds two proteins, Bcl10 and MALT1 (mucosa-associated lymphoid tissue lymphoma translocation gene 1) [176]. This membrane bound complex can activate IκB kinase (IKK) that phosphorylates IκB. IκB is found associated with NF-κB in the cytosol; however upon phosphorylation, IκB becomes ubiquitinated and degraded allowing NF-kB to translocate to the nucleus to

stimulate transcription of genes involved in T cell survival, effector function and homeostasis [176].

1.3.2 T cell homeostasis

The maintenance of the peripheral T cell pool occurs through complex homeostatic mechanisms [174]. The major T cell homeostatic signals are through the TCR and interleukin-7 receptor (IL-7R) (**Figure 1.15**) [172]. Naïve T cells emerge from the thymus after under going a series of developmental and selection processes. Positive selection ensures that T cells can receive signals through their T cell receptor (TCR) when low affinity contact occurs with self peptide-MHC. On the other hand, T cells with high affinity for self peptide-MHC will be deleted through negative selection [287]. Therefore, peripheral T cells will not become activated through self peptide-MHC interaction. Instead, contact with a diverse repertoire of self peptide-MHC provides survival signals [174]. Despite the requirement of TCR signalling, the exact intracellular survival signalling pathway remains unclear.

IL-7 also plays an essential role in naïve T cell survival. This was demonstrated in several studies where naïve T cell survival was impaired when contact with IL-7 was blocked either by injection of an IL-7 monoclonal antibody or adoptive transfer of T cells into an IL-7 deficient host [288-291]. Furthermore, overexpression of IL-7 in a murine model was shown to increase the naïve T cell pool [292, 293]. IL-7 signals through the IL-7R composed of two chains: a unique α chain, CD127 and a common cytokine receptor γ chain, CD132. IL-7R signalling is mediated through the Janus kinase signal transducer and activator of transcription (JAK-STAT) signalling pathway [174]. Binding

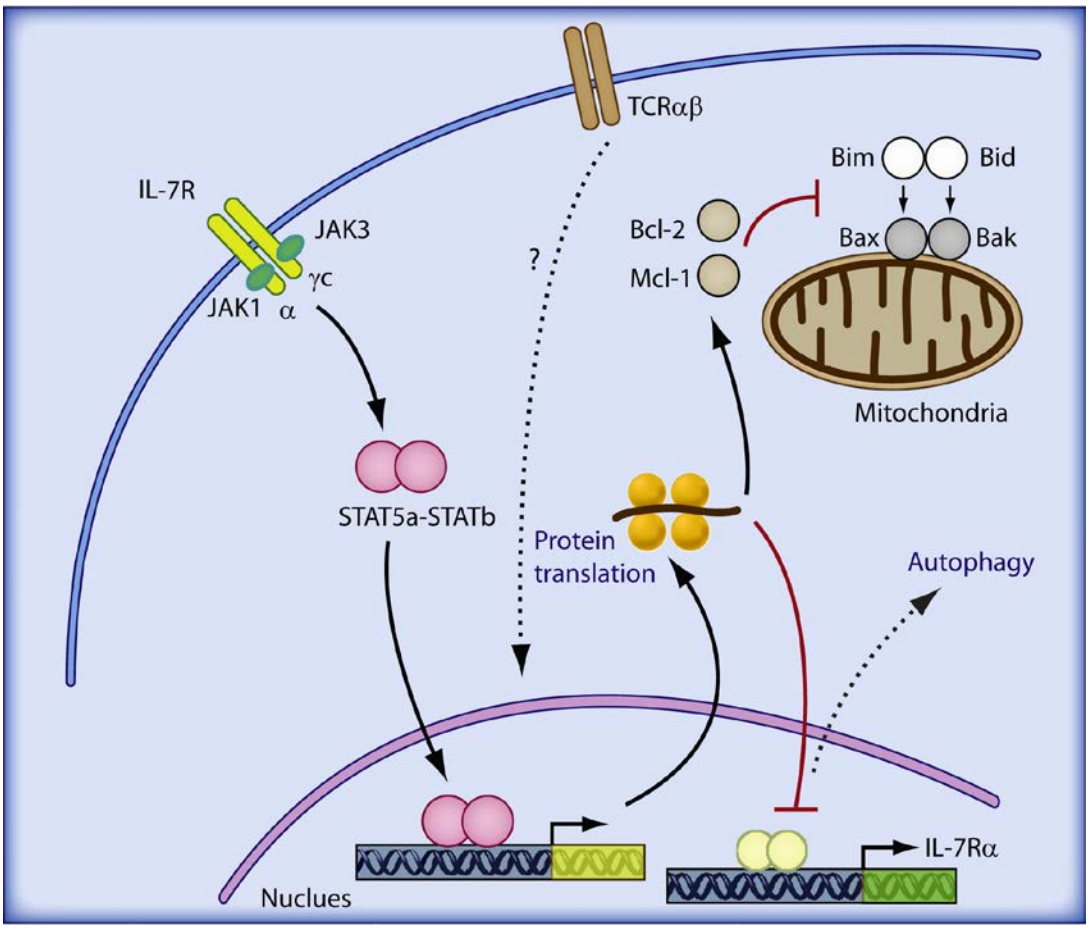

Figure 1.15. Naïve T cell survival signalling.
For survival, naïve T cells require signals generated when IL-7R binds IL-7 and TCRαβ contacts self-peptide/MHC. The exact details of TCR signalling in homeostasis are not yet clear. IL-7R signalling involves activation of receptor-bound JAK1/3, which in turn activates the STAT5a/b dimer. The result is initiation of synthesis of several anti-apoptotic factors proteins including BCL-2 and MCL1 and subsequent inhibition of various pro-apoptotic factors such as BAD, BAK, BAX, BIM and BAD. Adapted from Immunity, 29/6, Charles D. Surh and Jonathan Sprent, Homeostasis of Naive and Memory T Cells, 848-862, Copyright (2008), with permission from Elsevier.

of IL-7 activates JAK1 and JAK3, which are associated with CD127 and CD132, respectively. Activated JAK1/3 phosphorylates the IL-7 receptor recruiting STAT5a/b that in turn becomes phosphorylated. STAT5a/b subsequently dimerize and then can enter the nucleus to regulate gene transcription [174]. In response to IL-7R signalling the expression of the anti-apoptotic factors B cell lymphoma 2 (BCL-2) and myeloid cell leukemia sequence 1 (MCL1) are induced. BCL-2 and MCL1 are thought to block the death effector activity of Bcl-2–associated X protein (BAX) and Bcl-2 homologous antagonist/killer (BAK) that induce apoptosis by causing release of cytochrome c and other pro-apoptotic factors that induce the caspase pathway [174]. In addition, the activity of the pro-apoptotic proteins BH3-interacting domain death agonist (BID), BCL-2 interacting mediator of cell death (BIM) and BCL-2 antagonist of cell death (BAD) is inhibited [174]. In this way, IL-7 supports naïve T cell survival by preventing induction of apoptosis.

1.4 Specific aims

1.4.1 Dendritic cells

1.4.1.1 CD74 and cross presentation in DCs

To initiate an effective immune response against an invading pathogen, DCs must be able to cross prime naïve T cells. For cross presentation to occur, exogenous antigen and MHC I must localize to the same phagolysosomal or endolysosomal compartment. Previously, the Jefferies lab has shown that cell surface MHC I can enter such a compartment and this is mediated by a conserved tyrosine motif in the cytoplasmic tail

[59, 65]. Alternatively, newly synthesized MHC I may traffic straight from the ER directed by the chaperone protein, CD74. The first portion of my thesis will address the role of CD74 in MHC trafficking and cross presentation *in vivo*. These observations define a new model of MHC I antigen presentation and highlight the significance of the endolysosome as the organelle for cross presentation in DCs.

1.4.1.2 HIV-Nef immune evasion in DCs

Given the critical role that cross presentation plays in the generation of immune responses, it is understandable that viruses would employ mechanisms to interfere with its function. HIV can infect DCs and is in a position to disrupt important antigen presentation pathways [117]. Nef, a protein expressed early in the HIV replication cycle, has been shown to interfere with MHC I trafficking causing a downregulation of surface expression; however, the impact of this on DC antigen presentation has not been sufficiently assessed [136, 294]. The second portion of this thesis examines the impact of Nef-mediated disruption of MHC I trafficking in DCs with particular focus on the impact of Nef on the cross presentation pathway. DC cross priming is essential for activation of immune responses against HIV and secondary infections that are fatal to HIV-infected individuals. HIV's potential to infect and impair this pathway could potentially be a factor leading to immunosuppressive characteristic of AIDS.

1.4.2 T cells

1.4.2.1 $Ca_V1.4$ channels in T cells

In order for DCs to initiate immune response, naïve T cells need to be present and poised to interact with the cross presenting DCs [172]. One key signal regulating naïve T cell homeostasis is through the TCR [174]. The TCR can initiate several signalling pathways through various second messengers including Ca^{2+} ions. In lymphocytes, Ca^{2+} signals serve to regulate cell activation, proliferation, differentiation and apoptosis [188, 189]. Previously in the lab, the existence of an L-type Ca^{2+} channel, $Ca_V1.4$, in T cells was demonstrated [240, 241]. However, the function of $Ca_V1.4$ in T cell biology remains unclear [188, 189]. The final section of this thesis investigates the physiological role $Ca_V1.4$ plays in T cell homeostasis. Collectively, this study provides a new framework for the function of L-type channel in the storage of intracellular Ca^{2+} within T cells and in operative Ca^{2+} regulation of antigen receptor-mediated signal transduction.

CHAPTER 2. MATERIALS AND METHODS

2.1 *In vitro* studies

2.1.1 Cell lines and culture conditions

The DC2.4 [295], B3Z cells (a T cell hybridoma expressing a TCR recognizing $OVA_{257-264}$ in the context of H-$2K^b$ with a beta-galactosidase reporter driven by NFAT elements from the IL-2 promoter) [296] and RMA-S cells were maintained in completed RPMI (Roswell Park Memorial Institute) 1640 medium (Invitrogen) supplemented with 10% fetal bovine serum (FBS) (Invitrogen), 2 mM L-glutamine, 20 mM 4-(2-hydroxyethyl)piperazine-1-ethanesulfonic acid (HEPES), 1 mM sodium pyruvate, 0.1 mM nonessential amino acids (NEAA) and 5 x 10^{-5} M 2-mercaptoethanol.

2.1.2 Molecular biology

2.1.2.1 Cloning of Nef pMX-pie

The coding sequence of *nef* (Accession number: AF324493) was amplified by PCR from the pNLV102 vector [297] with BamHI containing sense primer (5'GATCGAGGGATCCCCTCCTGGAACGCCC3') and EcoRI containing anti-sense primer (5'GATCGAGGAATTCGCAACATACCTACAA3'). The PCR reaction was conducted with Platinum Pfx DNA Polymerase (Invitrogen) in the Whatman Biometra UnoII Thermocycler using the following conditions: 94°C for 2 min; 94°C for 15 sec, 55°C for 30 sec, 68°C for 45 sec for 35 cycles; 68°C for 10 min. The PCR fragment was

resolved on a 1% agarose gel and visualized by SYBRSafe (Invitrogen) staining. The fragment was gel purified using the Qiaex II Purification Kit (Qiagen). The *nef* fragment and pMX-pie vector (**Figure 2.1**) were digested with BamHI and EcoRI restriction enzymes (Invitrogen) at 37°C for 3 hours and the digestion products were resolved on a 1% agarose gel with SYBRSafe (Invitrogen). The digested *nef* fragment and pMX-pie vector were gel purified using the Qiaex II Purification Kit (Qiagen) and incubated in a 1:5 (vector: insert) ratio with T4 DNA ligase (Invitrogen) at room temperature for 1 hr. Correct insertion of the *nef* sequence into the pMX-pie vector was confirmed by sequencing (NAPS, UBC).

2.1.2.2 Cell transfection

DC2.4 (5 x 10^6) cells were combined in a 4-mm diameter electroporation cuvette with 30 μg of DNA in 0.7 ml of Opti-MEM media (Invitrogen). The mixture was incubated on ice for 10 min then electroporated at 280 V and 950 μF. The mixture was incubated on ice for another 5 min then at room temperature for 5 min. The cells were transferred to 24-well plates in RPMI completed media. After 24 hours, the media was supplemented with 20 μg/ml of puromycin (Calbiochem). Following selection with puromycin, cells were sorted for GFP expression in bulk by FACS (BD FACSVantage). The stably transfected cell cultures were maintained in RPMI completed media with 10 μg/ml puromycin (Calbiochem).

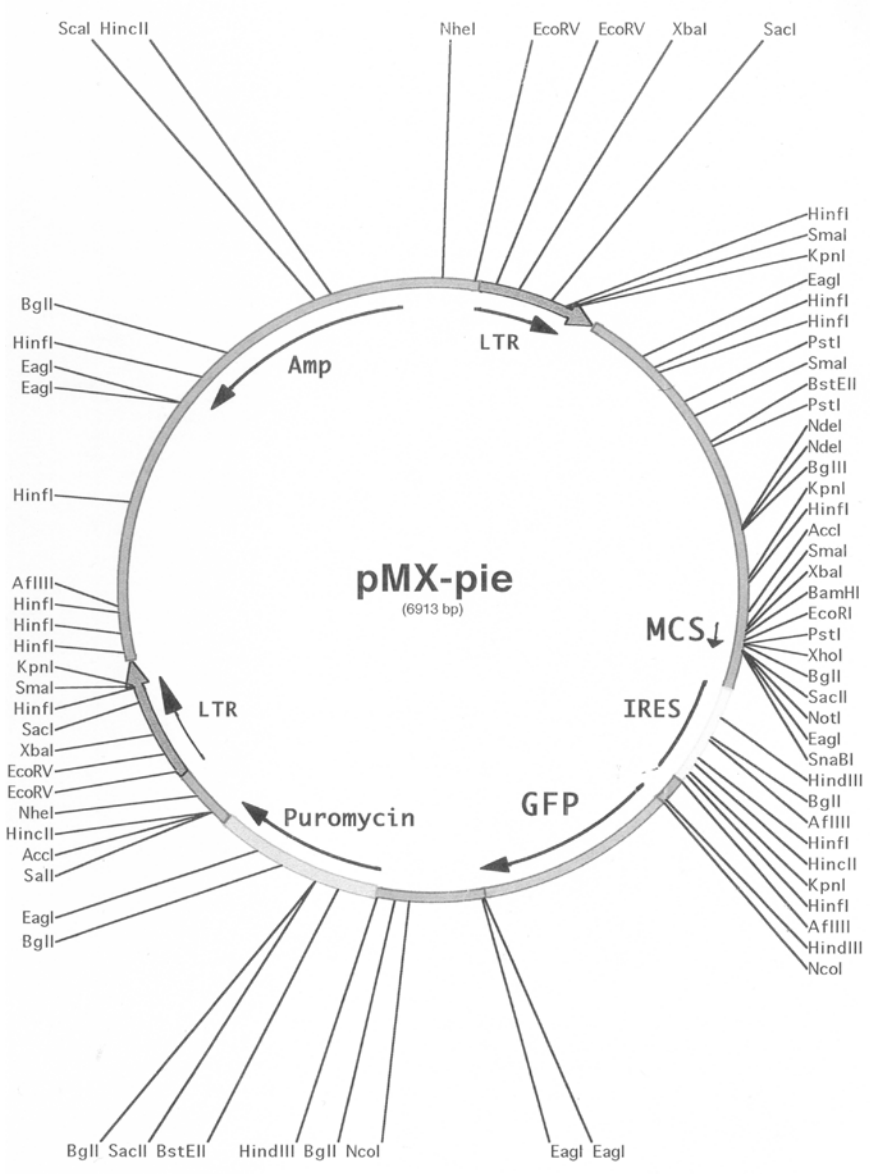

Figure 2.1. The pMX-pie vector map.
The pMX-pie vector contains a long terminal repeat (LTR) promoter, a multiple cloning site (MCS) followed by an internal ribosomal entry site (IRES) linked to the GFP coding sequence. The Nef sequence was ligated into the MCS through BamHI and EcoRI restriction enzyme sites. The pMX-pie vector contains the drug-resistant genes, ampicillin (Amp) for bacterial selection and puromycin for selection in mammalian cells.

2.1.2.3 RNA isolation and cDNA generation

RNA was isolated from cell lines or single-cell suspensions prepared from tissue samples. RNA was isolated from 5-10 x 10^6 cells using Trizol reagent (Invitrogen) according to manufacturer's directions. Contaminating DNA was removed from RNA preparations by digestion with 1 unit of RNA-free DNAse I (Fermentas) per 1 μg of RNA for 30 min at 37°C. The digestion was inactivated by incubation at 65°C for 10 min with 1μl of 50mM EDTA per unit of DNase I. cDNA was synthesized from 1 μg of digested RNA using the RevertAid First Strand cDNA Synthesis Kit (Fermentas). This cDNA was used as a template in PCR reactions with Taq DNA Polymerase (Fermentas) using the Whatman Biometra UnoII Thermocycler. PCR fragments were resolved on a 1% agarose gel and visualized by SYBRSafe (Invitrogen) staining.

2.1.2.4 PCR

Nef was detected by amplification of a 500 bp sequence with sense primer: NefF2 (5'TGATTGGATGGCCTGCTGTAA3') and anti-sense primer: NefR2 (5'TCTTGAAG TACTCCGGATGCA). The primer design was based on the n*ef* published sequence (Genbank accession number AB023804). PCR reactions were conducted with conditions as follows: 94°C for 5 min; 94°C for 30 sec, 56°C for 30 sec, 72°C for 30 sec for 35 cycles; 72°C for 10 min. The PCR product was sequenced at NAPS DNA Sequencing Facility of UBC.

CD4 expression was detected by amplification of a 553 bp sequence with sense primer: mouse CD4 Set 2 Forward (5'TTCAAAGTGACCTTCAGTCCGGGT3') and anti-sense primer: mouse CD4 Set 2 Reverse (5'TGATGCAGTGTCCCTTTGTCCA

GA3'). PCR reactions were conducted with the following conditions: 94°C for 5 min; 94°C for 30 sec, 60°C for 30 sec, 72°C for 30 sec for 35 cycles; 72°C for 10 min.

To detect *Cav1.4* in tissues an initial PCR was performed with sense primer (5′-CAT ACTGGAGGAAAGCCAGGA -3′) and anti-sense primer (5′-TGGAGTGTGTGGAGC GAGTAGA-3′). PCR reactions were conducted with the following conditions: 94°C for 5 min; 94°C for 60 sec, 55.5°C for 30 sec, 72°C for 30 sec for 28 cycles; 72°C for 2 min. A subsequent nested PCR reaction amplified a 324 bp fragment with sense primer (5′-GAC GAATGCACAAGACATGC-3′) and anti-sense primer (5′-CAAGCACAAGGTTGAGG ACA-3′). PCR reactions were conducted with the following conditions: 94°C for 5 min; 94°C for 60 sec, 55.5°C for 30 sec, 72°C for 30 sec for 28 cycles; 72°C for 2 min. The PCR product was subcloned into pCR2.1-TOPO vector (Invitrogen) and sequenced using the m13R primer at NAPS DNA Sequencing Facility of UBC. To detect the Cav1.4 mutated mRNA the first round PCR was performed with sense primer (5'-CATACTGGAGGAAAGCCAGGA-3') and anti-sense primer (5'CGTCCCTCTTCAG CAAGAGAA-3'). PCR reactions were conducted with the following conditions: 94°C for 5 min; 94°C for 30 sec, 56°C for 30 sec, 72°C for 30 sec for 26 cycles; 72°C for 2 min. A second nested PCR with sense primer (5'-GCCCATAACTTCGTATAA TGTATGC-3') and anti-sense primer (5'-CAAGCACAAGGTTGAGGACA-3') was performed to amplify the mutation cassette that introduces a premature stop codon in exon 7 of $Ca_V1.4$ mutated mRNA. PCR reactions were conducted with the following conditions: 94°C for 5 min; 94°C for 60 sec, 54°C for 30 sec, 72°C for 30 sec for 30 cycles; 72°C for 2 min.

S15 was amplified as a positive control for template DNA integrity. A 361bp fragment was amplified using the sense primer (5'-TTCCGCAAGTTCACCTACC-3') and the anti-sense primer (5'-CGGGCCGGC CATGCTTTACG-3'). PCR reactions were conducted with conditions as follows: 94°C for 5 min; 94°C for 30 sec, 56°C for 30 sec, 72°C for 30 sec for 35 cycles; 72°C for 10 min.

2.1.3 Protein analysis

2.1.3.1 Western blot

Primary antibodies used for Western blotting are as follows: rat anti-CD74 antibody (In-1, Fitzgerald), mouse anti-MHC Class I antibody (KH95; Santa Cruz Biotechnology), sheep anti-Nef polyclonal antibody (a kind gift from Victor Garcia, University of Texas Southwestern Medical Center; Dallas, Texas), rabbit anti-$Ca_V1.4$ polyclonal antibody (provided by Dr. John McRory), rabbit anti Phospho-p44/p42 MAPK antibody (9101, Cell Signalling), rabbit anti-ERK2 antibody (sc-154, Santa Cruz Biotechnology), rabbit anti Phospho-SAPK/JNK antibody (9251, Cell Signalling), rabbit anti-SAPK/JNK antibody (9252, Cell Signalling), mouse anti-p21Ras antibody (RAS10; Upstate Biotechnology), using mouse anti-NFATc1 (7A6, Thermo Scientific) antibody, mouse anti-GAPDH (MAB374, Chemicon), mouse anti-HDAC1 (10E2, Santa Cruz). To visualize primary antibody binding the following secondary antibodies were used: goat anti-rat IgG antibody conjugated to Alexa-680, goat anti-sheep IgG antibody conjugated to Alexa-680, goat anti-rabbit IgG antibody conjugated to Alexa-680 (Invitrogen); goat anti-mouse IgG antibody conjugated to Alexa-680, goat anti-mouse IgG antibody conjugated to IRDye-800CW (LI-COR Biosciences).

Cell lines or single-cell suspensions derived from tissue samples were lysed in RIPA buffer (10mM phosphate buffer pH7.2, 150mM NaCl, 1% NP-40, 1% sodium deoxycholate, 0.1% SDS, 0.2mM EDTA) containing a protease inhibitor cocktail (Roche) for 30 minutes on ice. The protein levels in the samples were quantified using the BCA Protein Assay according to the manufacturer's directions (Pierce). Equalized amounts of protein for each sample were mixed with 5x sample buffer (250mM Tris pH6.8, 0.02% bromphenol blue, 50% glycerol, 10% SDS, 25% β-mercaptoethanol) and boiled for 5 minutes. The samples were separated by SDS- polyacrylamide gel electrophoresis (PAGE) (10-12% separating/5% stacking). Proteins were transferred to a nitrocellulose membrane by wet transfer for 1 hour and 20 minutes at 70 Volts. The membrane was subsequently blocked with Odyssey Blocking Buffer (LI-COR Biosciences) for 1 hour at room temperature. The blots were probed with primary antibody overnight at 4°C. The blots were washed 3 times with TBS-T (Tris buffered PBS + 0.1% Triton-X) then probed for 1 hour with corresponding secondary antibody. After 3 washes with TBS-T, the blots were visualized using the Odyssey Infrared Imaging (LI-COR Biosciences). Signal intensities were quantified using the Odyssey software

2.1.3.2 Immunoprecipitation

Bone marrow derived dendritic cells (BmDCs) or single cell suspension prepared from tissue samples (prepared as described in Section 2.2.4) were lysed in 0.5% Nonidet P-40 (NP-40) buffer (120 mM NaCl, 4 mM $MgCl_2$, 20mM Tris-HCl pH 7.6) containing a protease inhibitor cocktail (Roche) and 40 μg/mL PMSF. Protein levels in the samples were quantified using the BCA Protein Assay according to the manufacturer's directions

(Pierce). Samples normalized for protein concentration were precleared overnight with normal rabbit serum and Protein A-sepharose (Pharmacia). Immunoprecipitation with anti-I-A/I-E antibody (M5/114.15.2, Becton Dickinson), anti-H-2K^b antibody (AF6.88.5, BD Biosciences) recognizing fully-folded MHC Class I, anti-exon-VIII antibody (a kind gift of Professors David Williams and Brian Barber, University of Toronto, Canada) that recognizes all MHC Class I or anti-transferrin receptor (H68.4, Invitrogen) was performed overnight with rotation. This was followed by binding to Protein A/G agarose beads (Santa Cruz) for one hour with rotation at 4^oC. Samples were analyzed on a 10-12% SDS -PAGE. Proteins were transferred onto a nitrocellulose membrane and Western blot analysis was performed (as in Section 2.1.3.1) with anti-CD74 antibody (In-1, Fitzgerald). For the endoglycosidase H experiments, bmDCs cell lysates were immunoprecipitated with anti-CD74 antibody (In-1; Fitzgerald) and digested with $EndoH_f$ enzyme (200 mIUB, New England Biolabs) according to manufacturer's directions. Western blot analysis was performed with an anti-MHC Class I antibody (KH95; Santa Cruz Biotechnology).

2.1.3.3 Metabolic labelling and immunoprecipitation

BmDCs (prepared as in Section 2.2.4) were used at $1x10^7$ cells per sample. Cells were washed once in Cystine/Methionine-Free DMEM (Dulbecco's Modified Eagle Medium; CellGro, Mediatech) supplemented with 5% dialyzed FBS (Gibco) then starved for one hour at 37°C in the same media. Cell cultures were supplemented with ~100 uCi of EasyTag Express Protein Labelling Mix [^{35}S] (Perkin Elmer) and incubated for a further 30 min at 37°C. Media was removed and DCs were lysed in 0.5% Nonidet P-40

(NP-40) buffer (120 mM NaCl, 4 mM $MgCl_2$, 20mM Tris-HCl pH 7.6) containing a protease inhibitor cocktail (Roche) and 40 μg/mL PMSF. The amount of ^{35}S labelled protein in each sample was quantified following TCA precipitation. Briefly, 5 μl of labelled protein reaction was added to 250 μl of 1M NaOH in a glass tube and allowed to incubate at room temperature of 10 min to deacylate charged ^{35}S-Met-tRNA. Paper filters were soaked in 10% Trichloroacetic acid **(**TCA, Sigma) and allowed to dry. The NaOH-treated reaction (20 μl) was spotted on the filter and the filter was incubated shaking in a beaker containing 100 ml of ice-cold 10% TCA for 15 min on ice. The TCA wash was repeated 3 times then followed by a wash with 100% ethanol. The filters were allowed to dry then counted in a liquid scintillation counter (Packard). Normalized amounts of labelled protein were precleared overnight with normal rabbit serum and Protein A-sepharose (Pharmacia). Immunoprecipitation was performed with anti-H-$2K^b$ antibody (AF6.88.5, BD Biosciences) recognizing fully-folded MHC Class I, anti exon-VIII antibody (a kind gift of Professors David Williams and Brian Barber, University of Toronto, Canada) that recognizes all MHC Class I, anti-I-A/I-E antibody (M5/114.15.2, Becton Dickinson) and anti-CD74 antibody (In-1, Fitzgerald). Samples were analyzed on a 10-12% SDS-PAGE. Gels were fixed by soaking overnight in Gel Fixing Solution (30% methanol, 10% Acetic Acid). To aid in amplification of the signal, the gels were soaked in Amplify (GE Healthcare) for 30 min then Gel Soaking Solution (1% glycerol, 5% PEG8000) for 30 min. The gels were dried and exposed to a film (Biomax MR, Kodak) at -80°C for 7-14 days. The film was developed using the Kodak M35A X-OMAT processor.

2.1.3.4 Pulse chase experiments

DC2.4 cells were seeded at $1x10^6$ per 60mm tissue culture plates in RPMI complete media and were allowed to adhere overnight. Cells were metabolically labelled with ^{35}S-Cystine and Methionine as in Section 2.1.3.3. Following the 30 min labelling, cells were washed with RPMI completed media then incubated with RPMI completed media at 37°C. At indicated time points, samples were placed on ice, washed with ice-cold PBS and then lysed in 1mL of RIPA buffer (10mM phosphate buffer pH7.2, 150mM NaCl, 1% NP-40, 1% sodium deoxycholate, 0.1% SDS, 0.2mM EDTA) containing a protease inhibitor cocktail (Roche) for 30 minutes on ice. Cell lysates were spun at 10,000xg at 4^oC for 15 min, and the supernatant was pre-cleared overnight with pre-washed Protein A sepharose beads (Amersham Biosciences). The amount of ^{35}S labelled protein in each sample was quantified following TCA precipitation as described in Section 2.1.3.3. Normalized amounts of labelled protein from each sample were precipitated with a rabbit anti-H-$2K^b$ polyclonal (P8) (courtesy of Jacques Neefjes, The Netherlands Cancer Institute) [298] overnight with rotation, followed by binding to Protein A sepharose beads for one hour with rotation at 4^oC. Samples were washed three times with RIPA buffer and split into two samples. One sample was suspended in $EndoH_f$ buffer and digested with $EndoH_f$ enzyme (New England Biolabs) according to manufacturer's protocol. The samples were then mixed with 5X protein sample buffer and separated by SDS-PAGE (12% separating/5% stacking) then fixed and analyzed as in Section 2.1.3.3.

2.1.3.5 Surface protein isolation

T cells were isolated from splenocyte single cell suspensions (prepared as in Section 2.2.4) using the using the EasySep Mouse T Cell Enrichment Kit (Stemcell Technologies) according to manufacturers` instructions. Cell surface proteins were biotinylated and isolated using the Pierce Cell Surface Protein Isolation Kit (Pierce). Protein levels between samples were normalized using the BCA Protein Assay (Pierce) and separated by SDS- PAGE (8% separating/5% stacking). Proteins were transferred to a nitrocellulose membrane and a Western blot analysis was performed as in Section 2.1.3.1 using a rabbit anti-$Ca_V1.4$ polyclonal antibody (provided by Dr. John Mcrory).

2.1.4 Immunofluorescence assays

2.1.4.1 Flow cytometry

Antibodies against H-$2K^b$ (AF.6-88.5), I-A^b (AF6-120.1), CD86 (GL1), CD4 (GK1.5), CD8a (53-6.7), CD11b (M1/70), CD11c (HL3), CD40 (3/23), CD44 (IM7), pan-NK (DX5), anti-Bcl-2 (3F11) were obtained from BD Biosciences. Antibodies against CD3ε (2C11), CD8b (53.58), TCRβ (H57-597), CD19 (ebio1D3), CD24 (M1/69), CD25 (PC61.5), CD62L (MEL-14), CD69 (H1.2F3), CD127 (A7R34), Thy1.1 (HIS51), Thy1.2 (53-2.1), CD45.2 (104), PD-1 (J43), PD-L1 (MIH5) and CCR7 (EBI-1) were purchased from eBioscience. Anti-TLR4 antibody (MDS510) was obtained from Santa Cruz Biotechnology. The H-$2K^b$/$OVA_{257–264}$ (25.D1.16) antibody was purified from the supernatant of the 28.14.8S hybridoma [299] and directly conjugated to Phycoerythrin (PE) by the UBC antibody facility. The following reagent was obtained through the AIDS

Research and Reference Reagent Program, Division of AIDS, NIAID, NIH: HIV-1 Nef monoclonal antibody (AE6) from Dr. James Hoxie.

All antibodies against surface proteins were incubated on ice with saturating amounts of antibody for 30 min except with anti-CCR7 (EBI-1, eBioscience) that was performed at 37° C for 30 min. The cells were then washed three times with cold PBS. For viability analysis, cells were labelled with relevant surface antibodies then incubated with Annexin V-Alexa-647 (Southern Biotech) for 15 min at room temperature in HEPES with 140 mM NaCl containing 2.5 mM Ca^{2+}. For intracellular analysis of Bcl-2 expression, cells were fixed in 2% formaldehyde, washed with PBS, and then permeablized by incubation in 90% methanol for 30 min on ice. Intracellular staining with anti-Bcl-2 (3F11; BD Biosciences) was conducted at room temperature for 30 min [300]. Data were acquired using either FACScan or FACSCalibur/CellQuest software (BD Biosciences) or LSRII/FACSDiVa software (BD Biosciences). Data were analyzed with Flowjo software (Treestar, Inc).

2.1.4.2 Phospho-flow cytometric signalling analysis

Thymocytes were incubated in Hank's Balanced Salt Solution (HBSS; Invitrogen) with 10 mM HEPES for 30 minutes prior to stimulation. For stimulations, thymocytes were incubated for 15 minutes at 4°C with 10 mg/ml of biotinylated anti-CD3ε antibody (clone 145-2C11; eBioscience) then with 20 μg/mL streptavidin diluted in prewarmed PBS at 37°C for the indicated time. For determination of STAT5 phosphorylation, cells were fixed with 2% formaldehyde for 10 min, pelleted by centrifugation and permeablized overnight in 90% methanol at -20°C. Permeabilized cells were treated with

anti-STAT5- AlexaFluor647 (pY649), anti-CD8a-PE (53-6.7) and anti-CD4-PE-Cy7 (GK1.5) antibodies (BD Biosciences) for 1 h at room temperature. For flow cytometric determination of ERK activation [301], cells that were activated in a 200 µl volume were fixed by adding 50 µl of 10% formaldehyde, and incubated for 10 min at 37°C. Following centrifugation, thymocytes were resuspended in ice-cold methanol and incubated on ice for 30 min. Permeabilized cells were incubated with anti-p-ERK1/2 (9101, Cell Signalling Technology) for 20 min at room temperature. Bound antibody was detected with anti-rabbit Ig $F(ab')_2$-PE (Jackson ImmunoResearch Laboratories) by incubation for 20 minutes on ice. Cell surface labelling with anti-CD4 (GK1.5) and CD8a (53-6.7) antibodies (BD Biosciences) was carried out by incubation on ice for 20 min. Data were acquired using either FACSCalibur/CellQuest software (BD Biosciences) or LSRII/FACSDiVa software (BD Biosciences). Data were analyzed with Flowjo software (Treestar, Inc).

2.1.4.3 Confocal microscopy

To aid in the adherence of cells, coverslips were coated with poly-D-lysine. Briefly, coverslips were incubated shaking at room temperature for 2 hours with 1 mg/ml poly-D-lysine. The coverslips were washed 3 times with PBS then sterilized by autoclaving. For analysis of antigenic loading by immunofluorescence, splenic DCs isolated using $CD11c^+$ magnetic beads following manufacturer's directions (Miltenyi Biotech**),** were incubated with 5 mg/mL OVA or control protein, Bovine Serum Albumin (BSA), for 10 hrs in the presence of GM-CSF with or without 10 ng/mL TNFα. Cells preincubated with OVA or not, were allowed to adhere to the sterile coverslips by incubation in 10 cm plates for 18

hours in RPMI completed media. The coverslips were then washed with PBS. The cells adhering to the coverslips were fixed with 4% paraformaldehyde for 20 min at room temperature then permeabilized and blocked for 1hr with 0.1% saponin/1% BSA in PBS at room temperature. The cells were stained for 1 hour at room temperature with: rabbit anti-Giantin antibody (PRB-114C, Covance), rabbit anti-furin convertase antibody (ab3467, Abcam), goat anti-LAMP1 antibody (N19, Santa Cruz Biotechnology), mouse anti-H-2K^{b} antibody (AF6-88.5, BD Biosciences), mouse anti-H-2K^{b}/OVA$_{257-264}$ antibody (25.D1.16) [299], rat anti-CD74 antibody (In-1, Fitzgerald). Cells were washed five times with 0.1% saponin/1% BSA in PBS, then incubated for 1 hour at room temperature with secondary antibodies: rabbit anti-goat IgG (H+L) conjugated to Alexa488, goat anti-mouse IgG (H+L) conjugated to Alexa488, rabbit anti-mouse IgG (H+L) conjugated to Alexa568, goat anti-rat IgG (H+L) conjugated to Alexa568, goat anti-rabbit IgG (H+L) conjugated to AlexaFluor568, rabbit anti-goat IgG (H+L) conjugated to Alexa568 goat anti-mouse IgG (H+L) conjugated to AlexaFluor647, (all from Molecular Probes). Cells were washed five times in 0.1% saponin/1% BSA in PBS and incubated for 10min with Slow Fade (Molecular Probes) equilibration buffer. The coverslips were mounted in Slow Fade glycerol solution and sealed to the slide with clear nail polish. Confocal microscopy was performed on a Nikon TE2000 inverted microscope with EZ-C1 software version 3.0, with 633nm, 543 nm and 488nm laser lines. Data analysis was performed with ImageJ.1 to select single slices and Adobe Photoshop for colour merging.

For studies with primary splenic DCs, 50 DCs were examined at 60X magnification using Open*lab* software to determine relative fluorescent intensity. The relative

fluorescent intensity of all individual colors was then expressed as percent of total fluorescence intensity (mean +/- SD). Alternatively for DC2.4 studies, co-localization was quantified by calculating the Mander's coefficient using ImageJ Colocalization Threshold software (NIH).

2.1.5 Signalling assays

2.1.5.1 T cell receptor signalling analysis

For signalling analysis, thymocytes were prepared as in Section 2.2.4. Thymocytes incubated for 15 minutes at 4°C with 10 mg/ml of biotinylated anti-CD3ε antibody (clone 145-2C11; eBioscience) were stimulated at 37°C for the indicated time by the addition of 20 μg/mL streptavidin diluted in prewarmed PBS. As a positive control for activation, thymocytes were incubated with 100 ng/mL PMA for 10 min at 37°C. Immediately following stimulation, the cells were lysed in RIPA buffer (10mM phosphate buffer pH7.2, 150mM NaCl, 1% NP-40, 1% sodium deoxycholate, 0.1% SDS, 0.2mM EDTA) containing a protease inhibitor cocktail (Roche) for 30 minutes on ice. Protein levels in the samples were quantified using the BCA Protein Assay according to the manufacturer's directions (Pierce). Equalized amounts of protein for each sample were separated by SDS-PAGE. Phosphorylated and total ERK and JNK were detected by Western blotting (Section 2.1.3.1). The fold increase in phosphorylation was expressed as a ratio of total protein and was normalized to the unactivated wild type control.

Ras activity was assessed as previously described [302]. Briefly, thymocytes were stimulated as above and lysed in 1% NP-40 buffer (200 mM NaCl, 5 mM $MgCl_2$, 50mM Tris-HCl pH 7.5, 15% glycerol) containing a protease inhibitor cocktail (Roche) and 40

μg/mL PMSF. Protein levels in the samples were quantified using the BCA Protein Assay according to the manufacturer's directions (Pierce). Activated p21Ras (Ras-GTP) was affinity-precipitated from lysates that were normalized for protein concentration, using glutathione Sepharose beads coupled to a recombinant fusion protein of GST and the Ras-binding domain of Raf-1 (GST-RBD). The beads were washed in lysis buffer then boiled in sample buffer. The eluted proteins were resolved by SDS-PAGE and analyzed by Western blot (Section 2.1.3.1) using an anti-p21Ras antibody (clone RAS10; Upstate Biotechnology). Whole cell lysates were analyzed in parallel to quantify total Ras protein in each sample. The fold increase in activation was expressed as a ratio of total Ras protein and was normalized to the unactivated wild type control.

2.1.5.2 NFAT mobilization assays

Single-cell suspensions from thymi of wild type or $Ca_V1.4^{-/-}$ mice were prepared (as in Section 2.2.4) and incubated for 16 hours with plate-bound anti-CD3ε antibody (145-2C11, eBioscience; used at 10 μg/ml) and soluble anti-CD28 (used at 1 μg/ml) antibody or media alone. Whole cells were lysed for 10 minutes in RIPA buffer (10mM phosphate buffer pH7.2, 150mM NaCl, 1% NP-40, 1% sodium deoxycholate, 0.1% SDS, 0.2mM EDTA) containing a protease inhibitor cocktail (Roche). Nuclear and cytoplasmic fractions were prepared using NE-PER Nuclear/ Cytoplasmic Extraction Kit as directed by the manufacturer (Thermo Scientific). Western blot analysis was performed as described above (Section 2.1.3.1) using anti-NFATc1 (7A6, Thermo Scientific) antibody and anti-GAPDH (MAB374, Chemicon) or anti-HDAC1 (10E2, Santa Cruz) as loading

controls. The fold increase in activation was expressed as a ratio of the appropriate loading control and was normalized to the unactivated wild type control.

2.1.6 *In vitro* antigen presentation assays

2.1.6.1 *In vitro* cross presentation assay

For cross presentation analysis, DC2.4 cells or splenic DCs (isolated as in Section 2.1.4.3) were examined. DCs were incubated for 18 hours with indicated concentrations of soluble ovalbumin (OVA) (Worthington Biochemical Corp) or 1 μg/ml of $OVA_{257–264}$ peptide in RPMI completed media then washed 3 times with PBS. Cells were incubated for 30 minutes on ice with Fc blocker (2.4G2 FcγIII/II blocker, BD Biosciences) to prevent non-specific binding of antibodies by FC receptors on the DC cell surface. Next, cells were stained with antibodies to detect total $H\text{-}2K^b$ or $H\text{-}2K^b$/ $OVA_{257–264}$ complexes and subsequently analyzed by flow cytometry (as in Section 2.1.4.1).

For analysis of cross priming, DC2.4 cells incubated with OVA as above were fixed for 10 min with 0.005% glutaraldehyde. Primary splenic DCs were incubated with OVA as above in addition to 15 ng/mL GM-CSF (Sigma) with or without 10 ng/mL TNF-α, or 10 ng/mL IFN-γ (both from R & D Systems). Next, 1 x 10^5 cells were incubated for 18 hours in a 1:1 ratio with B3Z T cells. For analysis of primary DCs, 15 ng/ml GM-CSF was included during co-culture with T cells. Individual cultures were lysed by addition of 100 μl of CPRG lysis buffer (100 mM 2-Mercaptoethanol, 9 mM $MgCl_2$, and 0.125% Nonidet P-40, and 0.15 mM chlorophenol red ß-galactoside in PBS). Plates were read at 595nm subtracting 655 nm background at 24 or 48 hours to obtain a measure of the

production of the β-galactosidase reporter under NF-AT elements by the B3Z TCR recognizing H-2K^b/SIINFEKL complexes [296].

2.1.6.2 *In vitro* classical MHC I antigen presentation assay

For analysis of MHC I presentation of endogenous antigen, DC2.4 cells were infected with vaccinia virus-expressing OVA (VV-OVA). Briefly, DCs were incubated with VV-OVA at indicated MOI in 50 μl of RPMI completed media at 37°C for 2 hours. Then, RPMI completed media was added to bring the total volume to 2 ml and the cells were incubated at 37°C for 18 hours. The DCs were washed three times with PBS then assessed for total H-2K^b or H-2K^b/ OVA$_{257–264}$ complexes on the cell surface as well as for the ability to prime B3Z T cells (as in Section 2.1.6.1).

2.1.7 MHC I trafficking assays

For analysis of the rate of MHC I internalization, cells were first incubated for 30 minutes on ice with Fc blocker (2.4G2 FcγIII/II blocker, BD Biosciences) to prevent non-specific binding of antibodies by FC receptors on the DC cell surface. Then, DCs were labelled with an H-2K^b specific monoclonal antibody (AF6-88.5, BD Biosciences) conjugated to biotin for 30 min on ice. Samples were placed at 37°C or for a negative control at 4°C. At indicated time points, the DCs were fixed in 2% paraformaldehyde, labelled with streptavidin-PE (Jackson Immunoresearch) for 30 min on ice then analyzed by flow cytometery (as in Section 2.1.4.1). The percent H-2K^b remaining on the cell surface was calculated by normalizing the MFU of the samples incubated at 37°C to the

MFU of the equivalent sample incubated at 4°C. A two-tailed Student's T-test was performed at each time point to identify statistical differences.

To determine the rate of MHC I trafficking to the cell surface, DCs were stripped of surface MHC I by acid wash and the return of H-2K^b was analyzed over time [303]. Briefly, DCs were washed in PBS containing 0.1% BSA and incubated in acid stripping buffer (0.2 M citric acid/0.2 M Na_2HPO_4 buffer; pH 3.0) on ice for 2 min. Excess ice-cold PBS/BSA was added to neutralize the cell suspension. The cells were centrifuged then immediately stained for FACS analysis or recovered by incubating at 37°C in completed RPMI with or without 10 μg/ml of cycloheximide (Sigma). At indicated time points, DCs were harvested and fixed in for 10 minutes in 2% PFA at room temperature. To determine the amount of H-2K^b returning to the cell surface, the DCs were stained with anti-H-2K^b (AF.6-88.5, BD Biosciences) and analyzed by flow cytometery (as in Section 2.1.4.1). The amount of MHC I transported to the cell surface was calculated by subtracting the MFU of the samples immediately after acid stripping from the corresponding sample at each time point. The amount of newly synthesized MHC I transported to the cell surface was determined by subtracting the MFU of the cycloheximide-treated cells from the MFU of the untreated cells. This number was normalized by then subtracting the corresponding MHC I staining remaining immediately after stripping. A linear regression was performed and the slopes of the linear regression lines were analyzed to identify significant differences.

2.1.8 Ca^{2+} flux assay

Splenocytes or thymocytes (10^7 cells/mL) in Hanks Balanced Salt Solution (HBSS) supplemented with 2% FCS were labelled with 1 μM Fluo-4, 2 μM Fura Red and 0.02% pluronic (all from Invitrogen) for 45 min at room temperature. Following washing, cells were stained with anti-CD44-APC (IM7), CD8a-APC-eFluor-780 (53-6.7) and anti-CD4-PE (GK1.5) antibodies (BD Biosciences) for 20 min on ice. Samples were suspended in RPMI (contains ~0.4 mM Ca^{2+}) and prewarmed for 15 min at 37° C. Thapsigargin (1 μM) and ionomycin (1 μg/mL) stimulations and the adding back of free extracellular Ca^{2+} (0.5 mM) were performed as described previously [304]. Chelation of extracellular Ca^{2+} was carried out by supplementation of RPMI media with 0.5 mM EGTA. For TCR stimulations, splenocytes pre-coated with 5 μg/mL of biotinylated anti-CD3ε antibody (145-2C11; eBioscience) were activated by the addition of 20 μg/mL streptavidin. Ca^{2+} flux data was acquired on a BD™ LSR II flow cytometer using FACSDiva™ software or BD FACSCalibur using CellQuest software and analyzed with Flowjo (Treestar, Inc), electronically gating on the indicated T cell subsets and plotting Fluo-4/Fura Red ratios versus time.

2.1.9 Naïve T cell survival assays

Single cell suspensions (prepared as described in Section 2.2.4) generated from lymph nodes and spleen of C57Bl/6 (Thy1.1^{+-}) and Cav1.4$^{-/-}$ (Thy1.2^{+}) mice were stained with anti-CD44 (IM7), anti-CD4 (GK1.5) and anti-CD8a (53-6.7) antibodies (BD Biosciences) and subsequently, naïve (CD44^{lo}) CD4^{+} and CD8^{+} T cells were isolated using a BD FACSAria. The vast majority (>99 %) of sorted T cells were considered

naïve as they expressed high levels of L-selectin. Purified wild type and mutant naïve $CD4^+$ and $CD8^+$ T cells were mixed at equivalent ratios (1:1:1:1) and 200,000 total cells per well were cultured in 96 well flat-bottom plates. Cells were treated either with the indicated dose of mIL-7 (eBioscience) or cultured in wells pre-coated with 10 μg/mL of anti-CD3ε (145-2C11, eBioscience) antibody. After 24 hours, viability was determined by labelling samples with anti-CD8a (53-6.7) and anti-Thy1.1 (HIS51) antibodies and Annexin V (as described in Section 2.1.4.1) for analysis by flow cytometery.

2.2 *In vivo* studies

2.2.1 Mice

C57Bl/6 and C3H mice were purchased from Charles River. Beta-2-microglobulin $(\beta 2m)^{-/-}$, transporter associated with antigen presentation $(TAP)1^{-/-}$, OT-I T cell transgenic, B6.PL-Thy1^{a}/Cy (Thy 1.1^+), B6.SJL-Ptprca Pep3b/BoyJ (Ly5.1^+), B6.$Rag1^{-/-}$ ($Rag1^{-/-}$ on a C57Bl/6 background) and BALB/c.$Rag1^{-/-}$ ($Rag1^{-/-}$ on a BALB/c background) were acquired from The Jackson Laboratory. OT-II T cell transgenic mice were a kind gift from Jan Dutz (Child and Family Research Institute, University of British Columbia). $CD74^{-/-}$ mice were a kind gift of Diane Mathis (C.U. Strasbourg, France and The Harvard Stem Cell Institute, Boston, MA). $Ca_V1.4^{-/-}$ mice were obtained from Torben Bech-Hansen (University of Calgary) [305]. All mice were bred and maintained at the University of British Columbia Small Animal Facility at South Campus. All studies followed guidelines set by both the University of British Columbia's Animal Care Committee and the Canadian Council on Animal Care.

Nef transgenic mice were created for this thesis. The *nef* gene was amplified from the pNLV102 vector [297] with the upstream primer (5'-GATCGAGGTCGACGAATT CGCAATCATACCTACAA-3') introducing the SalI and EcoRI restriction enzyme sites and the antisense primer (5'-GATCGAGCACGTCGACCCTCCTGGAACGCCCC-3') introducing the SalI site. The PCR reaction was conducted with Platinum Pfx DNA Polymerase (Invitrogen) in the Whatman Biometra UnoII Thermocycler using the following conditions: 94°C for 2.5 min; 94°C for 30 sec, 65°C for 1 min, 72°C for 1 min for 35 cycles; 72°C for 10 min. The *nef* PCR product was purified using the QIAquick PCR Purification Kit (Qiagen). The purified fragment was digested with SalI restriction enzyme (New England Biolabs), resolved on a 1% agarose gel then purified using the Qiaex II Gel Extraction Kit (Qiagen). Simultaneously, the p783 vector (from Dr. Nigel Kileen, UCSF) containing the murine CD4 promoter, enhancer and silencer [306] was digested with SalI restriction enzyme (New England Biolabs), resolved on a 1.5% agarose gel, purified using the Qiaex II Gel Extraction Kit (Qiagen) then treated with Calf Intestinal Alkaline phosphatase (Invitrogen) to remove 5' phosphate groups and prevent self-ligation. The digested *nef* transgene and p783 vector were ligated using T4 DNA Ligase (Invitrogen) and correct insertion of the Nef sequence into the vector was confirmed by sequencing (NAPS, UBC). The CD4/*nef* construct was microinjected into fertilized murine oocytes (derived from mating CBA and C57Bl/6) which were subsequently transplanted into the uteri of pseudo-pregnant female mice. The transgenic pups obtained were examined for the incorporation of the CD4/*nef* transgene into the genome. Genomic DNA was isolated from ear clips. Briefly, the ear clips were incubated in 20 μl of digestion buffer (50mM Tris pH8.0, 2mM NaCl, 10mM EDTA, 1% SDS) plus

1 mg/ml Proteinase K (Invitrogen) for 20 min at 55°C. The samples were vortexed for 30 seconds then incubated for another 20 min at 55°C. The digestion was diluted with 300 μl of MilliQ H_2O then incubation at 95°C for 10 min to inactivate the Proteinase K. An additional 700 μl of MilliQ H_2O was added to each sample and then used as a template in PCR reactions. PCR amplification using *nef* specific primers was performed as above. The transgenic offspring confirmed to contain the *nef* transgene were backcrossed to C57Bl/6 mice for ten generations. To create a homozygotic line, mice testing positive for the *nef* transgene were crossed to each other. Real-time PCR was used to quantify the *nef* transgene copy number per mouse. Briefly, DNA was prepared from earclips as above and amplified using the LightCycler FastStart DNA Master^{Plus} SYBR Green I Reaction Mix (Roche) in the LightCycler System (Roche) according to manufacturer's protocols. The C_T (threshold cycle) value was determined and normalized to an S15 housekeeping gene control. The fold differences between the normalized CT values were calculated to determine relative differences in *nef* gene copy number.

2.2.2 Bone marrow chimeric mice

To generate chimeric mice, bone marrow from 8 weeks-old donor mice was labelled with biotinylated anti-Thy1.1 (HIS51, eBioscience) or anti-Thy1.2 (53-2.1, eBioscience) antibodies for 30 min on ice and subsequently depleted with streptavidin-linked Dynabeads according to manufacturer's instructions (Invitrogen). Next, $1x10^7$ bone marrow cells were injected intravenously into sublethaly irradiated (1200 rad) recipients. Three months following reconstitution, chimeric mice were tested for complete graft

reconstitution by flow cytometry analysis (as in Section 2.1.4.1) following staining with anti-CD8a (53-6.7) and CD4 (GK1.5) antibodies (BD Biosciences).

2.2.3 Depletion of $CD4^+$ cell population from mice

To deplete $CD4^+$ cells, mice were injected intravenously with 100 µg GK1.5 antibody immediately prior to challenge and 48 hours prior to T cell collection. Peripheral blood was analyzed to confirm depletion of $CD4^+$ cells [307]. Briefly, peripheral blood mononuclear cells were isolated by centrifugation in Ficoll-Paque™ Plus reagent (GE Healthcare). The cells were labelled with anti-CD8a (53-6.7) and CD4 (GK1.5) antibodies (BD Biosciences) and analyzed by flow cytometry (as in Section 2.1.4.1).

2.2.4 Single-cell preparation from tissue

Tissue samples (spleen, thymus, liver, and lymph node) were isolated from the appropriate mice. Tissue was mashed into a single-cell suspension through a wire mesh to disrupt the connective tissue. In the case of DC isolation from spleen, the spleen was chopped and incubated with 1mg/ml collaganase D for 1 hour at 37°C. The red blood cells contaminating the tissue preparations were next lysed with MRCRB buffer (0.15M NH_4Cl, 0.01M Tris base PH 7.2) for 2-3 minutes at room temperature. The digestion was stopped by the addition of RPMI completed media. The mix was centrifuged and the resultant cell pellet was resuspended for use in further assays as a single-cell suspension.

Specific cell populations were isolated from the above tissue-derived single cell suspension. Briefly, the cells were stained with antibodies against cell-specific markers using the staining protocol for flow cytometry (as in Section 2.1.4.1) and the cells were isolated using a BD FACSAria or BD FACSVantage as above. If not otherwise indicated, the following markers were used to identify specific cell subsets: dendritic cells were sorted as $CD11c^+$, macrophages were sorted as $CD11b^+$ and T cells were sorted as $CD3^+$.

For isolation of bone marrow, the femur and tibia were first removed. The bone marrow was flushed out with RPMI completed media using a 25G5/8 needle. The bone marrow was washed twice with media and then used for further assays. Alternatively, bone marrow precursors were used to derive dendritic cells. Bone marrow was cultured in 1% X63-Ag8-plasmacytoma-derived GM-CSF [308] (gift from David Gray, University of Edinburgh, UK) in RPMI completed media for 10-12 days. The purity of the culture was confirmed by flow cytometry (as in Section 2.1.4.1) using the following antibodies: anti - CD11c (HL3), anti- H-$2K^b$ (AF.6-88.5), anti-I-A^b (AF6-120.1) (BD Biosciences).

2.2.5 Immune challenges and infections

2.2.5.1 Cell-associated ovalbumin

C3H-derived bone marrow-derived DCs (prepared as in 2.2.4) were incubated with 10 mg/ml ovalbumin (Worthington) overnight at 37°C. The cells were washed 2 times with PBS then injected intraperitoneally at 5 x 10^6 cells/mouse in 200 μl of PBS.

2.2.5.2 Vesicular stomatitis virus

Vesicular Stomatitis Virus (VSV) was injected intraperitoneally at 1-2 x 10^5 $TCID_{50}$ (dose that infects 50% of a tissue culture cell monolayer) as indicated.

2.2.5.3 *Listeria monocytogenes*

The OVA recombinant form of *Listeria monocytogenes* (rLMOVA), derived from the wild type strain 10403s, expresses ovalbumin under the Listeriolysin O promoter [309, 310]. Bacteria were cultured overnight in brain heart infusion (BHI) broth at 37°C with constant agitation. Bacteria were cultured for a further 2 hours following a 1:10 dilution to have bacterial growth in log phase for infections. The concentration of bacteria was estimated spectrophotometrically. Mice were inoculated intravenously with $1x10^2$ - $1x10^4$ CFU/mouse in 100 μl PBS. Actual CFU were calculated following infection by plating dilutions of the inoculum.

For evaluation of memory responses [311], mice were intravenously injected with $1x10^4$ CFU/mouse in 100 μl of PBS for a primary rLMOVA infection. After 14, 28 and 64 days, a secondary infection was established by intravenous injection of $1x10^5$ CFU/mouse in 100 μl.

2.2.6 Detection of immune responses

2.2.6.1 Tetramer staining

Spleens from challenged mice were harvested on day 7 post-challenge. Splenocytes were examine directly *ex vivo* or stimulated *in vitro* for 5 days in RPMI 1640 completed

medium plus 1 μM of the H-2K^b-restricted OVA$_{257-264}$ (SIINFEKL) peptide or VSV nucleocapsid NP$_{52-59}$ (RGYVYQGL) peptide. Splenocytes were stained with anti-CD8a (53-6.7, BD Biosciences), when required with anti-CD44 (IM7, BD Biosciences) antibodies and with H-2K^b-VSV-NP$_{52-59}$ or H-2K^{b}OVA$_{257-264}$ tetramers (iTag MHC Tetramer, Beckman Coulter) to identify the VSV$_{52-59}$ or OVA$_{257-264}$- specific CD8$^+$ T cells. Cells were examined using the FACSCalibur (Becton Dickinson) and analyzed using FlowJo software.

2.2.6.2 Cytokine production

Seven days following rLMOVA infection (1x10^4 CFU/mouse), antigen-specific T cells were detected through *ex vivo* peptide stimulations and cytokine secretion [312]. Briefly, splenocytes (2x10^6 cells/well) were cultured for 5 h in 96-well, flat-bottom plates, in 0.2 ml of RPMI completed medium supplemented with 1 μl/ml of Golgi Plug (BD Biosciences) to block cytokine secretion. Cells were either left unstimulated in media alone or stimulated with 1 μM of the H-2K^b-restricted peptide OVA$_{257–264}$ (SIINFEKL), or 10 μM of the I-A^b-restricted *Listeria monocytogenes*-derived peptide LLO$_{190–201}$. For anti-TCR stimulations, splenocytes were incubated in wells that had been precoated with 10 μg/ml anti-CD3ε antibody (145-2C11, eBioscience). As a positive control of T cell stimulation, splenocytes were incubated with 20 ng/ml phorbol 12-myristate 13-acetate (PMA) and 2 μg/ml Ionomycin. After culture, cells were stained with anti-CD4 (GK1.5) and anti-CD8a (53-6.7) antibodies (BD Biosciences) then fixed for 15 min in 2% paraformaldehyde/PBS solution at room temperature. The cells were subsequently permeabilized for 15 min with 0.2% saponin/PBS or 0.2% Tween-20/PBS

at room temperature and stained with anti-IFN-γ antibody (XMG1.2, BD Biosciences). Cells were analyzed by flow cytometry as above (Section 2.1.4.1).

2.2.6.3 Proliferation assays

$CD8^+$ T cells were isolated from single cell suspensions of spleen and lymph node from OT-I transgenic mice using the EasySep Mouse CD8a Positive Selection Kit (StemCell Technologies). Alternatively, $CD4^+$ T cells were isolated from single cell suspensions of spleen and lymph node from OT-II transgenic mice using the EasySep Mouse CD4 Positive Selection Kit (StemCell Technologies). Isolated cells were labelled with 2.5 μM CFSE (Molecular Probes) for 10 minutes at 37°C in 0.1% BSA/PBS. Labelled cells were washed 2 times with media then intravenously injected at 5×10^6 cells/mouse in 100 μl of PBS on the same day as immune challenge. Three days later, splenocytes from mice injected with OT-I or OT-II CFSE-labelled cells were stained with either an anti-CD8a (53-6.7) or CD4 (GK1.5) antibody (BD Biosciences), respectively. Proliferation of $CD8^+$ OT-I or $CD4^+$ OT-II cells was assessed by CFSE dilution using flow cytometry (Section 2.1.4.1).

2.2.6.4 Detection of CTL degranulation

Detection of CD107a and CD107b on the surface of $CD8^+$ cells was used to evaluate CTL degranulation [313]. Splenocytes were isolated seven days following rLMOVA infection (1×10^4 CFU/mouse) and incubated for 5 hours in 96-well flat bottom plates as in the cytokine production procedure with the addition of 1 μl/ml Golgi Stop (BD

Biosciences) and 0.1 μg anti-CD107a (1D4B) and 0.5 μg anti-CD107b (ABL-93) antibodies (BD Biosciences). Following incubation, the splenocytes were stained, fixed, permeablized and analyzed as in the cytokine production procedure (Section 2.2.6.2).

2.2.6.5 CTL killing assays

Cytotoxicity was assessed with a standard ^{51}Cr release assay [59]. Splenocytes were isolated following a seven day infection with rLMOVA or VSV and either used directly *ex vivo* or incubated for 5 days in RPMI completed media supplemented with 1 μM of the H-2K^{b} peptide OVA$_{257–264}$ (SIINFEKL) or VSV nucleocapsid NP$_{52-59}$ (RGYVYQGL) peptide. For CTL assays with Ca$_{V}$1.4$^{-/-}$ mice, CD8^{+} T cells were isolated by staining splenocyte suspensions with rat anti-CD4 (GK1.5) and subsequently depleting CD4^{+} and Ig^{+} cells with anti-rat Ig-linked Dynabeads per manufacturer's instructions (Invitrogen). RMA-S target cells were incubated with 1 μM OVA$_{257–264}$ peptide and 100 μCi of sodium chromate (Amersham or GE Healthcare) for 1 hour at 37°C. The target cells were washed 3 times with PBS then resuspended in RPMI completed media. Effector cells were incubated for 4 h at 37 °C with target cells (1×10^{4} cells per well in 96-well plates) at various effector/target ratios. Spontaneous ^{51}Cr release by labelled cells was measured in the absence of CTL, and maximum release was quantified by lysis of target cells in 2.5% Triton X-100 detergent. All experiments were done in triplicate, and specific ^{51}Cr release was calculated as follows: % specific ^{51}Cr release = [(experimental release – spontaneous release) / (maximum release – spontaneous release)] × 100%.

2.2.6.6 Clearance of bacterial infections

The clearance of infection was analyzed by determining the bacterial load per spleen 1, 3 and 5 days following infection with rLMOVA [311]. On indicated day, spleens were removed and mashed through a metal wire mesh. The splenocytes were lysed with 1 ml of 0.1% NP-40/PBS to release bacteria and lysates were serial diluted. Dilutions (100 μl) were plated on BHI plates and colonies counted to enumerate bacterial load. The limit of detection for this assay was 10 CFU's per spleen.

2.2.7 *In vivo* cross presentation assay

C57Bl/6 and $CD74^{-/-}$ bmDCs ($H\text{-}2K^b$) (prepared as in Section 2.2.4) were incubated with 10 mg/ml OVA protein or 1 μM $OVA_{257\text{-}264}$ peptide for 2 hours at 37°C. BmDCs were washed 3 times with cold PBS and injected at 1 x 10^7 cells/ mouse intravenously (*iv*) into $RAG1^{-/-}$ mice on a BALB/c background ($H\text{-}2D^b$). After 24 hours, CFSE-labelled OT-I transgenic $CD8^+$ T cells were prepared (as in Section 2.2.6.3) and injected *iv* at 5 x 10^6 cells/mouse. Three days later, proliferation of OT-I derived ($H\text{-}2K^b$), $CD8^+$ cells was assessed by CFSE dilution using flow cytometry (as in Section 2.2.6.3).

2.2.8 Bone marrow repopulation assays

Bone marrow cells were prepared from thigh bone extracts of Thy1.1 wild type ($Thy1.1^+CD45.2^+$) or $Ca_V1.4^{-/-}$ ($Thy1.2^+CD45.2^+$) mice. Mature T cells were stained with biotinylated anti-Thy1.1 (HIS51) or anti-Thy1.2 (53-2.1) antibodies (eBioscience) and subsequently depleted with streptavidin-linked Dynabeads according to manufacturer's

instructions (Invitrogen). Wild type and mutant BM cells were then mixed 50:50 before being transferred intravenously into sub-lethally irradiated (1000 rads) CD45.1^{+} hosts (Thy1.2^{+}CD45.1^{+}). Cells from spleen and thymus were recovered 30 days after adoptive transfer. The cells were labelled with anti-Thy1.1 (HIS51), Thy1.2 (53-2.1) and CD45.2 (104) antibodies (eBioscience) to discriminate wild type and mutant donor cells and anti-CD8a (53-6.7), CD4 (GK1.5) and CD44 (IM7) antibodies (BD Biosciences) to identify T cell populations. Analysis was performed by flow cytometry (Section 2.1.4.1).

2.2.9 Homeostatic proliferation assay

For naïve T cell transfers, C57Bl/6 (Thy1.1^{+}) and $Ca_V1.4^{-/-}$ (Thy1.2^{+}) splenocytes (prepared as described in Section 2.2.4) were stained with anti-CD44 (IM7), CD4 (GK1.5) and CD8a (53-6.7) antibodies (BD Biosciences). Naïve (CD44^{lo}) CD4 and CD8 T cells were isolated using a BD FACSAria and mixed at a 1:1:1:1 ratio. Isolated cells were labelled with 2.5 µM CFSE (Invitrogen) for 10 minutes at 37°C in 0.1% BSA/PBS. Labelled cells were co-injected intravenously into Rag1$^{-/-}$ hosts. One-week post-transfer, splenocytes were isolated and stained with anti-Thy1.1 (HIS51, eBioscience), Thy1.2 (53-2.1. eBioscience), CD4 (GK1.5, BD Bioscience) and CD8a (53-6.7, BD Bioscience) antibodies to discriminate the donor wild type and mutant T cells. Proliferation of cells was assessed by CFSE dilution using flow cytometry.

2.3 Statistical analysis

Two-tailed Student's t-test was used to compare the difference between two populations as required. The difference was considered statistically significant if $p < 0.05$. Error bars represent standard deviation (SD) or standard error (SE) as indicated.

CHAPTER 3. IDENTIFICATION OF A CD74-DEPENDENT MHC I CROSS PRESENTATION PATHWAY

3.1 Introduction

During primary immune responses, dendritic cells (DCs) are the principal antigen presenting cells (APCs) that initiate adaptive immune responses predominantly through cross presentation and cross priming of T cells. This involves extracellular antigen uptake, digestion of cell-associated antigenic fragments and presentation of proteolytic peptide products on both MHC I and II molecules [314]. For MHC I molecules, two main pathways have been described that may explain how this process occurs: the cytosolic pathway [42, 52-54] shown to function convincingly *in vitro*, and the vacuolar pathway, shown to play a major role *in vivo* for select antigens [59, 62, 63]. In the vacuolar pathway, proteases generating antigenic peptides that are loaded onto peptide-receptive MHC I molecules have recently been identified [57]. However, the source of MHC I in the endocytic compartment, the mechanism of its transport and the site of peptide loading remain areas of active study [59, 65].

Spontaneous internalization of MHC I into endosomes has been demonstrated [315, 316]. Furthermore, studies from the Jefferies lab have demonstrated the importance of a tyrosine motif in the cytoplasmic tail of MHC I in directing MHC I to an endolysosomal compartment presumably from the plasma membrane [59, 65]. Therefore, the plasma membrane is thought to be one source of MHC I [56]. Likewise, transport of MHC I from

A version of Chapter 3 is prepared for publication: Genc Basha*, Kyla Omilusik,* Anna T. Reinicke, Nathan Lack, Kyung Bok Choi, and Wilfred A. Jefferies. (2011). Identification of a CD74-Dependent MHC Class I Cross-Presentation Pathway. (* denotes co-first authorship)

the endoplasmic reticulum (ER) to the endocytic compartment has also been proposed. This could occur by a mechanism of phagosome and ER fusion [51]. Alternatively, CD74 (invariant chain) bound to MHC I could transport a fraction of the MHC I to the vacuolar-endocytic compartment [60, 61] using sorting signals present in the CD74 cytoplasmic tail [317]. This mechanism would place peptide-receptive MHC I in the same or similar compartment with exogenous antigen and perhaps MHC II molecules [318], thereby facilitating antigenic peptide binding to the MHC I. This pathway could be independent of the TAP transporters as CD74 may occupy the binding groove of MHC I to avoid peptide loading on the passage to the endolysosome.

MHC I interaction with CD74 and their coincident localization in the same compartment has been previously demonstrated in human cell lines [60, 61, 318]. Based on older paradigms, Tourne *et al* concluded that a CD74 interaction was unlikely to control the fate of MHC I transport to endosomes under physiological conditions [319]. However, subsequent studies demonstrated that CD74-transfected cells substantially increased surface expression of diverse MHC I alleles suggesting that the MHC I-CD74 interaction may have functional significance [320]. In this chapter, the functional relevance of MHC I interaction with CD74 *in vivo* is investigated and a clear and critical role for CD74 in cross presentation of exogenous antigen and subsequent cross priming by DCs is described.

3.2 Results

3.2.1 CD74 is required for the generation of primary antiviral immune responses

DCs may be directly infected and utilize classical MHC I presentation to activate naïve $CD8^+$ T cells. However, during infection with a low viral titre, direct infection of DCs is less likely and DC cross presentation is the dominant pathway responsible for generation of $CD8^+$ T cell responses [59, 321]. In order to address the role of CD74 in cross presentation to generate primary anti-viral immune responses, a low dose of 10^5 $TCID_{50}$ Vesicular Stomatitis Virus (VSV) was used [59, 321]. In addition, this virus has been demonstrated to generate primary and memory $CD8^+$ immune responses in the absence of $CD4^+$ T cells [322, 323]. In this way, the role of CD74 in cross presentation can be tested regardless of the impact on $CD4^+$ T cell responses. The percentage of $CD8^+$ T cells generated against the VSV-NP_{52-59} immunodominant epitope on MHC I (H-$2K^b$) was detected following the VSV infection [324]. $CD74^{-/-}$ mice had a significantly reduced capacity (5.0% vs 19.0%; $p<0.05$) to generate antigen specific $CD8^+$ T cells (**Figure 3.1A,B**). In addition, $CD74^{-/-}$-derived CTLs had reduced killing capacity (14.0% vs 34.0%; $p < 0.05$) relative to C57Bl/6-derived CTLs when the maximum effector: target ratio was assessed (**Figure 3.1C**).

Bone marrow chimeras were constructed to further exclude the dependency of MHC I cross priming on T cell help in the $CD74^{-/-}$ mice following VSV infection [322, 323]. Additionally, the chimeras would confirm whether the deficiency in generating immune responses is dependent on the haematopoietic derived DCs ability to cross present antigen and prime T cells. Normal levels of $CD8^+$ and $CD4^+$ cells were found in the periphery of C57Bl/6→C57Bl/6 and the $CD74^{-/-}$→C57Bl/6 mice. However, reduced

A

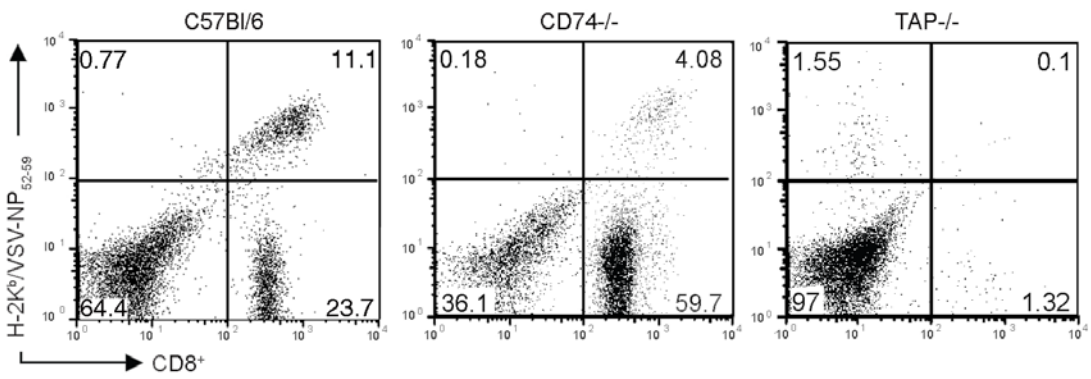
C57Bl/6
CD74-/-
TAP-/-
0.77
11.1
64.4
23.7
0.18
4.08
36.1
59.7
1.55
0.1
97
1.32
H-2K^b/VSV-NP$_{52-59}$
CD8$^+$

B

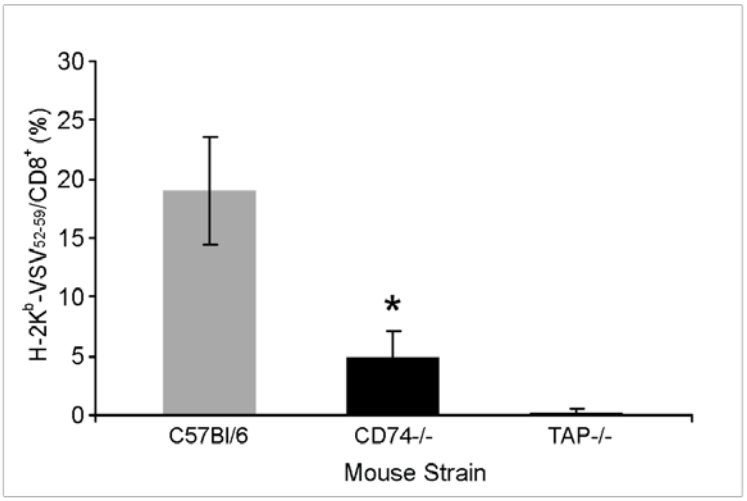
H-2K^b-VSV$_{52-59}$/CD8$^+$ (%)
30
25
20
15
10
5
0
*
C57Bl/6
CD74-/-
TAP-/-
Mouse Strain

C

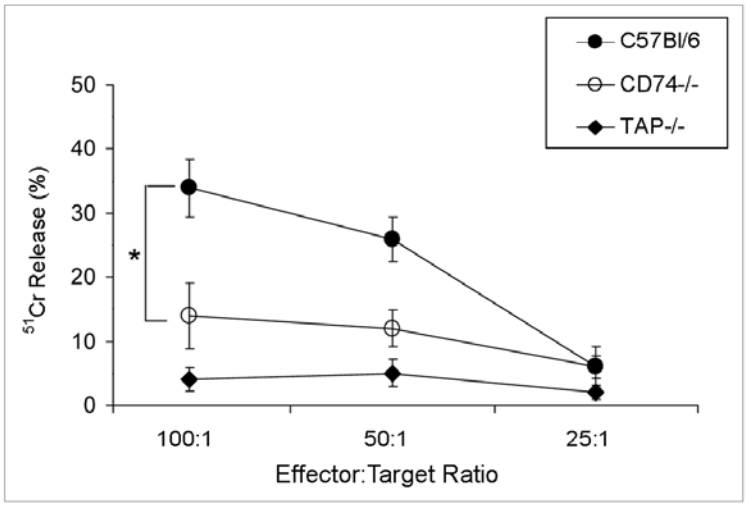
C57Bl/6
CD74-/-
TAP-/-
^{51}Cr Release (%)
50
40
30
20
10
0
*
100:1
50:1
25:1
Effector:Target Ratio

Figure 3.1. CD74$^{-/-}$ mice generate weak antiviral primary immune responses.
C57Bl/6, CD74$^{-/-}$ and TAP1$^{-/-}$ mice were infected with a low dose of VSV (2 x 10^5 $TCID_{50}$ per mouse). **(A)** Six days following viral infection, splenocytes were isolated and following a 5-day stimulation with VSV-NP_{52-59}, the number of VSV-NP_{52-59}-specific $CD8^+$ T cells generated was assessed. Percentages of VSV-NP_{52-59}-specific $CD8^+$ T cells in representative mice are shown. **(B)** Mean percentages (± SD) of H-$2K^b$-VSV-NP_{52-59}-specific $CD8^+$ T cells of three mice are shown. **(C)** The cytolytic capacity of CD74$^{-/-}$-derived CTLs is severely impaired. Standard ^{51}Cr-release assays were performed using CTLs generated following VSV infection and *in vitro* boosting. Error bars represent SD. * $p<0.05$.

$CD4^+$ and somewhat increased $CD8^+$ cell numbers were seen in the $CD74^{-/-}$→$CD74^{-/-}$ and C57Bl/6→$CD74^{-/-}$ mice. This indicated that positive selection in recipient $CD74^{-/-}$ mice was impaired due to reduced levels of MHC II in the $CD74^{-/-}$ thymic epithelium (**Figure 3.2**).

To examine antiviral responses, chimeric mice were infected with a low titre of VSV and tetramer analysis was performed (**Figure 3.3A**). Remarkably, C57Bl/6→$CD74^{-/-}$ mice, with low $CD4^+$ T cell numbers, were able to produce VSV-NP_{52-59}-specific $CD8^+$ T cells similar to wild type C57Bl/6→C57Bl/6 chimeras (1.1% vs 1.2%). However, the $CD74^{-/-}$→C57Bl/6 mice were grossly impaired in the generation of VSV-NP_{52-59} specific $CD8^+$ cells (0.2%; $p<0.05$) despite having normal $CD4^+$ T cells. This suggests that the generation of VSV specific CTL response is independent of $CD4^+$ T cell numbers. Importantly, bone marrow-derived APCs expressing CD74 were required and allowed $CD74^{-/-}$ mice to produce a robust antiviral immune response comparable with that of C57Bl/6 mice. The efficacy of elicited CTLs to lyse target cells was also tested. The CTLs obtained from C57Bl/6→C57Bl/6 and $CD74^{-/-}$→$CD74^{-/-}$ showed very different ability to lyse their targets (18.0% vs 4.5%; $p<0.05$; **Figure 3.3B).** In addition, CTLs from $CD74^{-/-}$→C57Bl/6 mice exhibited reduced killing capacity similar to $CD74^{-/-}$ mice ($p<0.05$). Conversely, C57Bl/6→$CD74^{-/-}$ mice generated CTLs with killing capacity comparable with the C57Bl/6→C57Bl/6 controls (16.8% vs 1.9%; $p<0.05$). demonstrating that $CD4^+$ help is not required for the generation of primary antiviral responses [322]. Taken together, these data demonstrate that bone marrow-derived DCs (bmDCs) of $CD74^{-/-}$ mice are defective in initiating CTL responses indicating the requirement of CD74 for optimal cross presentation to generate anti-viral immunity.

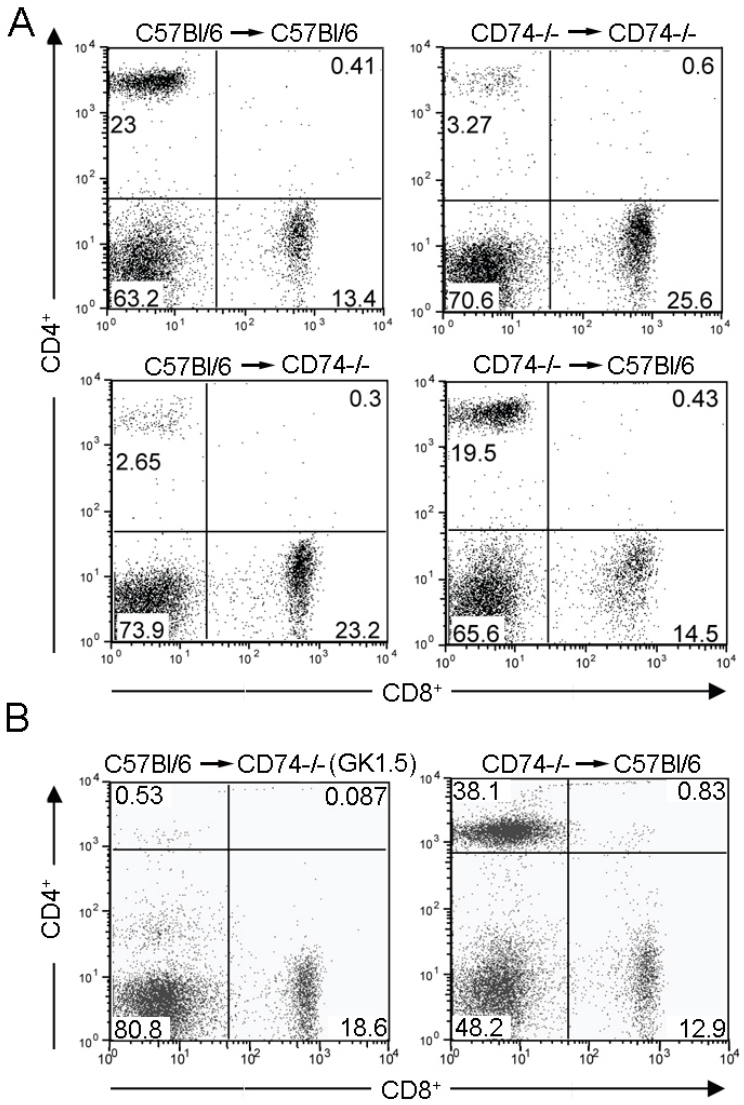

Figure 3.2. Peripheral analysis of chimeric mice.
(A) The CD8/CD4 profile in the blood of bone marrow chimera mice three months following reconstitution is presented. **(B)** C57Bl/6→CD74$^{-/-}$ chimeras were depleted of CD4^{+} cells by *iv* injection of an anti-CD4 antibody (GK1.5). Representative CD4/CD8 FACS profiles are shown.

A

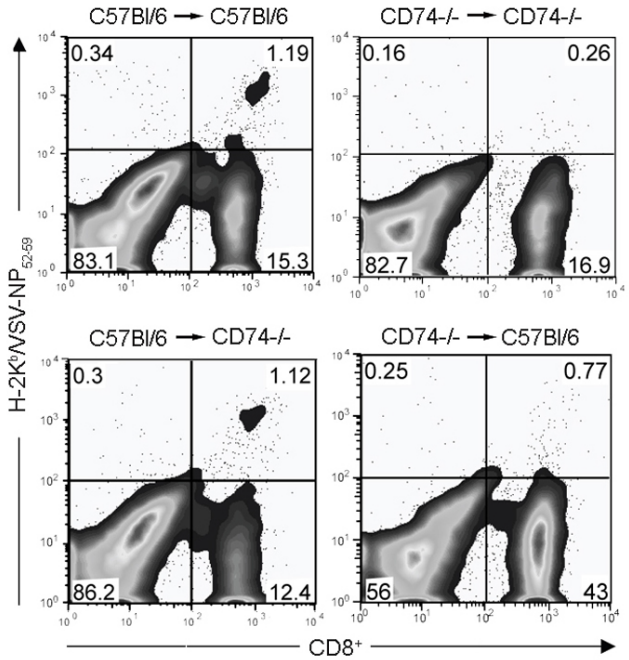
C57Bl/6 → C57Bl/6
0.34
1.19
83.1
15.3
CD74-/- → CD74-/-
0.16
0.26
82.7
16.9
C57Bl/6 → CD74-/-
0.3
1.12
86.2
12.4
CD74-/- → C57Bl/6
0.25
0.77
56
43
H-2Kᵇ/VSV-NP52-59
CD8+

B

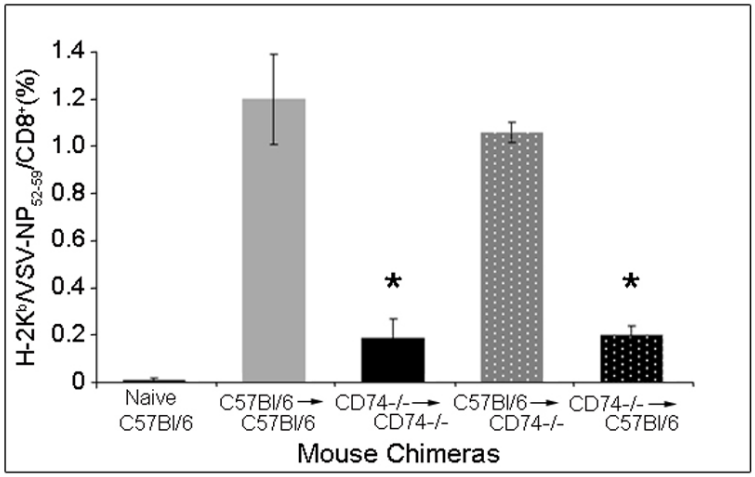
H-2Kᵇ/VSV-NP52-59/CD8+(%)
1.4
1.2
1.0
0.8
0.6
0.4
0.2
0
*
*
Naive C57Bl/6
C57Bl/6 → C57Bl/6
CD74-/- → CD74-/-
C57Bl/6 → CD74-/-
CD74-/- → C57Bl/6
Mouse Chimeras

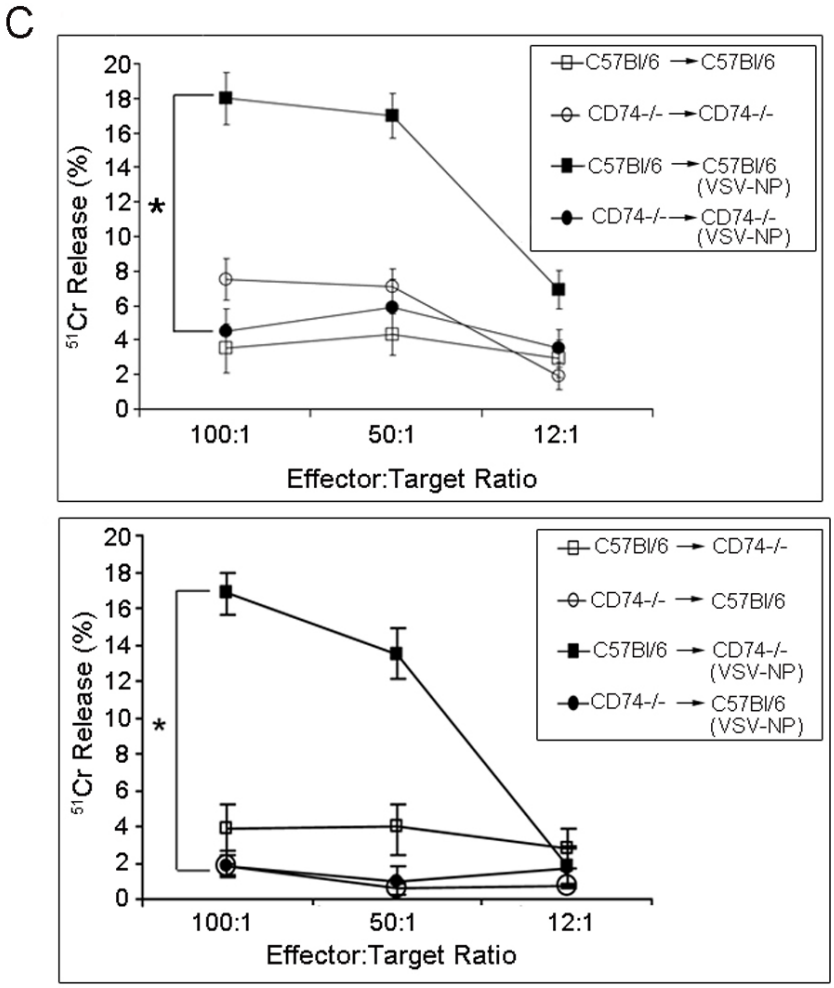

Figure 3.3. Deficiency of CD74$^{-/-}$ mice to elicit primary immune responses resides in their APCs.

(A) Chimeras were injected with 1 x 10^5 $TCID_{50}$ VSV and splenocytes were assessed for the generation of VSV-NP_{52-59} - specific $CD8^+$ cells. **(B)** The mean percentage (± SD) of three mice assayed following *in vitro* boosting with VSV NP_{52-59} peptide is shown. **(C)** Cytolytic capacity of CTLs from chimeras containing CD74$^{-/-}$ deficient APCs is severely impaired. Cytotoxicity assays were performed as described. Error bars represent SD. *$p<0.05$.

3.2.2 Depletion of residual $CD4^+$ cells in C57Bl/6→$CD74^{-/-}$ chimeras has no effect on anti-viral immune responses

Next, to eliminate the possibility that residual $CD4^+$ cells in the C57Bl/6→$CD74^{-/-}$ chimeras that result from dysfunctional positive selection in $CD74^{-/-}$ mice are contributing to the efficiency of anti-viral immune responses, during the course of the infection, the $CD4^+$ cells of C57Bl/6→$CD74^{-/-}$ chimeras were depleted with anti-CD4 antibodies. Although $CD4^+$ cells were virtually undetectable over background (**Figure 3.2B**), $CD4^+$ cell depleted C57Bl/6→$CD74^{-/-}$ chimeras generated significantly more $CD8^+$ VSV-NP_{52-59} specific T cells (13.5% vs 4.1%; $p<0.05$; **Figure 3.4A,B**) with increased lytic ability relative to $CD74^{-/-}$→C57Bl/6 chimeric mice (14.0% vs 4.9%; $p<0.05$; **Figure 3.4C**). Taken together, these data confirm that C57Bl/6→$CD74^{-/-}$ chimeras mount stronger responses than $CD74^{-/-}$→C57Bl/6 to viral infection. This is independent of $CD4^+$ cells as the reconstitution of $CD74^{-/-}$ mice with wild type DCs allowed for the restoration of fully functional anti-viral $CD8^+$ T cell responses.

3.2.3 MHC I cross priming of cell-associated antigens is dependent on CD74

It has been reported that cell-associated antigens derived from tumours are cross presented by APCs *in vivo* and that this process is TAP-dependent [325, 326]. In order to investigate the role of CD74 in primary immune response to cell-associated antigen, MHC I- mismatched OVA-pulsed DCs were used as a source of cell-associated antigen to activate antigen-specific CTLs in C57Bl/6, $CD4^+$-depleted (GK1.5-treated) C57Bl/6 and $CD74^{-/-}$ mice as well as in reconstituted mouse chimeras. Mice with a C57Bl/6 immune system, challenged with cell-associated OVA, were able to induce proliferation of OT-I-

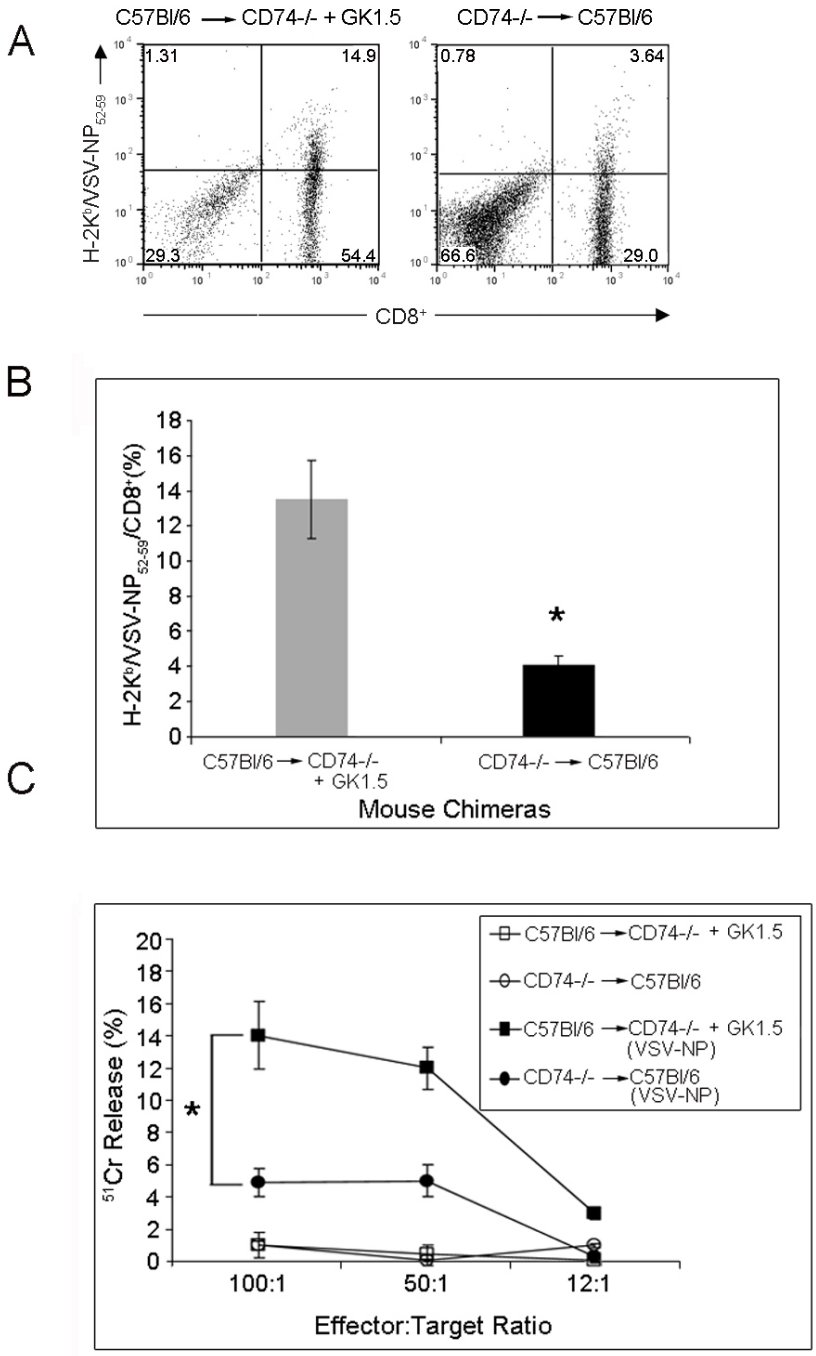

Figure 3.4. The deficiency of CD74$^{-/-}$ mice to elicit primary immune responses is independent of CD4^{+} T cells.
C57Bl/6→CD74$^{-/-}$ chimeras were depleted of CD4^{+} cells by *iv* injection of an anti-CD4 antibody (GK1.5) then assessed for immune function. **(A)** Mice chimeras infected with VSV were evaluated for the generation of H-2K^{b}-VSV-NP$_{52-59}$-specific CD8^{+} T cells. **(B)** The mean percentage (± SD) of tetramer^{+}CD8^{+} cells in the spleen of three mice is shown. **(C)** The lytic activity of these splenocytes was also assessed. Error bars represent SD**.** * $p < 0.05$.

derived $CD8^+$ T cells (**Figure 3.5**). However, with the same challenge of cell-associated OVA, mice with the haemopoetic system deficient for CD74 had a substantially reduced ability to stimulate proliferation of OT-I $CD8^+$ cells (**Figure 3.5**).

3.2.4 CD74-dependent MHC I cross priming is independent of $CD4^+$ T cells and CD74-mediated cell motility and homing

To focus specifically on DC cross priming defects and eliminate extraneous factors including the requirement for CD4-help, $CD74^{-/-}$ and C57Bl/6 DCs incubated with OVA protein or $OVA_{257-264}$ peptide were injected with CFSE-labelled purified $CD8^+$ OT-I cells into T cell deficient $RAG1^{-/-}$ mice on a BALB/c background. The ability of the DCs to cross prime the OT-I cells was assessed (**Figure 3.6**). $CD74^{-/-}$ DCs incubated with OVA protein induced lower OT-I proliferation in comparison to the C57Bl/6 control DCs (18% vs 48%). However, when provided with the immunodominant peptide $OVA_{257-264}$, as a positive control, $CD74^{-/-}$ DCs were as competent as C57Bl/6 control DCs at activating purified $CD8^+$ OT-I cells (59.5% vs 60.0%). In addition, in this setting, this control eliminates a possibly confounding role for CD74 in DC motility and homing [327] from the site of injection to the spleen, where CSFE -labelled T cells were assessed. With these findings, we conclude that CD74 plays a critical role in MHC I cross presentation of cell-associated antigen and $CD8^+$ T cell priming *in vivo* and this is unrelated to $CD4^+$ T cell help or CD74-mediated DC motility and homing.

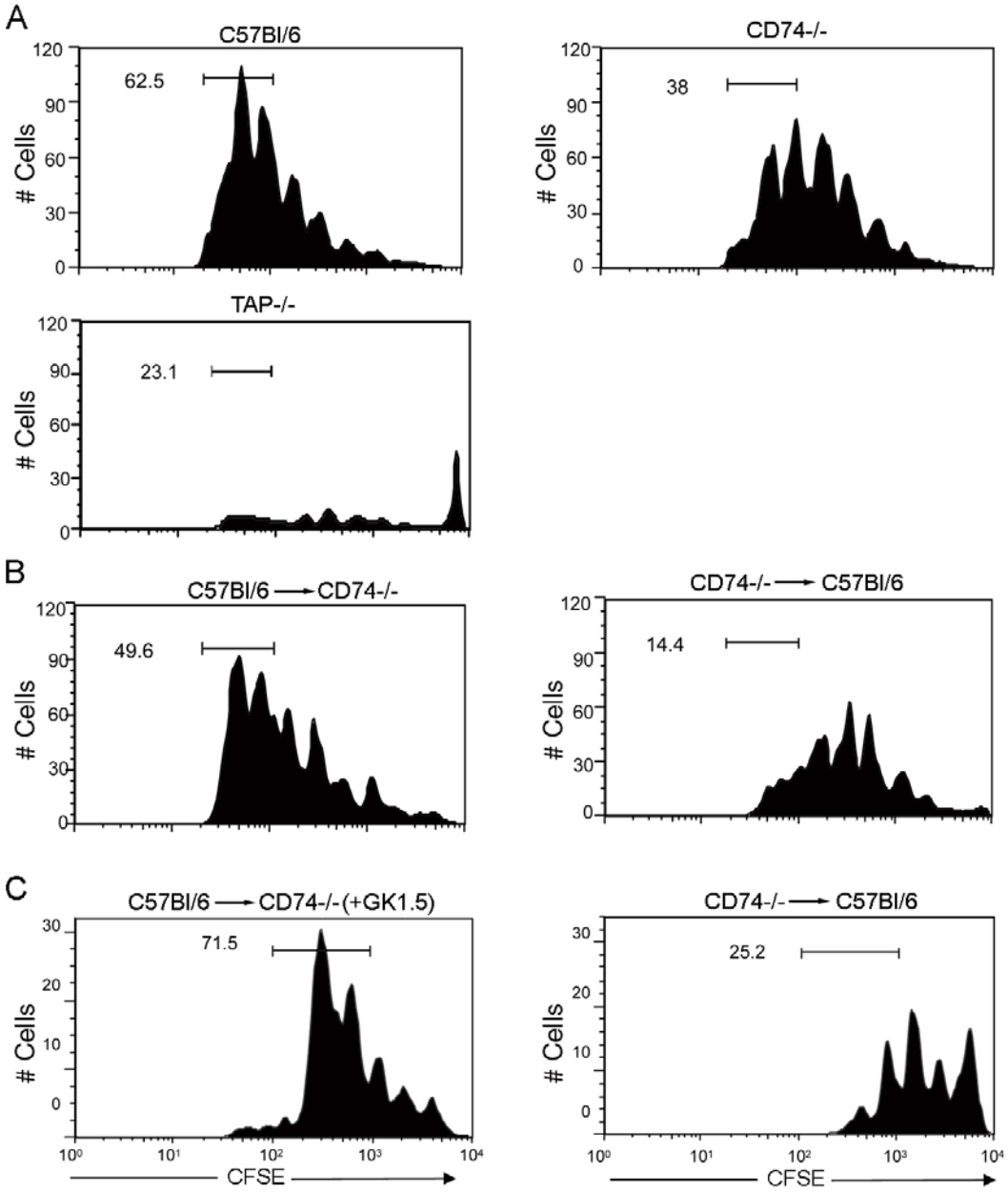
A
C57Bl/6
62.5
CD74-/-
38
TAP-/-
23.1
B
C57Bl/6 → CD74-/-
49.6
CD74-/- → C57Bl/6
14.4
C
C57Bl/6 → CD74-/-(+GK1.5)
71.5
CD74-/- → C57Bl/6
25.2
Cells
CFSE

D

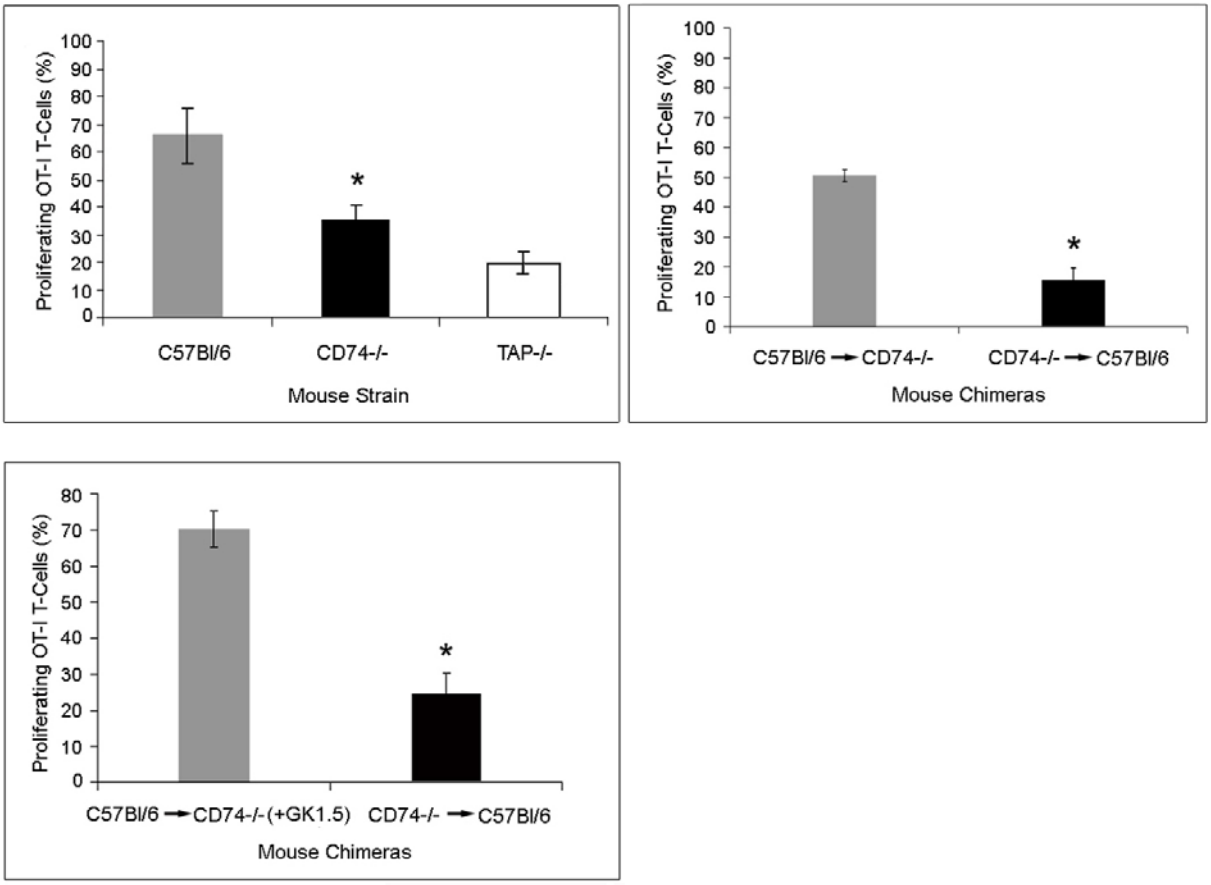

Figure 3.5. CD74$^{-/-}$ mice are unable to cross present cell-associated antigens *in vivo* to generate an effective primary immune response.
(A, B) OVA-pulsed C3H-derived bmDCs (H-2K^{k} haplotype) were injected (*ip*) then OT-I transgenic CFSE-labelled T cells were injected (*iv*) into mice and chimeras. CFSE/CD8^{+} populations were examined and data represent proliferating OT-I–derived T cells from spleen of representative mice or chimeras as indicated (n=3). **(C)** C57Bl/6→CD74$^{-/-}$ chimeras were depleted of CD4^{+} cells by *iv* injection of an anti-CD4 antibody (GK1.5) during immunization with cell-associated OVA then assessed for their ability to activate CFSE-labelled adoptively transferred OT-I–derived T cells. **(D)** The mean percentage (± SD) of OT-I cells proliferating is shown. Error bars represent SD**.** * $p < 0.05$

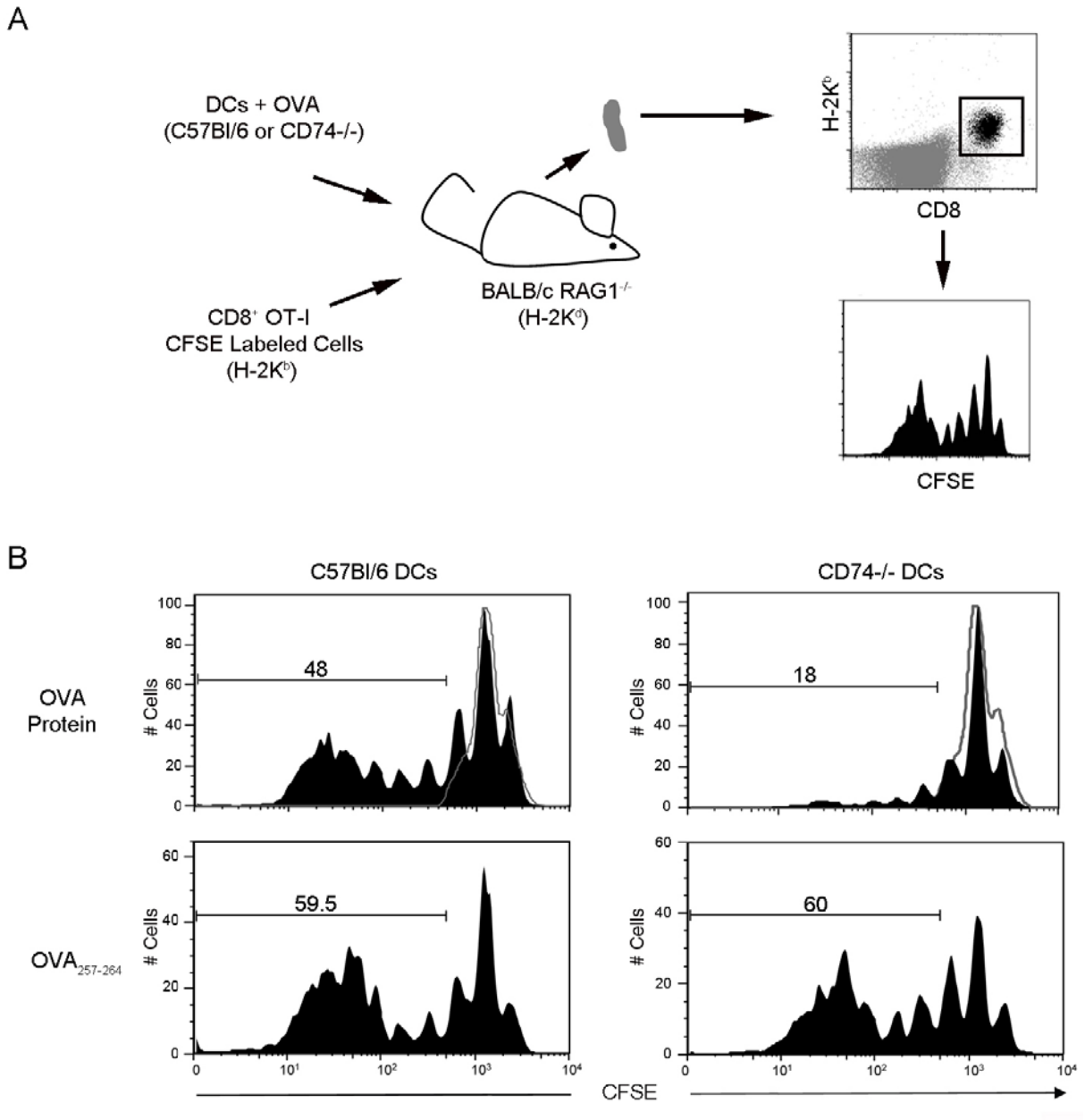

Figure 3.6. CD74$^{-/-}$ DCs are unable to cross present cell-associated antigens *in vivo* to prime antigen-specific CD8^{+} T cells.
(A) OVA protein or OVA$_{257-264}$ pulsed CD74$^{-/-}$ or C57Bl/6 DCs were injected with CD8^{+} OT-I CFSE-labelled T cells into RAG1$^{-/-}$ mice on a BALB/c background. Three days later, H-2K^{b}CD8^{+} T cells were assessed for proliferation. **(B)** Black histograms represents proliferating OT-I derived T cells from the spleens of representative mice (n=3).Grey histograms represent unproliferating OT-I T cells.

3.2.5 CD74-deficient DCs have an impaired ability to express MHC I/antigen complexes at the cell surface and prime T cells

Spleen-derived DCs from different mouse strains were examined for their ability to cross present the well-characterized, H-2K^b-restricted ovalbumin epitope OVA$_{257-264}$ *in vitro*. DCs were incubated with soluble OVA, with or without cytokines, and stained with anti-H-2K^b/OVA$_{257-264}$ antibody or co-cultured with B3Z, a T cell hybridoma that is activated following recognition of H-2K^b in association with the OVA$_{257-264}$ peptide [296]. Despite similar levels of total surface MHC I, CD74$^{-/-}$ DCs displayed substantially reduced levels of H-2K^b/OVA$_{257-264}$ complexes following OVA incubation compared to C57Bl/6 DCs (11.7 MFU vs 19.9 MFU; **Figure 3.7A**). It has been shown that cross priming capacity of DCs is differentially regulated by inflammatory mediators that induce upregulation of costimulatory and MHC molecules, and reduce endocytosis [328, 329]. This results in an increased capacity of T lymphocyte priming but lowers the ability of DCs to capture and present soluble antigens on MHC molecules. To test T cell activation in a situation resembling *in vivo* conditions that involves co-stimulation, OVA-pulsed DCs were incubated with B3Z T cells with and without cytokines. In the presence of TNF-α and IFN-γ, a significant difference in the ability of C57Bl/6 and CD74$^{-/-}$ DCs to activate B3Z T cells was observed (TNF-α: 880 vs 543 units; IFN-γ: 811 vs 420 units; $p<0.05$; **Figure 3.7B**) suggesting an important role for CD74 in T cell priming. As expected, no T cell activation was detected following incubation with OVA-pulsed DCs derived from TAP1$^{-/-}$ in the presence of cytokines.

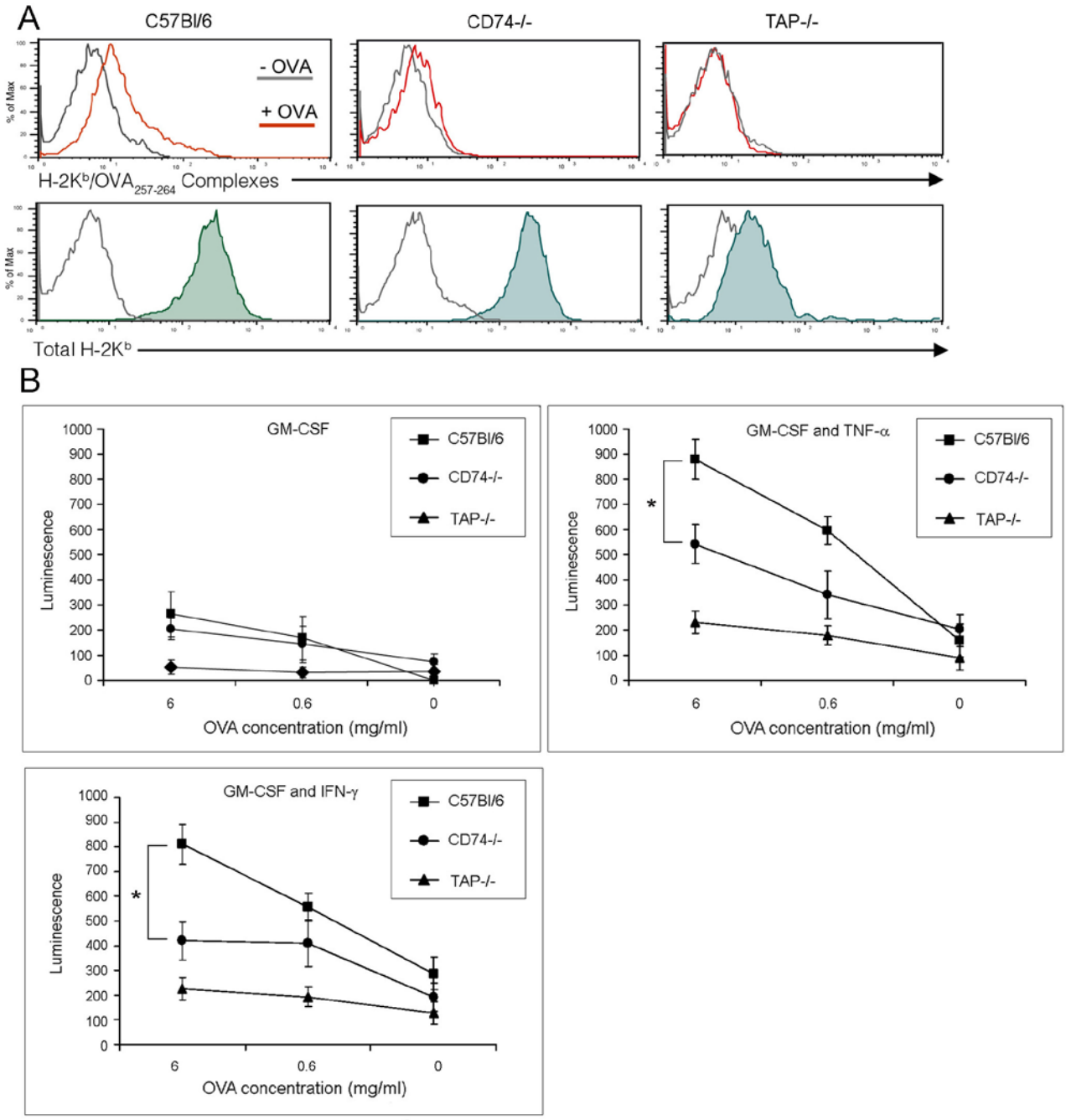
A
C57Bl/6
CD74-/-
TAP-/-
- OVA
+ OVA
% of Max
H-2K^b/OVA$_{257-264}$ Complexes
Total H-2K^b
B
GM-CSF
GM-CSF and TNF-α
GM-CSF and IFN-γ
C57Bl/6
CD74-/-
TAP-/-
Luminescence
OVA concentration (mg/ml)
6
0.6
0
*

Figure 3.7. Cross presentation and cross priming is defective in CD74$^{-/-}$ derived DCs. **(A)** Formation of H-2K^{b}/OVA$_{257-264}$ complexes on splenic DCs with (red) or without (grey) incubation with soluble OVA as well as total H-2K^{b} was measured by flow cytometry. Mean fluorescence intensities of one representative experiment are shown. **(B)** CD74$^{-/-}$ derived spleen DCs are less efficient in activating B3Z T cells. Spleen-derived DCs were incubated with soluble OVA as indicated, in the presence of GM-CSF plus TNF-α or IFN-γ. Activation of B3Z T cells was measured using a chemiluminescent assay. Data depict means (± SD) of triplicate samples for each OVA concentration. Similar results were observed in 3 separate experiments. * $p < 0.05$

3.2.6 CD74-deficient DCs have reduced MHC I loading in cross priming compartment

To better understand the mechanism of cross priming and presentation deficiency at a molecular level, comparative immunofluorescent confocal microscopy (ICM) was used to determine the intracellular localization, trafficking and distribution of $OVA_{257-264}$ loaded MHC I in C57Bl/6 and $CD74^{-/-}$ DCs with and without TNF-α. Intracellular staining was performed with antibodies against $H\text{-}2K^b/OVA_{257-264}$ (red) and the late endosome marker, LAMP1 (green), following incubation with OVA protein. Of the C57Bl/6 splenic DCs staining positive for $H\text{-}2K^b/OVA_{257-264}$ complexes, colocalization with the late endosomal marker was detectable in a considerable number of cells when no TNF-α was added to the culture (**Figure 3.8**). In the $CD74^{-/-}$ and $TAP1^{-/-}$ DCs, some $H\text{-}2K^b/OVA_{257-264}$ complexes were identified; however, colocalization with late endosomes was not observed. Following treatment with TNF-α, more than 80% of C57Bl/6 DCs demonstrated strong colocalization of $H\text{-}2K^b/OVA_{257-264}$ complexes with late endosomal marker (**Figure 3.8**). In contrast, insignificant numbers of $H\text{-}2K^b/OVA_{257-264}$ complexes were observed in late endosomal compartments in $CD74^{-/-}$-derived DCs indicating that the $H\text{-}2K^b/OVA_{257-264}$ complex formation in late endosomes was reduced. Quantification of the ICM data indicated that in the presence of TNFα, $CD74^{-/-}$-derived DCs had significantly less $OVA_{257-264}$ loaded onto $H\text{-}2K^b$ in the late endosomes (62% vs 32%; $p<0.05$; **Figure 3.8**). In all, the data suggests that a CD74-dependent MHC I antigen processing pathway exists in DCs that is required for the cross presentation of exogenous antigens.

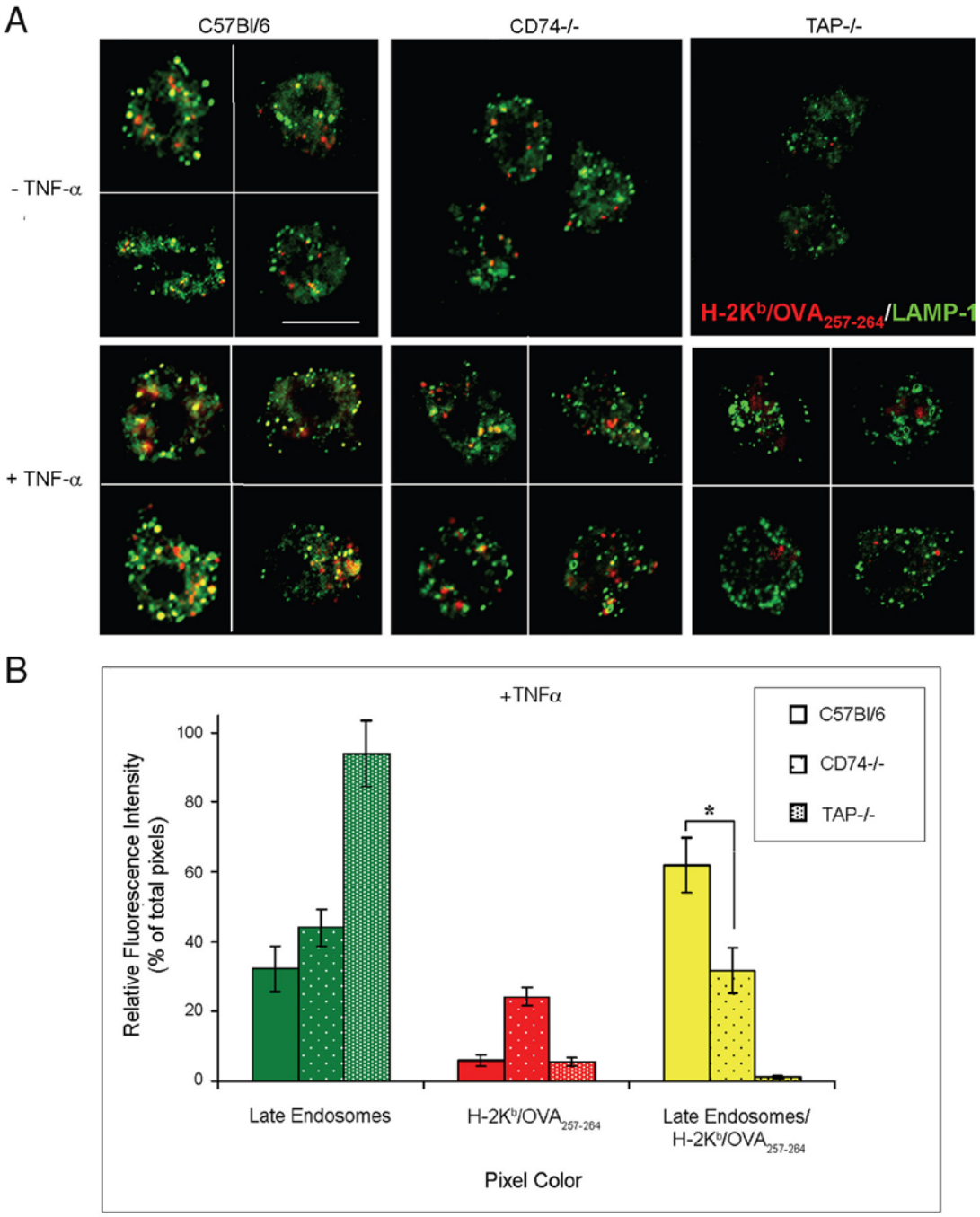
A
C57Bl/6
CD74-/-
TAP-/-
- TNF-α
+ TNF-α
H-2K^b/OVA$_{257-264}$/LAMP-1
B
+TNFα
C57Bl/6
CD74-/-
TAP-/-
Relative Fluorescence Intensity
(% of total pixels)
100
80
60
40
20
0
*
Late Endosomes
H-2K^b/OVA$_{257-264}$
Late Endosomes/
H-2K^b/OVA$_{257-264}$
Pixel Color

Figure 3.8. Cross presentation and cross priming is defective in CD74$^{-/-}$-derived DCs.

(A) The presence of H-2K^b/OVA$_{257-264}$ complexes in endolysosomal compartments of CD74$^{-/-}$-derived spleen DCs following overnight incubation with OVA is reduced compared to C57Bl/6 DCs. Mature spleen-derived DCs incubated with OVA were costained with H-2K^b/OVA$_{257-264}$ specific antibody (red) and LAMP1 (green). The figure shows optically merged images representative of the majority of cells examined by ICM. Scale bar, 5 μm. **(B)** Quantitative assessment of K^b/OVA$_{257-264}$ in late endosomes of DCs with TNFα treatment. Graph depicts individual color pixel percentages per total pixels ± SD. * $p < 0.05$

3.2.7 CD74 interacts with MHC I in the ER and directs transport to the cross priming compartment

The interaction of CD74 with MHC I in DCs as a prerequisite of targeting MHC I to the cross priming compartment was investigated at the molecular level. Spleen-derived DCs were isolated from C57Bl/6 and CD74$^{-/-}$ mice for analysis by ICM. DCs were stained with antibodies against H-2K^{b} (green) and CD74 (red). H-2K^{b} molecules were found to be distributed at the cell surface and to localize intracellularly mainly to vesicular-like compartments. Importantly, the microscopy analysis showed that CD74 molecules colocalized markedly with these intracellular compartments (**Figure 3.9A**, top panel). In the endolysosomes of TAP1$^{-/-}$ DCs, a reduced colocalization of H-2K^{b} with CD74 was observed, presumably due to the restricted availability of H-2K^{b} to traffic to the endolysosomes from the plasma membrane. To identify the compartment where these molecules colocalize, spleen DCs were co-stained with antibodies recognizing H-2K^{b} (green) and LAMP1 (red) that detects late endosomes. A considerable proportion of late endosomes contained H-2K^{b} in C57Bl/6 DCs, confirming that a substantial amount of MHC I reside in the endocytic compartment [59, 330]. In contrast, a reduced fraction H-2K^{b} colocalized with late endosomes in CD74$^{-/-}$ DCs (**Figure 3.9A**, mid panel). This was confirmed by quantification of ICM images and suggests that fewer MHC I molecules were targeted to the endolysosomal compartment in CD74$^{-/-}$ vs C57Bl/6 DCs (73% vs 47%; **Figure 3.9B**). Co-localization was even less evident in the TAP1$^{-/-}$ DCs possibly due to the impaired targeting of H-2K^{b} molecules to endolysosomes in the absence of TAP1. From the data, it can be concluded that a substantial fraction of MHC I

A

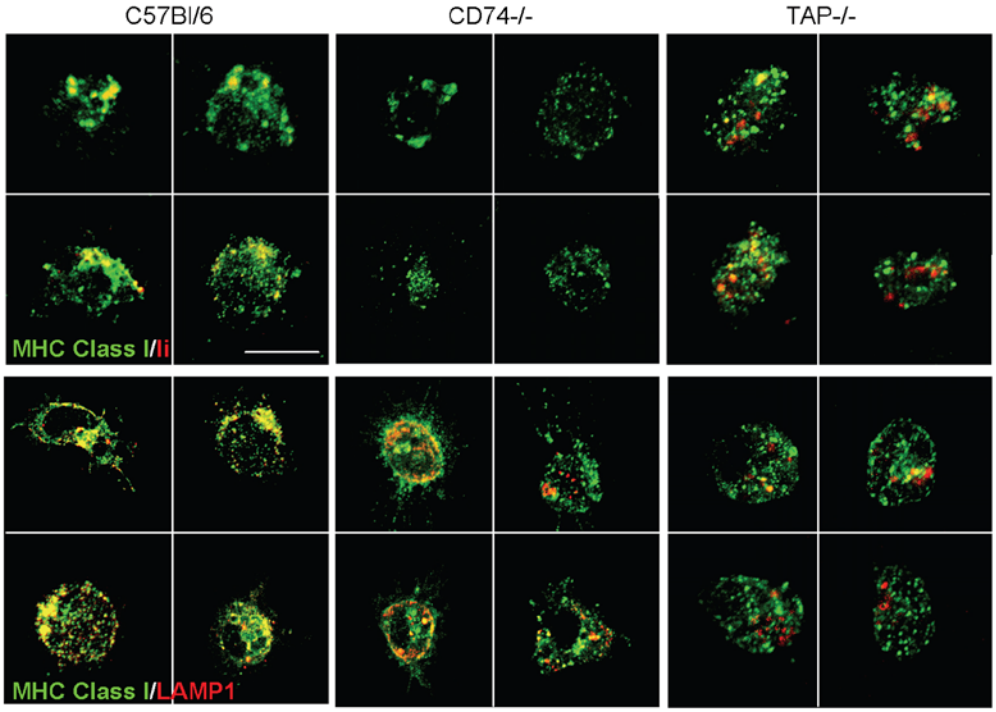
C57Bl/6
CD74-/-
TAP-/-
MHC Class I/Ii
MHC Class I/LAMP1

B

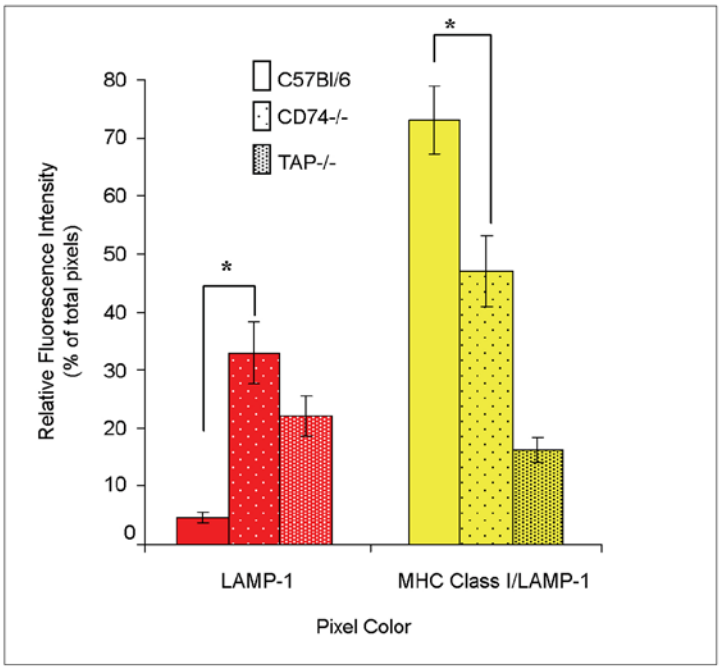
C57Bl/6
CD74-/-
TAP-/-
Relative Fluorescence Intensity
(% of total pixels)
80
70
60
50
40
30
20
10
0
*
*
LAMP-1
MHC Class I/LAMP-1
Pixel Color

Figure 3.9. CD74 controls MHC I localization to endolysosomes in DCs.
(A) A small fraction of MHC I reach late endosomes in $CD74^{-/-}$ DCs. Mature splenic DCs were stained with anti-H-$2K^b$ (green) and anti-CD74 (red) or anti-LAMP1 (red) antibodies. Representative images as examined by ICM are shown. Scale bar, 5 μm. **(B)** Quantitative assessment of MHC-I in $LAMP1^+$ compartments was performed (50 DCs/mouse strain). Graphs depicts individual color pixel percentages/total pixel (mean ± SD). * $p < 0.05$

molecules interact with CD74 facilitating their transport to the endolysosomes compartment of DCs likely from the ER.

3.2.8 CD74 and MHC I molecules form a molecular complex in DCs

Demonstration of a direct molecular interaction between MHC I and CD74 in DCs would further strengthen the argument that this is a yet undescribed pathway of antigen presentation in DCs. To this end, bmDCs from various knock-out and wild type mice were ^{35}S-labelled, and MHC I (H-2K^{b}), MHC II (I-A^{b}) or CD74 bound complexes were co-immunoprecipitated and proteins in these complexes were identified based on apparent molecular weight. MHC II co-immunoprecipitated with the abundant 41 and 31 kDa isoforms of CD74 (**Figure 3.10A**). Importantly, the anti-H-2K^{b} antibody also co-precipitated these same proteins corresponding to the CD74 isoforms (**Figure 3.10A**). These 41 and 31 kDa proteins were not present in the CD74$^{-/-}$ DCs (**Figure 3.10A**) demonstrating that they are indeed the previously reported isoforms of CD74 that have been shown to co-immunoprecipitate with MHC II molecules. In addition, the CD74 isoforms were co-immunoprecipitated with H-2K^{b} in TAP1$^{-/-}$ DCs, showing that CD74 binding to MHC I is "TAP independent". Finally, we demonstrated that there is a greater amount of 31 kDa CD74 isoform co-precipitated with MHC I from β_2m$^{-/-}$-derived DCs suggesting that while CD74 binds the folded β_2m-associated MHC I complex there exists a preference for unfolded and peptide-free MHC I heavy chain of newly synthesized MHC I molecules (**Figure 3.10A**). This suggests a complex cycle of MHC I-CD74 interaction in which stable β_2m-dependent peptide loading is not required for the formation for the CD74-MHC I complex.

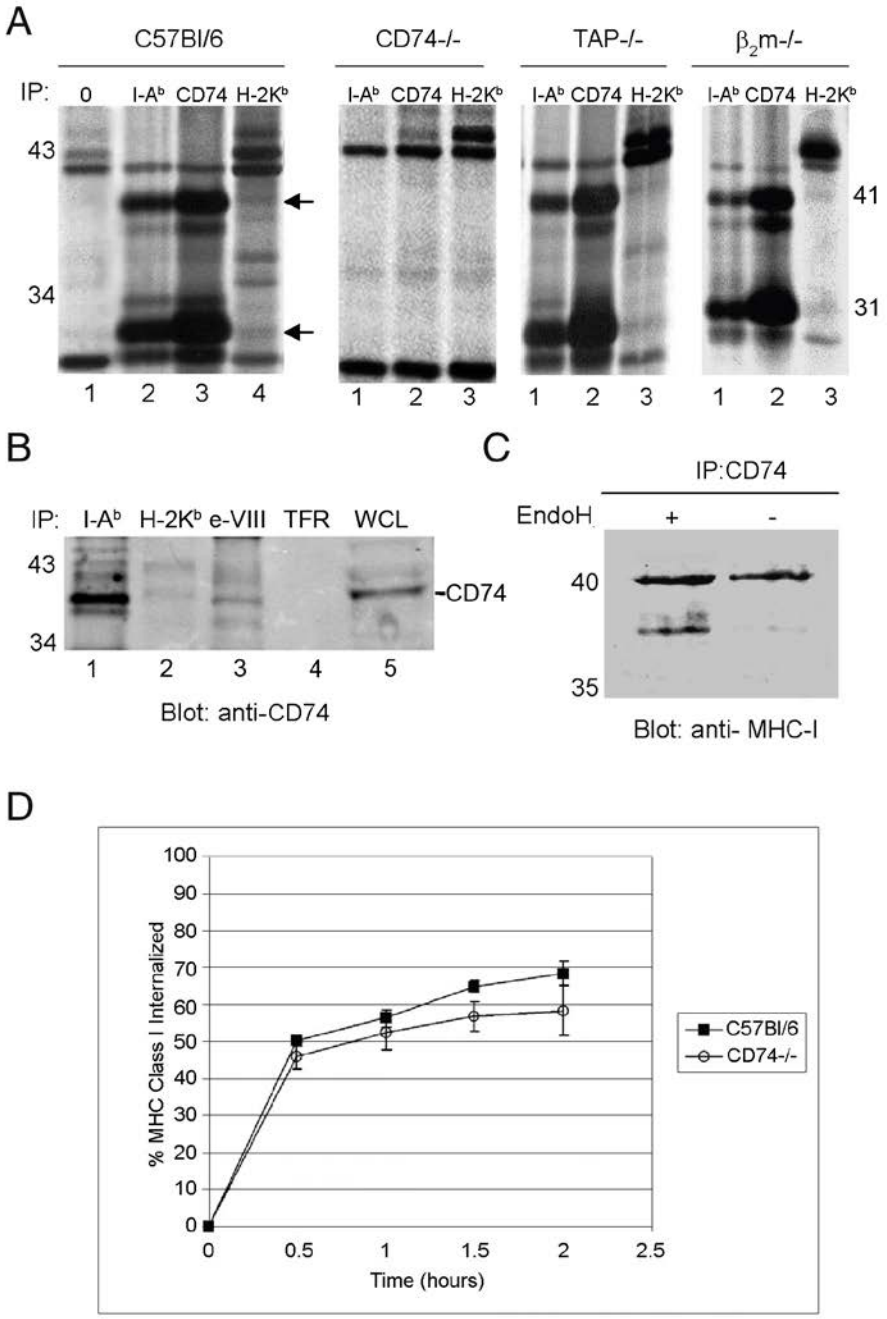
A
C57Bl/6
CD74-/-
TAP-/-
β2m-/-
IP:
0
I-Ab
CD74
H-2Kb
43
34
41
31
1 2 3 4
1 2 3
1 2 3
1 2 3
B
IP: I-Ab H-2Kb e-VIII TFR WCL
43
34
CD74
1 2 3 4 5
Blot: anti-CD74
C
IP:CD74
EndoH
+
-
40
35
Blot: anti- MHC-I
D
% MHC Class I Internalized
Time (hours)
C57Bl/6
CD74-/-

Figure 3.10. CD74 controls MHC I ER-to-endolysosome trafficking in DCs.
(A) CD74 associates with MHC I. Immunoprecipitation using anti-H-2K^b, anti-I-A/I-E and anti-CD74 antibodies was performed on [^{35}S]methionine-labelled bm-derived DC. The CD74 41 and 31 kDa protein bands are indicated. **(B)** Immunoprecipitation with antibodies against I-A^b, H-2K^b (conformationally dependent), H-2K^b cytoplasmic domain (e-VIII; conformationally independent) and transferrin receptor (TFR) was performed with C57Bl/6 DC lysates. The identity of the co-immunoprecipitated proteins was confirmed by blotting with anti-CD74 antibody. Whole cell lysate (WCL) was blotted as a control. **(C)** DC lysates were immunoprecipitated with an anti-CD74 antibody and digested with endoglycosidase H. Western blotting with anti-MHC I antibody was used to assess the MHC I fraction precipitated by CD74 antibody and to visualize the acquisition of EndoH resistance of the MHC I subset interacting with CD74. **(D)** DCs labelled with an anti-H-2K^b antibody were assessed overtime for MHC I internalization measured by flow cytometry as a reduction in mean fluorescence intensities over time. Error bars represent SD.

Western blotting was then performed to confirm the identity of the CD74 isoforms bound to MHC I molecules. Immunoprecipitation with antibodies against I-A^b, H-$2K^b$ and the exon-VIII region of the MHC I molecule as well as an irrelevant antibody against transferrin receptor (TFR) was followed by blotting with an anti-CD74 antibody. CD74 was precipitated with H-$2K^b$ confirming that this interaction is detectable and stable (**Figure 3.10B**).

3.2.9 CD74 and MHC I form a complex in a pre-Golgi compartment rapidly after synthesis

Next, in order to unequivocally demonstrate the kinetics and origin of the MHC I-CD74 interaction, we used biochemical means to further deduce the intracellular compartment where the CD74 and MHC I interaction takes place. Proteins within the secretory pathway acquire Endo H resistance as they traffic from the endoplasmic reticulum through the Golgi compartment and there, undergo cleavage by mannosidase II [331]. It is well accepted that Endo H sensitivity acts as an indication that proteins are localized to the ER or in “transitional elements” between the ER and cis-Golgi. CD74-bound MHC I was immunoprecipitated from C57Bl/6 bmDCs with an anti-CD74 antibody and treated with Endo H. Western blotting was performed with an anti-MHC I antibody to visualize the Endo H sensitivity of the CD74-bound MHC I subset. We clearly identify that a significant fraction of MHC I that associates with CD74 is Endo H sensitive as determined by the presence of a 38 kDa MHC I band (**Figure 3.10C**). This suggests that the CD74 interaction with the MHC I originates in the ER where the CD74 binds the ‘immature’ fraction of MHC I molecules and from here initiates trafficking to

the cross priming compartment. Altogether, these data confirm that a substantial amount of CD74 is bound to MHC I as a prerequisite to the transport of a subset of the ER pool of MHC I molecules to the endolysosomal compartment that plays a crucial role in cross presentation, T cell priming and primary immune responses [59, 65].

3.2.10 CD74 does not affect cell surface internalization of MHC Class I

Lastly, to further examine the source of MHC I that binds CD74, the role of CD74-mediated MHC I trafficking from the plasma membrane was examined. To determine if CD74 functions in surface receptor recycling, we followed the internalization of MHC I in C57Bl/6 and CD74$^{-/-}$ DCs. BmDCs were stained with anti-H-2K^{b} antibodies and flow cytometric analysis was used to follow internalization over time. As shown in **Figure 3.10D**, C57Bl/6 and CD74$^{-/-}$ DCs have very similar dynamics of MHC I internalization. This indicates that CD74 is not interacting with MHC I at the cell surface to cause internalization into an intracellular compartment for cross presentation. This contrasts our other studies that demonstrate a tyrosine-based motif in the cytoplasmic domain of MHC I molecules is crucial for internalizing MHC I molecules into the endolysosomal cross priming compartment from the plasma membrane [59, 65] and thus reveals a unique pathway of CD74-dependent MHC I trafficking.

3.3 Discussion

The dichotomy of MHC II molecules presenting exogenous peptides versus Class I molecules displaying cytosolic peptides has been revised [59, 62, 332, 333]. Not only

does MHC I cross presentation demonstrate the blurring of this division, but it also shows that for specific cell types such as DCs this phenomenon plays a major role in generating primary immune responses *in vivo* [59]. In addition, the presentation of endogenously-derived peptides on MHC II molecules demonstrates that MHC I and II pathways likely intersect and that they may share the same antigen-loading compartments [334, 335]. Although CD74 is classically recognized as a major chaperone in MHC II presentation, MHC I and CD74 have also been shown to interact [60, 61, 336, 337]. However, the physiological contribution of CD74 to MHC I mediated immune responses *in vivo* has not been investigated and the previous identification of CD74-MHC I interaction was largely discounted as biological curiosity. Thus, to our knowledge, this is the first demonstration that CD74 contributes significantly to MHC I antigen processing pathways including cross presentation and cross priming in DCs. These studies demonstrate a major role for CD74-dependent cross priming in the generation of responses against viral and cell-associated antigen.

In order to undertake this work, previous work of others that demonstrated that CTL responses against viruses such as VSV are CD4-independent [322, 323] and thus independent of the function of MHC II/CD74 was confirmed. To dissect direct endogenous and cross presentation in T cell priming, low viral doses were used to mimic a physiological situation where DCs would presumably be spared from infection and other infected cells would act as antigenic peptide donors (**Figure 3.1**). The observation that mice lacking CD74 are significantly impaired in their ability to generate MHC I-restricted CTL responses, particularly against low viral doses where cross priming is likely to dominate over direct priming by DCs, supports the conclusion that MHC I cross

presentation is the primary mechanism by which antiviral $CD8^+$ T cell-mediated immunity is generated under physiological conditions *in vivo* [59, 338, 339].

The generation of bone marrow chimeras made it possible to study the performance of myeloid $CD74^{-/-}$ derived DCs on a different host background (**Figure 3.2**). These studies led to the conclusion that CD74's priming defect was of DC origin and indicated that the deficit lies at the level of DC cross presentation. Further, CD74-dependent cross priming was revealed as a major MHC I antigen presentation pathway as the absence of CD74 resulted in a greater than 50% decrease in the number of anti-VSV CTLs. (**Figure 3.1 and Figure 3.3**). In addition, the findings obtained by mouse chimeras support the observations that the CD74 deficiency in generating primary immune responses against VSV, as previously shown, is independent of the reduced $CD4^+$ T cells [322, 340]. This is in accordance with other recent data that demonstrate that T_H cells are required for secondary, but not primary CTL expansion [341]. C57Bl/6→$CD74^{-/-}$ chimeras exhibited virtually no $CD4^+$ T cells above the controls. However, they were able to generate significant numbers of VSV specific $CD8^+$ T cells and produce effectors with a killing capacity equivalent to C57Bl/6→C57Bl/6 controls. In contrast, $CD74^{-/-}$→C57Bl/6 chimeras containing normal $CD4^+$ numbers proved severely deficient in antiviral response supporting others' suggestions that costimulation of the $CD8^+$ CTL by B7 molecules, along with TCR stimulation, can be sufficient to elicit $CD8^+$ CTL without T cell help [322]. In addition, it is entirely possible that two distinct lineages of $CD8^+$ CTLs precursors exist whereby the T_H-independent population provides the predominant response to various viruses resulting in no loss of CTL function in the absence of $CD4^+$ T cells [340].

As visualized by ICM, the loading of MHC I with the OVA epitope in endolysosomes of DCs was reduced by 50% when CD74 was absent (**Figure 3.8**). The deficiency of $CD74^{-/-}$ or $CD74^{-/-}\rightarrow$C57Bl/6 -derived DCs to cross present was confirmed by assaying the inability of $CD74^{-/-}$ or $CD74^{-/-}\rightarrow$C57Bl/6 -derived DCs to induce proliferation in $OVA_{257-264}$ specific T cells in an *in vivo* model of cell-associated antigen (**Figure 3.5**). The activation of OVA antigen specific $CD8^+$ T cells, however, could be rescued in C57Bl/6-repopulated $CD74^{-/-}$ mice despite their low $CD4^+$ T cell numbers confirming that the deficiency resides with DCs and is T_H independent [342, 343]. Additionally, the deficiency of $CD74^{-/-}$ DCs to activate $CD8^+$ T cell in $RAG^{-/-}$ mice that completely lack $CD4^+$ T cells, unequivocally demonstrates that the defect in DC cross priming function is due to the absence of CD74. This experiment further addresses previous observations that CD74 plays a role in cell migration as assessed using *in vitro* assays of motility that employ microfabricated channels that mimic the confined environment of peripheral tissues [327]. Here, it is demonstrated *in vivo* that CD74 deficient and wild type DCs pulsed with exogenous peptide and injected *iv* were equally capable to prime $CD8^+$ T cells transferred into $RAG^{-/-}$ mice as assessed by CFSE dilution in $CD8^+$ cells recovered from the spleen (**Figure 3.6**). This data demonstrates that the CD74-deficiency does not alter DC homing and motility in our *in vivo* system and supports the conclusion that a CD74-dependent MHC I dendritic cell cross priming pathway is a physiologically important process.

Using direct biochemical analyses, the first example of an association between MHC I molecules and CD74 under physiological conditions in DCs is provided. The CD74 protein was consistently co-precipitated by anti-MHC I antibodies. Inversely, the MHC I

interaction was also confirmed by co-precipitation with anti-CD74 antibodies. Interestingly, the amount of CD74 protein was increased in DCs lacking β_2m. This indicates that the conformational change following MHC I assembly with β_2m is not an absolute requirement for CD74 binding with MHC I [60] suggesting that CD74 association with MHC I is independent of stable peptide loading in the ER. It also suggests that upon CD74 dissociation in endolysosomes, the reassembly of MHC I heavy chain with β_2m and antigenic peptides could then take place in the endolysosomal compartment [344] (**Figure 3.8**). In this context, we have directly demonstrated that the MHC I-CD74 complex remains localized in vesicular-like compartments identified as late endosomes (**Figure 3.9**). Furthermore, we have established that CD74 influences the presence of MHC I in endolysosomes confirming previous observations that an MHC I-CD74 interaction results in targeting of a subset of MHC I molecules to the endolysosomal pathway [61], though in this case it was inferred, likely incorrectly, that they had entered this pathway from the cell surface (**Figure 3.9**). Similar to studies in human B cell lines, the 31 kDa isoform of CD74 was consistently co-immunoprecipitated with MHC I in TAP1$^{-/-}$ DCs (**Figure 3.10**) indicating that the MHC I-CD74 interaction occurs in the absence of TAP [60]. Nonetheless, our ICM studies showed that the overall presence of MHC I in late endosomes of TAP1$^{-/-}$ DCs was reduced. In contrast to the cytoplasmic tail tyrosine mutants we previously described [59, 65, 66], it is unlikely that a stable interaction between CD74 and MHC I molecules occurs at the plasma membrane as the absence of CD74 in DCs does not appear to influence MHC I internalization (**Figure 3.10**). Our results support a model that both MHC I recycling from the plasma membrane through recognition of the tyrosine internalization signal found in the MHC I

cytoplasmic and those targeted from the ER through the binding of the CD74 chaperone contribute to the pool of MHC I molecules in the endolysosomal pathway that are receptive to exogenous antigenic peptides. Thus, in an analogous manner to MHC II molecules, the MHC I-CD74 complex is formed in the ER and may be held in a conformation that masks peptide binding as they transit to the cross priming compartment. In support of this, two independent studies have shown that CD74 peptides, including a smaller peptide derived from the core CLIP peptide, can be eluted from MHC I molecules [345, 346]. Such peptides are therefore strong candidates for the MHC I equivalents of CLIP (MRMATPLLM). This CLIP-derived (CLIPD) peptide may prevent premature peptide binding akin to MHC II situation [345, 347]**.** In this model, following CD74 digestion and removal, MHC I could be loaded with high affinity cathepsin S-derived exogenous peptides and progress to the cell surface where they could efficiently prime T cell precursors to become activated. Finally, previous reports that a pool of MHC I transports to late endosomes in a TAP-dependent manner [318], suggests that CD74 assembly with MHC I at a post-ER location, perhaps in a post-Golgi compartment can not be excluded.

The dichotomy of MHC II molecules presenting exogenous peptides versus MHC I molecules displaying cytosolic peptides has been revised [59, 62, 332, 333]. Not only does MHC I cross presentation demonstrate the blurring of this division, but it also shows that for specific cell types such as DCs this phenomenon plays a major role in generating primary immune responses *in vivo* [59]. In addition, the presentation of endogenously-derived peptides on MHC II molecules demonstrates that MHC I and II pathways likely intersect and that they may share the same antigen-loading compartments [334, 335].

Although CD74 is classically recognized as a major chaperone in MHC II presentation, MHC I and CD74 have also been shown to interact [60, 61, 336, 337]. However, the CD74 contribution to MHC I mediated immune responses *in vivo* has not been investigated and the previous identification of CD74-MHC I interaction was largely discounted as biological curiosity. Thus, to our knowledge, this is the first demonstration that CD74 contributes significantly to MHC I antigen processing pathways including cross presentation and cross priming in DCs.

CHAPTER 4.THE MOLECULAR EFFECTS OF HIV-NEF ON DC ANTIGEN PRESENTATION FUNCTION *IN VITRO*

4.1 Introduction

Activation of cytotoxic T-lymphocytes (CTLs) is essential for immune responses against viruses. This includes responses against Human Immunodeficiency Virus (HIV) and secondary infections that are fatal to HIV-infected individuals [103, 348]. This is best evidenced through examination of 'elite controllers' (EC), a group of individuals that test positive for HIV-1 yet have extremely low rates of disease progression and appear to control viral levels in the body [349, 350]. Maintenance of polyclonal anti-HIV $CD8^+$ effector cells capable of degranulation and production of cytokines has been identified as one key distinguishing factor of ECs [103, 351-353].

The process of activation, proliferation and differentiation of naive T cells into armed effector CTLs is dependent on activation by antigen presenting cells (APCs). Dendritic cells (DCs) are thought to be the key APCs in this process as they have the capacity to cross present antigen. The cross presentation pathway allows for the presentation of exogenous antigen and is critical for establishing $CD8^+$ T cell responses against viruses [41]. The vacuolar model of cross presentation requires the trafficking of major histocompatability complex I (MHC I) from the cell surface or endoplasmic reticulum (ER) to an endolysosomal compartment where antigenic loading with exogenous peptides can take place [53, 59, 62]. From here, MHC I can travel to the cell

A version of Chapter 4 is prepared for publication: Kyla Omilusik, Anna T. Reinicke, and Wilfred A. Jefferies. (2011). HIV-1Nef Impairs Dendritic Cell MHC I Cross-Presentation.

surface for activation of effective $CD8^+$ T cell responses.

Many viruses have evolved effective immune-evasion mechanisms to survive in their host and HIV is no exception. HIV appears to have developed a means to disrupt CTL responses. In HIV-infected individuals, it has been documented that downregulation of human leukocyte antigen (HLA)-A and HLA-B but not HLA-C from the cell surface of infected cells occurs [354, 355]. HIV presumably uses this as an escape mechanism to avoid detection by CTLs and effectively persist in its host [103]. Nef, a HIV accessory protein that is not essential for replication but is important for viral pathogenicity [147, 154], has been implicated in this function. In fact, the expression of Nef appears to reduce the susceptibility of HIV-infected cells to CTL lysis [356, 357]. Nef has no enzymatic activities but has been likened to an adaptor protein that binds host proteins and diverts them from their normal trafficking routes and subsequently disrupts their functions [358, 359].

HIV predominately infects $CD4^+$ T cells and macrophages; however, myeloid DCs, plasmacytoid DCs and Langerhans cells have been shown to be support HIV infection as well (reviewed in [117]). At infection sites, DCs are one of the first cells to encounter HIV [360]. Upon interaction with HIV, DCs migrate to lymphoid organs rich in $CD4^+$ T cells that are susceptible to HIV infection [117]. It has been proposed that DCs may act as long-lived, motile HIV reservoirs disseminating virus throughout the blood and tissues [95, 117]. To allow HIV survival in DCs and subsequent transfer of virus to $CD4^+$ T cells, HIV must interfere with the DC's function. This has been observed in HIV positive individuals as deregulation of DC cytokine production [141, 361, 362], decreased costimulatory molecule expression [143] and a reduction in the ability to stimulate

allogenic T cells [142, 363, 364]. DC modulation may function as a key viral immune evasion mechanism preventing activation of virus-infected CTLs and consequently facilitating viral persistence [365, 366].

As the HIV protein, Nef, is an important molecule in HIV pathogenicity [147, 154] and functions as a virulence factor, it presumably plays a role in impairing the function of HIV infected DCs. Changes in DC morphology and function upon expression of Nef have been documented including the downregulation of surface MHC I [136, 169, 366-368]. This suggests that Nef is influencing the trafficking of MHC I in DCs. One disconcerting consequence of this would be improper routing of MHC I through the antigen presentation pathways. Importantly, Nef may affect the efficiency of DC cross presentation and subsequent $CD8^+$ T cell cross priming. Cross presentation to activate immune responses is a vital function of DCs and essential to the proper clearance of infection. Therefore, Nef-mediated interference of this pathway would be beneficial to immune evasion, allowing HIV persistence in the host.

The role Nef plays in subverting recognition of infected cells that would normally be targets for CTLs has been described; however, the effects of Nef in DCs, the cells responsible for activating the CTLs in the first instance is unclear. In this chapter, a Nef-expressing DC line was created to study the impact of Nef on MHC I classical and cross presentation in DCs. The results of this study collectively demonstrate that Nef exploits trafficking in DCs. Nef appears to manipulate the DC sorting pathways to block trafficking of newly synthesized MHC I-peptide complexes at the trans Golgi network (TGN) and to remove MHC I–peptide complexes from the cell surface. The result is that MHC I classical and cross presentation of viral antigen is disrupted and subsequent

priming of naïve immune responses is impaired. HIV's potential to infect and impair this pathway could potentially be a factor leading to the immunosuppressive characteristics of acquired immunodeficiency syndrome (AIDS).

4.2 Results

4.2.1 Nef reduces the surface expression of MHC I, MHC II and co-receptors

To study the role of HIV-1 Nef in DC function, a Nef-expressing DC line was created. DC2.4 cells [295] were transfected to stably express wild type HIV-1 Nef (pNL432; Nef accession number: AF324493) and GFP or with empty vector to express GFP alone. Bulk cell cultures of both lines expressed GFP at similar levels (**Figure 4.1A**). Expression of the Nef protein was confirmed by both RNA and protein analysis (**Figure 4.1B,C**). Upon expression of Nef, the surface level of several receptors important for activation of immune responses decreased as compared to the vector alone control (**Figure 4.2A**). Nef-expressing DCs had a 1.4-fold dowregulation of surface MHC I ($p<0.01$) and a 1.5-fold downregulation of surface MHC II ($p<0.05$) while the co-receptors CD40 and CD86 were reduced 2.2 ($p<0.001$) and 1.2 times ($p=0.07$), respectively (**Figure 4.2B**). When activated during an immune response, DCs upregulate costimulatory molecules and MHC. This allows for efficient priming of T cell responses [369]. To determine if Nef expression affects the degree of receptor upregulation, DCs were activated with interferonγ (IFNγ) [370] and examined by flow cytometry. Following DC maturation, overall surface expression levels were increased in the presence of Nef; however, distinct dowregulation of surface MHC I, MHC II and CD40 as compared to

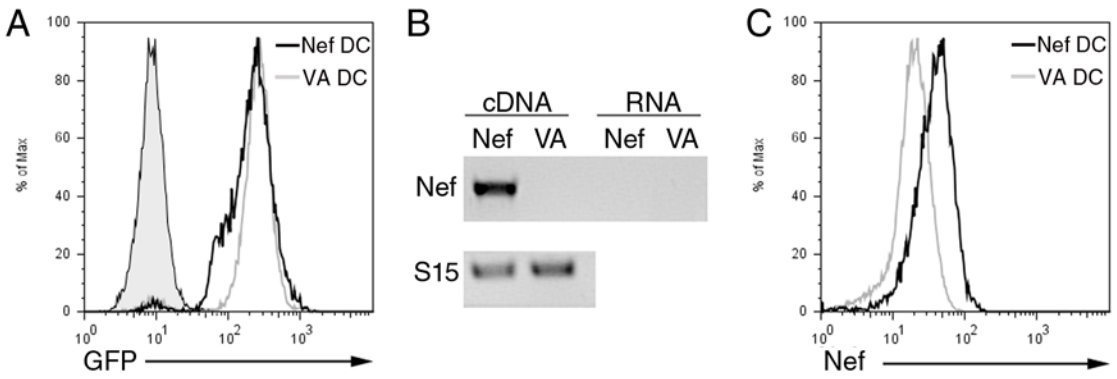

Figure 4.1. Expression of Nef in DCs.
DC2.4 cells were transfected with Nef pMX-PIE Vector (Nef) or pMX-PIE Vector alone (VA). Cells were selected with puromycin and bulk sorted for **(A)** GFP expression. Nef expression was confirmed by **(B)** RT-PCR with *nef* specific primers and by **(C)** FACS analysis. Black = Nef DCs; Grey = VA DCs; Shaded = untransfected DCs

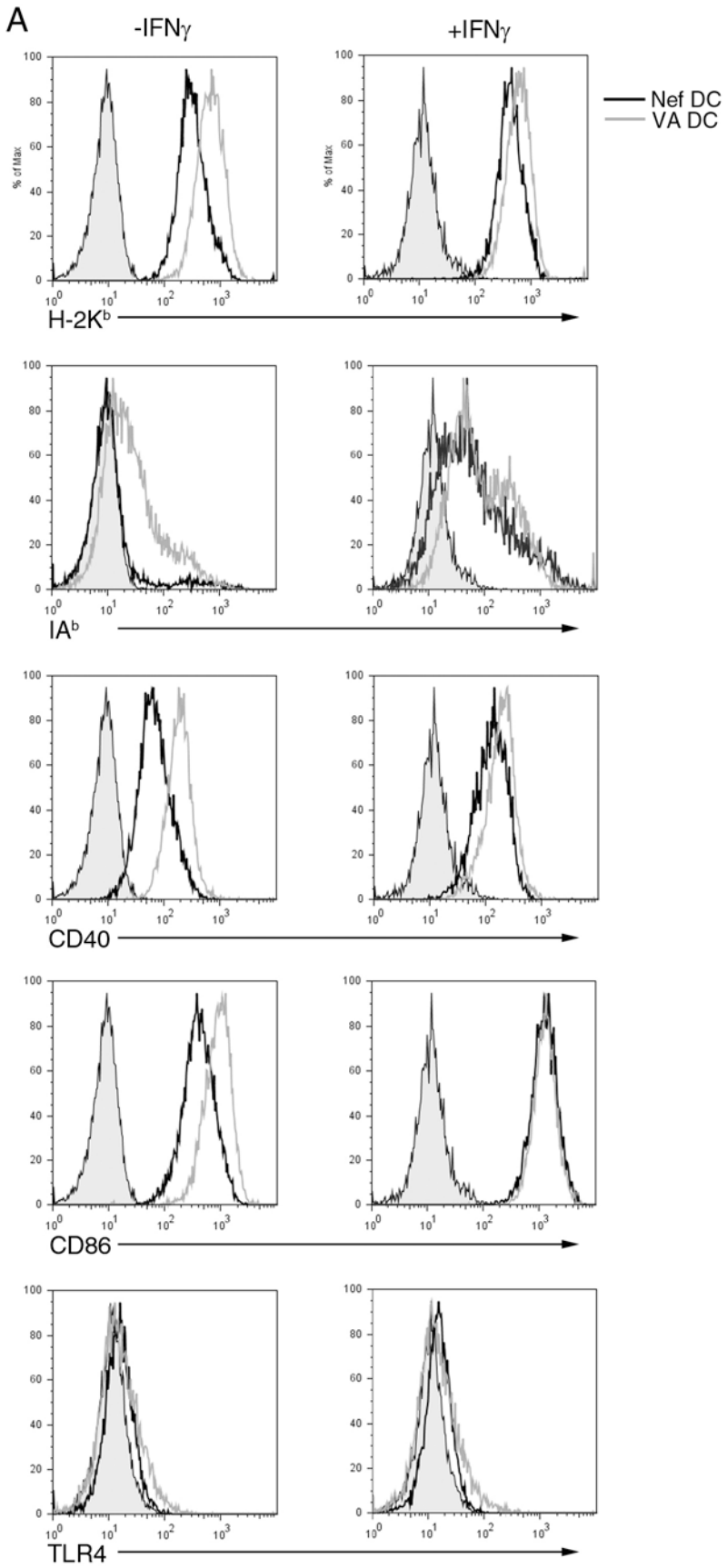
A
-IFNγ
+IFNγ
Nef DC
VA DC
% of Max
H-2K^b
IA^b
CD40
CD86
TLR4

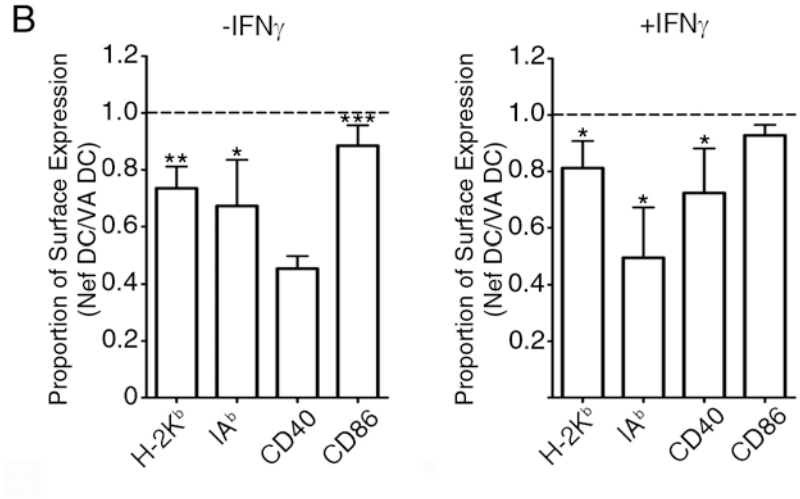

Figure 4.2. Nef downregulates DC surface markers contributing to deficient immune activation.

(A) FACS analysis was performed on unactivated (no IFNγ) and IFNγ activated Nef-expressing and vector alone (VA) DCs to determine the degree of down-regulation associated with Nef expression. Black = Nef DCs; Grey = VA DCs; Shaded = Negative Staining Control. **(B)** The fold difference in mean fluorescent units (± SE) between Nef and VA DCs was calculated and expressed as the proportion of Nef DC surface expression compared to VA DCs. (no IFNγ: n=14-15; with IFNγ: n=3-4). *$p<0.05$; **$p<0.01$; ***$p<0.001$

control DCs was still maintained at 1.2 ($p<0.05$), 2.0 ($p<0.05$) and 1.4-fold ($p<0.05$) respectively (**Figure 4.2**). Deficient surface expression of immune receptors on Nef-expressing DCs suggests a deficiency in activation of immune responses against HIV and secondary infections.

4.2.2 Nef decreases antigen presentation and priming ability

Dendritic cells function to efficiently capture and present antigen for T cell activation. Therefore, the effect of Nef on the DCs ability to present antigen and subsequently prime T cells was investigated. First, the ability of Nef-expressing DCs to cross present was examined. Nef and VA DCs were incubated overnight with graded doses of the well-characterized exogenous protein antigen, ovalbumin (OVA). To assess the ability of DCs to take up OVA and cross present it in the context of MHC I, the formation of OVA-MHC I complexes on the cell surface was evaluated (**Figure 4.3A**). VA DCs could present OVA on H-2K^b in a dose-dependent manner and this ability was almost completely abolished in the Nef-expressing DCs. The defect was quantified by determining the fold decrease of H-2K^b/OVA on the cell surface of Nef DCs compared to VA DCs. The Nef DCs presented 4.3 ($p<0.01$) to 4.1-fold ($p<0.01$) less H-2K^b/OVA on the cell surface with a high and low dose of OVA, respectively (**Figure 4.3B**). To account for the reduction of total surface MHC I on Nef DCs, the percentage of total H-2K^b presenting OVA peptide was calculated. The fold decrease on Nef DC surface in relation to VA DCs is represented in **Figure 4.3C**. A reduction in cross presentation ability in Nef-expressing DCs was still observed (2.2-fold; $p=0.05$ to 3.3-fold; $p=0.06$).

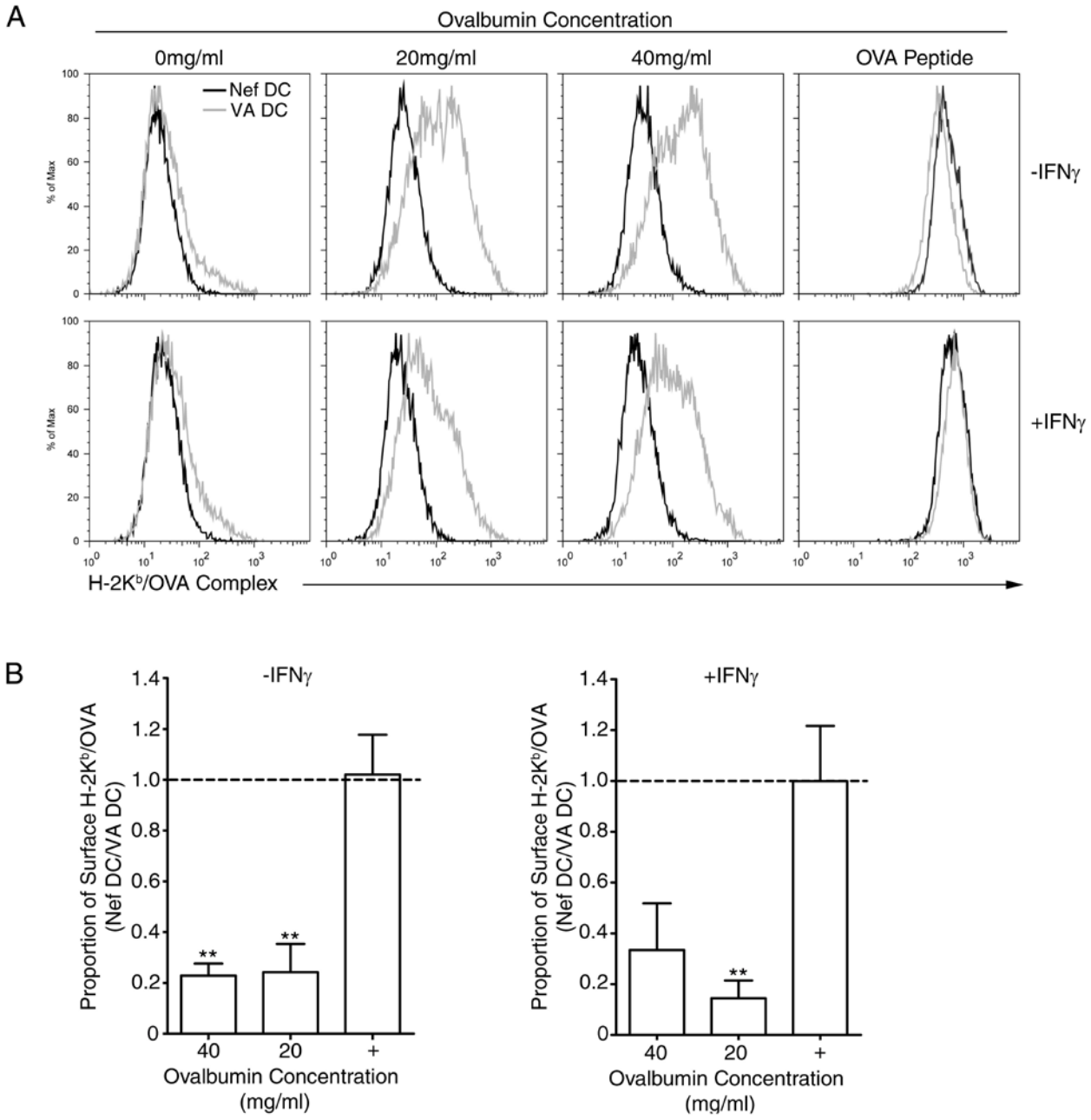
A
Ovalbumin Concentration
0mg/ml
20mg/ml
40mg/ml
OVA Peptide
Nef DC
VA DC
% of Max
-IFNγ
+IFNγ
H-2K^b/OVA Complex
B
-IFNγ
+IFNγ
Proportion of Surface H-2K^b/OVA (Nef DC/VA DC)
**
40
20
+
Ovalbumin Concentration (mg/ml)

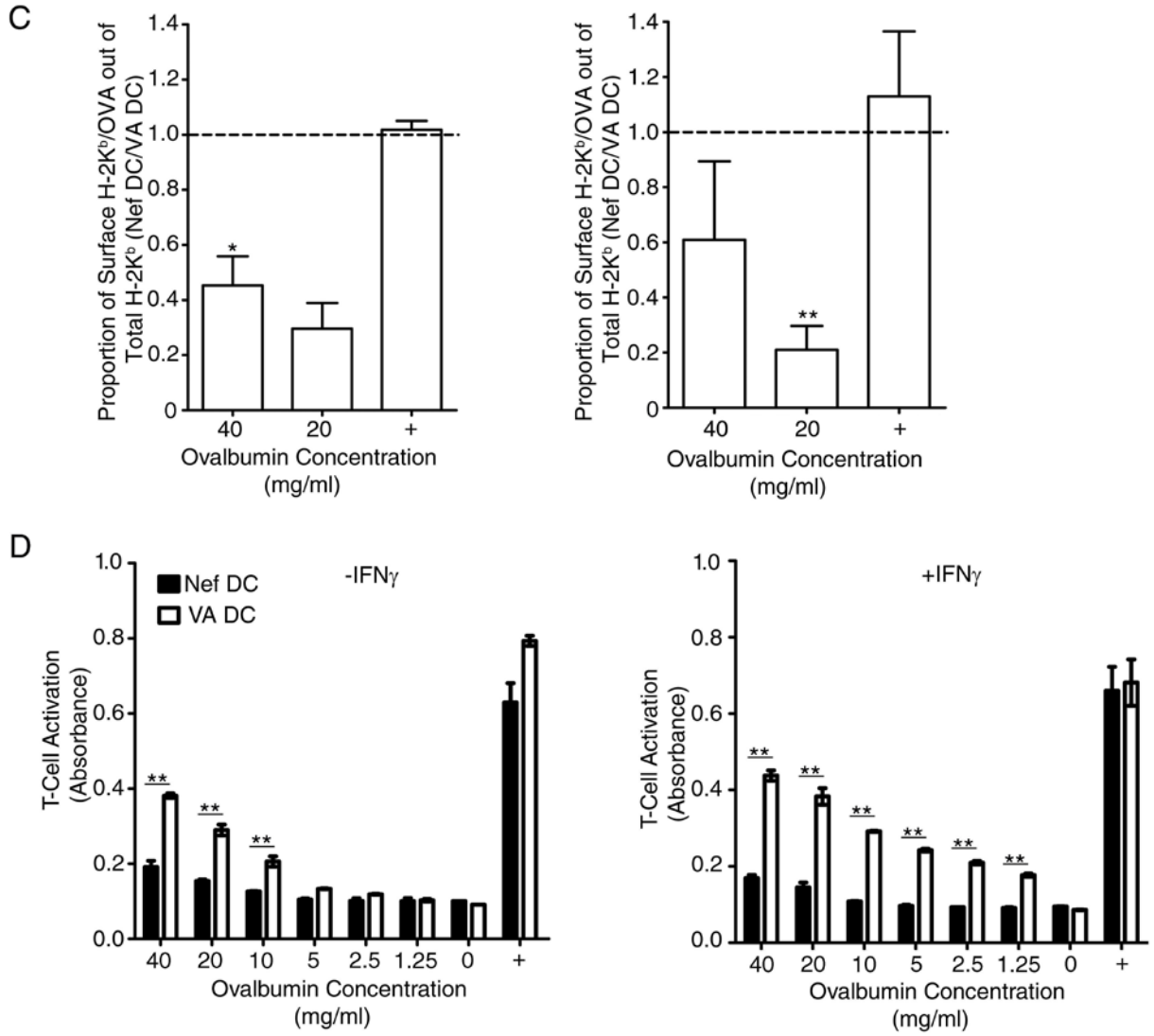

Figure 4.3. Nef-expressing DCs have decreased ability to cross present soluble ovalbumin and cross prime CD8$^+$ T cells.

(A) Nef-expressing (black) and VA DCs (grey) were incubated with soluble OVA with or without IFNγ. Flow cytometry was used to determine the number of H-2K^b/OVA complexes on the surface of the DCs. **(B)** The fold difference in mean fluorescent units between Nef and VA DCs was determined and expressed as the proportion of Nef DC surface H-2K^b/OVA complexes compared to VA DCs (no IFNγ: n=8-10; with IFNγ: n=3). **(C)** The difference in H-2K^b/OVA complexes normalized to total H-2K^b on the cell surface was calculated and represented as the proportion of surface expression on Nef DCs compared to VA DCs (no IFNγ: n=5-6; with IFNγ: n=3). **(D)** Activation of ovalbumin specific B3Z T cells was assessed using a colorimetric CPRG assay. Figure represents 3-6 experiments. Error bars represent SE. **p<0.01;*p=0.05

When DCs were activated with IFNγ to mimic an immune response situation, the cross presentation defect was still evident (**Figure 4.3A-C**). The fold decrease of H-2K^b/OVA on the cell surface of Nef DCs was 3.0 ($p=0.07$) to 6.9-fold ($p<0.01$) depending on OVA dose. The difference was still observed when evaluated against the total H-2K^b on the surface (1.6-fold; $p=0.06$ and 4.8-fold; $p<0.01$).

Next, the ability of Nef-expressing DCs to cross prime T cells was evaluated. Nef and VA DCs were allowed to process and present soluble OVA overnight, as above. After 18 hours, the DCs were incubated with B3Z cells, a T cell hybridoma with a T cell receptor (TCR) that specifically recognizes the $OVA_{257-264}$ peptide in the context of the MHC I allele, H-2K^b, and T cell activation was assessed [296]. Without IFNγ activation, both Nef and VA DCs were able to activate B3Z T cells at higher doses of OVA, in a dose-dependent manner. However, Nef DCs had significantly impaired cross priming ability when compared to the VA DC controls (**Figure 4.3D**; $p<0.001$). Matured DCs are more potent at priming T cell responses [369]. This is evident in the IFNγ treated DCs as VA DCs could prime T cells with lower doses of OVA. Similar results were obtained following IFNγ treatment whereby Nef-expressing DCs were inept at cross priming T cells (**Figure 4.3D**; $p<0.001$). This indicates that Nef significantly modulates primary T cell responses by interfering with the cross priming function of DCs.

To examine the effect of Nef on direct or endogenous MHC I antigen presentation, a viral vector was used to introduce OVA into the cytosol of the DCs. Specifically, Nef-expressing and VA DCs were infected with empty recombinant vaccinia virus (VV) or recombinant vaccinia virus expressing full-length ovalbumin (VV-OVA). After culture for 16 h, the DCs were evaluated for the formation of OVA-MHC I complexes on the cell

surface via FACS analysis as described above (**Figure 4.4A**). Nef-expressing DCs had reduced MHC I/OVA peptide complexes on the cell surface. The effect was most evident at MOI of 5; therefore, quantification was performed using this dose (**Figure 4.4B**). At MOI 5, 1.5-fold ($p<0.01$) more H-2K^b/OVA was presented on the cell surface of VA DCs. Furthermore, when the difference in total surface MHC I expression was considered, the percentage of MHC I presenting OVA peptide on the cell surface was reduced 1.4-fold when Nef was expressed (**Figure 4.4C**). To determine if the reduction in cell surface MHC I/OVA peptide complexes translates to reduced priming ability, the virally infected DCs were incubated with B3Z T cells, as above. As expected, the VV-Vector (lacking OVA expression) infected DCs were unable to activate the OVA$_{257-264}$ peptide T cells (**Figure 4.4C**). Concurrently, both the VV-OVA infected Nef and VA DCs were able to active T cells in a MOI-dependent manner. Importantly, the Nef-expressing DCs had significantly reduced levels of T cell activation at all MOI's examined (**Figure 4.4C**; $p<0.001$). Taken together, the results show that both exogenous and endogenous MHC I responses are altered in DC's when Nef is present.

4.2.3 Nef alters MHC I trafficking and subcellular localization

The effect of Nef on DC cross presentation is likely attributed to Nef ability to alter MHC I trafficking. To investigate this, the effect of Nef-MHC I interaction on the localization of MHC I in DCs was assessed. Nef-expressing and VA DCs were stained with an H-2K^b-specific antibody (blue) in combination with a Golgi-specific antibody, Giantin or Furin Convertase (red). Increased colocalization of H-2K^b and Golgi markers (pink) was observed in Nef-expressing DCs as compared to the VA controls

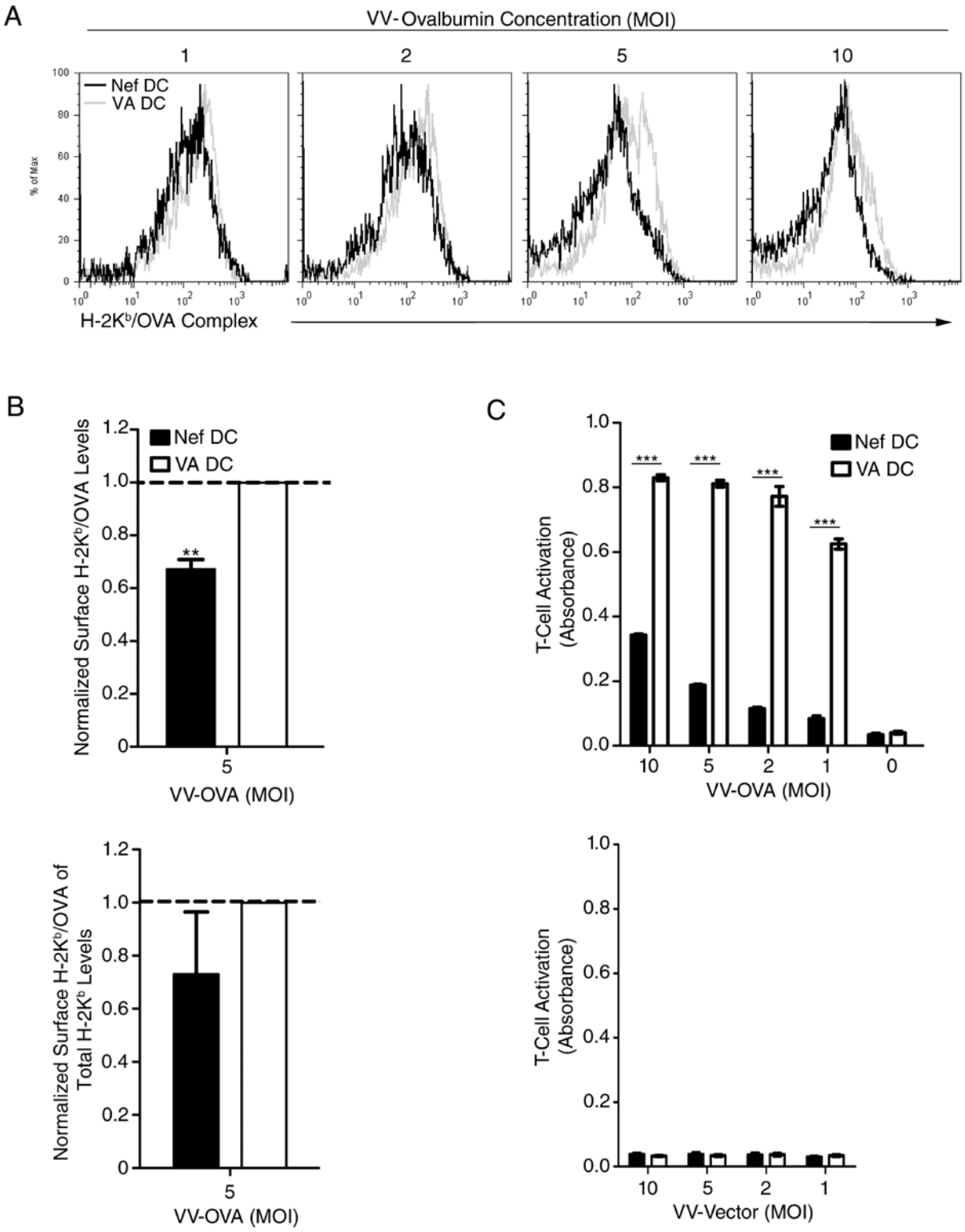
A
VV-Ovalbumin Concentration (MOI)
1
2
5
10
Nef DC
VA DC
% of Max
H-2Kb/OVA Complex
B
Nef DC
VA DC
Normalized Surface H-2Kb/OVA Levels
**
VV-OVA (MOI)
Normalized Surface H-2Kb/OVA of Total H-2Kb Levels
VV-OVA (MOI)
C
Nef DC
VA DC
T-Cell Activation (Absorbance)
***
VV-OVA (MOI)
T-Cell Activation (Absorbance)
VV-Vector (MOI)

Figure 4.4. Nef-expressing DCs have decreased ability to present virus-associated ovalbumin and prime $CD8^+$ T cells.

Nef-expressing and VA DCs were infected with vaccinia virus-expressing ovalbumin (VV-OVA) and vaccinia virus vector alone (VV-Vector). **(A)** Flow cytometry was used to determine the number of $H\text{-}2K^b$/OVA complexes on the surface of the DCs infected with VV-OVA at various multiplicities of infection (MOI). Black = Nef DCs; Grey = VA DCs. **(B)** The fold difference in mean fluorescent units at MOI 5 was calculated (n=4). The difference in $H\text{-}2K^b$/OVA complexes out of total $H\text{-}2K^b$ on the cell surface is represented (n=3). **(C)** Activation of ovalbumin specific B3Z T cells by VV-OVA or VV-Vector infected DCs was assessed using a colorimetric CPRG assay. Figure represents 4 experiments. Error bars represent SE. $^{**}p<0.01$; $^{***}p<0.001$

(**Figure 4.5A,B**). Quantification of this colocalization indicated that when Nef was present 8% ($p<0.05$) and 17% ($p<0.001$) more MHC I molecules colocalized with Giantin and Furin Convertase, respectively (**Figure 4.5C**). This indicates that Nef can sequester MHC I in the Golgi compartment in DCs.

To determine the origin of the Golgi-localized MHC I, MHC I internalization from the cell surface was investigated. Briefly, Nef-expressing and VA DCs were labelled with an anti- H-2K^b antibody and flow cytometric analysis was used to follow MHC I internalization over time. Nef-expressing DCs were found to have less MHC I remaining on the cell surface over 8 hours as compared to the VA control (**Figure 4.6A**; $p<0.05$). This indicates that Nef is interacting with surface MHC I to cause internalization into an intracellular compartment.

The endogenous MHC I presentation and priming pathway was also significantly impaired by the presence of Nef indicating that the ER to cell surface trafficking of MHC I is altered by Nef. Therefore, the transport kinetics of newly synthesized MHC I molecules was next analyzed. Nef-expressing and VA DCs were acid-stripped by low pH treatment to destabilize and remove surface MHC I and then examined by flow cytometry for the appearance of MHC I on the cell surface over time. The rate of total MHC I, both newly synthesized and recycled, returning to the cell surface was reduced in Nef-expressing DCs (**Figure 4.6B**; $p<0.05$). Cyclohexamide inhibits protein synthesis by blocking translational elongation [371]. DCs treated with cyclohexamide will not synthesize new MHC I so only recycling MHC I will traffic to the cell surface. To remove the effect of MHC I recycling to the cell surface, the difference in the amount of MHC I returning to the cell surface in cyclohexamide-treated and untreated cells over

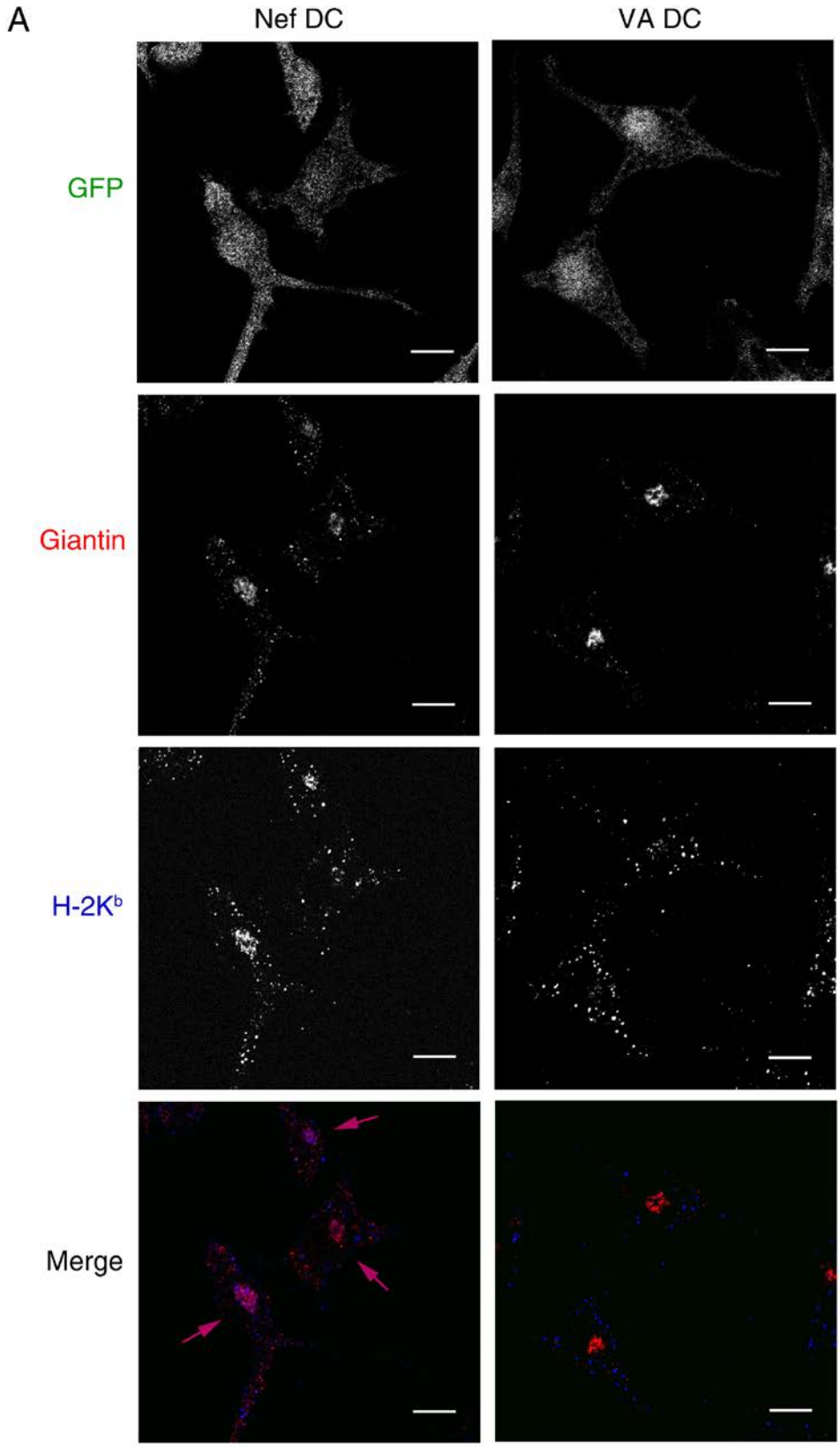
A
Nef DC
VA DC
GFP
Giantin
H-2K^b
Merge

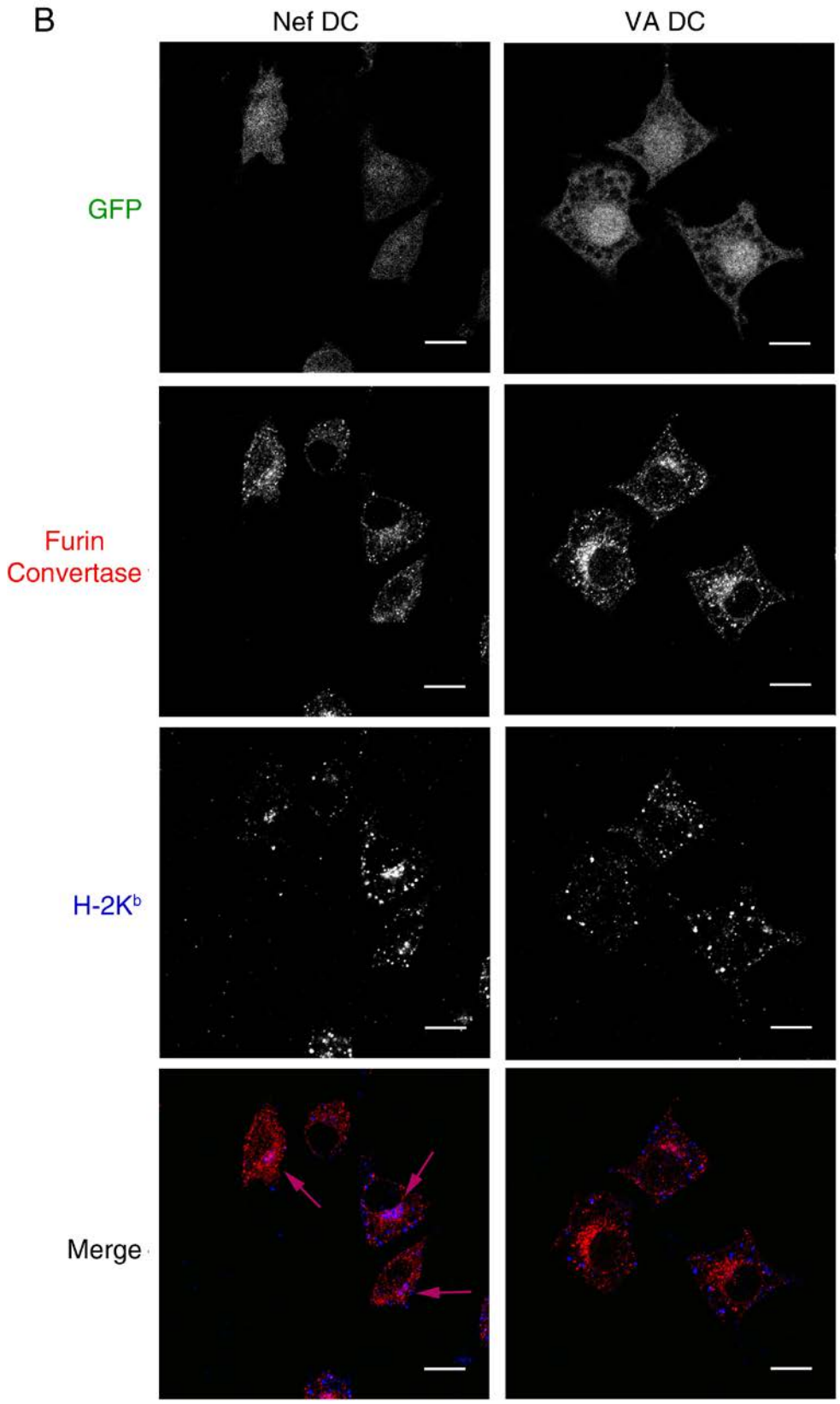
B
Nef DC
VA DC
GFP
Furin
Convertase
H-2K^b
Merge

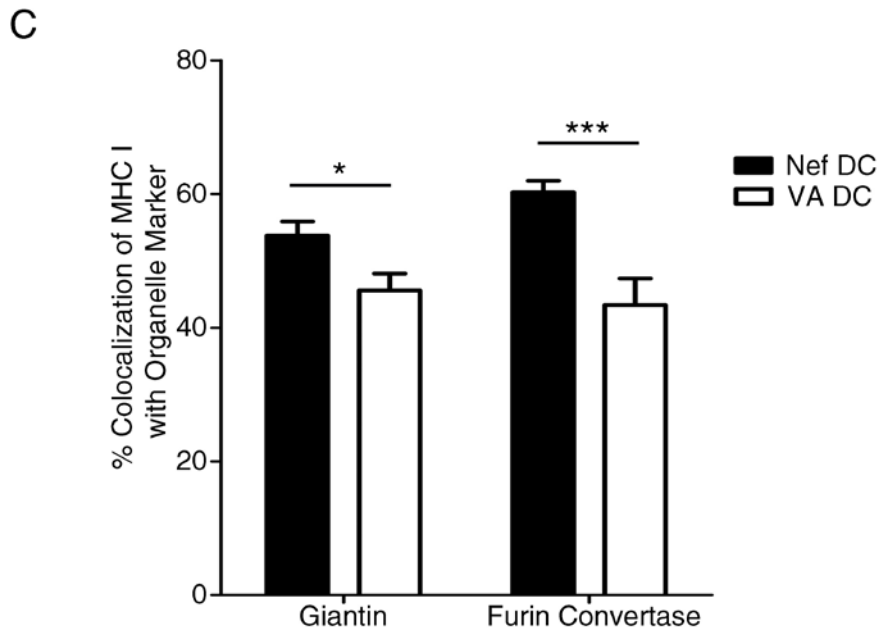

Figure 4.5. **Nef causes an accumulation of MHC I in a Golgi-like compartment**.
(A,B) Confocal analysis was used to colocalize (pink) MHC Class I (blue) with Golgi marker, Giantin (red) and trans-Golgi network marker, Furin Convertase (red). Scale bar = 10 μm. **(C)** Colocalization was quantified by calculating the Mander's coefficient. Error bars represent SE. *$p<0.05$; ***$p<0.001$

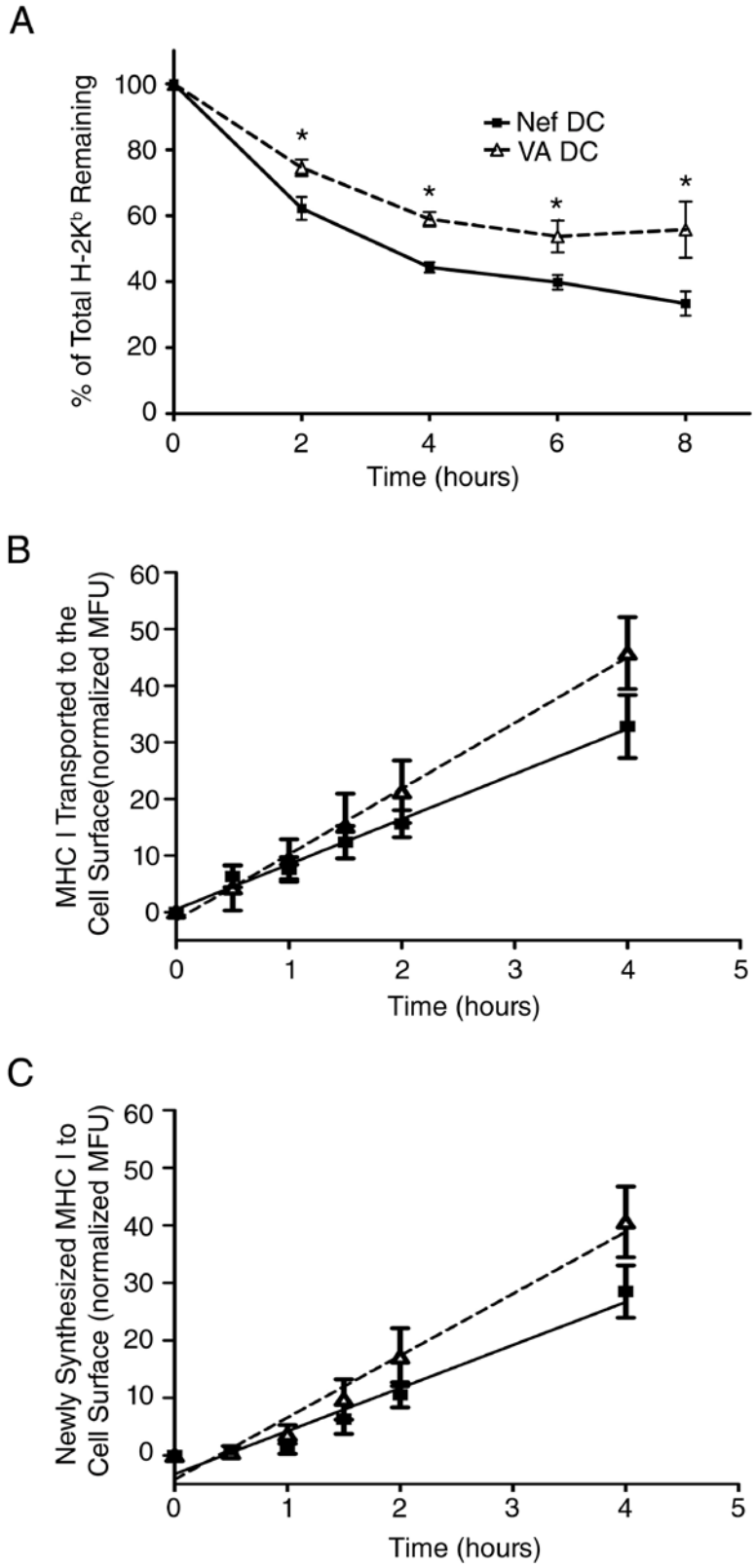
A
% of Total H-2K^b Remaining
100
80
60
40
20
0
Nef DC
VA DC
*
*
*
*
0
2
4
6
8
Time (hours)
B
MHC I Transported to the Cell Surface(normalized MFU)
60
50
40
30
20
10
0
0
1
2
3
4
5
Time (hours)
C
Newly Synthesized MHC I to Cell Surface (normalized MFU)
60
50
40
30
20
10
0
0
1
2
3
4
5
Time (hours)

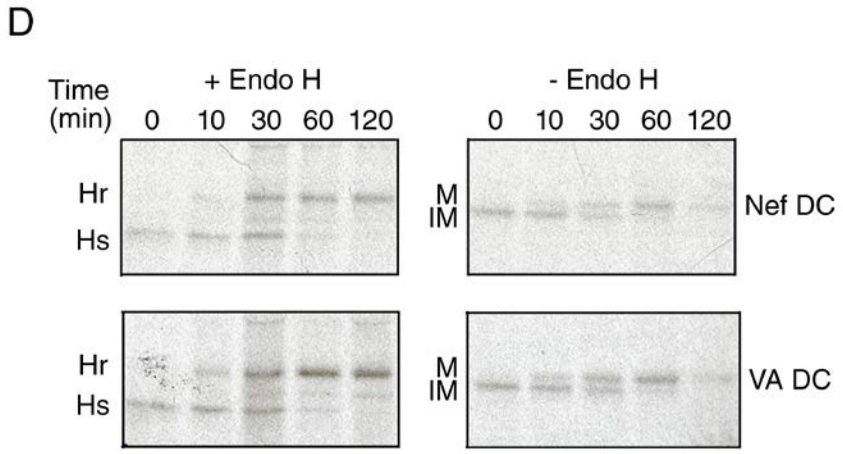

Figure 4.6. Nef inhibits MHC I trafficking to and from the cell surface in DCs.
(A) Surface MHC I on Nef-expressing and VA DCs was labelled with biotinylated anti-H2-K^b antibody. At various time points, the cells were fixed and labelled with strepatavidin-PE. The percent of MHC I remaining on the cell surface was determined by flow cytometry (n=3). **(B)** MHC I on Nef-expressing and VA DCs was acid stripped. Cells were incubated with or without cycloheximide and MHC I recycling to the cell surface was monitored over time by flow cytometery. The total MHC I transported to the cell surface was calculated by normalizing the mean fluorescence units for each sample to the zero time point. By linear regression, the rates were determined to be statistically significant (p=0.028; n=4). (**C**) The amount of newly synthesized MHC I transported to the cell surface was calculated by subtracting the cyclohexmide-treated sample from the corresponding untreated cell sample. By linear regression, the rates were determined to be statistically significant (p=0.019; n=4). **(D)** Nef-expressing and VA DCs were labelled with ^{35}S and chased for various amounts of time. MHC I was immunoprecipitated and treated or not with Endo H. Samples were run on an SDS-PAGE gel. Treated (+ Endo H) samples were examined for the disappearance of an Endo H sensitive (Hs) and the appearance of an Endo H resistant (Hr) band. Untreated (-Endo H) samples were assessed for the disappearance of an immature MHC I form (IM) and the appearance of a mature, glycosylated form (M). Error bars represent SE. *p<0.05.

time was assessed (**Figure 4.6C**). The Nef-expressing DCs had a statistically reduced rate of transport of newly synthesized MHC I as compared to the VA DCs This shows that in addition to affecting MHC I internalization, Nef can also impair trafficking of newly synthesized MHC I.

To locate the point of Nef-mediated MHC I trafficking impairment, the maturation of newly synthesized MHC I through the Golgi was examined. MHC I was immunoprecipitated from DCs that had been pulsed with ^{35}S and chased for various amounts of time. Immature MHC I (IM) moves through the Golgi and acquires glycosylation so in its mature state (M), MHC I has a higher mass. This is evidenced by the appearance of a higher molecular weight band at about 10 minutes in Nef and VA DCs (**Figure 4.6D**). The mature form of MHC I appears at the same time whether Nef is present or not suggesting Nef does not affect MHC I movement through the Golgi. To further confirm this point, Endoglycosidase (Endo) H analysis of the immunoprecipitated MHC I was performed. Since proteins become Endo H resistant when they traffic through the Golgi compartment and undergo cleavage by mannosidase II [331], Endo H sensitivity of MHC I can be followed overtime (**Figure 4.6D**). The appearance of Endo H resistant (Hr) MHC I and the disappearance of End H sensitive (Hs) MHC I occurs similarly in Nef-expressing and control DCs. Taken together, Nef does not impair maturation of MHC I through the Golgi but impairs trafficking from the Golgi to the cell surface.

4.3 Discussion

Dendritic cells are potent antigen presenting cells essential for initiating strong T cell responses [1]. However, persistent viruses can employ efficient mechanisms to manipulate DC function and circumvent the adaptive immune system [95, 372]. In this study, a murine bone marrow derived DC line, DC2.4 [295], was used to examine the effect of Nef on DC antigen presentation and priming ability. As previously reported [159, 168, 169, 373], Nef was found to downregulate the surface expression of MHC I and several other receptors important for activation of immune responses, including MHC II, CD40 and CD86. The new findings of this study show that Nef expression in DCs results in a significantly reduced MHC I endogenous and cross presentation capacity and diminished $CD8^+$ T cell priming ability. These effects may be attributed to Nef's ability to disrupt MHC I trafficking in DCs.

The DC2.4 cell line is a convincing model of DC function. This cell line was originally made by transducing bone marrow derived DCs with a retrovirus expressing GM-CSF and the oncogenes, *myc and raf* [295]. They retain DC morphology including dendritic processes and ruffled edges and express MHC, costimulatory molecules and DC-specific molecules, DEC-205 and 33D1[295]. Functionally, these DCs are immature with the ability to phagocytose antigen; however, maturation can be induced with IFNγ leading to increased T cell priming ability [370]. Using DC2.4 cells rather than primary murine bone marrow-derived or splenic DCs in the current study allowed for high transfections rates and the establishment of a stable *nef*-expressing DC2.4 cell line. This way, multiple experiments comparing various effects of Nef on DC functions could be performed with the same cell line. Consistent with results previously shown, when Nef is

present in the DC2.4 cells, the expression of MHC I and costimulatory molecules is reduced [159, 168, 169, 373]. Upon treating the DCs with IFNγ and inducing maturation, the downregulation of MHC I, MHC II and CD40 is still evident when Nef is present (**Figure 4.2**). This confirms that Nef-expressing DC2.4 cells are a valid model with which to study the effects of Nef on DC immune function.

Although it has been shown that Nef can influence the classical MHC I pathway [366], this is the first demonstration that Nef impacts the cross presentation of exogenous antigen on MHC I. Here, two model exogenous antigens were assessed. First, soluble OVA that enters the vacuolar pathway of cross presentation was used as a representative antigen [59]. In Nef-expressing DCs, fewer MHC I molecules were loaded with the OVA peptide showing cross presentation impairment by the HIV protein (**Figure 4.3**). Second, the recombinant viral system, VV-OVA, confirmed these findings. During vaccinia virus infections not only is direct MHC I presentation important for inducing CTL responses, cross presentation is also necessary for induction of immune responses for viral clearance [374]. Following infection with VV-OVA, Nef-expressing DCs were not proficient at expressing MHC I bound with OVA peptide on the cell surface (**Figure 4.4**). This demonstrates that VV-OVA proteins produced by the infected cell could not be presented on MHC I due to Nef's manipulation of the classical MHC I pathway. Importantly, MHC I in Nef-expressing DCs could also not access cellular/viral debris resulting from infection-induced cell death and so cross presentation was blocked too. Lizee *et al.* demonstrated the importance of MHC I accessing exogenous antigen for cross presentation [59, 65]. In DCs, recycling MHC I lacking a conserved tyrosine motif in the cytoplasmic tail were unable to access the endolysosomal compartments and instead

remained stuck on the cell surface. The result was reduced loading of MHC I with exogenous antigen, minimal cross presentation and impaired cross priming [59, 65]. Nef-expression may mimic this situation in that similar to the tyrosine motif mutation, Nef interaction blocks MHC I trafficking and subsequent contact with exogenous antigen. The end result is dysfunctional MHC I cross presentation.

The current studies also revealed the novel finding that DC cross priming of $CD8^+$ T cells is downregulated directly as a result of Nef expression. Nef appeared to impact T cell priming to a greater extend than antigen presentation itself (**Figure 4.3 and Figure 4.4**). Generally, T cell priming was reduced to a greater degree and Nef's effects on priming could be observed at lower OVA concentrations and MOI's. This may be explained by the reduction in co-stimulatory molecules on Nef-expressing DCs. The combination of reduced peptide-loaded MHC I and co-stimulatory molecules on the surface of supposedly mature DCs would inevitably lead to reduced ability for DCs to activate anti-viral effector T cells. This is a break through in understanding the significance of Nef's immune system inhibition since cross presentation and cross priming of $CD8^+$ T cells has been shown to have great importance in alerting viral immune responses.

The effect of Nef on costimulatory molecules has been previously investigated. One explanation for reduced expression may be that Nef prevents complete DC maturation promoting a generalized downregulation of surface immune receptors necessary to prime T cells. Recently, a hypothetical model was proposed suggesting that Nef activation of PAK2 and Rac1 via the signalling molecule DOCK180 may result in negative regulation of DC activation and the maintenance of a phagocytic immature phenotype [169, 375].

Although consensus exists that Nef interacts and activates PAK2, the functional relevance of this is yet to be demonstrated [153]. Alternatively, Nef has been proposed to function as a viral adaptor protein trafficking host molecules to improper locations and promoting aberrant function [153]. Pathways of surface downregulation have been described not only for MHC I but also for costimulatory molecules. In monocytes expressing Nef, CD80 and CD86 have been observed to be rapidly internalized through a dynamin-independent pathway [376, 377]. From here, CD80/CD86-containing vesicles acquire Rab11 in a PI3K-dependent manner to localize to the Golgi region [377]. The exact mechanism Nef utilizes to impair costimulatory molecules in DCs is unknown but is the focus of future studies.

Trafficking of MHC I in DCs was examined to provide insight into how Nef exerts its effects on MHC I. Nef-expressing DCs had an accumulation of intracellular MHC I in a Golgi-like compartment (**Figure 4.5**). This was evidenced as an increased in colocalization with Giantin, a marker of the cis and medial Golgi [378]. Nef-mediated MHC I Golgi localization was even more obvious when compared to the trans Golgi protein, Furin Convertase, an endoprotease that activates proprotein secretory pathway compartments [379]. Nef-expressing DCs were found to have an increased rate of MHC I internalization from the cell surface (**Figure 4.6**). Additionally, the rate of appearance of newly synthesized MHC I on the cell surface was found to be decreased when Nef was present. Further analysis of this showed that transport through the Golgi was unaffected indicating that transport from the Golgi to the cell surface is compromised. Therefore, Nef is having a two-pronged effect on DC antigen presentation. First, Nef blocks the classical MHC I pathway. Newly synthesized MHC I loaded with endogenous antigen in

the ER enters the secretory pathway but is blocked by Nef at the Golgi. MHC I that does escape and egresses to the cell surface is rapidly internalized by Nef back to the Golgi. Although MHC I can be loaded with endogenous antigen, Nef reduces the amount of endogenous antigen presented at the cell surface. Second, Nef blocks cross presentation by immobilizing MHC in the Golgi. MHC I can not traffic to an endolysosomal compartment to access exogenous antigen so MHC I can not be loaded for cross presentation. Ultimately, Nef's manipulation of trafficking and immobilization of MHC I results in the reduced ability for DCs to present endogenous and exogenous antigens in complex with MHC I on the cell surface.

This MHC I trans Golgi localization has been reported for other cell types distinct from DCs [159, 162, 294, 380-382]. Through analysis of T cells and other cell lines (for example HeLa cells), two models have been constructed to explain this phenomenon. First, Thomas and colleagues propose a model in which Nef accelerates ARF6 mediated MHC I endocytosis then blocks the recycling of the MHC I back to the cell surface [161-163]. Second, an interaction with Nef links MHC I to AP-1 interrupting trafficking to the plasma membrane and diverting MHC I to a paranuclear compartment [164, 165]. This second mechanism may intersect with the latter part of the first in that this interaction may be responsible for blocking recycling of MHC I [383]. The relative contribution of increased internalization and diminished egress to the plasma membrane seems to differ depending on the cell type studied [156]. A comparison between cell types concluded that blockage of MHC I export to the cell surface was more prevalent in T cells than in HeLa cells [162, 384, 385]. These differences have been attributed to the rate in which MHC I

traffics from the ER through the secretory pathway. The slower this occurs the more time Nef has to exert its effects [385].

Dendritic cells function to efficiently capture and present antigen for T cell activation. DC cross priming is essential for activation of immune responses against HIV and secondary infections that are fatal to HIV-infected individuals. Therefore, manipulation of this pathway in DCs by Nef provides an advantage for escape of immune surveillance and for the establishment of persistence. HIV's potential to infect and impair this pathway could potentially contribute to the immunodeficiency typical of AIDS.

CHAPTER 5. CONSTRUCTION AND ANALYSIS OF A NEF TRANSGENIC MOUSE

5.1 Introduction

A small animal model would greatly help the study of Human Immunodeficiency Virus (HIV) and Acquired Immunodeficiency Syndrome (AIDS). However, rodent cells inefficiently support an HIV infection and obstruct HIV replication at several points [386, 387]. The best studied barrier to HIV replication in rodent models is a blockage of HIV entry. To enter cells, HIV uses the glycoprotein gp120 to bind both the host cell surface receptor CD4 and a coreceptor, either CCR5 or CXCR4 [388]. Upon binding, a second HIV glycoprotein gp41 causes fusion of the cellular membrane and viral envelope allowing the viral genome and associated proteins to enter the cytoplasm [388]. HIV envelope proteins may bind mouse CD4 and chemokine receptors to some degree, but not with high enough affinity to induce virion fusion and HIV entry into the cell [387, 389, 390]. Upon fusion, HIV cDNA integrates into the host chromosomal DNA in order to get viral mRNA transcribed. This is dependent on host factors in addition to viral enzymes. At this step, murine T cells have been shown to restrict HIV replication presumably due to incompatible host factors [387]. In addition, during viral mRNA production, HIV uses an accessory protein, Tat, that binds cyclin T1 to increase transcription efficiency [391, 392]. Tat interacts with rodent cyclin T1 less effectively than with the human version leading to inefficient mRNA elongation [393-395]. Posttranslational blocks also occur. In murine cells, the viral structural proteins are not properly targeted to the membrane for viral assembly but become trapped in cytoplasmic vesicular structures. This leads to

incomplete processing of the viral structural protein, Gag, and the production of very few virulent viral particles [390]. Despite the generation of murine HIV disease models that express human factors to overcome these blocks, a HIV mouse model has yet to be established [396, 397].

As an alternative method, HIV genes can be expressed in transgenic mice alone or in provirus constructs. Most pertinent to this thesis, several groups have expressed Nef in mouse hematopoietic cells and under the regulation of T cell specific regulatory elements with mixed success [386]. Despite varied phenotypes, all studies noted several similar effects due to Nef that paralleled *in vitro* and clinical results such as downregulation of CD4 from the cell surface [386]. These results demonstrate that at least some of the effects of cell perturbations caused by Nef can be studied using transgenic animals.

In this thesis and previous studies, Nef has been shown to affect MHC I trafficking (reviewed in [153]). This disruption not only occurs in T cells but also in dendritic cells (DCs) important for immune activation [169, 366]. Specifically, this thesis demonstrated the inhibition of the MHC I cross presentation pathway in DCs that is essential for the activation of immune responses. Taken together, the expression of Nef in murine DCs would presumably affect the ability of DCs to activate immune responses against secondary viral and bacterial infections. Here, a Nef transgenic (Tg) mouse model was created in order to study the impact of Nef on the generation of immune responses *in vivo*. Due to HIV receptor requirements, HIV is targeted to T cells, macrophages and DCs. To mimic this tropism, *nef* was expressed under the control of a CD4 promoter. Using this model, Nef was shown to have some impact on the generation of immunity to viral and bacterial infections.

5.2 Results

5.2.1 Construction of Nef Tg mice

To examine the function of Nef in an *in vivo* setting, a Nef Tg mouse was created on a C57Bl/6 background. To model HIV viral tropism, the *nef* gene was expressed on a CD4 promoter for transgenic expression in the $CD4^+$ cell lineage. This vector allows expression of *nef* in T cells, macrophages and DCs. To confirm insertion of the transgene, PCR was performed with *nef*-specific primers on genomic DNA isolated from the transgenic line (**Figure 5.1A**). The *nef* transgene was detected in the Nef Tg mice but not in the C57Bl/6 wild type controls. Next, a homozygotic mouse line was created to double the copy number of the transgene and increase Nef protein levels in the $CD4^+$ cells. In addition, this aided in breeding because the mating of homozygotic animals would produce entire litters containing the *nef* transgene insertion. To generate homozygotic mice, heterozygotic animals were mated and pups with the *nef* transgene insertion were identified by genotyping as above. DNA from littermates testing positive were further analyzed using real-time PCR to quantify the amount of *nef* transgene present in their genome (**Figure 5.1B**). In this way, each mouse could be identified as having single or double amounts of the *nef* transgene in their genomic DNA. Mice with two times the amount of *nef* transgene were considered homozygotic.

Next, correct expression of the transgene was examined. $CD4^+$ cells were isolated from the spleen of Nef Tg and C57Bl/6 mice. The presence of the Nef protein was confirmed in the Nef Tg $CD4^+$ cells by Western blot (**Figure 5.2A**)**.** Nef expression was further examined by RT-PCR in mouse tissues and cell populations. As expected, spleen, thymus, lymph node, bone marrow and liver were all identified to have CD4-expressing

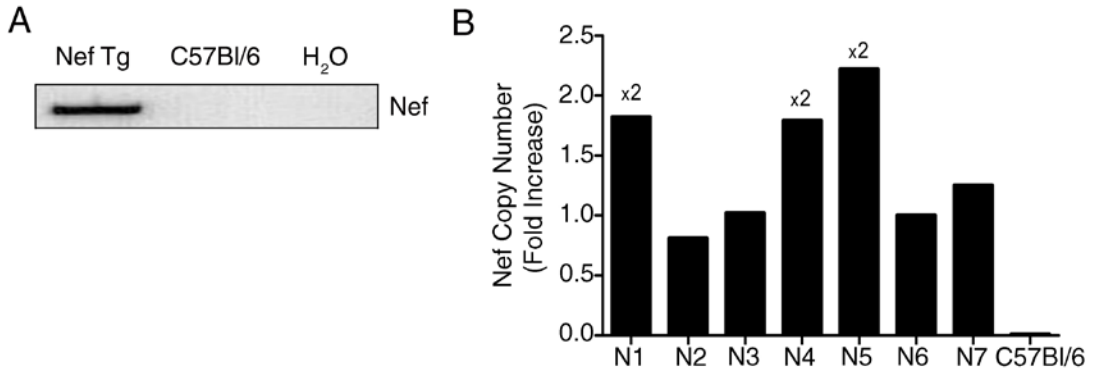

Figure 5.1. Presence of the Nef transgene in heterozygotic and homozygotic mice. **(A)** DNA was isolated from earclips of Nef Tg and C57BL/6 mice. The presence of the *nef* transgene was confirmed by PCR with Nef-specific primers. **(B)** To create a homozygotic mouse, Nef Tg mice were mated and DNA from earclips was isolated from the litter (N1-N7). Relative *nef* transgene copy number was assessed by real-time PCR with *nef* specific primers. Nef transgenic pups with two times (x2) the amount of *nef* transgene were considered homozygotic.

A

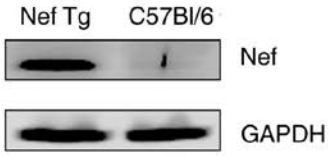
Nef Tg
C57Bl/6
Nef
GAPDH

B

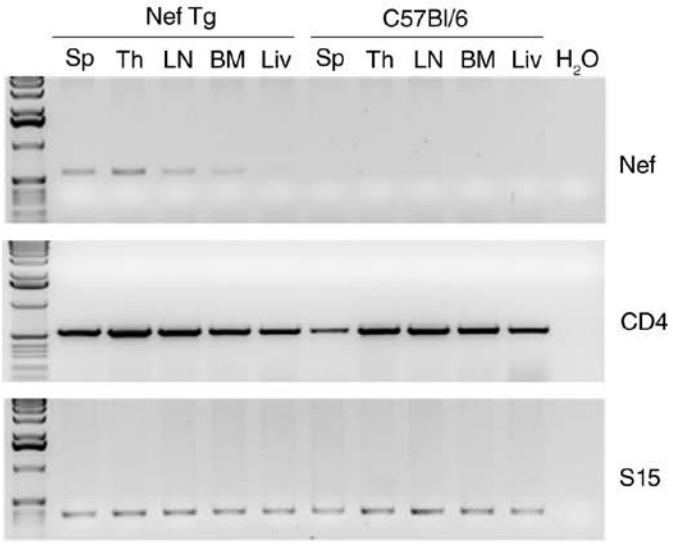
Nef Tg
C57Bl/6
Sp Th LN BM Liv Sp Th LN BM Liv H2O
Nef
CD4
S15

C

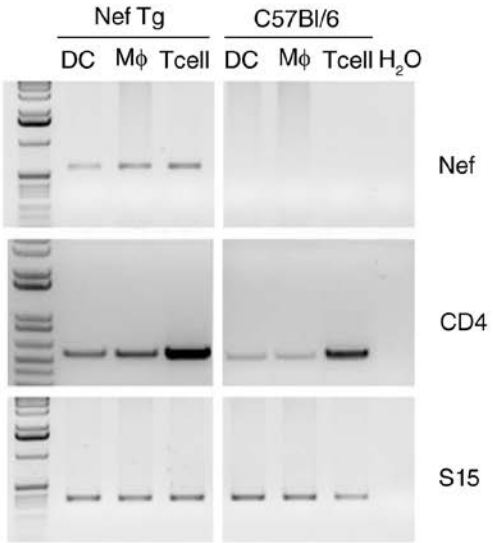
Nef Tg
C57Bl/6
DC Mϕ Tcell DC Mϕ Tcell H2O
Nef
CD4
S15

Figure 5.2. Nef transcript and protein is selectively present in $CD4^+$ tissues and cell populations of the Nef Tg mouse.

(A) $CD4^+$ cells were isolated from the spleen of Nef Tg mice and Western blot analysis was performed. GAPDH was detected as a loading control. **(B)** RNA from spleen (Sp), thymus (Th), lymph node (LN), bone marrow (BM) and liver (Liv) was isolated. *CD4* and *nef* transcripts were detected by RT-PCR using gene-specific primers. S15 primers were used as a loading control. **(C)** Dendritic cells (DC), macrophages (MØ) and T cells were sorted from the spleen using cell-specific markers. RNA was isolated and analyzed by RT-PCR as above.

cells (**Figure 5.2B**). In the Nef Tg mice the *nef* RNA was also detected to some degree in these tissues with the liver having the lowest amount. Further to this, DCs, macrophages and T cells were isolated from the spleens of Nef Tg and C57Bl/6 mice. These cells were confirmed to express CD4 and additionally, in the Nef Tg cells, *nef* transgene expression was detected (**Figure 5.2C**).

5.2.2 Characterization of cell populations in Nef Tg mice

To begin to characterize the effect of Nef on immune function, the thymic and splenic cell populations were examined. In the Nef Tg mice, the thymi were smaller with 1.5 times fewer thymocytes than the C57Bl/6 controls (**Figure 5.3A**). To account for this loss in cell number, the $CD4^+$ and $CD8^+$ populations were examined. The Nef Tg mice had a smaller $CD4^+$ population (**Figure 5.3B).** This was most evident when the $CD4^+$:$CD8^+$ ratios were calculated with the Nef Tg mice having a significantly reduced ratio compared to the wild type controls (1.8 vs 2.6, $p<0.05$) (**Figure 5.3C**). Further to this, the cell numbers in the thymic populations were evaluated and the CD4-expressing cells ($CD4^+$ and $CD4^+CD8^+$ cells) were found to be significantly decreased in the Nef Tg mice (**Figure 5.3D**).

To see if this defect extended to the periphery, splenic populations in the Nef Tg mice were next assessed. Surprisingly, it was noted that the Nef Tg spleens were on average larger than the C57Bl/6 controls (**Figure 5.4A**). In an attempt to understand this, several cell populations were examined using flow cytometry. The percentage of cells expressing surface $CD4^+$ and MHC I^+ decreased and a population emerged in the Nef Tg that was $CD4^-$ and MHC I^- (**Figure 5.4B, C**). As described in previous studies and in this

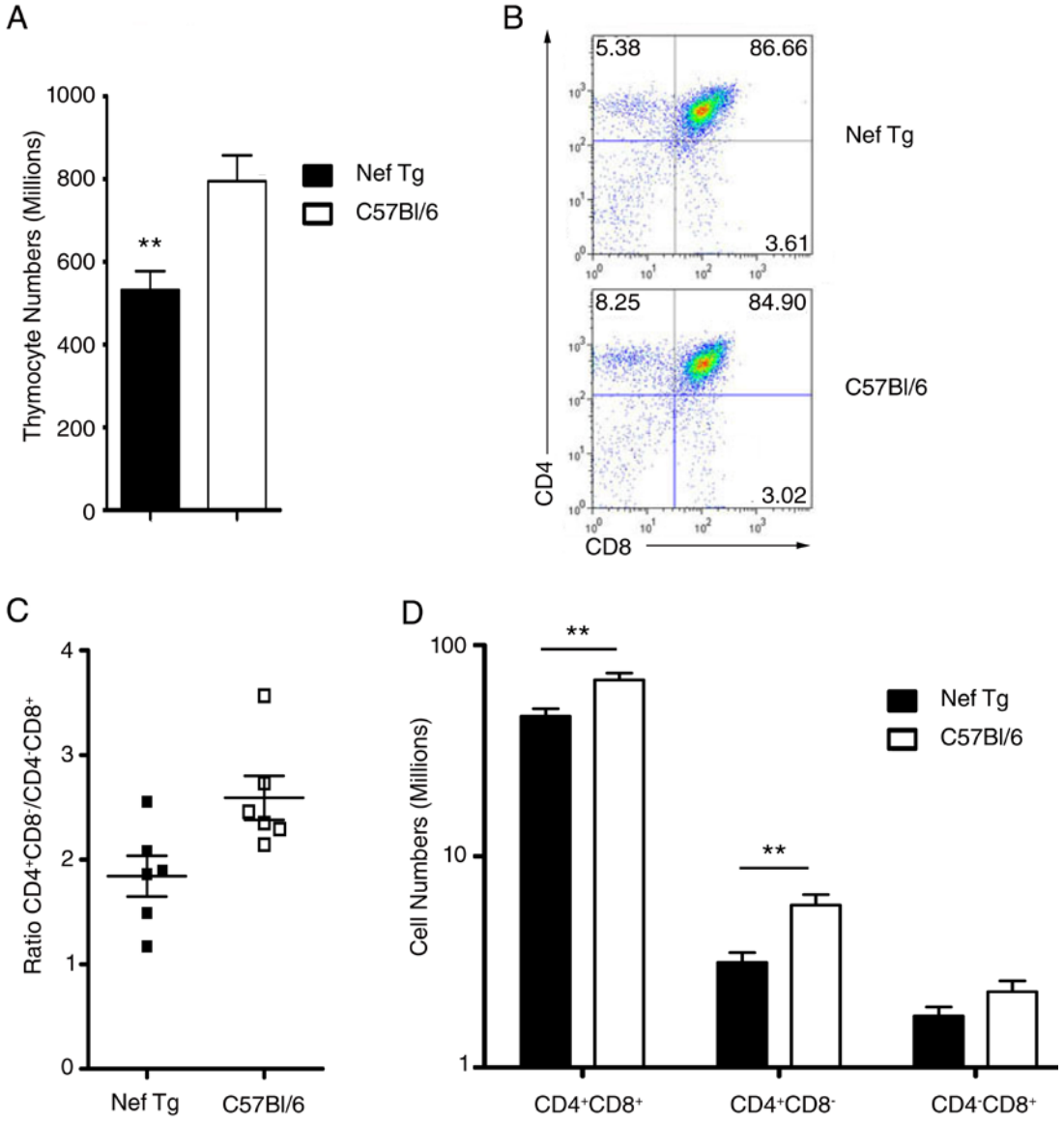

Figure 5.3. Nef expression results in a decreased CD4$^+$ T cell population in the thymus.

(A) Thymi were removed from C57BL/6 and Nef Tg mice and total thymocyte numbers were determined. **(B)** Flow cytometry was used to analyze the thymocyte cell subsets present. **(C)** The CD4$^+$CD8$^-$/CD4$^-$CD8$^+$ ratios were calculated. **(D)** Total numbers of cell populations were determined. Error bars represent SE. **p<0.01

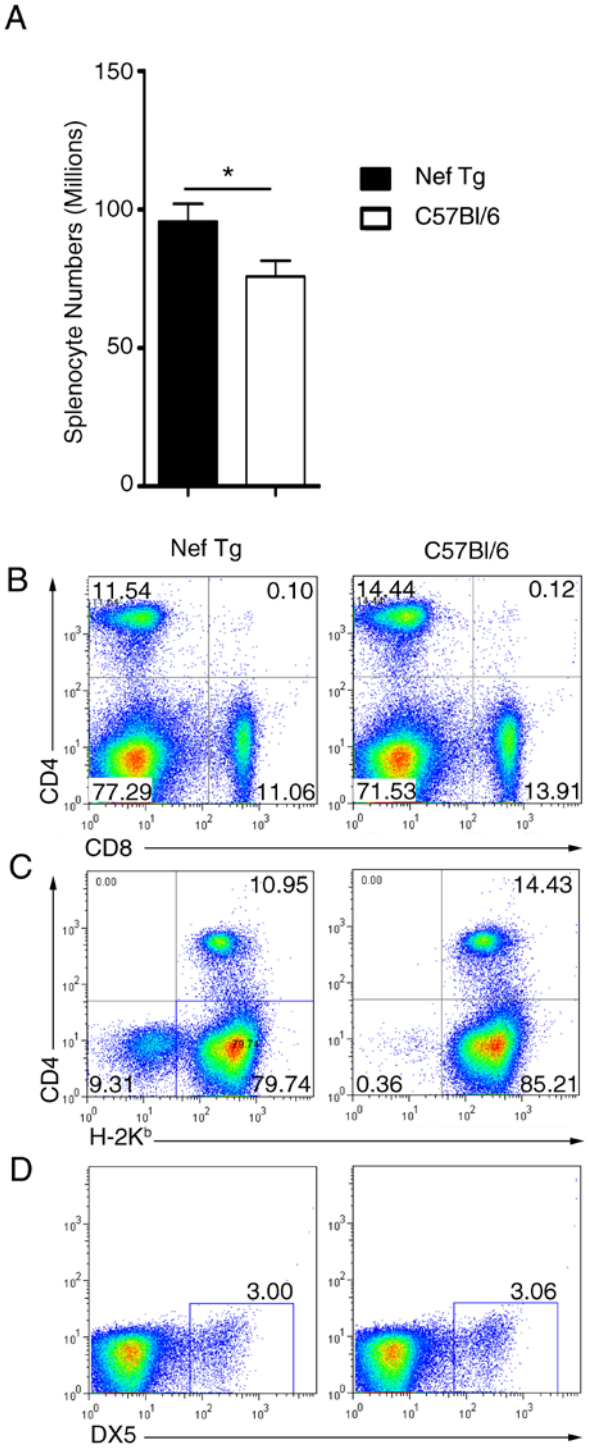
A
150
100
50
0
Splenocyte Numbers (Millions)
*
Nef Tg
C57Bl/6
Nef Tg
C57Bl/6
B
11.54
0.10
77.29
11.06
14.44
0.12
71.53
13.91
CD4
CD8
C
10.95
9.31
79.74
14.43
0.36
85.21
CD4
H-2K^b
D
3.00
3.06
DX5

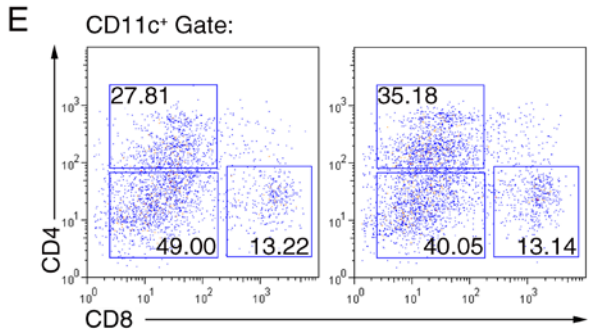

Figure 5.4. Nef expression in the periphery results in decreased CD4$^+$ and MHC I$^+$ cell populations.
(A) Spleens were removed from C57BL/6 and Nef Tg mice and cell numbers (± SE) were determined. Flow cytometry was used to analyze the proportion of **(B)** CD4$^+$ cells, **(C)** MHC I$^+$ cells, **(D)** NK cells and **(E)** CD11C$^+$ DCs . *$p<0.05$

thesis, Nef is known to affect MHC I surface expression. Natural Killer (NK) cells recognize downregulation or absence of MHC I on infected cells and target these cells for death. Therefore, the NK population was analyzed to determine if these cells were more abundant with Nef present. Using a pan-NK antibody (DX5), the NK population was found to be similar in Nef Tg and wild type controls. Finally, the $CD11c^+$ DC subsets in the spleen were investigated (**Figure 5.4D**). $CD8^+$ DCs appeared in similar proportion in the Nef Tg and C57Bl/6 spleen; however, the percentage of $CD4^+$ $CD11c^+$ cells was decreased with a corresponding increase in double negative $CD11c^+$ cells.

Immune dysfunction in HIV infections has been linked to T cell exhaustion resulting from chronic infection. In HIV-infected patients, the inhibitory receptor programmed death 1 (PD-1), a molecule associated with chronic infection, has been reported to be elevated on HIV $CD4^+$ and $CD8^+$ T cells [398-400]. Engagement of PD-1 with its ligands, PDL-1 or PDL-2, leads to impaired T cell function and a deficient immune response. Recently, Nef has been shown to be sufficient for PD-1 upregulation [401]. Furthermore, during chronic infection T cell dysfunction has been noted with the downregulation of the homing receptor, CD127, the migration receptor, CD62L, and activation marker, CD69 [402, 403]. Therefore, $CD4^+$ and $CD8^+$ peripheral cells from Nef transgenic mice were evaluated for activation and exhaustion markers. In this transgenic model of Nef function, there was no evidence of chronic exhaustion based on evaluation of the PDL-1, PD-1, CD69, CD127 and CD62L (**Figure 5.5**).

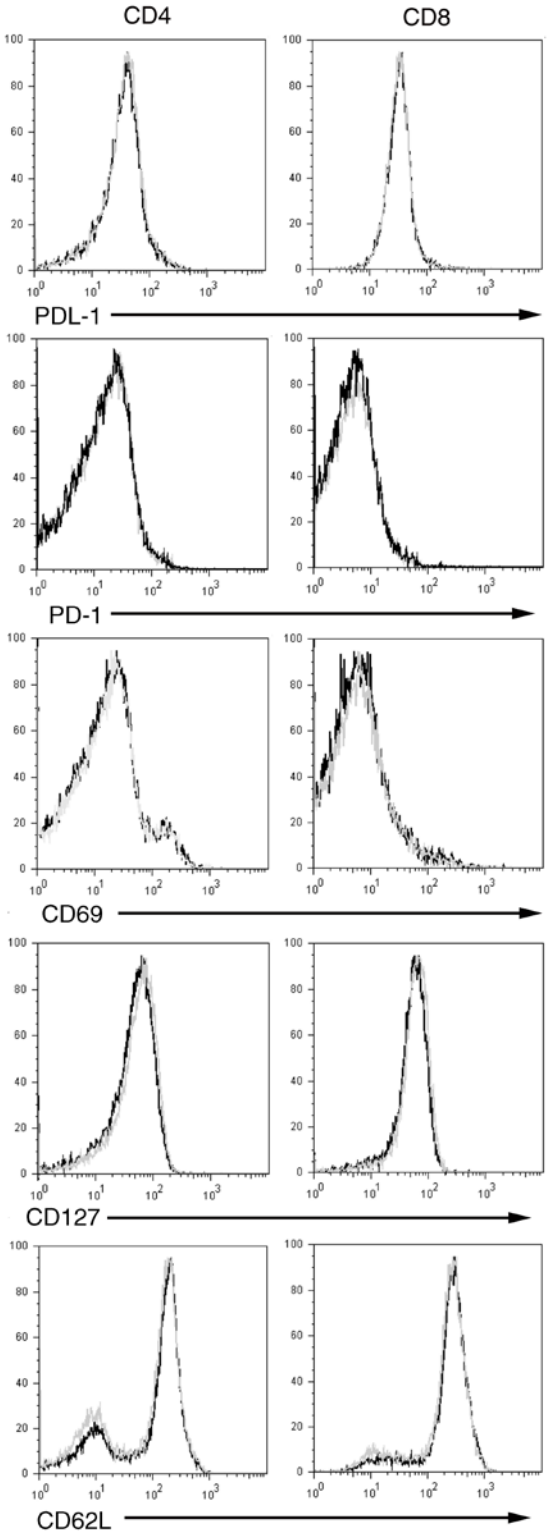
CD4
CD8
PDL-1
PD-1
CD69
CD127
CD62L

Figure 5.5. Nef Tg mice show no change to exhaustion or activation markers PDL-1, PD-1, CD69 and CD62L compared to wild type mice.
Splenocytes were removed from Nef Tg (black) or C57BL/6 (grey) mice. FACS analysis was performed to examine the $CD4^+$ and $CD8^+$ cells for activation/exhaustion markers.

5.2.3 Nef Tg mice can cross present antigen *in vivo*

In this thesis, Nef has been shown to inhibit DC cross presentation and subsequent cross priming *in vitro*. Nef is also expressed in DCs in the Nef Tg mouse; therefore, cross priming was investigated *in vivo*. MHC I mismatched bone marrow (bm) derived DCs (C3H-derived, H-2K^k) were incubated with model antigen, ovalbumin (OVA) and used as a source of cell-associated OVA. Nef Tg mice were injected intraperitoneally (*ip*) with OVA-pulsed DCs and the generation of OVA-specific CD8$^+$ T cells was assessed by tetramer staining (**Figure 5.6A,B**). Nef Tg mice had a trend towards decreased ability to generate antigen-specific CD8$^+$ T cells by cross presentation; however, this was not statistically significant (p=0.2, n=3). To confirm this observation, CFSE-labelled OT-I CD8$^+$ cells were transferred into Nef Tg and wild type mice at the time of antigen injection. OT-I-derived CD8$^+$ T cells recognize the OVA peptide when cross presented by host DCs in the context of H-2K^b. After 72 hours post-injection, OT-I T cell proliferation was detected in both C57Bl/6 and Nef Tg mice but not in the naïve controls (**Figure 5.6C**). The percent of proliferating OT-I cells was calculated and no significant difference was found between the Nef Tg and wild type mice (**Figure 5.6D**).

5.2.4 Nef Tg mice make deficient immune responses to viral infections

Although cross presentation was not inhibited in immune responses against cell-associated antigen, Nef may have an effect during infections with pathogens. Viral secondary infections are common among HIV-positive patients [404-406]; therefore, the effect of Nef expression in CD4$^+$ cells on anti-viral immune responses was next

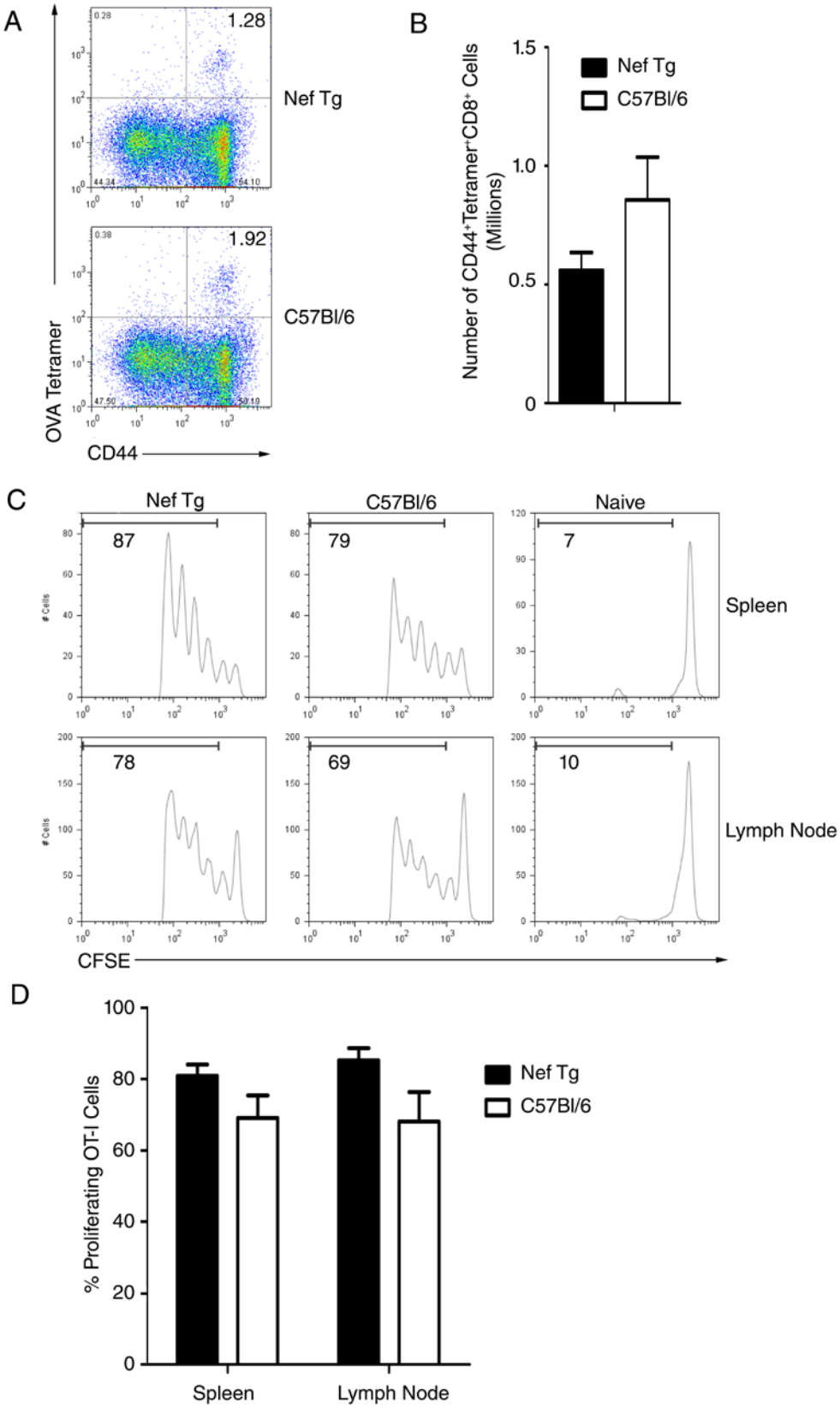
A
1.28
Nef Tg
1.92
C57Bl/6
OVA Tetramer
CD44
B
Number of CD44+Tetramer+CD8+ Cells (Millions)
1.5
1.0
0.5
0
Nef Tg
C57Bl/6
C
Nef Tg
C57Bl/6
Naive
87
79
7
Spleen
78
69
10
Lymph Node
Cells
CFSE
D
% Proliferating OT-I Cells
100
80
60
40
20
0
Nef Tg
C57Bl/6
Spleen
Lymph Node

Figure 5.6. Nef Tg mice can cross present cell-associated antigen and prime $CD8^+$ T cells.

(A) OVA-pulsed C3H-derived bmDCs (H-$2K^k$ haplotype) were injected *ip*. Splenocytes were examined *ex vivo* for H-$2K^b$/$OVA_{257-264}$ -specific $CD8^+$ T cells. **(B)** The mean percentage ± SE is shown. **(C)** OVA-pulsed C3H-derived bmDCs (H-$2K^k$ haplotype) were injected *ip* then OT-I transgenic CFSE-labelled T cells were injected *iv* into Nef transgenic and C57Bl/6 mice. CFSE/$CD8^+$ populations were examined. **(D)** The mean percentage ± SE of proliferating OT-I–derived T cells is shown.

examined. Nef Tg mice and C57Bl/6 controls were infected with Vesicular Stomatitis Virus (VSV). After a seven day infection, splenocytes were removed and analyzed for the presence of $CD8^+$ T cells against the H-$2K^b$ immunodominant VSV-nucleocapsid (NP_{52-59}) epitope (**Figure 5.7**). Nef Tg mice had a reduced number of antigen-specific $CD8^+$ T cells following infection. However, this trend was not statistically significant ($p=0.18$; $n=13$). The CTLs were further examined for their ability to lyse target cells. At three different effector-to-target ratios, the Nef Tg CTLs had a significantly reduced ability to kill VSV NP_{52-59}-specific target cells ($p<0.05$, $n=3$).

5.2.5 Nef Tg mice make deficient immune responses to bacterial infections

AIDS patients often succumb to secondary bacterial infections [406]. One such opportunistic infection associated with AIDS is *Listeria monocytogenes* [407]. To examine the impact of Nef on Ag-specific T cell responses to *Listeria*, a recombinant strain of *Listeria* (rLMOVA) that expresses OVA, was used to infect Nef Tg and C57Bl/6 mice [309]. OVA is fused to the signal sequence and promoter of the *hly* virulence gene which controls the expression of OVA in these bacteria. An I-A^b immunodominant epitope in $CD4^+$ T cell responses against *Listeria*, $LLO_{190–201}$, is known to originate from the endogenous virulence factor, Listeriolysin O (LLO). However, an H-$2K^b$ immunodominant epitope is not well defined. Therefore, the expression of OVA with the immunodominant epitope, $OVA_{257-264}$, during infection allows detection of *Listeria* specific $CD8^+$ T cell responses *in vivo.*

To begin to examine anti-bacterial immune responses, Nef Tg mice and C57Bl/6 controls were *iv* infected with a range of doses (10^2 to 10^4) of rLMOVA and the ability to

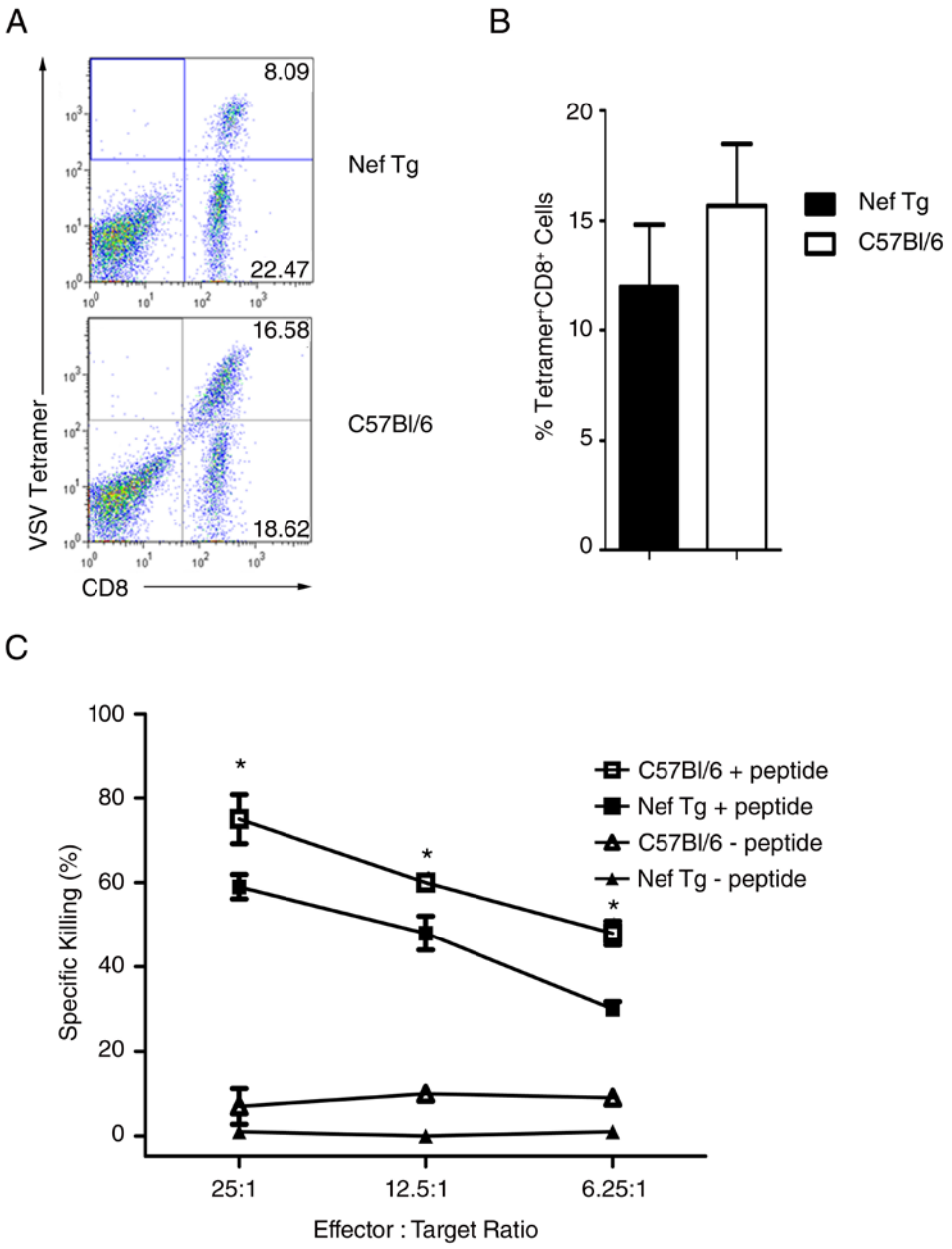
A
8.09
22.47
Nef Tg
16.58
18.62
C57Bl/6
VSV Tetramer
CD8
B
% Tetramer+CD8+ Cells
20
15
10
5
0
Nef Tg
C57Bl/6
C
Specific Killing (%)
100
80
60
40
20
0
C57Bl/6 + peptide
Nef Tg + peptide
C57Bl/6 - peptide
Nef Tg - peptide
25:1
12.5:1
6.25:1
Effector : Target Ratio

Figure 5.7. Nef Tg mice are deficient in anti-viral CTL responses.
Nef Tg and C57BL/6 mice were injected *ip* with VSV at 10^5 $TCID_{50}$ /mice. Seven days post-infection, spleens were removed. Splenocytes were restimulated in culture for 5 days with the VSV-derived H-$2K^b$-restricted peptide, RGYVYQGL. **(A)** The splenocytes were co-stained with an H-$2K^b$- VSV specific tetramer and an anti-CD8 antibody to quantify the VSV-peptide specific $CD8^+$ CTLs generated. **(B)** The mean percentage ± SE of VSV-specific lymphocytes was determined. **(C)** ^{51}Cr-release assays were performed to measure specific killing of target cells. Error bars represent SE. * $p < 0.05$

generate $CD8^+$ T cells responses was assessed by tetramer staining (**Figure 5.8**). At each dose, Nef Tg mice produced fewer antigen-specific $CD8^+$ T cells than the C57Bl/6 controls. This was quantified and a 1.4, 1.7 ($p=0.07$) and 1.5 ($p<0.05$) -fold reduction was found in Nef at each increasing dose increments, respectively.

As the generation of T cells appeared to be affected in the Nef Tg mice, the function of the T cells generated was next examined. First, $CD4^+$ and $CD8^+$ T cells were assessed for their ability to secrete IFNγ (**Figure 5.9**). Following a seven day infection with rLMOVA, antigen-specific T cells were stimulated with the immunodominant epitopes, $LLO_{190–201}$ or $OVA_{257-264}$. As a positive control, general T cell stimulation with PMA and ionomycin or an anti-CD3 antibody to cross-link the T cell receptor was performed. Intracellular staining for IFNγ was analyzed by flow cytometry and the number of IFNγ-secreting cells was calculated. There appeared to be no difference between the Nef Tg and C57Bl/6 $CD4^+$ and $CD8^+$ T cells to secrete IFNγ regardless of the stimulation used. Next, the ability for $CD8^+$ T cells to lyse target cells was assessed (**Figure 5.10**). At three different effector-to-target ratios Nef Tg mice were found to have an impaired ability to kill target cells. This indicates that Nef-expression may have selective effects on immune cell function. Finally, it was determined if the immune cell defects observed had an effect on the ability of Nef Tg mice to clear an infection. Nef Tg and C57Bl/6 mice were infected with rLMOVA. One, three and five days post-infection, spleens were removed and analyzed for the presence of bacteria (**Figure 5.11**). Both Nef Tg and wild type controls had detectable bacterial loads at each time point analyzed. However, at each time interval, the bacterial counts decreased in a similar manner indicating that the mice had a comparable ability to clear a bacterial infection.

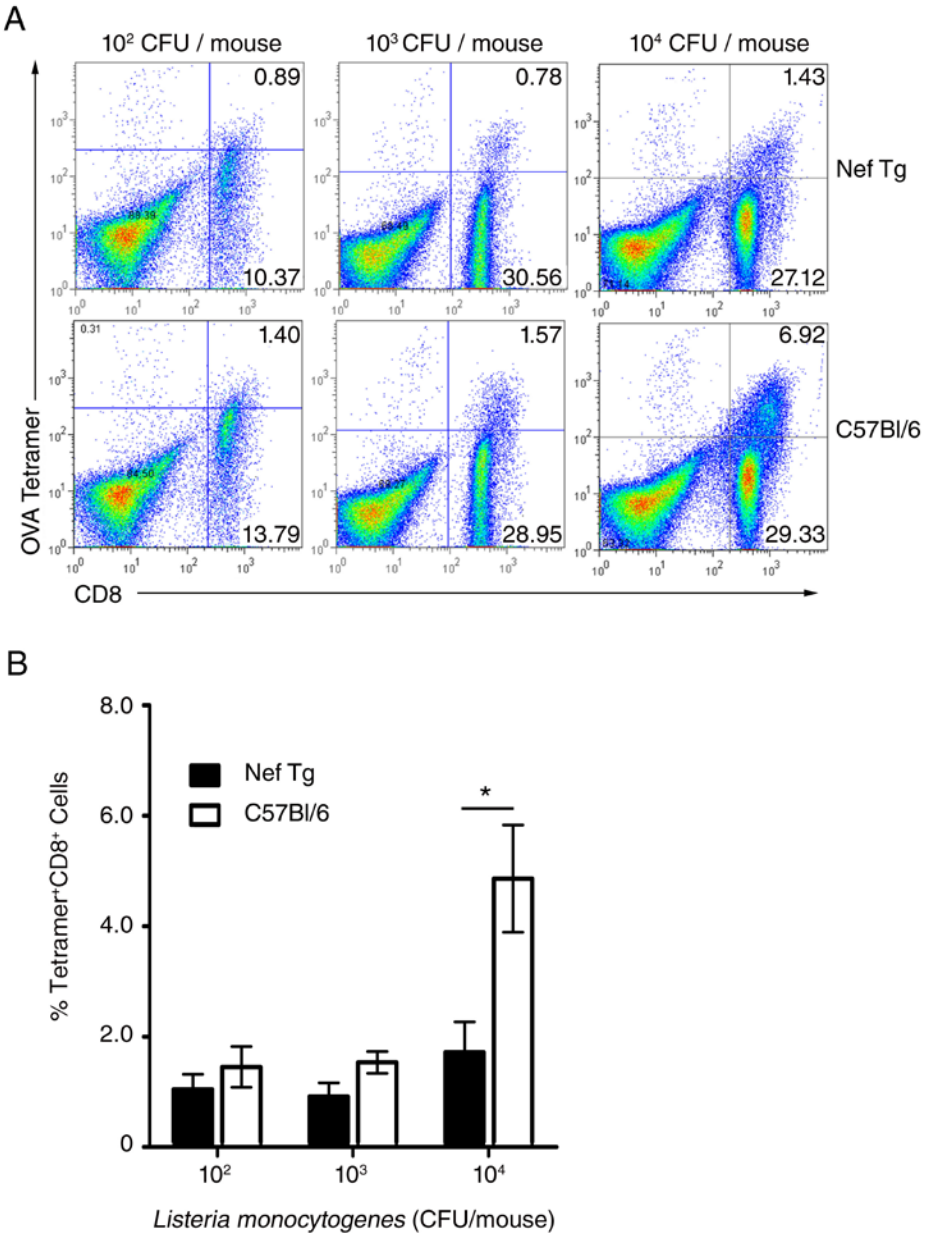
A
10² CFU / mouse
10³ CFU / mouse
10⁴ CFU / mouse
0.89
10.37
0.78
30.56
1.43
27.12
Nef Tg
1.40
13.79
1.57
28.95
6.92
29.33
C57Bl/6
OVA Tetramer
CD8
B
Nef Tg
C57Bl/6
*
% Tetramer⁺CD8⁺ Cells
8.0
6.0
4.0
2.0
0
10²
10³
10⁴
Listeria monocytogenes (CFU/mouse)

Figure 5.8. Nef Tg mice have a trend of impaired anti-bacterial CTL generation. Nef Tg mice and age-matched wild type mice (C57BL/6) were *iv* infected with a several doses of rLMOVA. Seven days post-infection, spleens were removed. Splenocytes were restimulated in culture for 5 days with the OVA derived H-2K^b-restricted peptide, SIINFEKL. **(A)** Following infection, splenocytes were co-stained with an H-2K^b-OVA specific tetramer and an anti-CD8 antibody to quantify the OVA-peptide specific CD8$^+$ CTLs generated. **(B)** The mean percentage ± SE of OVA-positive lymphocytes was determined. *$p<0.05$.

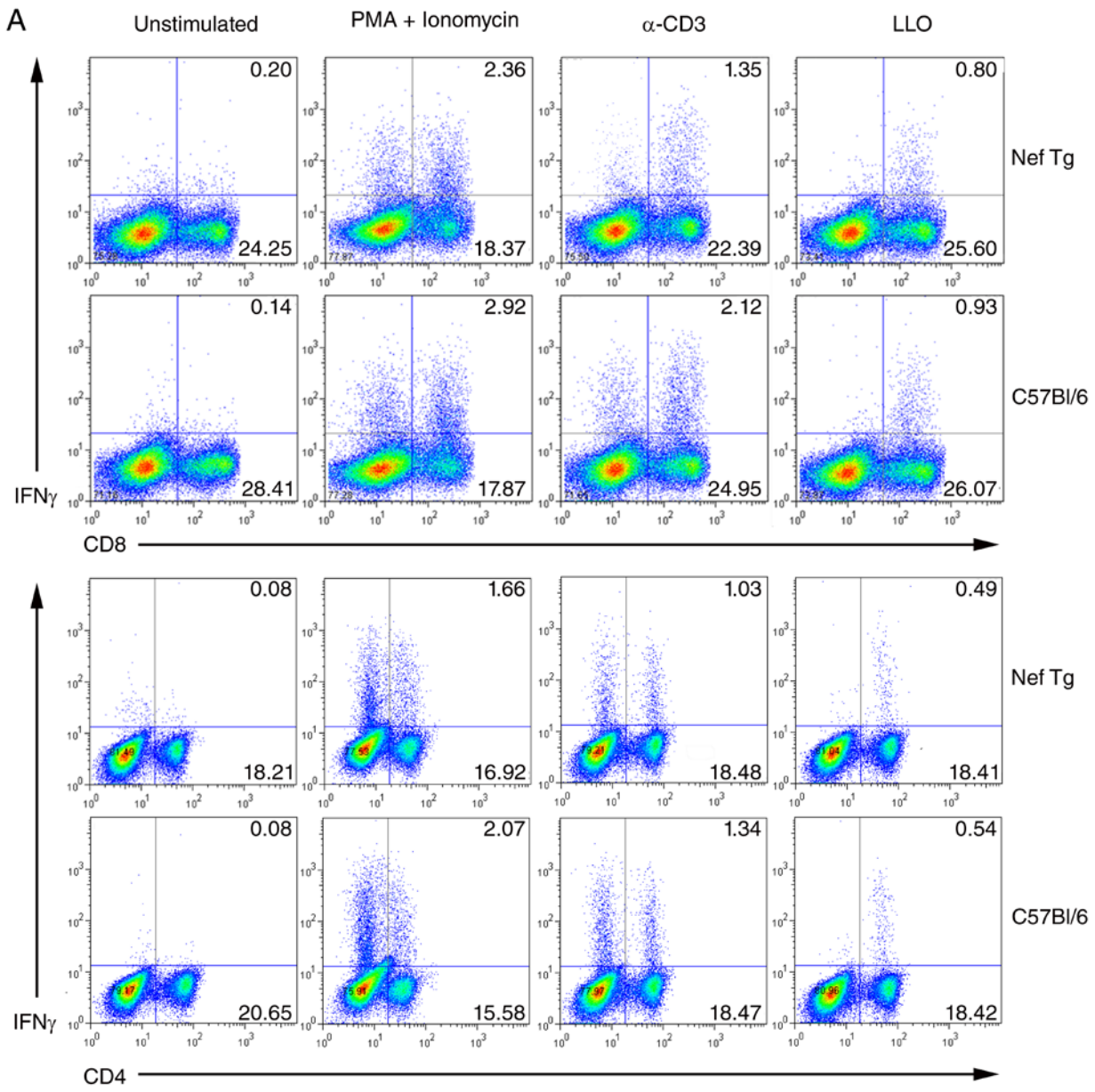
A
Unstimulated
PMA + Ionomycin
α-CD3
LLO
Nef Tg
C57Bl/6
IFNγ
CD8
CD4
0.20
24.25
2.36
18.37
1.35
22.39
0.80
25.60
0.14
28.41
2.92
17.87
2.12
24.95
0.93
26.07
0.08
18.21
1.66
16.92
1.03
18.48
0.49
18.41
0.08
20.65
2.07
15.58
1.34
18.47
0.54
18.42

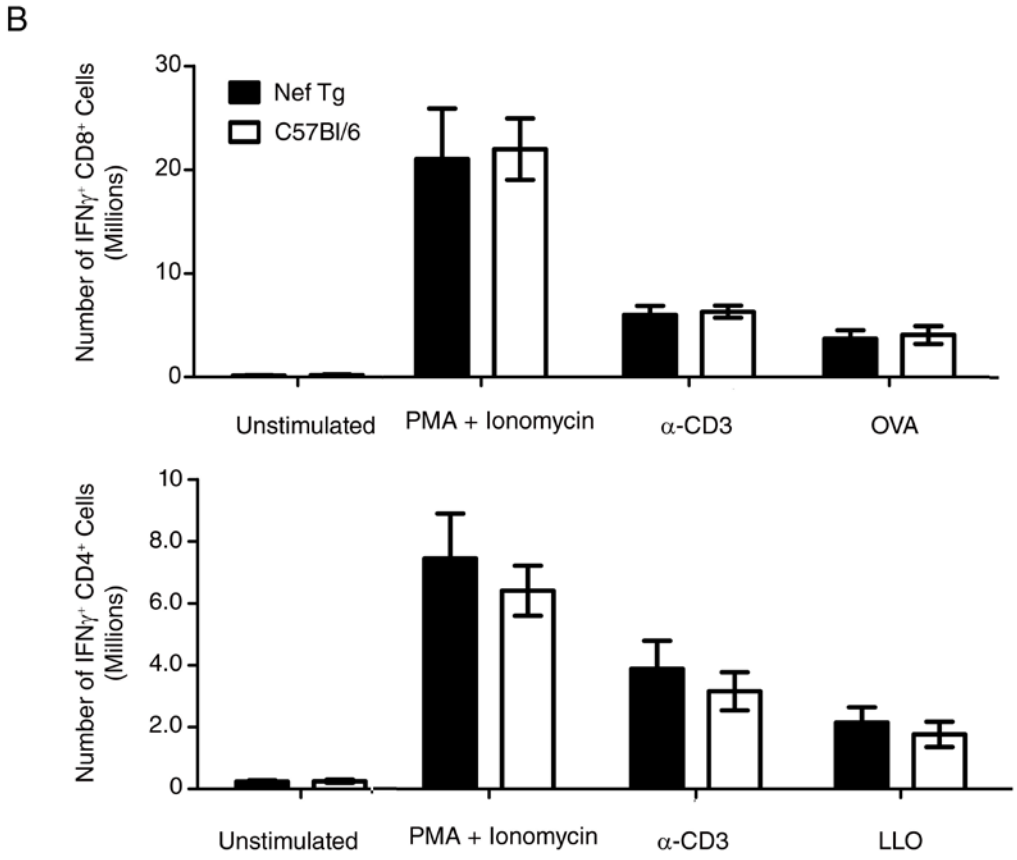

Figure 5.9. Nef Tg CD4$^+$ and CD8$^+$ T cells secrete IFNγ following bacterial infection. **(A)** Nef Tg mice and age-matched wild type mice (C57BL/6) were *iv* infected with rLMOVA. Seven days post-infection, spleens were removed. Splenocytes were treated *ex vivo* with GolgiPlug and stimulated with PMA + Ionomycin, an anti-CD3 antibody, MHC I or MHC II-restricted peptide or left unstimulated. Following a 5 hour incubation, intracellular IFNγ staining was performed to quantify the antigen-specific CD8$^+$ or CD4$^+$ T cells, respectively. **(B)** Mean number ± SE of CD8$^+$ or CD4$^+$ lymphocytes producing IFNγ.

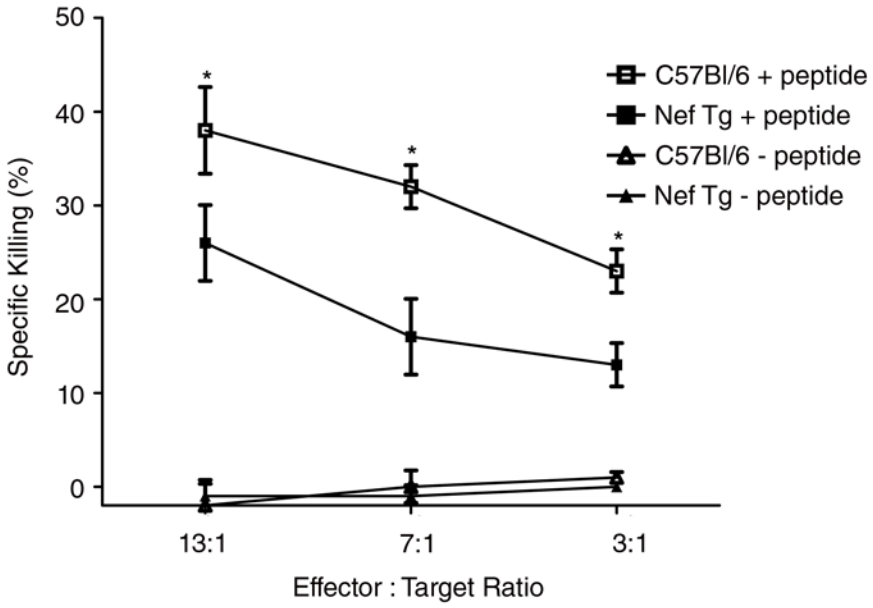

Figure 5.10. Nef Tg mice have impaired CTL function in response to *Listeria* infection.

Nef Tg mice and age-matched wild type mice (C57BL/6) were *iv* infected with rLMOVA. Seven days post-infection, spleens were removed. ^{51}Cr-release assays were performed *ex vivo* to measure CTL specific killing. Error bars represent SE. *$p<0.05$

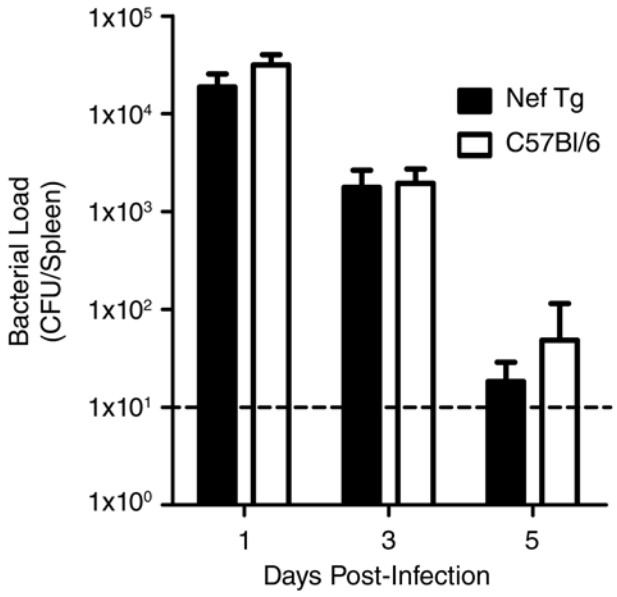

Figure 5.11. Nef Tg mice reduce bacterial burden in spleen similar to wild type mice following *Listeria* infection.
Following infection (1, 3, 5 days), splenocytes were lysed in 0.1% NP40. rLMOVA remaining in splenocytes was quantified by plating lysates on BHI media plates. Figure represents mean ± SE. Figures represent three experiments with at least three mice per group.

5.2.6 Nef Tg mice show impaired memory CTL killing ability following bacterial recall infection

Primary $CD8^+$ cytotoxic T cell responses to *Listeria monocytogenes* have been reported to be independent of $CD4^+$ T cell help [311, 408]. However, $CD4^+$ help is required for development of $CD8^+$ memory [311, 408]. Because Nef transgenic mice show a decreased proportion of $CD4^+$ cells in the periphery, memory development in the Nef transgenic may be affected. Therefore, the ability of Nef transgenic mice to resist a second challenge of *Listeria monocytogenes* was examined. Nef Tg and C57Bl/6 controls were infected with rLMOVA. On day 14, 28 and 64 post-infection, the mice were challenged a second time with rLMOVA and evaluated for the ability to clear the infection over three days (**Figure 5.12**). In the primary infection control, both Nef Tg and C57Bl/6 had similar detectable levels of bacteria in their spleens as seen previously. However, upon secondary infection, C57Bl/6 mice were able to clear the infection and no bacteria were detected regardless of the time the secondary infection occurred. Conversely, in the Nef Tg mice, bacteria could be detected following the secondary infection indicating that memory responses may be impaired.

The memory responses against *Listeria monocytogenes* in the Nef Tg mice were next evaluated. First, the generation of $CD8^+$ T cells following secondary infection was analyzed by tetramer staining at day 14, 28 and 64 following secondary infection (**Figure 5.13A**). The number of antigen-specific CTLs was quantified and no significant difference was noted between the Nef Tg and C57Bl/6 controls (**Figure 5.13B**). Next, the function of the T cells generated during a memory response was evaluated. On day 64 following a primary infection, mouse strains were infected with rLMOVA for a second

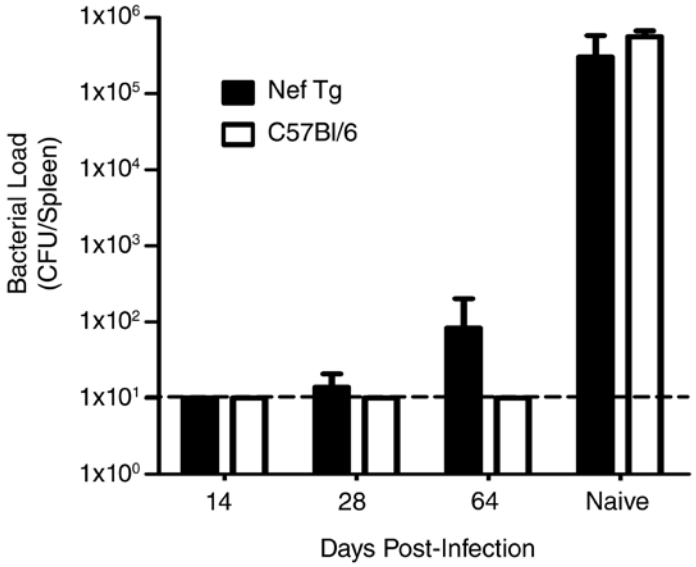

Figure 5.12. Nef Tg mice have impaired ability to clear bacteria from the spleen in recall responses.
Nef Tg mice and age-matched wild type mice (C57BL/6) were *iv* infected with rLMOVA at $1x10^4$ CFU/mouse. Day 14, 28 and 64 post-infection, the mice were reinfected with rLMOVA at $1x10^5$ CFU/mouse. Three days following the second infection, splenocytes were lysed in 0.1% NP40. rLMOVA remaining in splenocytes was quantified by plating lysates on BHI media plates. Figure represents mean ± SE.

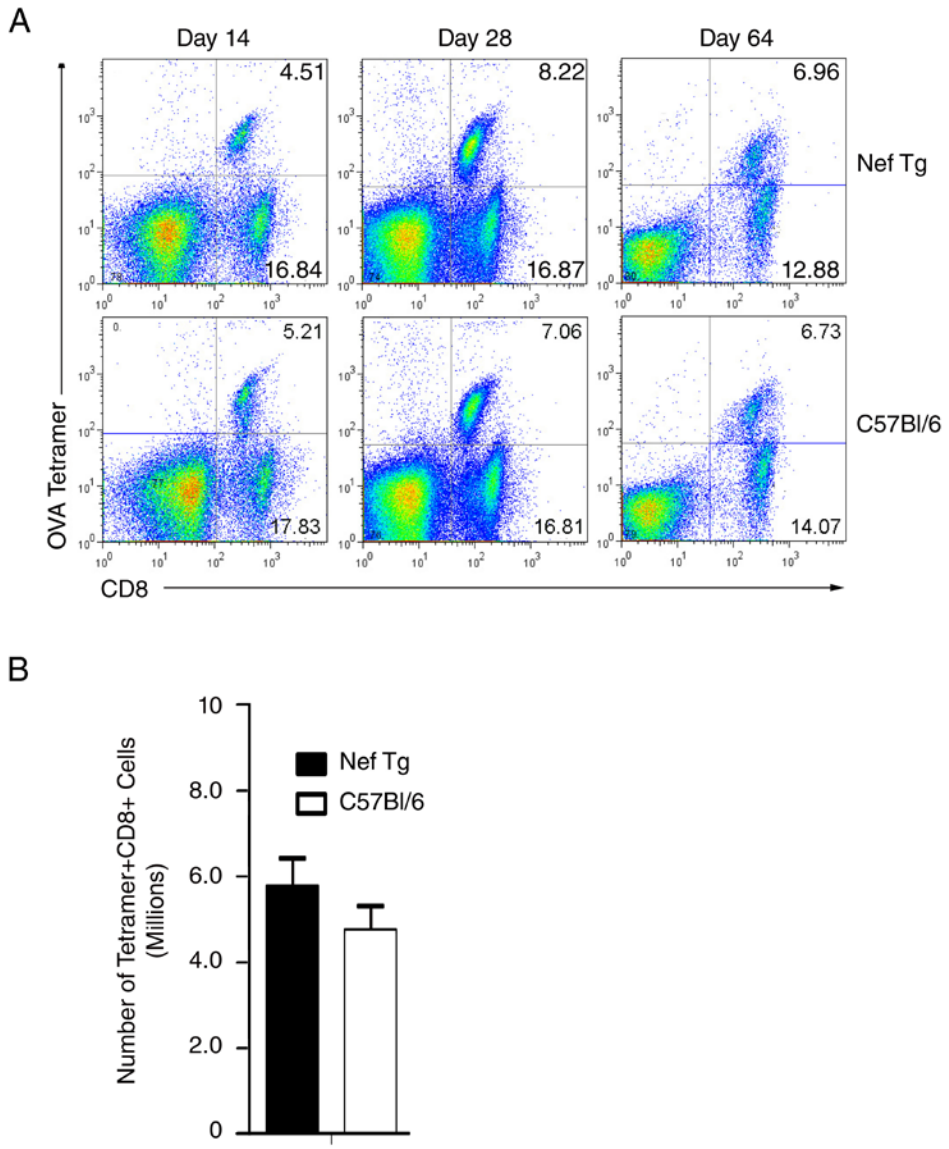

Figure 5.13. Nef Tg mice generate memory CD8$^+$ T cell against *Listeria* similar to wild type mice in recall responses.
(A) Following the second infection, splenocytes were co-stained with an H-2K^b-OVA specific tetramer and an anti-CD8 antibody to quantify the OVA-peptide specific CD8$^+$ CTLs generated. **(B)** The mean number ± SE of OVA-positive lymphocytes on Day 64 post-primary infection was determined.

time. Following a seven day secondary infection with rLMOVA, antigen-specific T cells were stimulated with the immunodominant epitopes, $LLO_{190–201}$ or $OVA_{257-264}$, PMA and ionomycin or an anti-CD3 antibody to cross-link the T cell receptor as above. Intracellular staining for IFNγ was analyzed by flow cytometry and the number of IFNγ-secreting cells was calculated (**Figure 5.14**). The ability to secrete IFNγ was similar between Nef Tg and C57Bl/6 mice. Finally, following a second infection on Day 64, $CD8^+$ splenocytes were evaluated for their ability to kill target cells (**Figure 5.15**). At various effector-to-target ratios Nef Tg had a reduce ability to lyse target cells displaying OVA in complex with $H\text{-}2K^b$. Taken together, $CD8^+$ memory responses are generated in Nef Tg mice but are functionally impaired when Nef is present.

5.2.7 Evaluation of $CD4^+$ T cell responses in Nef Tg mice

$CD4^+$ help has been suggested to play a role in initiation and persistence of CTL responses [409]. In several models, it has been shown that optimal $CD8^+$ responses require the presence of antigen-specific $CD4^+$ T cells [409]. Therefore, the ability of Nef Tg mice to generate $CD4^+$ T cells against foreign antigen was investigated. Cell associated OVA (as described in section 5.2.3), was injected together with CFSE-labelled $CD4^+$ OT-II cells. OT-II-derived $CD4^+$ T cells will proliferate when they recognize the OVA peptide in the context with host $I\text{-}A^b$. In this study, Nef Tg and C57Bl/6 mice had comparable levels of $CD4^+$ T cell proliferation when challenged with cell-associated OVA as visualized by the degree of CFSE dilution (**Figure 5.16A**). This finding was confirmed when the percentage of OT-II cells proliferating was quantified (**Figure 5.16B**).

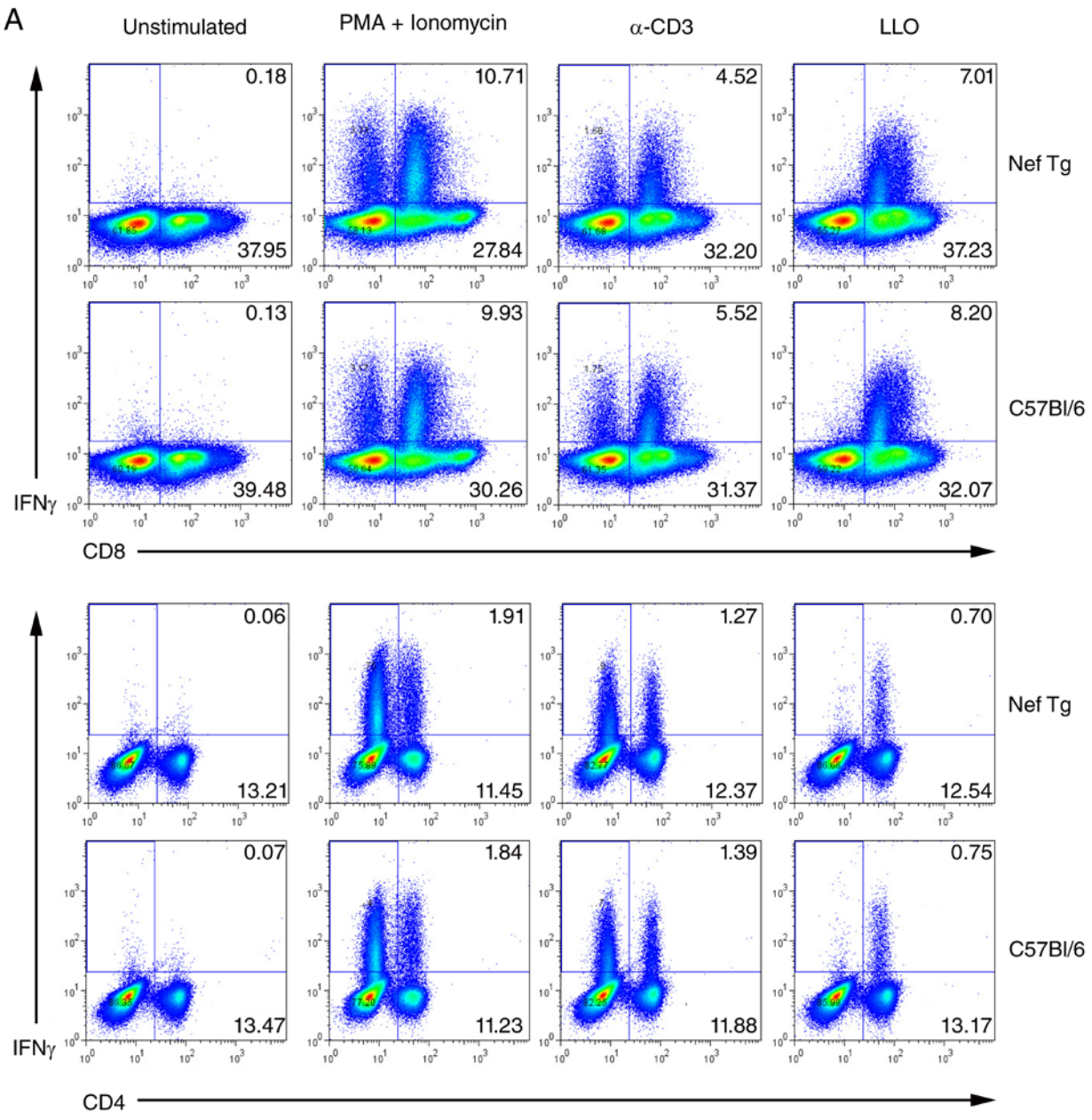
A
Unstimulated
PMA + Ionomycin
α-CD3
LLO
0.18
37.95
10.71
27.84
4.52
32.20
7.01
37.23
Nef Tg
0.13
39.48
9.93
30.26
5.52
31.37
8.20
32.07
C57Bl/6
IFNγ
CD8
0.06
13.21
1.91
11.45
1.27
12.37
0.70
12.54
Nef Tg
0.07
13.47
1.84
11.23
1.39
11.88
0.75
13.17
C57Bl/6
IFNγ
CD4

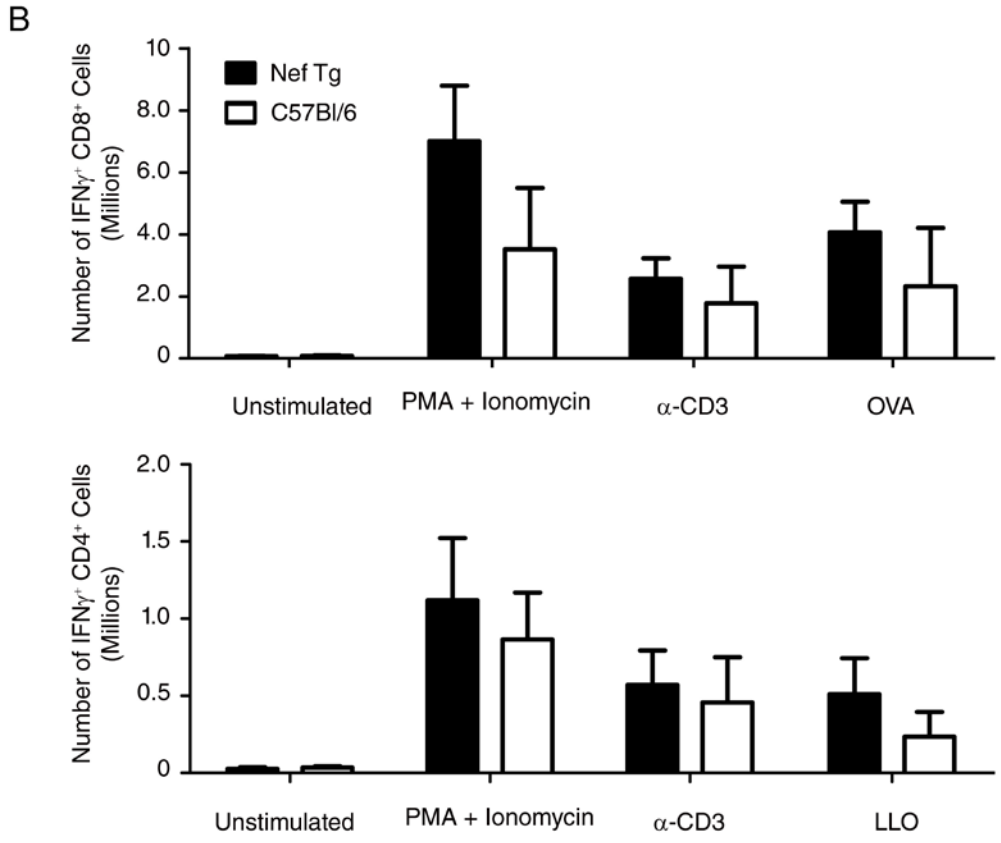

Figure 5.14. Nef Tg mice generate recall responses with T cells that produce IFNγ following *Listeria* infection

(A) Splenocytes from mice secondarily infected with rLMOVA on Day 64 were treated *ex vivo* with GolgiPlug and stimulated with PMA + Ionomycin, an anti-CD3 antibody, MHC I or MHC II-restricted peptide or left unstimulated. Following a 5 hour incubation, intracellular IFNγ staining was performed to quantify the antigen-specific $CD8^+$ or $CD4^+$ T cells, respectively. **(B)** The mean number ± SE of $CD8^+$ or $CD4^+$ lymphocytes producing IFNγ.

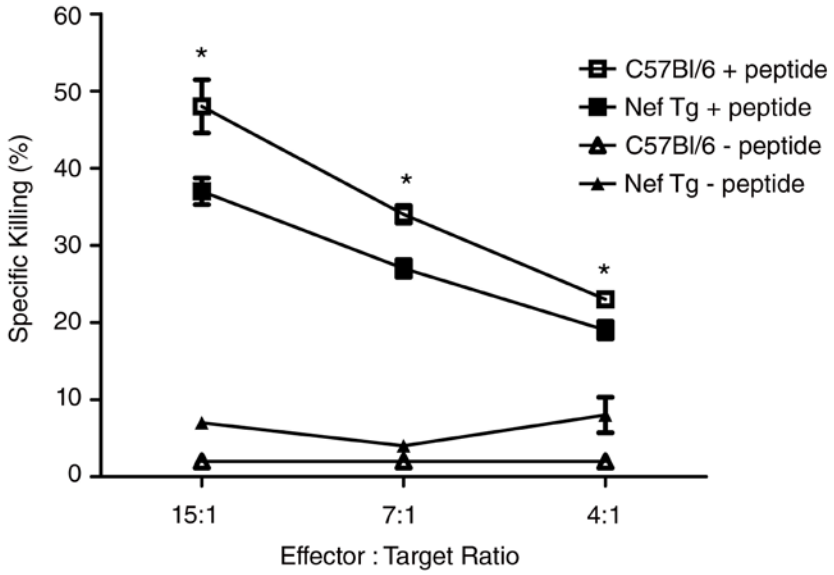

Figure 5.15. Nef Tg mice produce memory CTLs with impaired killing ability.
^{51}Cr-release assays were performed *ex vivo* on mice infected on Day 64 to measure CTL specific killing. Error bars represent SE. *p<0.05

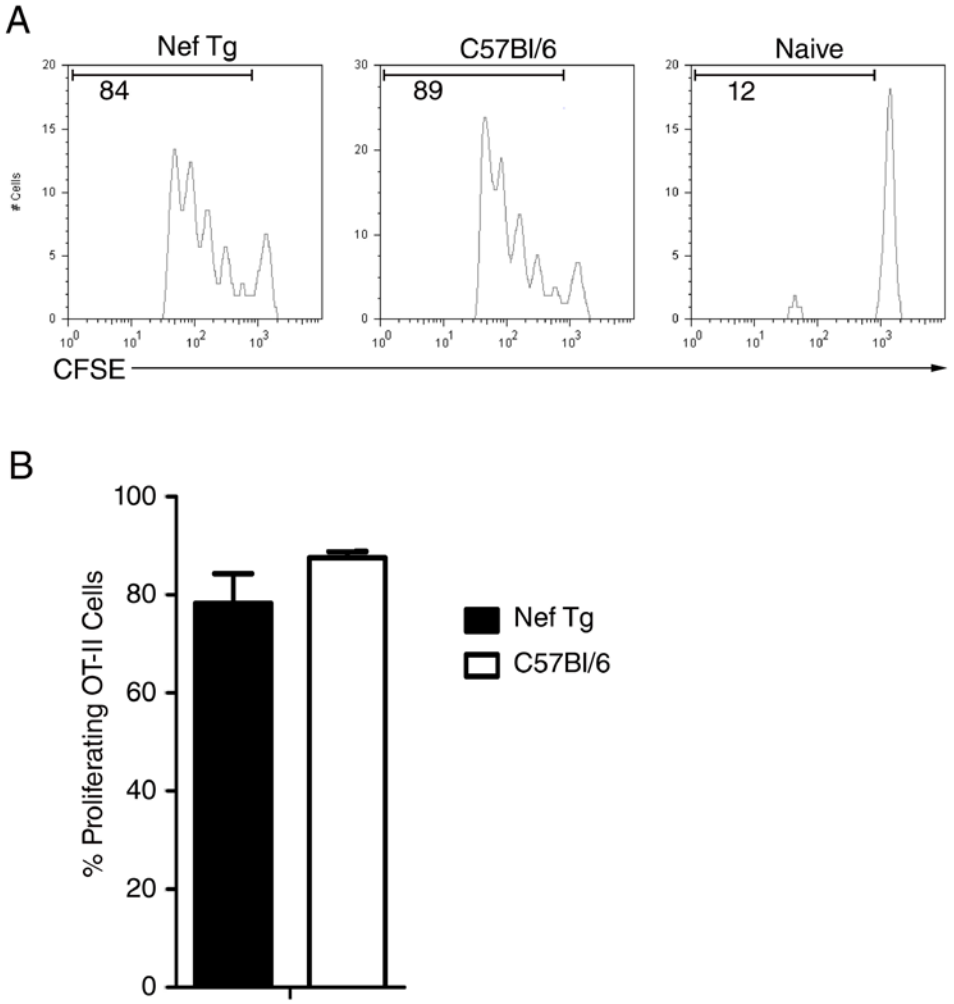

Figure 5.16. Nef Tg mice can present cell-associated antigen to CD4$^+$ T cells.
(A) OVA-pulsed C3H-derived bmDCs (H-2K^k haplotype) were injected (*ip*) then OT-II transgenic CFSE-labelled T cells were injected (*iv*) in Nef transgenic and C57Bl/6 mice. CFSE/CD4$^+$ populations were examined. **(B)** The mean percentage ± SE of proliferating OT-II–derived T cells is shown.

5.3 Discussion

The HIV protein, Nef, is a potent virulence factor crucial for high viral persistence and host progression of disease [410]. In this study, a murine model of Nef function in CD4-expressing cells was created to examine Nef's role in the modulation of immune responses to secondary infections. In this model, the $CD4^+$ cell population in the thymus and the $CD4^+$ and MHC I^+ cell populations in the periphery were decreased. The cross presentation function of Nef Tg mice was examined and contrary to the deficiency found *in vitro*, these mice were able to cross present cell-associated antigen *in vivo*. However, when challenged with a bacterial or viral infection, the Nef Tg mice had some deficiencies in generating immune responses.

The generation of Nef transgenic mice has previously been reported whereby the *nef* gene has been expressed using several promoter/enhancer systems including the CD3δ, CD2, TcR β chain and importantly CD4 elements [411-415]. The phenotypes of these mice included reduction in surface CD4, loss of T cells and some alterations in T cell activation but were by no means the same in terms of immune function [411-414]. The most striking phenotype was observed when *nef* was expressed using the CD4 regulatory elements. These mice had defects in their immune system as well as developed a wasting, multi-organ syndrome analogous to AIDS [415]. The disease course of this animal model correlated with the level of *nef* transgene expression [414, 415]. Differences in these animal models can be attributed to differences in *nef* alleles as well as variation in expression patterns and levels [386, 411, 412]. In the current study, a new Nef transgenic animal model with *nef* expression driven by a CD4 promoter/enhancer system was created in order to most accurately recapitulate the immune deficiency phenotype

associated with HIV infection. The model has been created to allow examination of specific effects of Nef on the essential immune function of antigen processing and presentation. The goal is to provide a model with which to examine in detail, Nef's alterations to immune functions in the context of secondary infections, an essential aspect of HIV-induced disease.

In our transgenic model, a severe wasting phenotype was not observed as described previously [414]. This is most likely due to lower levels of *nef* expression in our model and possibly due to differences in the transgene insertion sites. Despite this variation, a decrease in $CD4^+$ populations in the thymus and periphery was noted as previously described [414]. The ability to downregulate CD4 from the surface of HIV-infected cells is one of the best characterized functions of Nef [reviewed in [410]]. Nef achieves this by linking CD4 to AP-2 adaptor complexes increasing endocytosis and directing CD4 to lysosomes for degradation [410]. This removal of CD4 from the cell surface is thought to promote the release and infectivity of HIV particles [410, 416, 417]. Considering this function, the decrease in the $CD4^+$ cell population in the Nef Tg mice thymi and periphery may be a loss of CD4 receptor from the cell surface marking the cell population rather than a reduction in the number of cells themselves. However, it has been proposed that Nef can induce cell death. Restricted Nef expression in $CD4^+$ T cells has been shown to induce apoptosis [418]. In addition, expression of Nef has been shown to induce CD95 (Fas) that leads to apoptosis [419, 420]. It has also been noted that Nef can increase apoptotic responses by altering the expression of Bcl-2 and Bcl-X_L [421]. Furthermore, Nef may manipulate T cell signalling and induce a state of constitutive activation which

is known to cause cell death [414]. Therefore, the consequence of Nef-expression in $CD4^+$ cells could be a reduction in cell numbers.

In this study, the reduction in the $CD4^+$ population in the thymus was accompanied by a decrease in total cellularity, which is consistent with previous findings in transgenic models [411, 413, 414]. Considering this, cell death is a likely explanation of loss of cell numbers. In addition to direct cytopathic effects of Nef, aberrant selection in the thymus may also be occurring. Decreased CD4 on thymocytes would interrupt the interaction between the T cell receptor complex on developing thymocytes and MHC II on the thymic epithelium impairing positive selection resulting in fewer mature $CD4^+$ T cells. Mice deficient in MHC II [422] or hemizygous for CD4 [423] have impaired $CD4^+$ T cell development presumably due to reduced CD4-MHC II contact demonstrating the importance of this interaction.

In HIV-infected individuals, $CD4^+$ T cell depletion from the thymus is observed [424]. This study suggests that despite $CD4^+$ T lymphopenia in the thymi of HIV infected adults thymopoiesis is still occurring [424]. Instead, direct viral lysis and activation leading to high turnover and exhaustion are proposed as the relevant mechanisms impacting the thymus [424]. On the other hand, loss of thymic function may be a major factor contributing to disease in paediatric HIV infections [425, 426]. In comparison to uninfected children, HIV-positive children have fewer T cell receptor rearrangement excision circles (TREC) indicating a reduced thymic output [427]. In this transgenic model, Nef is expressed throughout mouse development analogous to paediatric AIDS.

In the periphery, a reduction in the $CD4^+$ population is also evident. Surprisingly, increased cellularity was noted in the spleen of Nef Tg mice. In previous studies of Nef

Tg mice, enhanced apoptosis and reduced $CD4^+$ T cell numbers were noted when Nef was expressed in the cell lineage [411-414, 418]; however, this was not consistent among all transgenic lines and a dose threshold was observed with lower transgene expression showing minimal or no alterations in the peripheral T cell populations [411, 412]. Additionally, splenomegaly was noted in several Tg lines [413, 415, 418]. Nef expressed under the control of the TCR β chain promoter had an expansion of B cell and NK cell numbers in the periphery [413] while Nef expressed in $CD4^+$ lineages exhibited increased immature DC, B cell, macrophage, megakaryocyte and erythroid progenitor numbers in the spleen [415, 418]. Furthermore, enlarged spleens have been observed in SIV infection in rhesus macaques [428-432] and pigtailed macaques [433]. Spleen enlargement in this Nef transgenic model was accompanied with the appearance of $CD4^-$ and MHC I^- cells. With the lack of MHC I, this cell population may have developed in the periphery without the detection of the immune system.

As *nef* expression is driven by CD4 promoter/enhancer element, Nef protein was present in DCs in this transgenic model. Upon analysis of DC populations in the spleen of transgenic model, the proportion of $CD4^+CD11c^+$ population was decreased; however, the $CD8^+CD11c^+$ population was similar to wild type controls. This indicates that Nef is impacting the $CD4^+$ DC population in which it is expressed possibly by direct cytotoxicity or altering DC phenotype. Nef-mediated alteration in DCs subsets has been noted in other Nef transgenic mouse models including impaired maturation and distribution in lymphoid organs [434]. Although murine DC populations are not equivalent to those in humans, general comparisons can be made. In HIV-infected individuals, a decreased number of DCs in the blood has been noted [138, 435, 436]. This

may be a result of altered migration of DCs with reduced localization in the blood as well as direct depletion of the DC populations [95].

Interference with DC location, maturation-state and general health by HIV, will have an impact on DC function, including antigen presentation, and may represent a key aspect of viral immune evasion. DCs isolated from HIV-positive patients have been shown to have reduced ability to prime allogenic T cells in comparison to those from healthy donors [141, 364] In addition, DCs isolated from infected individuals have dysregulated cytokine production with reduced IL-12 and IFNα and upregulated IL-10 secretion [141, 361, 362]. Furthermore, DCs from individuals with acute HIV have reduced surface expression of costimulatory molecules and DCs infected in culture have been shown to have reduced ability to mature [140, 142, 143]. Nef in particular may affect DCs and contribute to the immunodeficiency observed during HIV infections. Nef has been shown to downregulate MHC I trafficking in DCs possibly impairing antigen presentation [169, 366, 367]. Specifically, in this thesis, Nef was shown to affect not only classical MHC I presentation but also cross presentation when expressed in DCs *in vitro*. When examined *in vivo,* Nef Tg mice had similar ability as wild type controls to cross present cell-associated antigen. This discrepancy may be attributed to Nef expression levels. *In vitro*, Nef expression was driven by a viral promoter producing higher protein levels than achieved using the CD4 promoter *in vivo*. Nef-mediated MHC I manipulation has been shown to require a threshold level of expression [380]. Lower amounts of Nef can modulate CD4 cell surface location but have no affect on surface expression of MHC I [380]. Alternatively, Nef expression in DCs *in vivo* would occur in accordance with CD4 promoter activity allowing Nef to be expressed only in $CD4^+$ DCs and some

plasmacyotid DCs (pDCs) [9]. Analysis of precise function of individual DC subsets, although still limited, suggests that the $CD8^+CD4^-$ DC subset is the most efficient at cross presenting exogenous antigen on MHC I while $CD4^+CD8^-$ DCs appear to be better at presentation of exogenous antigens by MHC II [437]. In this way, Nef-expression in $CD4^+$ DCs may not be a major inhibitor of cross presentation during immune challenge *in vivo*.

Opportunistic infections are an important cause of disease in HIV infected individuals [438]. AIDS patients often succumb to secondary bacterial infections such as *Listeria monocytogenes*. *Listeria* infection is markedly increased in immunocompromised patients with AIDS patients having approximately a 100 to 300 fold higher risk of infection than the general population [407]. In addition, viral opportunistic infections are common in HIV-infected adults and cause considerable morbidity and mortality [439]. The impact of Nef on immune responses against bacterial and viral infection was examined in the Nef Tg mice. Nef Tg mice generated diminished $CD8^+$ immune responses to VSV and *Listeria* infections evidenced by reduced CTL lytic activity. These novel results establish that Nef's effects are directly responsible for immune deficiency towards two major secondary pathogens and suggest Nef is a major influencing factor of host-pathogen interactions in HIV infected individuals.

There are several factors that may be involved in the Nef-mediated dampening of immune responses against secondary infections. First, this could still be attributed to Nef-mediated reduction in MHC I antigen presentation as impaired generation of $CD8^+$ T cells following infection was noted. $CD4^+$ DCs have been shown to cross present in certain cases such as when antigen is in the form of immune complexes [440]. The cross

presentation pathway in Nef Tg mice was functional when evaluated with cell-associated protein. However, different antigens may use different cross presentation paths [86] and immune impairment in the Nef Tg mice may depend on the type of antigen encountered. Furthermore, L*isteria monocytogenes* has been shown to infect DCs directly [441] and VSV binds phosphatidylserine, a near-universal cell-surface component, giving VSV a broad tropism that would allow direct DC infection [442]. In this way, antigen would access the classical MHC I pathway for $CD8^+$ T cell priming which may be compromised by Nef expression. Another possibility may be that Nef is affecting MHC II presentation and therefore reducing the $CD4^+$ help available to activate efficient CTL responses. $CD4^+$ T cells secrete cytokines and chemokines and also interact directly with the DCs 'licensing' them to induce potent CD8 responses [409, 443, 444]. As mentioned above, $CD4^+$ DCs, that are expressing Nef, appear to be most efficient at stimulating $CD4^+$ T cell responses by utilizing the MHC II pathway. In several instances, including *in vitro* studies in this thesis, Nef has been known to influence MHC II trafficking [168-170]. Therefore, the generation of $CD4^+$ T cell help may be impaired in the Nef transgenic mice during immune responses.

Additionally, in this model, $CD4^+$ T cells are expressing Nef which could cause reduced numbers and altered function [145, 368]. Nef has been documented to affect T cell function in several ways. Nef can downregulate chemokine receptors, CXCR4 and CCR5, which may affect migration and distribution of $CD4^+$ cells [445, 446]. Interaction of CXCR4 with Nef may also cause T cell apoptosis contributing to T cell depletion [368, 447]. Further to this, Nef alters T cell activation to create an environment to maximize viral replication and cell survival [145] as a result rendering $CD4^+$ T cells against

secondary infections less than efficient. Nef has been shown to affect T cell signalling by interfering with events downstream of the T cell receptor (TCR) [412, 448]. Furthermore, it has recently been shown that Nef can interrupt the immunological synapse formation by misrouting Lck and TCR from the T cell-APC contact sites [449, 450] and instead aids in formation of a virological synapse for cell-cell mediated viral spread [451, 452]. In addition, Nef-mediated removal of cell surface molecules affects T cell activation. Downregulation of the costimulatory molecule, CD28, from the cell surface has been observed [453]. This would suppress the immune response and lead to T cell anergy. Again, reduction of CD4 on T cells weaken the T cell receptor complex interaction with MHC II on antigen presenting cells reducing activation of $CD4^+$ T cell responses [410, 454] Taken together, Nef can not only affect generation of $CD4^+$ responses but also the function of $CD4^+$ T cells themselves leading to poor anti-viral immunity. In most HIV-infected patients, the acute phase of infection has an obvious lack of $CD4^+$ proliferative responses and weak CTL activity [455, 456]. Conversely, long-term non-progressors have significant levels of $CD4^+$ cell proliferation accompanied by strong CTL responses and low viral loads [457, 458]. This highlights the importance of $CD4^+$ help for efficient CTL activity.

Proliferation of $CD4^+$ cells was evaluated in the Nef transgenic mice following inoculation with cell-associated antigen and no difference was noted between Nef transgenic mice and wild type controls. However, generation of $CD4^+$ T cell immunity in an infection setting needs to be evaluated. The pathogens used here, VSV and rLMOVA, are not be ideal for examining $CD4^+$ T cell responses. This thesis and other studies have demonstrated that VSV-specific primary and memory $CD8^+$ immune responses can be

generated in the absence of $CD4^+$ T cells. [322, 323, 459]. Furthermore, mice lacking $CD4^+$ T cells generate primary CTL responses to *Listeria monocytogene* that are equivalent to wild type and can efficiently clear the infection [311]. However, protective memory is defective and wanes over time [311]. Following both VSV and rLMOVA infection, some deficiency in primary infection are observed likely due to compounding effects of Nef. Analogous to mice missing $CD4^+$ help [311], Nef transgenic mice immune responses' following secondary rLMOVA infection diminished over time resulting in suboptimal CTL killing function and incomplete bacterial clearance most prevalent at day 64 following primary infection. The importance of $CD4^+$ T cell help has been demonstrated in other HIV and Nef-specific murine models of fungal infection [418, 460, 461]. Oropharyngeal candidiasis (OPC) is a common fungal infection plaguing patients with impaired cell-mediated immunity including those positive for HIV [462]. $CD4^+$ helper T cells are directly required for recovery from OPC [463]. Expression of Nef in $CD4^+$ cells results in increased susceptibility to OPC suggesting that Nef impairs $CD4^+$ T cell function *in vivo*.

In the absence of faithful small animal models for HIV, many of the details of Nef mediated immuno-subversion that contributes to a generalized immunodeficiency are yet to be fully appreciated. Analysis of DCs and CD8-mediated immunity in a Nef transgenic mouse model revealed functional impairment. Further analysis of DC priming and subsequent function $CD4^+$ T cells will likely uncover further immune defects. Nef's expression pattern and multifaceted manipulation of several distinct cell types culminates into a complex immune evasion strategy that likely contributes to the characteristics of AIDS.

CHAPTER 6. THE LONG LASTING-TYPE CALCIUM CHANNEL $CA_V1.4$ IS A CRITICAL REGULATOR OF T CELL RECEPTOR SIGNALLING AND NAÏVE T CELL HOMEOSTASIS

6.1 Introduction

Calcium (Ca^{2+}) ions act as universal second messengers in virtually all cell types, including cells of the immune system. In lymphocytes, Ca^{2+} signals modulate the activation of calcineurin/NFAT and Ras/MAPK pathways, serving to regulate cell activation, proliferation, differentiation and apoptosis [188, 189]. TCR stimulation invokes rises in intracellular Ca^{2+} through the activation of PLCγ1 and the associated hydrolysis of phosphatidylinositol-3,4-bisphosphate (PIP_2) into inositol-1,4,5-trisphosphate (IP_3) and diacylglycerol (DAG). Subsequently, IP_3 binds IP_3 receptors in the endoplasmic reticulum (ER) and induces Ca^{2+} release from ER stores, triggering store-operated Ca^{2+} entry (SOCE) from outside the cell via plasma membrane channels [188, 189]. For Ca^{2+} signalling to affect T cell fate or effector functions, sustained Ca^{2+} influx via plasma membrane channels is likely necessary for a number of hours, maintaining cytoplasmic Ca^{2+} concentrations higher than resting baseline levels [189].

The identity and number of plasma membrane channels mediating sustained Ca^{2+} entry into T cells are unclear [190, 464]. One well-characterized mechanism of entry is through Ca^{2+} release-activated calcium (CRAC) channels [465]. In the CRAC pathway, the Ca^{2+} sensor STIM1 responds to decreases in ER Ca^{2+} stores by associating with the

A version of Chapter 6 is currently accepted for publication at *Immunity*: Omilusik KD*, Priatel JJ*, Chen X*, Wang, YT*, Xu H, Choi KB, Gopaul R, McIntyre-Smith A, Teh HS, Tan R, Bech-Hansen NT, Waterfield D, Fedida D, Hunt SV, Jefferies WA, (2011), The $Ca_V1.4$ Calcium Channel Is a Critical Regulator of T Cell Receptor Signaling and Naive T Cell Homeostasis, Immunity, doi:10.1016/j.immuni.2011.07.011. (* denotes co-first authorship).

CRAC channel pore subunit ORAI1 and activating SOCE. However, loss of ORAI1 in naïve T cells has been found to have minimal effects on their ability to flux Ca^{2+} or proliferate upon TCR stimulation [207, 209]. Other candidate plasma membrane Ca^{2+} channels operating in lymphocytes include P2X receptor, transient receptor potential (TRP) cation channels, TRP vanilloid channels, TRP melastatin channels and voltage-dependent Ca^{2+} channels (VDCC). It is unknown whether the repertoire of Ca^{2+} channels operating in T cells remains constant or changes during various stages of development or differentiation.

VDCC are a group of plasma membrane voltage-gated Ca^{2+} (Ca_V) channels whose functions have been primarily characterized in excitable cells. Ca_V complexes are composed of a pore forming and voltage sensing α1 subunit along with auxiliary α2, β, δ, and γ subunits that modulate gating [466]. In mammals, ten Ca_V family members have been grouped into 5 groups (L, P/Q, N, R & T) based on electrophysiological /pharmacological properties, each likely serving distinct cellular signalling pathways. Previous work has described the discovery, expression and functions of L-type (long-lasting) Ca_V channels in mouse and human T cells [240, 241]. L-type Ca_V channels (includes 4 subtypes: Ca_V1.1, Ca_V1.2, Ca_V1.3 & Ca_V1.4) are closed under resting conditions and open up, leading to Ca^{2+} entry into the cell, following their activation by strong membrane depolarization events. Findings describing Ca_V1.4, an α1 Ca^{2+} channel subunit encoded by *Cacna1f*, message and protein in the spleen, thymus and T cells of rodents and humans suggest that this particular L-type channel may be important in regulating Ca^{2+} signalling in T cells [240, 241, 249-251] In addition, L-type calcium

channels appear to facilitate entry of Ca^{2+} into mitochondria and thus may contribute to the spatial and temporal characteristics of Ca^{2+} signals in many types of cells [467].

To investigate the physiological functions of $Ca_V1.4$ in T cell biology, analyses on developing thymocytes and peripheral T cells from $Ca_V1.4$-deficient ($Ca_V1.4^{-/-}$) mice were performed. In this chapter, it is demonstrated that $Ca_V1.4$ mediates critical roles in charging intracellular Ca^{2+} stores and regulating TCR-induced elevations in cytosolic free Ca^{2+} affecting TCR-induced Ras, ERK and NFAT activation. In addition, these studies demonstrate that $Ca_V1.4$ modulates naïve T cell survival and is essential for the generation of pathogen-specific T cell responses. Collectively, this study provides a new framework understanding the regulation of lymphocyte biology through the function L-type channel in the storage of intracellular Ca^{2+} within lymphocytes and operative Ca^{2+} regulation of antigen receptor-mediated signal transduction.

6.2 Results

6.2.1 $Ca_V1.4$ deficiency results in $CD4^+$ and $CD8^+$ T cell lymphopenia and spontaneous T cell activation

To characterize $Ca_V1.4$ expression in wild type mice, RNA analyses revealed expression in thymus, spleen and peripheral $CD4^+$ and $CD8^+$ T cells (**Figure 6.1A**). The observation that $Ca_V1.4$ is expressed in developing and mature T cells led to an investigation of T cells in $Ca_V1.4^{-/-}$ mice. $Ca_V1.4^{-/-}$ mice were previously generated through gene targeting, inserting a stop codon and prematurely terminating *Cacna1f* translation [305]. To verify gene targeting in $Ca_V1.4^{-/-}$ mice, RT-PCR was performed detecting the disrupted *$Ca_V1.4$* mRNA carrying a loxP site in the $Ca_V1.4^{-/-}$ mice

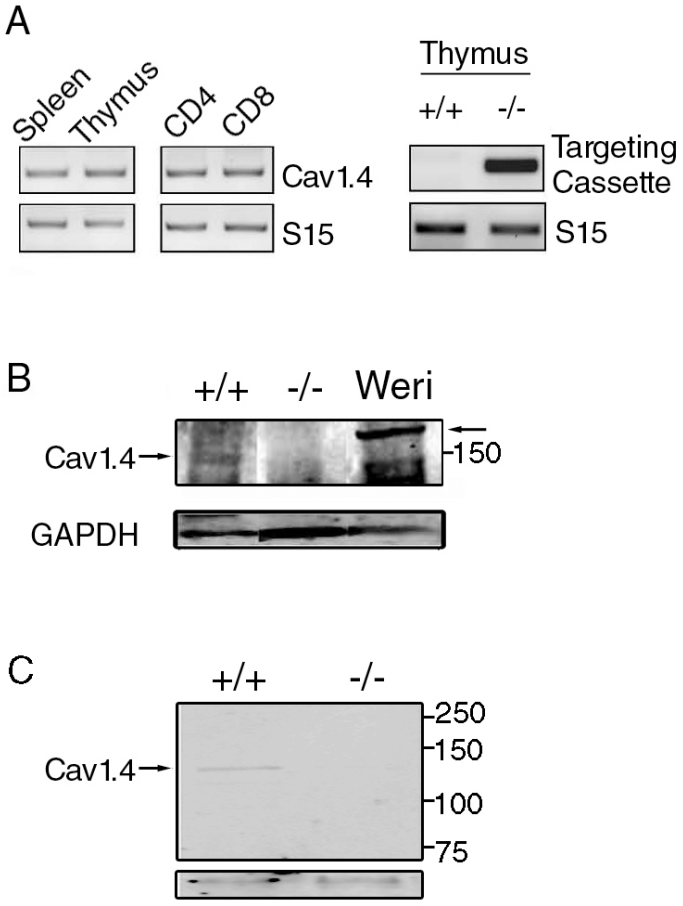

Figure 6.1. The expression of Cav1.4 in lymphoid tissue is disrupted in $Ca_V1.4^{-/-}$ mice.

(A) *$Ca_V1.4$* mRNA is expressed in lymphoid tissues and $CD4^+$ and $CD8^+$ T cells. Disruption of *$Ca_V1.4$* mRNA in mutant mice was confirmed by RT–PCR analysis of thymic transcripts for the presence of the targeting cassette. S15 mRNA was detected as a loading control. **(B)** Immunoblot analysis of $Ca_V1.4$ protein in whole cell extracts of wild type and $Ca_V1.4$-deficient splenocytes. Weri retinoblastoma cells were used as a $Ca_V1.4$-expressing positive control. Anti-GAPDH antibody staining is provided as a control for sample loading. **(C)** Surface proteins on wild type and $Ca_V1.4$-deficient splenic T cells were biotinylated and immunprecipitated with streptavidin sepharose beads. Equivalent amounts of protein were blotted with anti-$Ca_V1.4$ antibody. A non-specific low molecular size band on the same blot was used to confirm equal loading.

(**Figure 6.1A**). In addition, blotting experiments with anti-$Ca_V1.4$ antibody revealed the loss of protein expression in $Ca_V1.4^{-/-}$ splenic whole cell lysates (**Figure 6.1B**). Differences in size between $Ca_V1.4$ channels expressed in mouse lymphocytes relative to Weri retinoblastoma cells may be a product of alternative splicing [241] or cell-type specific post-translational modifications. To determine whether $Ca_V1.4$ is expressed at the T cell plasma membrane, the surface of wild type and $Ca_V1.4^{-/-}$ splenic T cells were biotinylated and immunoprecipitated with streptavidin-coupled beads (**Figure 6.1C**). These experiments detected the presence of $Ca_V1.4$ molecules at the plasma membrane of mature T cells.

Examination of thymocyte development in mice lacking a functional $Ca_V1.4$ channel revealed changes to T cell differentiation in $Ca_V1.4^{-/-}$ mice. In $Ca_V1.4^{-/-}$ mice, the ratio of $CD4^+$ versus $CD8^+$ SP thymocytes is skewed slightly towards the CD8 lineage ($Ca_V1.4^{-/-}$ = 1.32 ± 0.15 vs $Ca_V1.4^{+/+}$ = 2.34 ± 0.34; **Figure 6.2A,B**) and the proportion of mature thymocytes, distinguished by $CD24^{lo}TCR\beta^{hi}$ expression, were reduced relative to wild type ($Ca_V1.4^{-/-}$ = 3.3 ± 0.5 % vs $Ca_V1.4^{+/+}$ = 5.7 ± 0.4 %; & **Figure 6.2A**). The effect of $Ca_V1.4$-deficiency on T cell development is also reflected in a two-fold reduction in numbers of mature $CD4^+$ SP thymocytes ($Ca_V1.4^{-/-}$ = 4.1 ± 1.3 *vs* $Ca_V1.4^{+/+}$ = 8.0 ± 1.9) whereas the number of $CD8^+$ SP thymocytes is largely unchanged (**Figure 6.2C**). However, the expression of various maturation and activation markers on $Ca_V1.4^{-/-}$ DP and SP thymocytes closely paralleled levels seen on wild type subpopulations, expressing similar amounts of TCRβ, CD44, CD69 and CD62L (**Figure 6.2D**). Collectively, these findings suggest that $Ca_V1.4$-deficiency results in less efficient positive selection and that

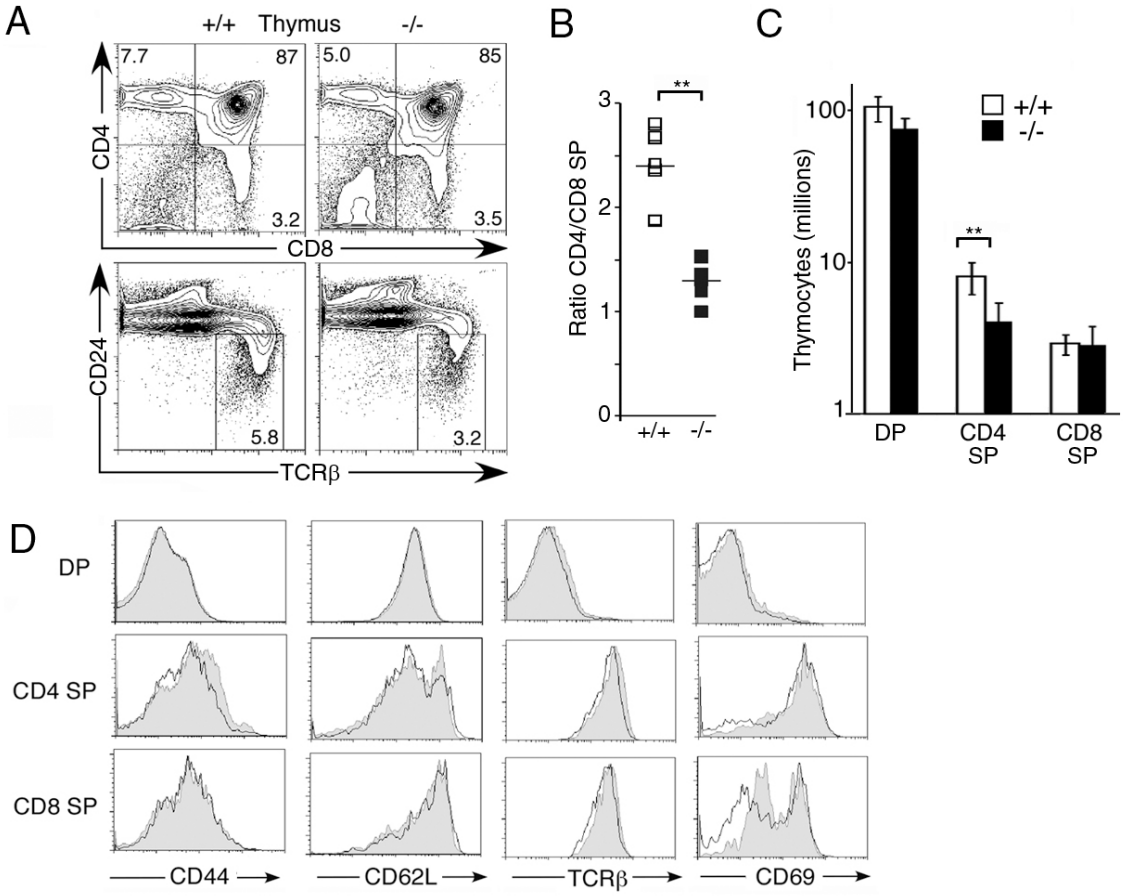

Figure 6.2. $Ca_V1.4$ deficiency results in subtle developmental defect.
(A) $Ca_V1.4^{-/-}$ thymi express a reduced fraction of mature SP thymocytes, as determined by electronic gating on $TCR\beta^{hi}$ and $CD24^{lo}$ cells (percentage is shown within rectangular gate on contour plot). **(B)** $Ca_V1.4$-deficiency reduces the proportion of $CD4^+$ versus $CD8^+$ SP thymocytes. **(C)** The abundance of various thymic subpopulations present in wild type (n = 6) and mutant mice (n = 7) was determined by staining with anti-CD4 and anti-CD8 antibodies. **(D)** Expression levels of CD44, CD62L, TCRβ and CD69 on wild type and $Ca_V1.4^{-/-}$ DP and SP thymocyte subpopulations. Error bars represent the SD. **$p<0.01$.

$Ca_V1.4$ function may play a more critical role for the positive selection of $CD4^+$ SP thymocytes relative to $CD8^+$ SP thymocytes.

The examination of peripheral lymphoid compartments, including spleen, lymph nodes (LN) and peripheral blood, revealed that $Ca_V1.4^{-/-}$ mice exhibit a decreased frequency of $CD4^+$ T cells and a reduced ratio of $CD4^+$ versus $CD8^+$ T cells relative to wild type mice (**Figure 6.3A**). Furthermore, $Ca_V1.4^{-/-}$ mice were found to be strikingly lymphopenic for $CD4^+$ T cell, $CD8^+$ T cell and B cell subsets based on splenic and lymph node cell recovery **(Figure 6.3B**). The loss of peripheral $CD4^+$ T cells (5.4-fold spleen; 5.0-fold LN) in $Ca_V1.4^{-/-}$ mice is considerably more dramatic than for $CD8^+$ T cells (2.5-fold spleen; 2.4-fold LN). Associated with the drop in T cell numbers, both $CD4^+$ $TCR\beta^+$ and $CD8^+$ $TCR\beta^+$ T cells showed signs of spontaneous acute T cell activation, expressing increased levels of CD44, CD122 and PD-1 and reduced CD62L (**Figure 6.3C**)**.** In summary, these findings demonstrate that $Ca_V1.4$-dependent Ca^{2+} signalling is essential for naïve $CD4^+$ and $CD8^+$ T cell homeostasis and quiescence.

6.2.2 $Ca_V1.4$ is critically required for TCR-induced and store-operated rises in cytosolic free Ca^{2+}

Wild type and mutant splenocytes, loaded with the Ca^{2+} indicator dyes, labelled with anti-CD4 and anti-CD8 antibodies plus anti-CD44 antibodies for the discrimination of Ca^{2+} responses by naïve ($CD44^{lo}$) or memory ($CD44^{hi}$) $CD4^+$ and $CD8^+$ T cells, were stimulated to investigate Ca^{2+} transport deficiencies in $Ca_V1.4^{-/-}$ mice (**Figure 6.4A**). To determine whether Ca^{2+} release from intracellular stores is competent for mediating Ca^{2+}

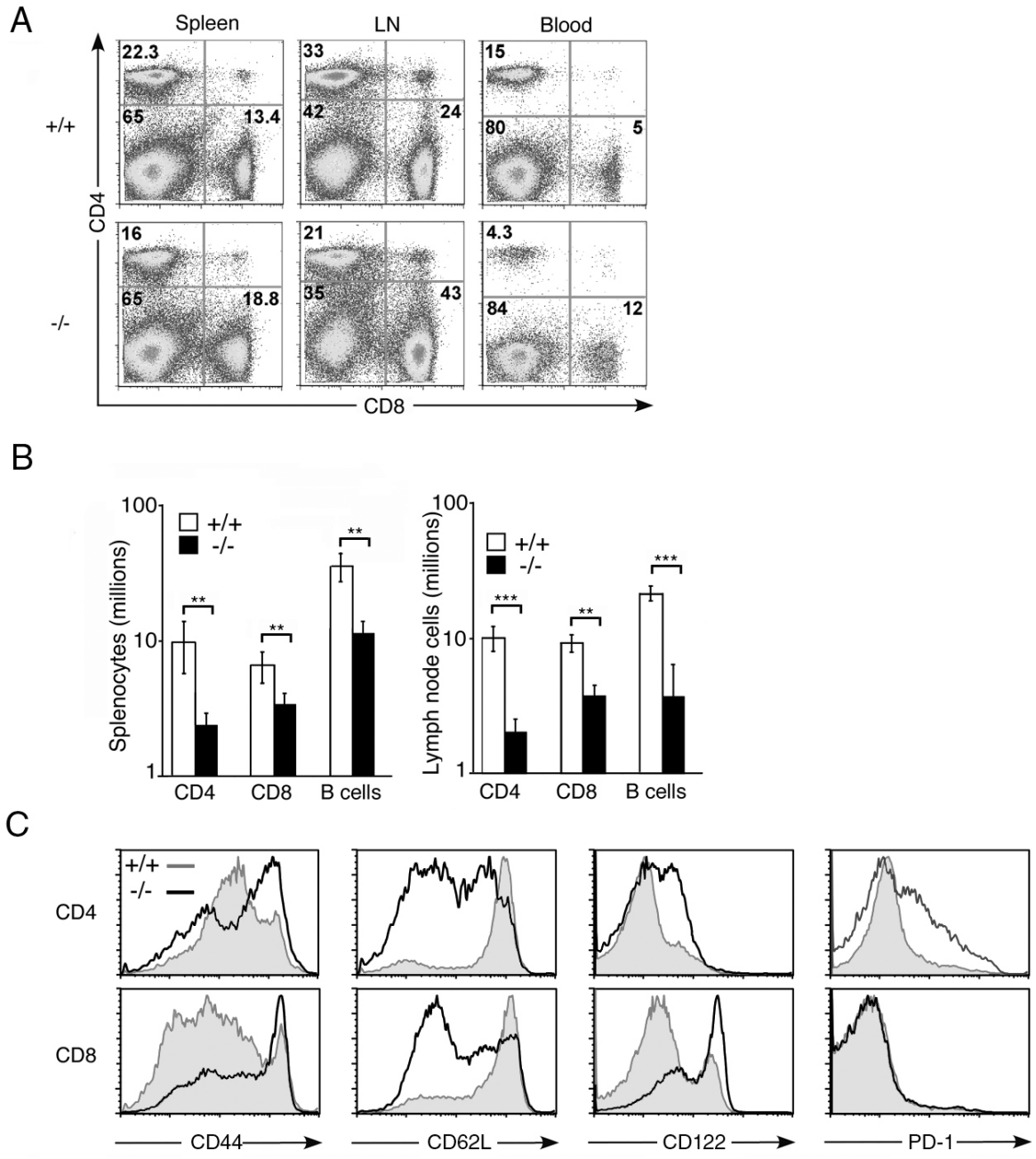

Figure 6.3. $Ca_V1.4$ deficiency results in $CD4^+$ and $CD8^+$ T cell lymphopenia and spontaneous T cell activation in the periphery.
(A) Peripheral lymph organs including spleen, lymph nodes (LN) and blood of $Ca_V1.4^{-/-}$ mice display abnormal ratios of $CD4^+$ versus $CD8^+$ T cells. The percentage of cells residing within each quadrant is shown within the density plot. **(B)** Spleens and lymph nodes of $Ca_V1.4^{-/-}$ mice exhibit greatly reduced T cell ($n \geq 6$) and B cell ($n = 3$) numbers as compared to wild type. Y-axis is a log scale. **(C)** Splenic $Ca_V1.4^{-/-}$ $CD4^+$ and $CD8^+$ T cells express markers of acute activation and T cell memory. Error bars represent the SD. **p<0.01, ***p<0.001.

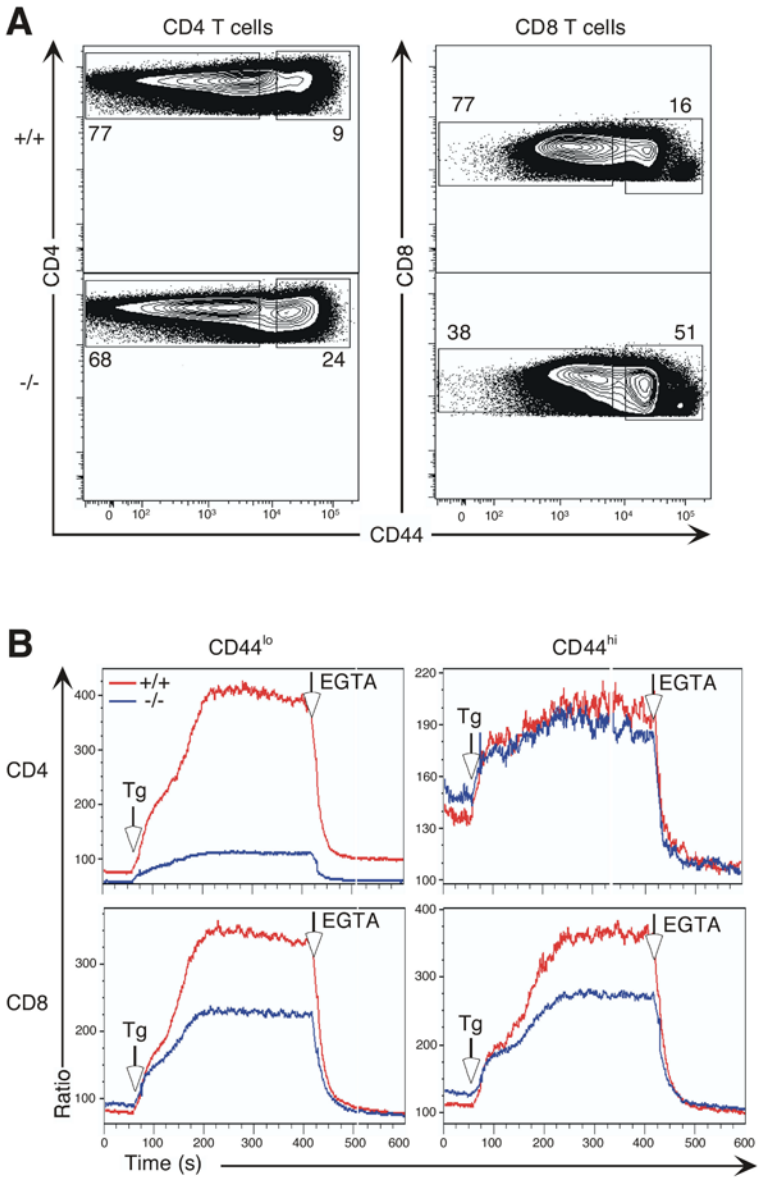
A
CD4 T cells
CD8 T cells
+/+
-/-
CD4
CD8
77
9
68
24
77
16
38
51
CD44
B
CD44lo
CD44hi
+/+
-/-
EGTA
Tg
CD4
CD8
Ratio
Time (s)

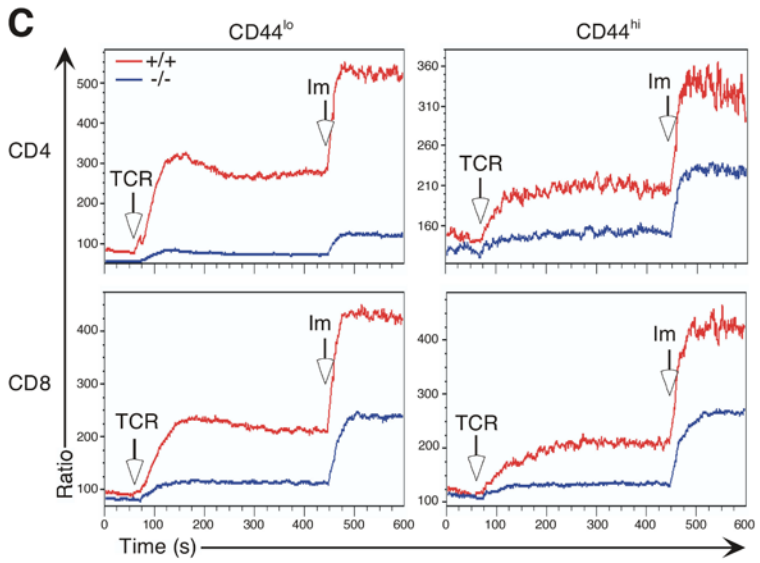
C
CD44lo
CD44hi
+/+
-/-
CD4
CD8
TCR
Im
Ratio
Time (s)

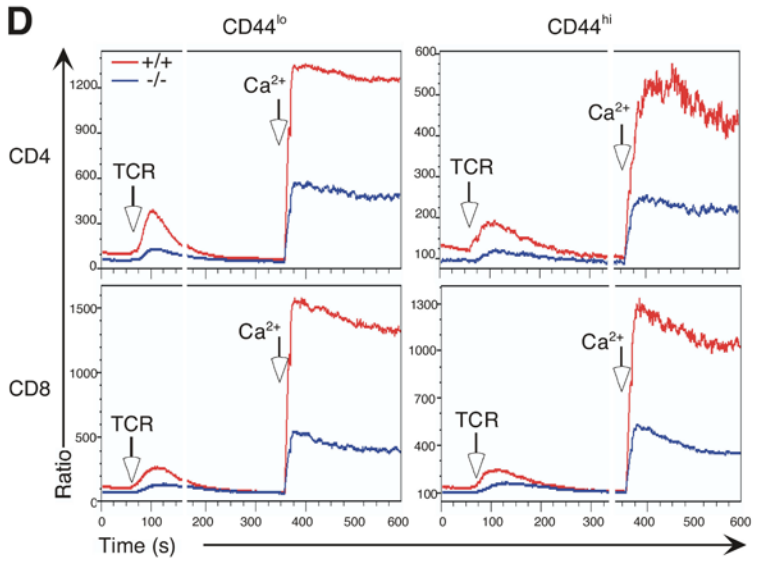
D
CD44lo
CD44hi
+/+
-/-
CD4
CD8
TCR
Ca2+
Ratio
Time (s)

Figure 6.4. Cav1.4 is critically required for both TCR- and thapsigargin-induced elevations in cytosolic free Ca^{2+} by naïve T cells.

Wild type (red line) and Cav1.4$^{-/-}$ (blue line) splenocytes were loaded with the Ca^{2+} indicator dyes Fluo-4 and Fura Red, surface stained and suspended in RPMI. To minimize the effects of variation in dye loading samples, intracellular Ca^{2+} levels were plotted as a median ratio of Fluo-4/Fura Red (FL-1/FL-3) over time. **(A)** Electronic gating (boxed area) used to discriminate CD44^{lo} and CD44^{hi} CD4^{+} and CD8^{+} T cells is indicated within the contour plot. **(B)** Splenocytes were stimulated with thapsigargin (Tg) and extracellular Ca^{2+} chelated by EGTA addition at the indicated time point. **(C)** Splenic T cells pre-coated with biotinylated anti-TCR antibodies were treated with streptavidin (SA) or ionomycin (Im) at the indicated times (marked by arrows). **(D)** TCR stimulations were performed in the absence of free extracellular Ca^{2+}. Sufficient EGTA (0.5 mM) was added to cell suspensions to chelate extracellular Ca^{2+} in RPMI (~0.4 mM Ca^{2+}), blocking cellular uptake.

influx via plasma membrane channels, splenic T cells were treated with thapsigargin, an inhibitor of a Ca^{2+}-ATPase of the ER (**Figure 6.4B**). Thapsigargin induces rises in cytosolic Ca^{2+} concentration by blocking the cell's ability to pump Ca^{2+} into sarco- and endo-plasmic reticula and secondarily, activates plasma membrane-bound Ca^{2+} channels, triggering Ca^{2+} entry from outside the cell. Remarkably, $Ca_V1.4^{-/-}$ $CD44^{lo}$ $CD4^+$ T cells exhibited greatly diminished increases in cytosolic Ca^{2+} upon thapsigargin stimulation and both $Ca_V1.4^{-/-}$ $CD44^{lo}$ and $CD44^{hi}$ $CD8^+$ T cells also showed marked reductions relative to their wild type counterparts (**Figure 6.4B**). On the other hand, Ca^{2+} efflux from $CD4^+$ and $CD8^+$ T cells does not appear to be compromised by $Ca_V1.4$ deficiency as demonstrated via addition of EGTA. In contrast to comparisons between naïve $CD4^+$ T cells, wild type and $Ca_V1.4^{-/-}$ $CD44^{hi}$ $CD4^+$ T cells displayed very similar Ca^{2+} responses. Together, these observations demonstrate that $Ca_V1.4$ channels are critically required for SOCE in $CD44^{lo}$ $CD4^+$ T cells and to a lesser extent in $CD44^{lo}$ and $CD44^{hi}$ $CD8^+$ T cells.

The observation that $Ca_V1.4$-deficiency impacts the ratio of $CD4^+$ SP versus $CD8^+$ SP thymocytes suggests that $Ca_V1.4$ channels might regulate TCR signalling. To investigate this hypothesis, wild type and mutant splenocytes, pre-coated with biotinylated anti-CD3 antibodies, were activated by streptavidin (SA) addition. In wild type T cells, TCR crosslinking induced cytosolic Ca^{2+} levels to rise rapidly and remain elevated for sustained duration (**Figure 6.4C**). Paradoxically to the responses observed for thapsigargin treatment, both $Ca_V1.4^{-/-}$ $CD4^+$ and $CD8^+$ T cells responded very weakly to TCR stimulus regardless of their surface CD44 phenotype. The basis for differential $CD4^+$ and $CD8^+$ T cell dependence on $Ca_V1.4$ function for thapsigargin but not TCR responses is unclear (**Figure 6.4B**). In addition, $Ca_V1.4^{-/-}$ T cells, particularly $CD44^{lo}$

$CD4^+$ T cell subset, reached greatly reduced peak Ca^{2+} levels relative to wild type upon treatment with ionomycin. Ionomycin increases cytosolic Ca^{2+} concentrations via its ionophoric properties releasing intracellular Ca^{2+} stores and subsequently, stimulating the opening of plasma membrane Ca^{2+} channels and Ca^{2+} influx from outside the cell. The findings that ionomycin responses are greatly blunted in $Ca_V1.4^{-/-}$ T cells suggests that $Ca_V1.4$ function contributes to the storage of intracellular Ca^{2+} or is critical for the importation of Ca^{2+} following its release from intracellular stores.

To determine whether $Ca_V1.4$ mediates one or both of the aforementioned processes involved in Ca^{2+} responses, Ca^{2+} responses were monitored after TCR stimulation when extracellular Ca^{2+} was chelated by EGTA, preventing Ca^{2+} intake and thereby uncovering Ca^{2+} release from intracellular stores. The transient cytosolic Ca^{2+} elevation observed following TCR ligation in the presence of EGTA was found to be decreased in $Ca_V1.4^{-/-}$ T cells relative to wild type (**Figure 6.4D**). Furthermore, the repletion of extracellular Ca^{2+}, facilitating Ca^{2+} influx across the plasma membrane, resulted in dramatic cytosolic Ca^{2+} surge in wild type T cells whereas climbs by $Ca_V1.4^{-/-}$ T cells were markedly less. In addition, $Ca_V1.4$ was found also to function in thymocytes and appears important for rises in cytosolic Ca^{2+} when TCR stimulations are performed in the absence of extracellular Ca^{2+} (**Figure 6.5**). Together, these data suggest that $Ca_V1.4$ is operated by TCR engagement and that it may serve to replenish intracellular Ca^{2+} stores in thymocytes and naïve T cells.

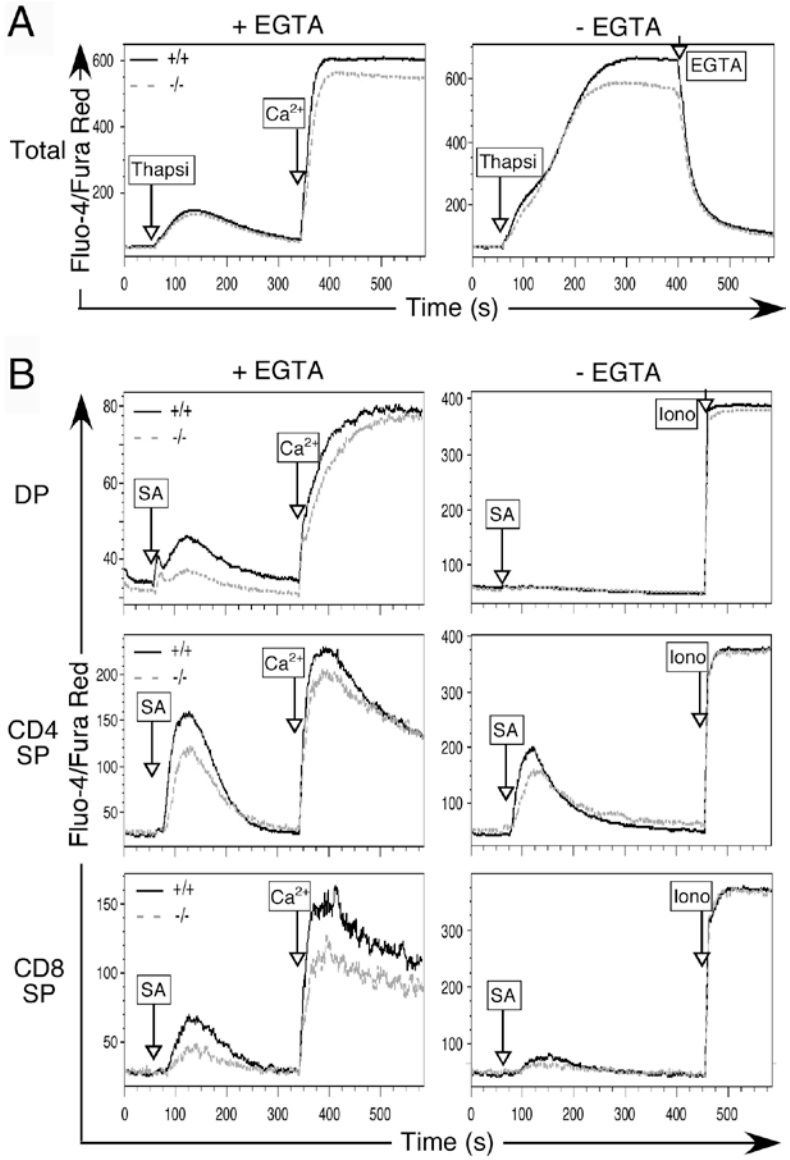
A
+ EGTA
- EGTA
Total
Fluo-4/Fura Red
+/+
-/-
Thapsi
Ca2+
EGTA
Time (s)
B
DP
CD4 SP
CD8 SP
SA
Iono

Figure 6.5. $Ca_V1.4$ is required for TCR-induced rises in cytosolic free Ca^{2+} during Ca^{2+} limitation.

(A) Wild type and mutant thymocytes (Total), loaded with the calcium indicator dyes Fluo-4 and Fura Red and suspended in RPMI, were stimulated with thapsigargin (Thapsi) in the presence or absence of extracellular EGTA (0.5 mM) sufficient to chelate Ca^{2+} present in RPMI (~0.4 mM). To minimize the effects of variation in dye loading samples, cytosolic Ca^{2+} levels were plotted as a ratio of FL-1/FL-3 over time. At the indicated time point, extracellular Ca^{2+} (0.5 mM) or EGTA (0.5 mM) was added midway through the stimulation. **(B)** Fluo-4/Fura Red-labelled thymocytes, stained with anti-CD4 and anti-CD8 antibodies for discrimination of thymic subpopulations, were activated with anti-TCR antibodies in the presence and absence of extracellular EGTA (0.5 mM). Midway through the time course, a second stimulus, extracellular Ca^{2+} (0.5 mM) or ionomycin (1 μg/mL), was added to samples.

6.2.3 $Ca_V1.4$ function regulates Ras/ERK activation and NFAT mobilization

To address whether $Ca_V1.4$ channels affect Ras/MAPK signalling, a pathway heavily implicated in controlling T cell survival and differentiation [468], studies to measure the activation status of these downstream effectors following TCR stimulation were initiated. For Ras signalling, wild type and $Ca_V1.4^{-/-}$ thymocytes were stimulated with anti-TCR antibody and subsequently, Ras activation was assessed by precipitation of Ras-GTP with Raf-1/GST fusion protein (**Figure 6.6A**). $Ca_V1.4^{-/-}$ thymocytes were found to be about two-fold less efficient at inducing Ras-GTP as compared to wild-type cells (2.2 versus 4.4 relative fluorescence intensities), normalizing to the amount of Ras in the whole cell lysate. By contrast, activated Ras levels were fairly comparable between genotypes when cells were stimulated with the DAG analog PMA. Next, an analysis was performed of the activation of downstream-acting MAP kinases ERK and JNK in total thymocytes at the indicated times post-TCR stimulation (**Figure 6.6B**). The intensity and duration of ERK activation following TCR crosslinking was reduced in $Ca_V1.4^{-/-}$ thymocytes relative to wild type. However, comparison of JNK phosphorylation between wild type and $Ca_V1.4^{-/-}$ thymocytes upon TCR stimulation revealed only marginal differences. By contrast, PMA treatment was found to induce strong ERK and JNK phosphorylation regardless of cell genotype. Collectively, these studies find that $Ca_V1.4$- deficiency selectively affects the activation of ERK following TCR engagement.

To assess whether ERK activation is affected in $Ca_V1.4^{-/-}$ mature SP thymocytes, a flow cytometric-based assay was employed to combine anti-phospho-ERK antibody labelling along with cell surface staining as described previously [301]. Wild type and $Ca_V1.4^{-/-}$ thymocytes were stimulated for 2 minutes by either TCR crosslinking or PMA

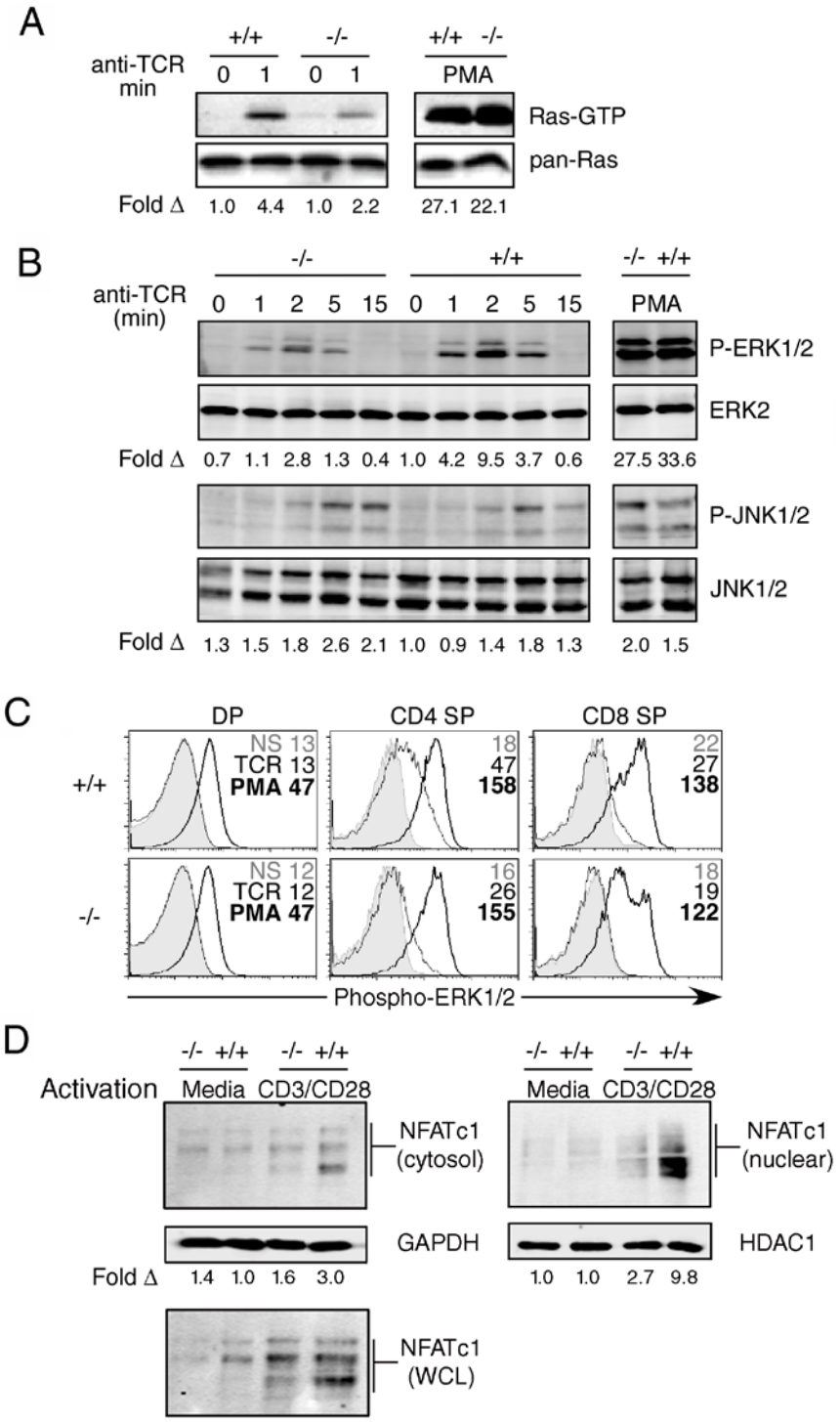
A
+/+
-/-
+/+ -/-
anti-TCR
min
0 1 0 1
PMA
Ras-GTP
pan-Ras
Fold Δ 1.0 4.4 1.0 2.2 27.1 22.1
B
-/-
+/+
-/- +/+
anti-TCR
(min)
0 1 2 5 15 0 1 2 5 15
PMA
P-ERK1/2
ERK2
Fold Δ 0.7 1.1 2.8 1.3 0.4 1.0 4.2 9.5 3.7 0.6 27.5 33.6
P-JNK1/2
JNK1/2
Fold Δ 1.3 1.5 1.8 2.6 2.1 1.0 0.9 1.4 1.8 1.3 2.0 1.5
C
DP
CD4 SP
CD8 SP
+/+
NS 13
TCR 13
PMA 47
18
47
158
22
27
138
-/-
NS 12
TCR 12
PMA 47
16
26
155
18
19
122
Phospho-ERK1/2
D
-/- +/+ -/- +/+
Activation
Media CD3/CD28
NFATc1
(cytosol)
GAPDH
Fold Δ 1.4 1.0 1.6 3.0
NFATc1
(nuclear)
HDAC1
1.0 1.0 2.7 9.8
NFATc1
(WCL)

Figure 6.6. $Ca_V1.4$ function regulates Ras/ERK activation and NFAT mobilization.
(A) Activated Ras was measured in wild type and $Ca_V1.4^{-/-}$ thymocytes following stimulation with either anti-TCR antibody or the DAG analog PMA using RAF-1/GST pulldown assays. Whole cell lysates (WCL) were immunoblotted for total Ras to verify equivalent protein expression. **(B)** Total thymocytes were stimulated with anti-TCR antibodies for the indicated period of time. Phosphorylation of ERK and JNK MAP kinases was measured by immunoblotting. Band intensities were quantified using the Odyssey software and ratios calculated for P-ERK2/ERK2, P-JNK1/JNK1. Unstimulated wild type thymocytes were arbitrarily given a score of 1. **(C)** To assess ERK signalling in specific thymic subpopulations, ERK activation in wild type and mutant thymocytes following stimulation with either anti-TCR antibody or PMA treatment for 2 min was determined using flow cytometry. Mean Fluorescence Intensities (MFU) for unstimulated (grey), TCR stimulated (black) and PMA-treated (bold) cells are shown within each histogram. **(D)** Thymoctyes from wild type and $Ca_V1.4^{-/-}$ mice were incubated for 16 hours with anti-CD3/CD28 or media alone. Immunoblotting for NFATc1 was performed on nuclear and cytoplasmic fractions and whole cell lysates (WCL). GAPDH or HDAC1 was detected as a loading control. Band intensities were quantified and ratios calculated as above.

treatment and monitored for ERK activation. $Ca_V1.4^{-/-}$ $CD4^+$ and $CD8^+$ SP thymocytes exhibited reduced ERK activation upon TCR engagement relative to wild type (**Figure 6.6C**; CD4 SP: 26 versus 47 mean fluorescence units (MFU); CD8 SP: 19 versus 27 MFU). These results indicate that $Ca_V1.4$-deficiency impacts the strength of ERK signalling in SP thymocytes.

To determine if deficient Ca^{2+} release following TCR ligation affected NFAT translocation and activation in $Ca_V1.4^{-/-}$ thymocytes, NFATc1 amounts in the cytosolic and nuclear fractions of wild type and $Ca_V1.4^{-/-}$ thymocytes was examined (**Figure 6.6D**). Following TCR stimulation for 16 h, $Ca_V1.4^{-/-}$ thymocytes had ~3.6 times less NFATc1 in their nucleus as compared to equivalent wild type cells. These experiments demonstrate that $Ca_V1.4$-dependent Ca^{2+} entry is required for activation of the NFAT-pathway.

6.2.4 T cell intrinsic $Ca_V1.4$ function is required for normal T cell homeostasis

To determine whether the loss of $Ca_V1.4$ function in T cells themselves contributes to the impaired T cell development and/or peripheral T cell maintenance, bone marrow transfer experiments were performed in which equivalent numbers of T cell-depleted wild type ($Thy1.1^+Ly5.2^+$) and $Ca_V1.4^{-/-}$ ($Thy1.2^+Ly5.2^+$) bone marrow was transferred into irradiated congenic ($Ly5.1^+$) hosts. After one-month post-transfer, evaluation of donor cell frequencies ($Ly5.2^+$) in the thymus and spleen revealed that $Ca_V1.4^{-/-}$ bone marrow cells competed very poorly with wild type for T cell reconstitution of the host (**Figure 6.7A**). The frequency of wild type donor $CD4^+$ and $CD8^+$ T cells in the thymus and periphery was substantially higher than that of the $Ca_V1.4^{-/-}$ $CD4^+$ and $CD8^+$ T cells,

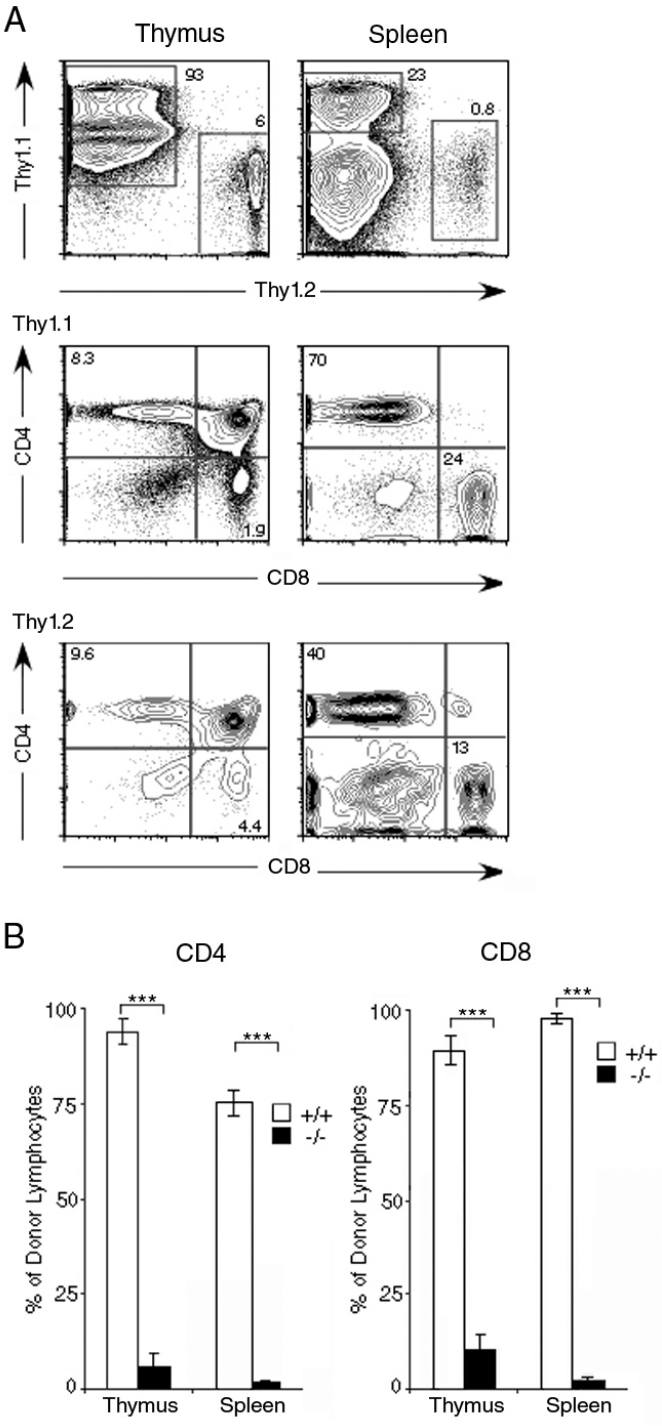
A
Thymus
Spleen
93
6
23
0.8
Thy1.1
Thy1.2
Thy1.1
83
70
24
1.9
CD4
CD8
Thy1.2
9.6
40
13
4.4
CD4
CD8
B
CD4
CD8
100
75
50
25
0
% of Donor Lymphocytes
***
+/+
-/-
Thymus
Spleen

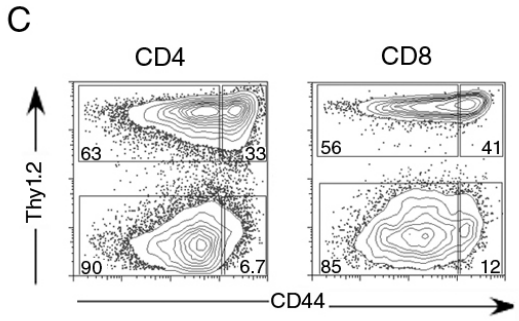

Figure 6.7. T cell intrinsic requirement for $Ca_V1.4$ function is required for normal T cell homeostasis.

Irradiated recipient mice (Thy1.2$^+$Ly5.1$^+$) were repopulated with *$Ca_V1.4^{-/-}$* (Thy1.2$^+$Ly5.2$^+$) and wild type (Thy1.1$^+$Ly5.2$^+$) bone marrow in a 1:1 ratio. **(A)** The origin of the Ly5.2$^+$ cells in the thymus, and spleen were assessed (top panel). *$Ca_V1.4^{-/-}$* cells (Thy1.2 gate) showed decreased survival in recipient mice as compared to wild type cells (Thy1.1 gate). Using Thy1 markers, donor lymphocytes were identified and the relative proportion of CD4$^+$ and CD8$^+$ T cells were determined (middle and bottom panel). The percentage of cells residing within each quadrant is shown within the density plot. **(B)** Percentage of donor wild type versus mutant T cells present in the thymus spleen of host mice one-month post bone marrow transfer (n = 5). Error bars represent SD. ***$p < 0.001$. **(C)** The relative proportion of CD44^{lo} and CD44^{hi} CD4$^+$ and CD8$^+$ T cells in donor lymphocyte populations are shown. The percentage of cells residing within each quadrant is shown within the density plot.

respectively (**Figure 6.7A,B**). Furthermore, comparison of the ratio of $CD44^{lo}$ versus $CD44^{hi}$ $CD4^{+}$ and $CD8^{+}$ T cells populations showed that $Ca_V1.4^{-/-}$ splenic donor T cells were skewed towards a memory phenotype relative to wild type donor T cells (**Figure 6.7C**). Moreover, these experiments suggest that the heightened frequency of $Ca_V1.4^{-/-}$ $CD44^{hi}$ T cells in $Ca_V1.4^{-/-}$ mice is not a consequence of lymphopenia but rather due to a failure of $Ca_V1.4^{-/-}$ $CD44^{lo}$ T cells to be maintained. Together, these results demonstrate a cell-intrinsic function of $Ca_V1.4$ in T cell progenitors and/or mature T cells that is necessary for efficient reconstitution of a recipient host.

6.2.5 $Ca_V1.4$ is an important regulator of naïve T cell homeostasis

The finding that $Ca_V1.4^{-/-}$ mice are lymphopenic and that a majority of the residual T cells possess an activated/memory surface suggested that $Ca_V1.4$ functions are essential for naïve T cell maintenance and quiescence. Moreover, comparison of naïve and memory phenotype T cells, using CD44 expression as a basis for discrimination, between wild type and mutant mice reveals that $Ca_V1.4^{-/-}$ mice exhibit a severe loss of naïve T cells (CD4: 16 ± 4% of wild type; CD8: 31 ± 7% of wild type; **Figure 6.8A,B**). By contrast, $CD44^{hi}$ T cell numbers were much less affected (CD4: 38 ± 10% of wild type;CD8: 84 ± 20% of wild type). To examine whether the paucity of $Ca_V1.4^{-/-}$ naïve T cells may be related to decreased survival, wild type and $Ca_V1.4^{-/-}$ splenocytes were stained with the apoptotic marker Annexin V to determine whether these cells had a heightened rate of cell turnover (**Figure 6.8C**). These experiments found that $Ca_V1.4^{-/-}$ $CD44^{lo}$ T cells exhibited enhanced reactivity to Annexin V than their wild type counterparts (CD4: 2.2-fold increase; CD8: 2.4-fold increase). By contrast, there was

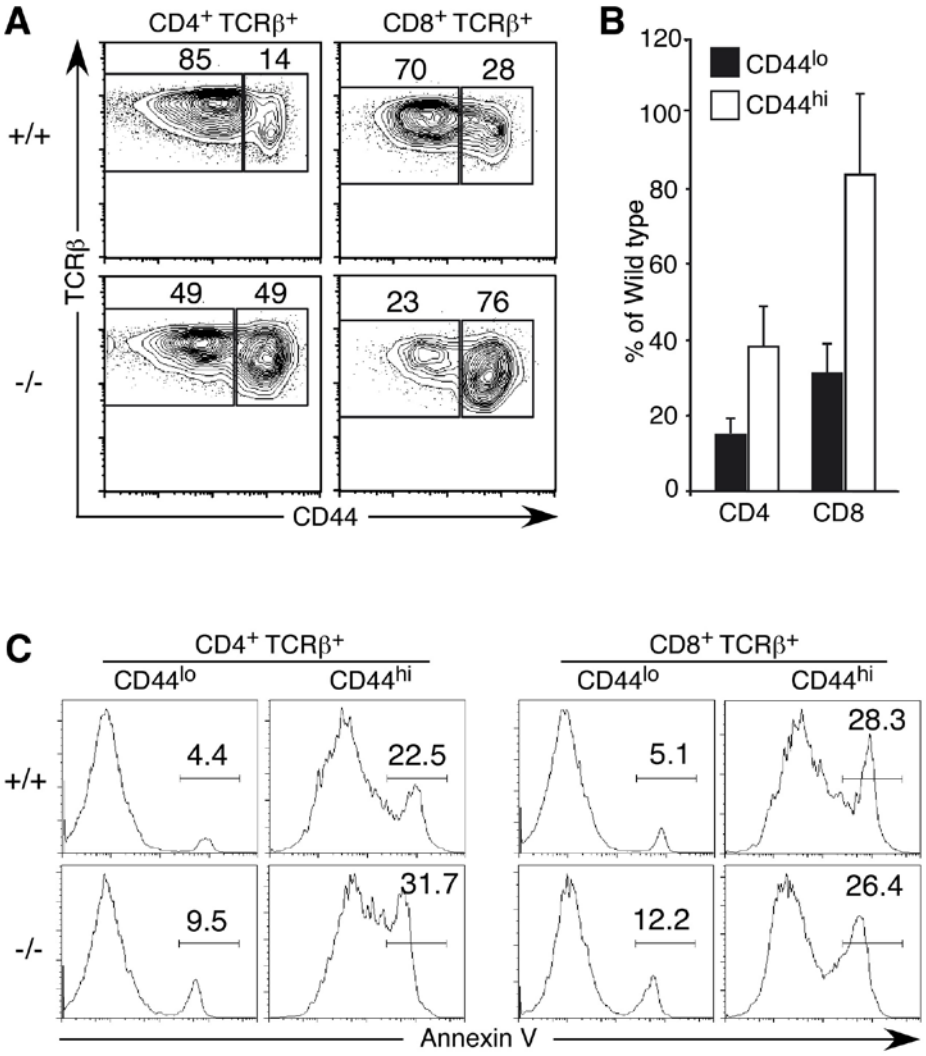

Figure 6.8. $Ca_V1.4$ deficiency results in decreased survival of T cells in the periphery.

(A) CD44 expression on splenic $CD4^+TCR\beta^+$ and $CD8^+TCR\beta^+$ T cells from wild type and mutant mice. **(B)** $Ca_V1.4^{-/-}$ mice exhibit a profound reduction in $CD44^{lo}$ $CD4^+$ and $CD8^+$ TCR β^+ T cells. Error bars represent SD. **(C)** $Ca_V1.4$-deficient $CD44^{lo}$ $CD4^+$ and $CD8^+$ TCR β^+ T cells show increased rates of spontaneous apoptosis.

greater correspondence in binding Annexin V between $CD44^{hi}$ T cells from $Ca_V1.4^{-/-}$ and wild type mice (CD4: 1.4-fold increase; CD8: 1.07 decrease). Examination of markers on $Ca_V1.4^{-/-}$ $CD44^{lo}$ T cells showed that they have a resting naïve surface phenotype, expressing wild type levels of CD62L and TCRβ (**Figure 6.9A**). Together, these data suggest that the limited number of $CD44^{lo}$ T cells in $Ca_V1.4^{-/-}$ mice is at least in part a consequence of their decreased fitness to survive.

Signalling through the IL-7 receptor (IL-7R), a heterodimer of IL-7Rα (CD127) and the common γ-chain (CD132), plays a governing role in naïve T cell homeostasis and loss of either IL-7 or IL-7R in both mice and humans results in T cell lymphopenia and severe immunodeficiency [174]. Therefore, whether $Ca_V1.4^{-/-}$ $CD44^{lo}$ T cells expressed normal IL-7R, an essential requirement for naïve T cell survival, was investigated (**Figure 6.9B**). Although $Ca_V1.4^{-/-}$ $CD44^{lo}$ T cells possessed normal CD132 expression, both $Ca_V1.4^{-/-}$ $CD44^{lo}$ $CD4^+$ and $CD8^+$ T cells expressed only about 50% of wild type CD127 levels. Comparison of $Ca_V1.4^{-/-}$ mature $CD4^+$ and $CD8^+$ SP thymocytes with $Ca_V1.4^{-/-}$ $CD44^{lo}$ peripheral T cells revealed an almost identical phenotype including increased Annexin V reactivity and reduced CD127 (**Figure 6.10**). Despite reduced CD127 expression, $Ca_V1.4^{-/-}$ $CD44^{lo}$ $CD4^+$ and $CD8^+$ T cells displayed normal levels of the pro- survival protein Bcl-2 (**Figure 6.9C**). These findings indicate that $Ca_V1.4$ affects CD127 expression on mature SP thymocytes and peripheral naïve T cells.

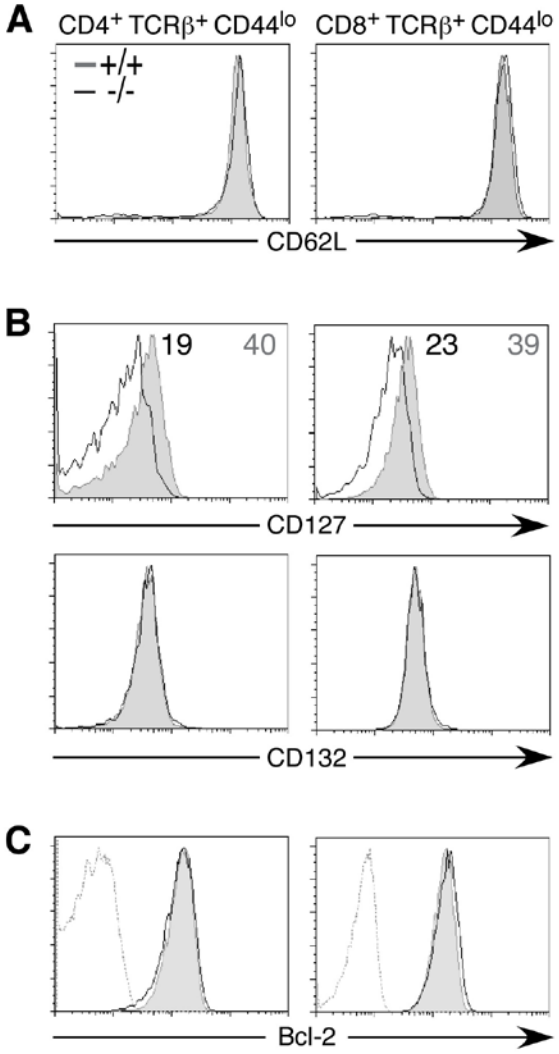

Figure 6.9. $Ca_V1.4$ deficient $CD44^{lo}$ T cells have a naïve surface phenotype with reduced CD127 expression.

(A) L-selectin levels on $CD44^{lo}$ $CD4^+$ and $CD8^+$ $TCR\beta^+$ T cells. **(B)** $Ca_V1.4$-deficient $CD44^{lo}$ $CD4^+$ and $CD8^+$ $TCR\beta^+$ T cells express reduced IL-7Rα levels. **(C)** Bcl-2 expression by $CD44^{lo}$ $CD4^+$ and $CD8^+$ $TCR\beta^+$ T cells was measured by intracellular flow cytometry.

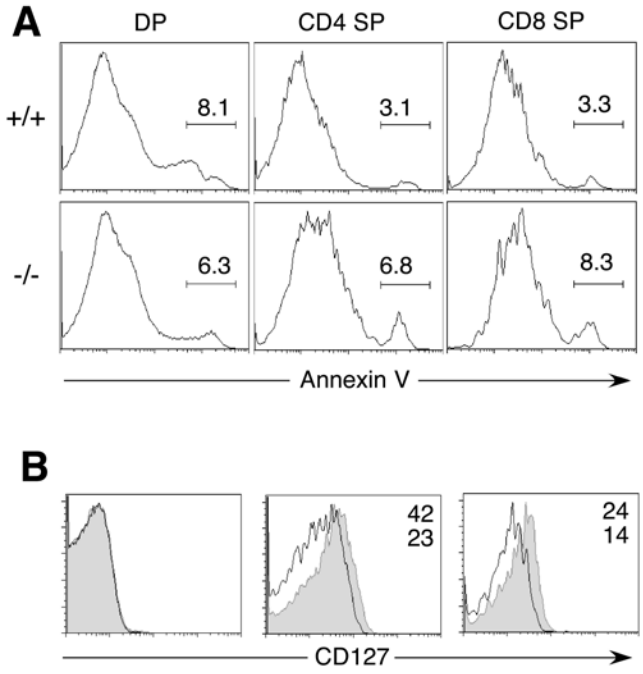

Figure 6.10. $Ca_V1.4$ deficiency results in decreased survival of thymic T cells with reduced CD127 expression.
(A) $Ca_V1.4$-deficient $CD4^+$ $TCR\beta^{hi}$ and $CD8^+$ $TCR\beta^{hi}$ SP thymocytes show increased rates of spontaneous apoptosis. **(B)** CD127 levels on $CD4^+$ $TCR\beta^{hi}$ and $CD8^+$ $TCR\beta^{hi}$ SP thymocytes.

6.2.6 $Ca_V1.4$ promotes survival signalling and homeostasis-induced T cell expansion

To determine whether $Ca_V1.4$-deficiency and its concomitant reduction in IL-7Rα expression is functionally significant, an assay was set up to monitor IL-7R signal transduction through the phosphorylation status of STAT5, a known downstream effector of IL-7R signalling. Wild type and $Ca_V1.4^{-/-}$ $CD4^+$ and $CD8^+$ SP thymocytes were stimulated with various doses of IL-7 for 5 min and STAT5 phosphorylation assessed using an anti-phospho-Y647 STAT5 specific antibody. $Ca_V1.4$-deficient $CD4^+$ and $CD8^+$ SP thymocytes showed a marked reduction in STAT5 phosphorylation at all doses of IL-7 tested (**Figure 6.11A**). These results suggest that $Ca_V1.4^{-/-}$ $CD4^+$ and $CD8^+$ SP thymocytes are less sensitive to IL-7 stimulation *in vitro* than wild type cells. To test the hypothesis that $Ca_V1.4$-deficiency affects IL-7's ability to promote survival, wild type and $Ca_V1.4^{-/-}$ $CD44^{lo}$ T cells were isolated by sorting, placed into culture with the indicated concentrations of IL-7 and their viability measured 24 h later using Annexin V staining (**Figure 6.11B**). These experiments found that $Ca_V1.4^{-/-}$ $CD44^{lo}$ T cells were much less capable than wild type cells of utilizing IL-7 to support their survival. Next, the impact of $Ca_V1.4$-deficiency on the ability of $CD44^{lo}$ T cells to receive survival signalling was examined through 24 h *ex vivo* culture in anti-TCR antibody coated wells (**Figure 6.11C**). $Ca_V1.4^{-/-}$ $CD44^{lo}$ $CD4^+$ T cells were discovered to be impaired in receiving survival signalling through the TCR. Collectively, these findings suggest that $Ca_V1.4$ channel protein impacts naïve T cell survival through the regulation of either IL-7 or TCR signalling.

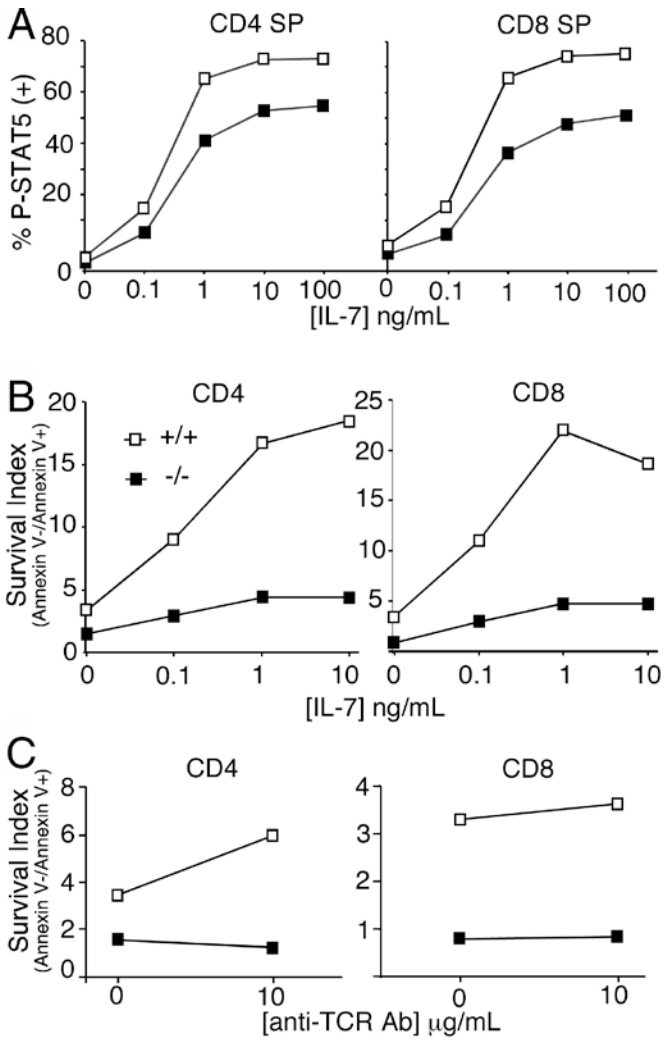
A
CD4 SP
CD8 SP
% P-STAT5 (+)
80
60
40
20
0
0
0.1
1
10
100
[IL-7] ng/mL
B
CD4
CD8
+/+
-/-
Survival Index
(Annexin V-/Annexin V+)
20
15
10
5
0
25
[IL-7] ng/mL
C
CD4
CD8
Survival Index
(Annexin V-/Annexin V+)
8
6
4
2
0
3
1
[anti-TCR Ab] μg/mL

Figure 6.11. $Ca_V1.4$ promotes survival signalling in T cells.
(A) Wild type and $Ca_V1.4$-deficient thymocytes were stimulated with the indicated concentration of IL-7 for 5 min and subsequently, assessed for the capacity to phosphorylate STAT5. The frequency of phospho-STAT5-positive mature $CD4^+$ and $CD8^+$ SP thymocytes was determined by flow cytometry. **(B)** Wild type ($Thy1.1^+$) and $Ca_V1.4^{-/-}$ ($Thy1.1^-$) naïve $CD4^+$ and $CD8^+$ T cells, electronically gated ($CD44^{lo}$) as shown in Fig. 5A, were purified by cell sorting, mixed at a 1:1:1:1 ratio and cultured with the indicated concentration of IL-7. After 24 h incubation, cell survival was determined by staining with Annexin V conjugated to Alexa647. **(C)** Wild type and mutant naïve T cells were isolated, prepared and cultured as in (B) except stimulated with anti-TCR antibody instead of IL-7. Viability was assessed after 24 h of *ex vivo* culture.

The two dominant forces controlling the size of the T cell compartment are the availability of self-peptides/MHC and the cytokine IL-7, providing TCR and IL-7R signalling respectively that is necessary for the maintenance of naïve T cells [174]. To examine the proliferative potential of $Ca_V1.4^{-/-}$ $CD44^{lo}$ T cells, wild type ($Thy1.1^+$) and $Ca_V1.4^{-/-}$ ($Thy1.2^+$) $CD44^{lo}$ $CD4^+$ and $CD8^+$ T cells were purified, mixed together at a 1:1:1:1 ratio, labelled with CFSE and co-injected into congenitally lymphopenic $Rag1^{-/-}$ hosts **(Figure 6.12A**). After residing for 7 days *in vivo*, donor T cells were recovered and their cellular proliferation assessed via CFSE dilution (**Figure 6.12B**). Using the congenic marker Thy1.1, the proportion of donor wild type cells recovered was found to be considerably greater than $Ca_V1.4^{-/-}$ cells (78.5 ± 5.1%; 3.7 fold more $Ca_V1.4^{+/+}$ than $Ca_V1.4^{-/-}$). By electronically gating on donor T cells likely responding to cues from IL-7 and self-peptides/self-MHC molecules [469], $Ca_V1.4^{-/-}$ $CD4^+$ and $CD8^+$ T cells were found to have undergone fewer cell divisions than wild type $CD4^+$ and $CD8^+$ T cells (**Figure 6.12C**). Collectively, our data strongly suggests cell-intrinsic $Ca_V1.4$ function is critical for T cells to respond appropriately to homeostatic and survival cues.

6.2.7 $Ca_V1.4$ functions are necessary for functional $CD4^+$ and $CD8^+$ T cell immune responses

To investigate the requirement of $Ca_V1.4$ function in an immune response, wild type and $Ca_V1.4^{-/-}$ mice were challenged with a recombinant *Listeria monocytogenes* strain expressing ovalbumin (rLMOVA) that possesses immunodominant $CD4^+$ and $CD8^+$ T cell epitopes. One week post-infection, splenocytes were examined for antigen-specific cells. $Ca_V1.4^{-/-}$ mice produced substantially reduced numbers of $CD8^+CD44^+$OVA/

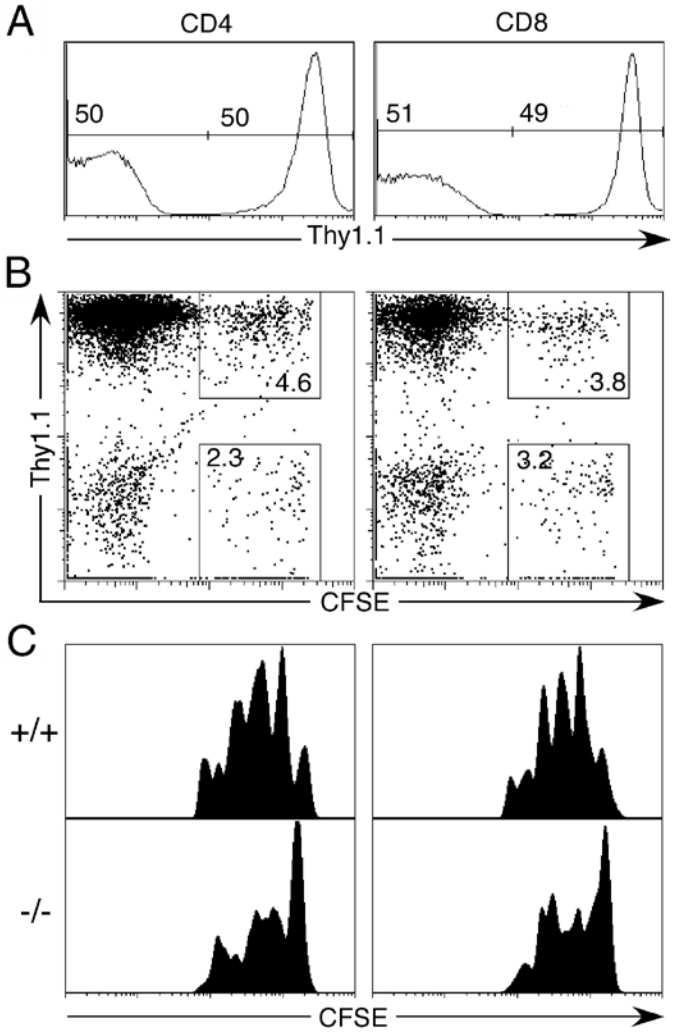

Figure 6.12. $Ca_V1.4$ promotes homeostasis-induced T cell expansion.
Naïve T cells from wild type (Thy1.1$^+$) and $Ca_V1.4$-deficient (Thy1.1$^-$) mice were purified, mixed at a 1:1:1:1 ratio, CFSE-labelled and co-injected into Rag1$^{-/-}$ hosts. **(A)** The percentage of wild type and $Ca_V1.4^{-/-}$ CD4$^+$ and CD8$^+$ T cells is shown prior to injection. **(B)** CFSE dilution indicates proliferation of transferred T cells. Boxed region within dot plots indicates proliferation driven by self-MHC molecules and IL-7 (homeostatic). **(C)** Histograms indicating homeostatic proliferation by wild type and mutant donor CD4$^+$ and CD8$^+$ T cells.

Tetramer$^+$ cells in response to rLMOVA infection (14-fold decrease) (**Figure 6.13A,B**). To determine the functional ability of the antigen-specific cells, splenocytes were stimulated with the MHC class I-restricted antigen $OVA_{(257–264)}$ or the endogenous MHC class II-restricted antigen $LLO_{(190-201)}$ and intracellular IFN-γ production was monitored (**Figure 6.13C,D**). Numbers of both antigen-specific $CD4^+$ (34-fold decrease) and $CD8^+$ (12-fold decrease) secreting IFN-γ were drastically reduced in $Ca_V1.4^{-/-}$ mice relative to wild type (**Figure 6.13E)**. To evaluate the numbers of effector T cells capable of producing IFN-γ, wild type and $Ca_V1.4^{-/-}$ splenocytes were also polyclonally activated with an anti-TCR antibody. Findings that $Ca_V1.4^{-/-}$ mice exhibited much smaller decline in numbers of IFN-γ producing (not-specific for LLO and OVA) effector $CD4^+$ (1.4-fold decrease) and $CD8^+$ (1.8-fold decrease) T cells argues that there is no intrinsic requirement for $Ca_V1.4$ function in eliciting IFN-γ production by activated T cells. To evaluate whether the decline in antigen-specific IFN-γ producing $CD8^+$ T cells in $Ca_V1.4^{-/-}$ mice is associated with reduced cytolytic activity of activated $CD8^+$ T cells, purified $CD8^+$ T cells from the spleens of mice infected 7 days earlier with rLMOVA were incubated with ^{51}Cr-labeled RMA-S targets that were either untreated or pulsed with OVA peptide (**Figure 6.13F**). Further to this, wild type or $Ca_V1.4^{-/-}$ CTLs from splenocytes of mice similarly infected with rLMOVA were stimulated with OVA peptide or polyclonally activated with an anti-TCR antibody and degranulation was assessed by CD107a/b surface staining (**Figure 6.13G,H**). These results uncovered that $Ca_V1.4^{-/-}$ mice exhibit greatly diminished capacity to generate antigen-specific killers and correlated with the reduced numbers of antigen-specific IFN-γ producing $CD8^+$ T cells in

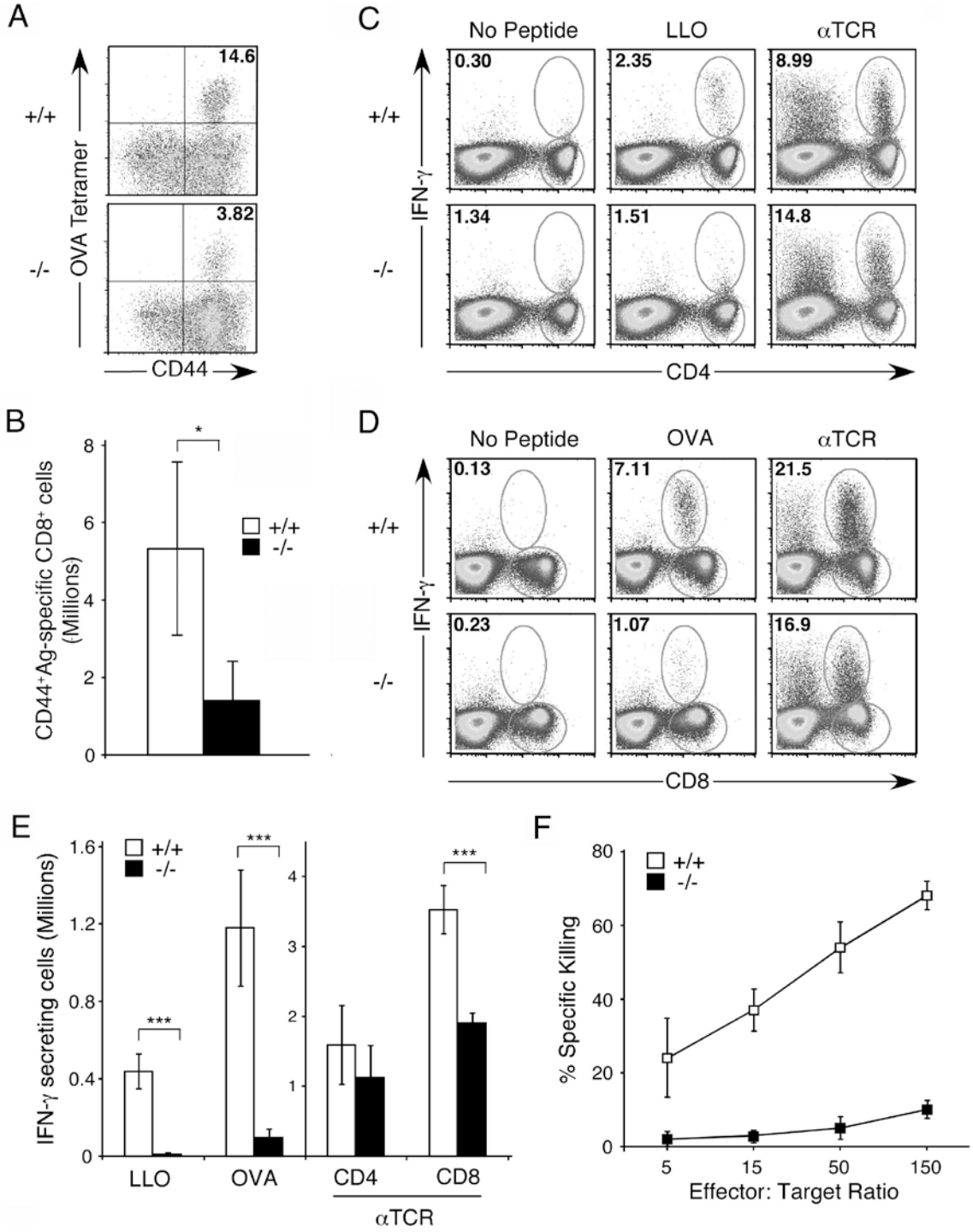
A
+/+
-/-
OVA Tetramer
CD44
14.6
3.82
B
CD44+Ag-specific CD8+ cells (Millions)
+/+
-/-
*
C
No Peptide
LLO
αTCR
IFN-γ
CD4
0.30
2.35
8.99
1.34
1.51
14.8
D
No Peptide
OVA
αTCR
IFN-γ
CD8
0.13
7.11
21.5
0.23
1.07
16.9
E
IFN-γ secreting cells (Millions)
+/+
-/-
***
LLO
OVA
CD4
CD8
αTCR
F
% Specific Killing
+/+
-/-
Effector: Target Ratio

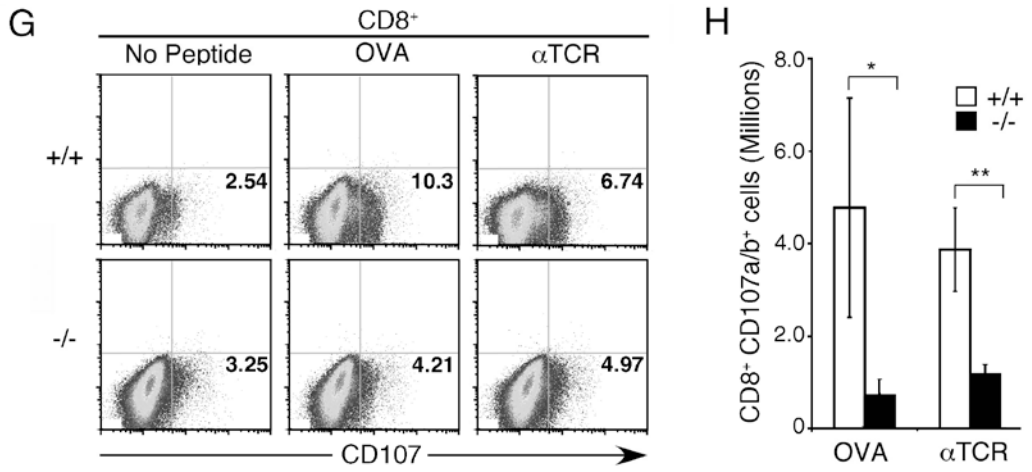

Figure 6.13. $Ca_V1.4$ is critically required for optimal antigen-specific $CD4^+$ and $CD8^+$ T cell immune responses.

Seven days post-infection with recombinant *L. monocytogenes*-OVA, mice were sacrificed and antigen-specific T cell immune responses were assessed. **(A)** The percentage of $CD44^+$ H-$2K^b$/OVA $tetramer^+$ cells in the $CD8^+$ population is shown within the density plots. **(B)** The mean number of antigen-specific $CD44^+$ $CD8^+$ cells is represented (n = 3). **(C,D)** Splenocytes from infected mice were stimulated with MHC class I-($OVA_{257-264}$)- and MHC class II-($LLO_{190-201}$)-restricted peptides and subsequently, assayed for IFN-γ secretion. To determine the frequency of T cells capable of secreting IFN-γ, splenocytes were separately stimulated with anti-TCR antibody alone. Numbers within density plots represent the percentage of IFN-γ secreting $CD4^+$ or $CD8^+$ T cells. **(E)** Cumulative data indicating the mean numbers of antigen-specific IFN-γ-producing T cells in wild type and $Ca_V1.4^{-/-}$ mice (n = 3). **(F)** $CD8^+$ T cells from the spleens of infected mice were purified and incubated with ^{51}Cr-labeled RMA-S targets that had either been untreated or pulsed with $OVA_{257-264}$ peptide. **(G)** Splenocytes from infected mice were stimulated with MHC class I-($OVA_{257-264}$)-restricted peptide or anti-TCR antibody. The number of $CD8^+$ T cells capable of degranulation was assessed by CD107a/b surface staining. Numbers within density plots represent the percentage of $CD8^+$ CD107a/b^+ cells. **(H)** Cumulative data indicating the mean numbers of CTLs degranulating following stimulation in wild type and $Ca_V1.4^{-/-}$ mice (n=3). Error bars represent the SD. *p=0.05; **p<0.01; ***p<0.001.

these animals (**Figure 6.13E**). Together, our studies show that $Ca_V1.4$ is essential for the generation of functional $CD4^+$ and $CD8^+$ T cell responses.

6.3 Discussion

Ca_V channels are major passageways controlling Ca^{2+} entry in excitable cells and regulate numerous processes including muscle contraction, neuronal signal transmission and gene transcription [191]. However, the biological roles of Ca_V channels in non-excitable cells such as lymphocytes are poorly defined. Identification of a mutation in the β4 subunit of VDCCs underlying the neurologic and immune system defects observed in the *lethargic* mouse line first implicated Ca_V function in immunoregulation [470]. In addition, subsequent to submission of the present study, a manuscript describing mice deficient in the β3 regulatory subunit has argued that Ca_V channels play a role in modulating TCR signalling and $CD8^+$ T cell homeostasis [249]. To investigate the physiological functions of the L-type $Ca_V1.4$ channel in developing and mature T cells, mice deficient in its pore-forming α1 subunit were analyzed. $Ca_V1.4$ channels were found to be critical for both the survival of naïve $CD4^+$ and $CD8^+$ T cells and the generation of pathogen-specific $CD4^+$ and $CD8^+$ T cell responses. In addition, naïve $CD4^+$ and $CD8^+$ T cells were shown to be dependent on $Ca_V1.4$ function for SOCE, TCR-induced rises in cytosolic Ca^{2+} and downstream TCR signal transduction.

The observation that $Ca_V1.4$ function affected SOCE suggests the possibility that it may function at the ER rather than the plasma membrane (**Figure 6.4**). Therefore, cell surface biotinylation and immunoprecipitation experiments were performed verifying that $Ca_V1.4$ molecules are indeed present on the plasma membrane (**Figure 6.1**). Consistent

with this notion, $Ca_V1.4^{-/-}$ deficiency was found to impair entry of extracellular Ca^{2+} (**Figure 6.4 and Figure 6.5**). In addition to our documentation of $Ca_V1.4$ residing on the T cell surface and regulating TCR-induced rises in cytosolic Ca^{2+} levels (**Figure 6.1 and Figure 6.4**), recent work indicates that $Ca_V1.4$ associates with TCR signalling components in lipid rafts [249]. However, neither our data nor the work of others currently precludes $Ca_V1.4$ from also functioning at intracellular membranes such as the ER.

Analyses of $Ca_V1.4^{-/-}$ mice revealed that T cells of various stages of development and differentiation showed differing relative dependence on $Ca_V1.4$ for mediating Ca^{2+} responses. For instance, $Ca_V1.4^{-/-}$ SP thymocytes exhibited more moderate decreases in TCR- or thapsigargin-induced rises in cytosolic free Ca^{2+} relative to wild type than what was observed when peripheral naïve and memory $Ca_V1.4^{+/+}$ and $Ca_V1.4^{-/-}$ T cells were compared (**Figure 6.4 and Figure 6.5**). Thus, our study hints at the great complexity involved in Ca^{2+} regulation, dynamically changing with T cell differentiation, and suggests that differential responses are important for functional outcomes upon TCR engagement. Alternative Ca_V splicing likely contributes to this complexity as different isoforms may yield channels with unique characteristics of Ca^{2+} regulation [240, 241]. For example, a specific isoform of CACNA1F mediates Ca^{2+} entry into the photoreceptors and promotes tonic neurotransmitter release [253]. Kotturi *et al.* found that two putative $Ca_V1.4$ splice isoforms (termed $Ca_V1.4\alpha$ and $Ca_V1.4\beta$) are expressed in Jurkat T cells and primary human T and B cells but are not present in human retina [241, 251]. Furthermore, truncated $Ca_V1.2$ and $Ca_V1.3$ channels are expressed in human T and B cells [244, 471]. Moreover, it is likely that Ca^{2+} signalling biology in lymphocytes

cannot be fully explained by the function of $Ca_V1.4$ and ORAI1 and that a variety of Ca^{2+} channels and associated isoforms may be responsible for currents necessary for lymphocyte activation, differentiation, migration and apoptosis.

$Ca_V1.4$-deficiency results in decreased positive selection, a reduced frequency and number of mature $CD4^+$ SP thymocytes and defects in the TCR-activation of the Ras/ERK cascade (**Figure 6.2 and Figure 6.6**), a pathway heavily implicated in the differentiation of DP thymocytes into mature T cells [468]. $Ca_V1.4$ channels may regulate the Ras/ERK cascade through its effects on RasGRP1, a Ras-guanyl nucleotide exchange factor. RasGRP1's two “EF hand” domains function by binding Ca^{2+}, dictating its cellular localization and the duration of Ras signalling [472]. In addition, the finding that the loss of $Ca_V1.4$ influences TCR signal transduction suggests that central or peripheral tolerance could be impaired in $Ca_V1.4^{-/-}$ mice. Although negative selection studies using $Ca_V1.4^{-/-}$ TCR transgenic mice have not been performed, $Ca_V1.4^{-/-}$ mice display a 2-fold reduction in splenic regulatory T cell numbers, defined as $CD4^+CD25^+FoxP3^+$ cells, relative to wild type ($Ca_V1.4^{-/-} = 0.84 \pm 0.23 \times 10^6$ vs $Ca_V1.4^{+/+} = 1.75 \pm 0.44 \times 10^6$). However, it appears that neither the deletion of autoreactive T cells in the thymus nor their suppression by regulatory T cells in the periphery is perturbed by $Ca_V1.4$-deficiency because old $Ca_V1.4^{-/-}$ mice, bred 13 generations onto a C57BL/6 background, appear healthy, lacking any gross histological abnormalities among various tissues examined, and remain lymphopenic.

Mutations in the *CACNA1F* have been found to lead to incomplete X-linked congenital stationary night blindness type 2 (CSNB2) or Åland Island eye disease (AIED) [473-475]. However, no published report has examined the immune cell function of these

patients. In addition, the existence of several types of *CACNA1F* mutant alleles associated with variable disease penetrance could complicate such a study as many of the identified mutations may not necessarily result in a Null allele like described here for *$Ca_V1.4^{-/-}$* mice [476]. The conclusions drawn from our study will be sure to stimulate investigation into the Ca^{2+} responses of CSNB2 patients' T cells as well as an assessment of their frequencies of memory relative to naïve T cells.

The finding that $Ca_V1.4$ is critical for naïve $CD4^+$ and $CD8^+$ T cell homeostasis suggests that this channel modulates signals required for their survival: low grade TCR signalling upon contact with self-peptides/MHC molecules and IL-7R signalling following IL-7 exposure [477]. Previous work has suggested that naïve T cell TCR recognition of MHC molecules on DCs triggers small Ca^{2+} responses that are necessary for their survival [478]. As a result, we hypothesize that naïve T cells require $Ca_V1.4$ for tonic filling of intracellular Ca^{2+} stores and that charged stores are critical for low-level TCR survival signalling. Therefore, we suspect that at least two secondary factors may contribute to the Ca^{2+} release defects observed by $Ca_V1.4^{-/-}$ T cells upon stimulation (**Figure 6.4**): (i) decreased ER Ca^{2+} stores resulting in reduced SOCE and (ii) diminished inward Ca^{2+} flux through CRAC channels collaborating to impair Ca^{2+}-dependent signalling. Notably, low-grade TCR signalling and naïve T cell homeostasis have been shown to be dependent on the Ca^{2+}-responsive molecule RasGRP1 [212, 301]. As $Ca_V1.4^{-/-}$ T cells possess reduced IL-7R levels and are hyporesponsive to IL-7 (**Figure 6.9, Figure 6.10 and Figure 6.11**), $Ca_V1.4$-dependent Ca^{2+} signals possibly mediated through TCR may be critical for maintaining IL-7R expression because, to the best of our knowledge, Ca^{2+} fluxes have not been implicated directly in regulating IL-7R signalling.

In conclusion, this study suggests that the Ca^{2+} current controlled by lymphoid-expressed $Ca_V1.4$ channels influence the viability of naïve T cells and may be essential for preserving a naïve T cell population that expresses a diverse repertoire of TCRs.

CHAPTER 7.CONCLUDING REMARKS AND FUTURE DIRECTIONS

7.1 General conclusions

7.1.1 Dendritic cells

7.1.1.1 CD74 and cross presentation in DCs

The results presented in the first section of this thesis describe a novel role for the chaperone protein, CD74 in the cross presentation pathway. Antigen cross presentation and cross priming of naïve T cells by dendritic cells (DCs) is the key event in stimulating most, if not all adaptive immune responses against foreign antigens [41]. Though critically important in harnessing the power of the immune system to eradicate disease, the cross presentation pathway in DCs is not yet clearly defined [41]. The existence of multiple cross presentation pathways have been hypothesized including a pathway leading major histocompatibility complex (MHC) I from the DC cell surface into an endolysosomal peptide loading compartment [59, 65]. The current studies establish an alternate route for MHC I to this loading compartment that involves and interaction between MHC I and CD74.

Using a CD74 deficient mouse model, MHC I cross priming responses *in vivo* were shown to be impaired when challenged with a model virus, Vesicular Stomatitis Virus (VSV) and a model of cellular exogenous antigen, cell-associated ovalbumin (OVA). As $CD74^{-/-}$ mice have few $CD4^{+}$ T cells in the periphery due to improper thymic selection, the possibility that incomplete $CD4^{+}$ T cell responses are responsible for the inadequate immune responses was eliminated. Anti-VSV cytotoxic T lymphocyte (CTL) responses in wild type mice have been shown to be independent of $CD4^{+}$ cells [322, 340]; therefore,

the use of this virus allows exclusion of MHC II priming in this model of infection, so the MHC I/CD74 pathway can be examined in isolation**.** In addition, the creation of bone marrow chimeric mice allowed for the analysis $CD74^{-/-}$ derived DCs on a wild type host background. These studies led to the conclusion that the immune response defect was of antigen presentation cell (APC) origin. Using confocal microscopy analysis of DCs, CD74 was shown to route MHC I to the endolysosomes in DCs. This CD74-mediated trafficking was shown to be required for efficient loading of MHC I with exogenous OVA antigen in endolysomes. Finally, biochemical approaches demonstrated the interaction between MHC I heavy chain and CD74. This interaction appears to take place first in the endoplasmic reticulum (ER) before egress to the endolysosomal-loading compartment occurs. CD74 mediated MHC I cross presentation constitutes a new pathway of antigen presentation *in vivo*. The CD74 pathway adds to the functioning cross presentation pathways already known to exist in DCs. With multiple pathways, DCs can use the one best suited to the physical nature of the antigen allowing for efficient antigen processing of all exogenous antigens.

In summary, the vacuolar pathway of cross presentation requires peptide loading of MHC I to take place within endolysosomal compartments [59, 479]. A significant subset of newly synthesized peptide-receptive MHC I can reach this compartment by a CD74-dependent trafficking from the ER (**Figure 7.1**) Data from published peptide elution experiments suggests that a CLIP peptide may occupy the MHC I binding cleft, inhibiting other peptides from binding, during this part of intracellular transport to the endolysosomal compartment. These and previous data [59, 93] highlight the significance of the endolysosome as the principle compartment for cross presentation in DCs and the

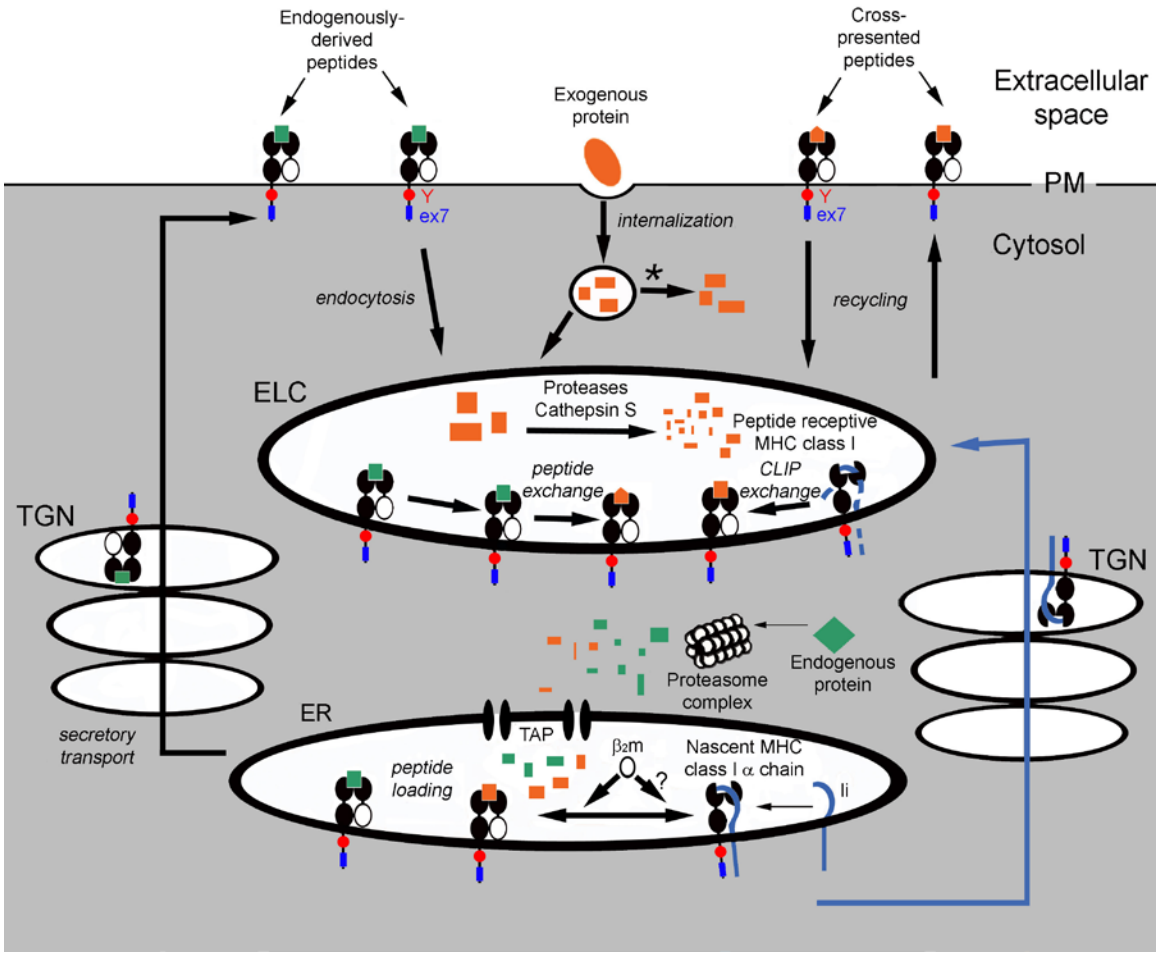

Figure 7.1. Model of DC MHC I trafficking and cross presentation.
Schematic representation of trafficking routes for MHC I molecules in DCs, depicting proposed intracellular sites of antigen acquisition. CD74 (blue) may bind a subset of MHC I molecules and re-route them from the secretory pathway directly into endolysosomal compartments. During cross presentation, exogenous protein antigens (orange) are internalized into endocytic vesicles, and then transported into endolysosomes, where they are degraded by resident proteases such as Cathepsin S into antigenic peptides. These peptides are then loaded onto the surface-derived MHC I molecules that are constitutively internalized by a tyrosine (Y) dependent mechanism. Alternatively, the high affinity exogenous peptides are loaded onto the ER-derived peptide receptive MHC I molecules shuttled through the endosomes/lysosomes by CD74 during cell activation. Adapted from [65].

present investigation establishes the structural and functional relevance of the CD74-MHC I interaction on the intracellular routing of MHC I and cross presentation function of DCs. These observations define a new pathway (**Figure 7.1**) for priming immune responses and therefore the complete elucidation of this process is of significant importance.

7.1.1.2 HIV-Nef immune evasion in DCs

The activation of viral specific CTLs by DCs is essential for the elimination of viral infections [40]. Therefore, to evade the immune response and establish in a host, many viruses have evolved mechanisms to interfere with the MHC I antigen presentation pathways [372]. The second section of this thesis describes the immune evasion mechanisms employed by HIV. Specifically, the role that the HIV virulence factor, Nef, plays in interfering with MHC I trafficking in DCs thereby impairing MHC I classical and cross presentation is established.

The effect of Nef on DC function was examined *in vitro*. Using a DC line, the expression of Nef was shown to downregulate the surface expression of MHC I, MHC II, CD40 and CD86. Using two model antigens, soluble OVA and vaccinia virus, Nef was shown to inhibit both the MHC I classical and cross presentation pathways by reducing the amount of antigenic-loaded MHC I on the DC surface. This corresponds with a significant decrease in the T cell priming ability of the DC. Nef appears to be exerting its effects by disrupting MHC I trafficking. By tracking MHC I through the DC, Nef was shown to interrupt the Golgi to cell surface transport of newly synthesized MHC I as well

as increase the internalization of surface MHC I. The result is an accumulation of MHC I in a Golgi-like compartment.

To extend the analysis *in vivo*, a Nef transgenic (Tg) mouse line was constructed that maintained the tropism of HIV and allowed for expression of Nef in $CD4^+$ T cells. In these mice, the $CD4^+$ cell populations in the thymus and periphery were decreased including the splenic $CD4^+CD11c^+$ DC population. Viral and bacterial opportunistic infections are common among HIV-positive patients and often lead to death [438]. This Nef Tg model allowed for the investigation of the impact of Nef on immune responses against secondary infections. Nef Tg mice exhibit a marked decrease in CTL specific killing when challenged with the model virus, VSV, and bacteria, *L. monocytogenes.*

As described for classical MHC I presentation, this thesis extends the consequences of Nef manipulation of MHC I to impairment of the cross presentation pathway. Endogenous antigen, such as viral or intracellular bacterial proteins, are processed by the proteosome and transported into the ER via the transporter associated with antigen processing (TAP). Here MHC I is loaded with peptide creating a stable complex that can egress through the Golgi to the cell surface. Nef may interact with this complex in the Golgi blocking the route to the cell surface (**Figure 7.2A**). Nef does not provide complete MHC I blockage at this point as a complete removal of MHC I from the cell surface of Nef-expressing cells is not seen. Any MHC I complexes escaping the block on the secretory pathway are subjected to a second disruption at the cell surface with Nef-mediated internalization to the Golgi. This eliminates the opportunity for surface MHC I to recycle to endolysosomal compartments for presentation of exogenous antigen. Instead, MHC I is sequestered in the Golgi and is unable to participate in antigen

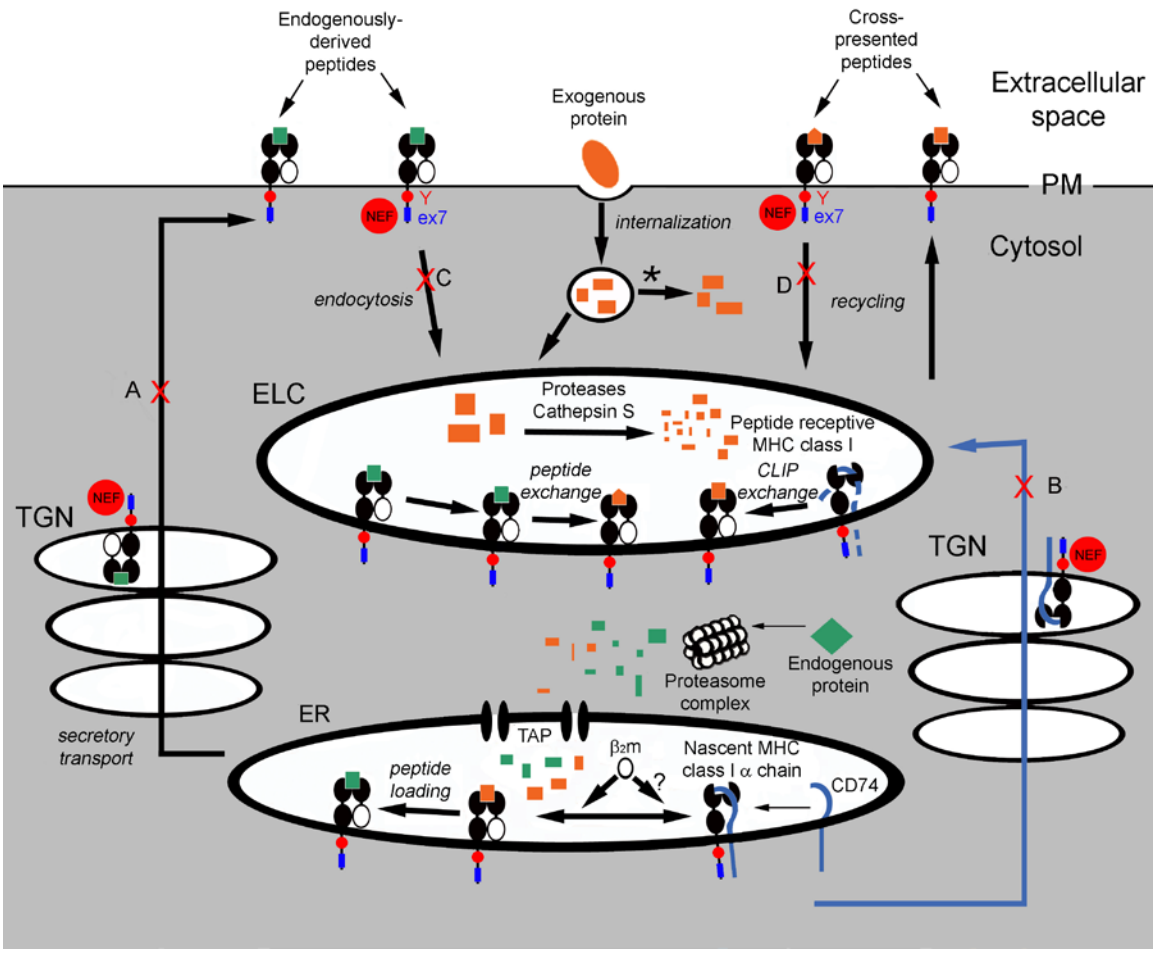

Figure 7.2. Model of Nef impairment in MHC I trafficking in DCs.
Newly synthesized MHC I is loaded with antigenic peptide in the ER. From here, the stable MHC I-peptide complex may traffic through the secretory pathway to the **(A)** plasma membrane (PM) or **(B)** with the help of CD74 to an endolysosomal compartment (ELC) for loading of cross presented antigen. Nef appears to block the transport of MHC I in these pathways at the TGN. MHC I-peptide complex that escapes this blockade is further disrupted by Nef at the PM and **(C, D)** recycling MHC I is inhibited from entering the ELC to undergo cross presentation. Instead Nef appears to direct MHC I to the TGN. Adapted from [65].

presentation (**Figure 7.2C,D**). Nef may further obstruct cross presentation by blocking MHC I complexed with CD74 en route to the ELC from the ER (**Figure 7.2B**). The utilization of multiple pathways to block MHC I antigen presentation is not surprising and is consistent with findings for other cell types [161-165]. This would be advantageous for viral survival in a host. Since HIV has tropism for several cell-types having various mechanisms of MHC I antigen presentation disruption would ensure that immune evasion could occur in several cell types regardless of the rate of transit through the secretory pathway or the efficiency of MHC I recycling. The combined affect of Nef-mediated impairment of antigen presentation ability and decreased costimulatory molecules cell surface expression impedes DCs from effectively activating CTLs to fight secondary infections likely contributing to the immune deficiency associated with Acquired Immunodeficiency Syndrome (AIDS).

7.1.2 T cells

7.1.2.1 $Ca_V1.4$ channels in T cells

For DCs to initiate strong immune responses capable of clearing infections, naïve T cells capable of responding to their cognate antigen need to be present. To maintain peripheral T cells, complex homeostatic mechanisms including signalling through the T cell receptor (TCR) and IL-7 receptor (IL-7R) are required [174]. Key components of these signalling events are the universal second messenger calcium (Ca^{2+}) and the calcium channels that regulate the intracellular Ca^{2+} levels [188, 189]. In the final section of this thesis, the importance of one long-lasting (L)-Type Calcium Channel, $Ca_V1.4$, was examined and its role in T cell homeostasis was established.

The $Ca_V1.4$ Ca^{2+} channel was found to be expressed on the cell surface of $CD4^+$ and $CD8^+$ murine T cells. This lymphocyte form was found to be smaller in size compared to a retinoblastoma version perhaps due to alternative splicing or cell-type specific post-translational modifications [241]. Using a loss of function murine model knocking out the pore forming subunit of Ca^{2+} channel, $Ca_V1.4$ was shown to play a T cell-intrinsic role in the survival and maintenance of naïve $CD4^+$ and $CD8^+$ T cells *in vivo*. $Ca_V1.4$ was shown to be essential for TCR-induced regulation of cytosolic free Ca^{2+} and downstream TCR signalling, impacting activation of the Ras/ERK and NFAT pathways, IL-7 receptor expression and IL-7 responsiveness. The loss of $Ca_V1.4$ and subsequently naïve peripheral T cells resulted in deficient immune responses when challenged with the model bacteria, *L. monocytogenes*. Taken together, this channel likely provides calcium current that is a tonic or set point flux enabling T cells to be poised to respond to their cognate antigen in primary or secondary/memory immune responses. The absence of tonic survival signals provided by $Ca_V1.4$ results in failure of naïve T cells to thrive and perpetuates a state of immunological activation and exhaustion.

Instead of being activated by store release as in the case of ORAI1, $Ca_V1.4$ may operate to create intracellular Ca^{2+} stores in the ER and perhaps mitochondria. Low-level TCR signalling through interactions with self-antigens (i.e. self-peptides/self MHC molecules) may result in $Ca_V1.4$-mediated Ca^{2+} influx from outside the cell, allowing the filling of intracellular stores and the initiation of a prosurvival program (**Figure 7.3**). The data in this thesis supports the concept that in the absence of $Ca_V1.4$, there is a reduction in the influx of extracellular Ca^{2+} coupled to self/MHC-TCR interaction, resulting in low cytoplasmic Ca^{2+} levels and depleted Ca^{2+} ER stores. Therefore, when $Ca_V1.4^{-/-}$ T cells

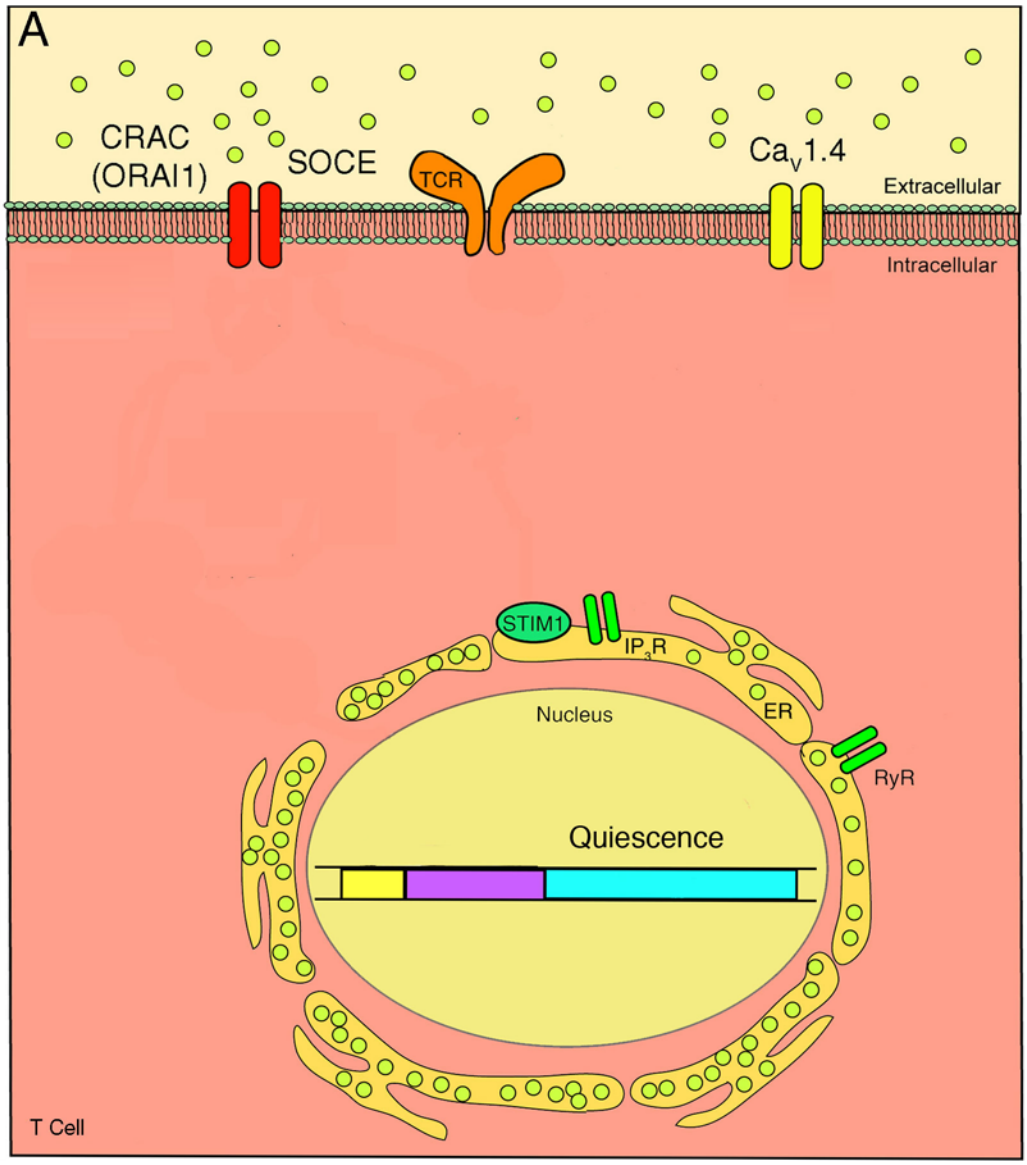
A
CRAC
(ORAI1)
SOCE
TCR
Ca$_V$1.4
Extracellular
Intracellular
STIM1
IP$_3$R
ER
Nucleus
RyR
Quiescence
T Cell

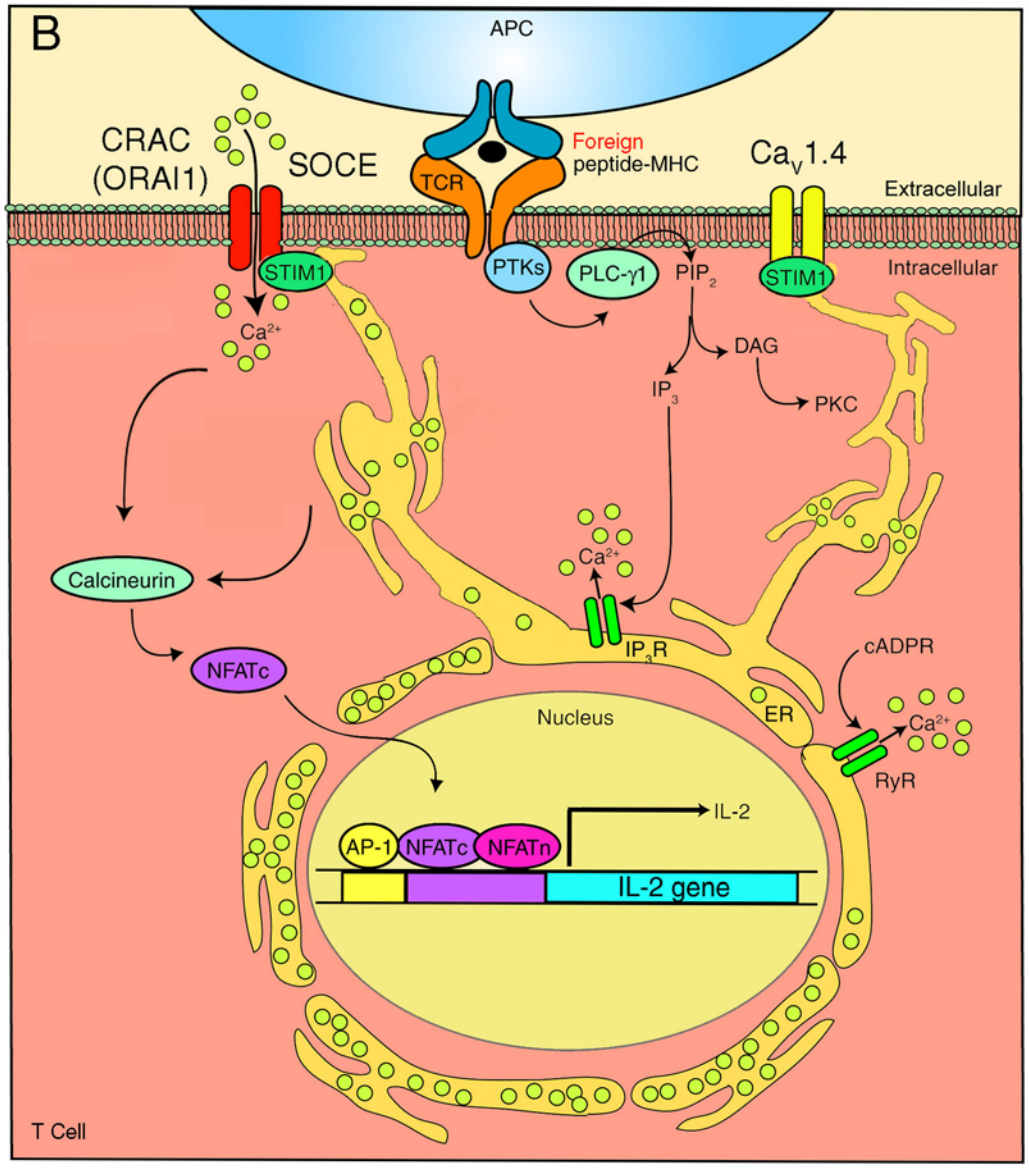
B
APC
CRAC
(ORAI1)
SOCE
TCR
Foreign
peptide-MHC
$Ca_V1.4$
Extracellular
Intracellular
STIM1
PTKs
PLC-γ1
PIP_2
STIM1
Ca^{2+}
DAG
IP_3
PKC
Calcineurin
Ca^{2+}
IP_3R
cADPR
NFATc
Nucleus
ER
Ca^{2+}
RyR
IL-2
AP-1
NFATc
NFATn
IL-2 gene
T Cell

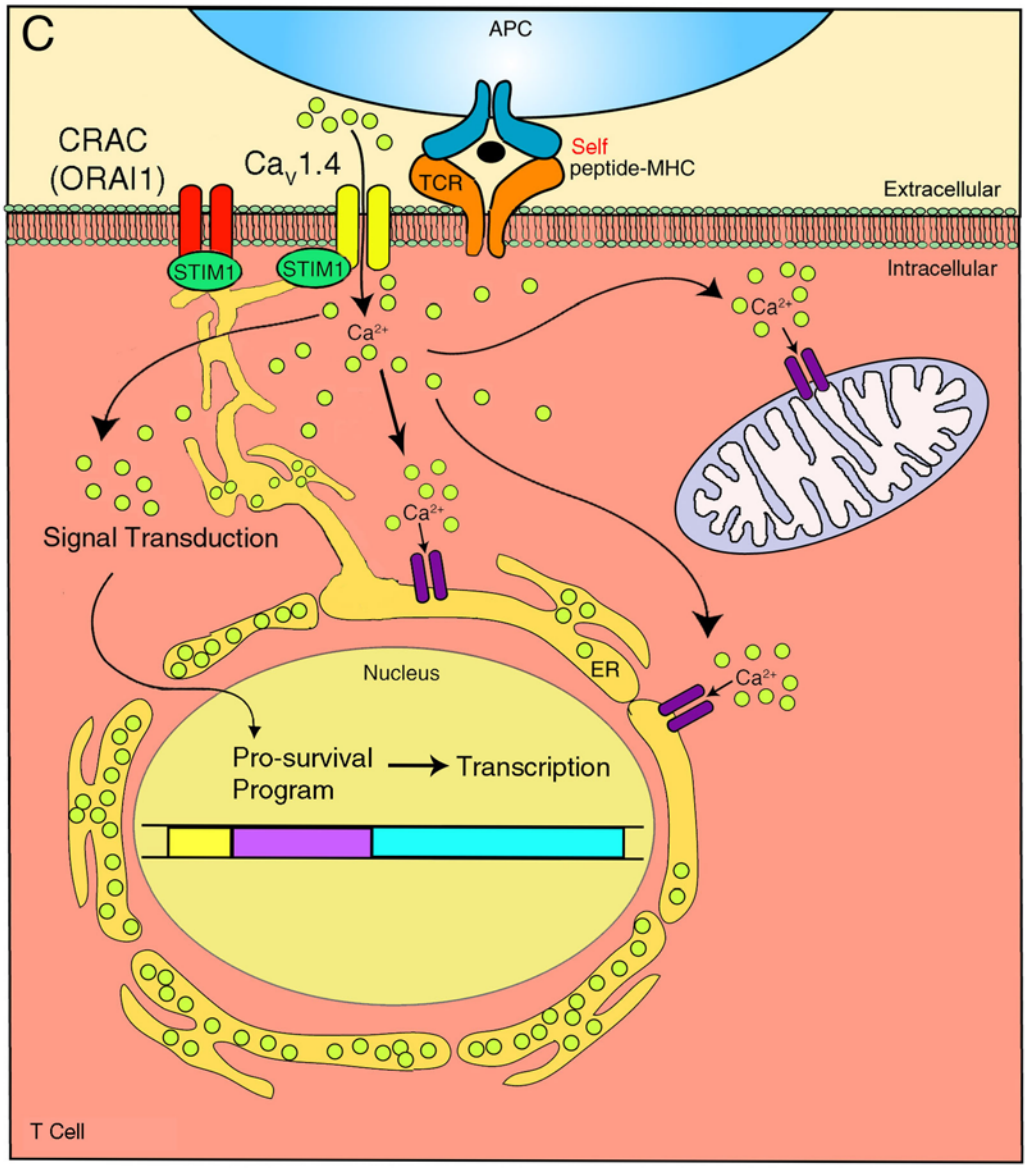
C
APC
CRAC
(ORAI1)
Ca$_V$1.4
TCR
Self
peptide-MHC
Extracellular
Intracellular
STIM1
STIM1
Ca^{2+}
Ca^{2+}
Ca^{2+}
Ca^{2+}
Signal Transduction
Nucleus
ER
Pro-survival
Program
Transcription
T Cell

Figure 7.3. Model of $Ca_V1.4$ function in T cells.
Ca^{2+} signals serve to regulate cell activation, proliferation, differentiation, survival and apoptosis (as reviewed in [188, 190, 191, 465]. **(A)** In a short-lived quiescent state, unactivated T cells with no antigen-MHC engagement have operative calcium stores in the ER while ORAI1 and Ca_V channels are closed. STIM1 resides in the ER membrane. **(B)** Strong T cell receptor (TCR) signalling through engagement by a foreign peptide-MHC, triggers rises in intracellular Ca^{2+} through the activation of PLCγ1 and the associated hydrolysis of phosphatidylinositol-3,4-bisphosphate (PIP2) into inositol-1,4,5-trisphosphate (IP3) and diacylglycerol (DAG) [188, 189]. Elevated levels of IP_3 in the cytosol lead to the release of Ca^{2+} from IP_3R Ca^{2+} channels located in the ER. TCR stimulation also leads to the generation of cyclic adenosine diphosphate ribose (cADPR) that binds and opens RyR Ca^{2+} channels located in the ER, leading to further Ca^{2+} release. After Ca^{2+} store depletion in the ER, STIM1 oligomers form at ER- plasma membrane junctions and STIM1 opens ORAI1 channels. Thus, Ca^{2+} release from the ER causes sustained Ca^{2+} influx from the extracellular space through store-operated Ca^{2+} entry (SOCEs) in the plasma membrane. During the activation phase STIM1 may become adjacent to Ca_V channels thereby inhibiting opening [480, 481]. Elevated intracellular Ca^{2+} activates the serine/threonine protein phosphatase, calcineurin that is responsible for dephosphorylating the cytoplasmic component of NFAT (NFATc), permitting the activated form of NFATc to translocate into the nucleus. NFATc associates with the newly synthesized nuclear subunit of NFAT (NFATn), and together the NFAT complex regulates the expression of several genes, through binding to response elements in gene promoter/enhancer regions, usually in association with activating protein-1 (AP-1). **(C)** Low-level TCR signalling through interactions with self-antigens (ie. self-peptides/self MHC molecules) results in $Ca_V1.4$-mediated Ca^{2+} influx from outside the cell, filling of depleted intracellular stores and induction of a signalling cascade to activate a pro-survival program within the naïve T cell. Thus, the interaction with self-MHC stimulates the production of survival factors leading to momentary quiescence before re-engagement with cells presenting self-MHC or foreign-MHC. This model depicts STIM1 activating Ca_V and reciprocally inhibits ORAI1 in this pro-survival process but this presently is an open question. Adapted from Trends in Pharmacological Sciences, 27/7, Maya F. Kotturi, Simon V. Hunt, Wilfred A. Jefferies, Roles of CRAC and Ca_V-like channels in T cells: more than one gatekeeper?, 360-367 Copyright (2006), with permission from Elsevier.

are stimulated through the TCR, there is a defective Ca^{2+} release from the ER as a result of less stored Ca^{2+}, decreased subsequent store-operated Ca^{2+} entry (SOCE), diminished inward Ca^{2+} flux through Ca^{2+} release-activated calcium (ORAI1/CRAC) channels leading to weakened Ca^{2+}-dependent signalling. Collectively, our study provides a new framework for understanding the regulation of lymphocyte biology through the function of L-type Ca^{2+} channels in the storage of intracellular Ca^{2+} and operative Ca^{2+} regulation during antigen receptor-mediated signal transduction. These findings have direct implications in designing modifying T cell responses using drugs that are known to modulate Ca_V activities. This information could be useful for designing specific drugs that can be used to inhibiting autoimmunity or as increasing the efficacy of vaccines.

7.2 Future directions

7.2.1 Dendritic cells

7.2.1.1 CD74

The CD74-mediated cross presentation pathway is one of several proposed mechanism to explain the processing and presentation of exogenous antigen on MHC I [41]. As distinct DC subsets exist, these pathways may be specialized to function in specific DC populations. Therefore, the function of CD74-mediated cross presentation in the different DCs could be examined. Using specific FACS sorting protocols based on unique surface marker expression (**Table 7.1**), DC subsets could be isolated from $CD74^{-/-}$ mice. The sorted cells could then be examined by the *ex vivo* cross presentation protocols that were used in this thesis to analyze the DCs as a whole. Alternatively, DC cross

Features	Lymphoid-organ-resident DC subsets			Migratory DC subsets		Monocyte derived
	CD4+ DCs	CD8+ DCs	DN DCs	Interstitial DCs	Langerhans cells	
Surface markers						
CD11c	+++	+++	+++	+++	+++	+++
CD4	+	–	–	–	–	–
CD8	–	++	–	–	–/+	–
CD205	–	++	–/+	+	+++	–/+
CD11b	++	–	++	++‡	++	++
Langerin	–	+	–	–	+++	–
CD24	+	++	+	ND	ND	ND
SIRPα	+	–	+	+	+	ND

Table 7.1. Mouse DC subsets.
The surface markers distinguishing the conventional DC subsets are listed. ‡ Absent in 'triple negative' DCs [482, 483]. Adapted by permission from Macmillan Publishers Ltd: [Nature Reviews Immunology] [9], copyright (2007)

presentation pathways may function in a number of DC subsets, however, be specialized for a specific exogenous antigen. Therefore, using the *ex vivo* cross presentation protocols, different antigens could be used to examine the capacity of DCs lacking CD74 to cross present. The antigens can be selected based on the route DCs use to internalize them and may include antigen that is phagocytosed such as bacteria (*L. monocytogenes*-OVA or *E.coli*-OVA) [90, 484] or antigen that is internalized by receptor mediated endocytosis such as immune complexes (anti-OVA antibody bound OVA) that bind Fc receptors or antigen directed against C-type lectins (anti-DEC205/anti-DCIR2 antibody conjugated to OVA) [91, 440].

Recently, DC migration has been linked to CD74 expression [327]. For DCs to migrate through narrow spaces such as parenchymal tissue, actin contraction controlled by the motor protein myosin II is important [485]. CD74 has been shown to interact with myosin II in order to traffic MHC II to endolysosome [486, 487]; however, this interaction affects the ability of myosin II to participate in mobility reducing the migration speed of the DC. Presumably, this decrease in DC speed allows for DCs to better sample the environment and maximize antigen uptake. When CD74 reaches the endolysosomes and is cleaved by proteases, the CD74-myosin II interaction is disrupted and DC migration is restored [327]. In our *in vivo* analysis of cross presentation, DCs are injected *iv* with TCR transgenic T cells. To eliminate the possibility that CD74-deficient DCs are not migrating to the spleen as efficiently as wild type DCs in this assay, DCs could be tracked. Labelled CD74-deficient and wild type DCs could be injected *iv* and tracked through the mouse over time. If migration is equivalent, these results would

conclusively demonstrate that a cross presentation defect is independent of migration defects experienced by $CD74^{-/-}$ DCs.

7.2.1.2 HIV-Nef

In this thesis, HIV Nef was shown to interfere with the cross presentation of exogenous antigen. This was demonstrated by a decrease in the amount of MHC I loaded with exogenous antigen on the cell surface. To confirm this observation in greater detail, it would be useful to determine if MHC I can traffic efficiently to endolysosomal cross presentation compartment for antigenic loading in the presence of Nef. Using confocal microscopy techniques described in this thesis and previously [59], the amount of MHC I localizing to endolysosomes ($LAMP1^{+}$ compartments) could be visualized. Furthermore, Nef-expressing and wild type DCs allowed to internalize antigen such as soluble OVA (or those listed above) could be analyzed for the formation of MHC I-OVA complexes in $LAMP1^{+}$ compartments. These results would confirm that the Nef impairment of MHC I specifically inhibits the vacuolar pathway of cross presentation.

HIV Nef is a virulence factor that has been likened to an adaptor protein that binds host proteins misdirecting them and thereby affecting their function in the cell. In this study of the effect of Nef on DCs, downregulation of MHC II was noted in addition to MHC I. This has previously been document in monocytes expressing Nef where MHC II delivery to the cell surface was retarded [170]. Further in monocytes, Nef has been shown to remove mature MHC II from the cell surface [168, 170, 171]. To expand on these findings, the role of Nef on MHC II function could be assessed in this DC model to determine if Nef impedes $CD4^{+}$ T cell activation. Specifically, the ability of DCs to

present antigen such as Hen Egg Lysozyme (HEL) on MHC II and activate HEL-specific $CD4^+$ T cells could be examined. Furthermore, using confocal microscopy the cellular localization of MHC II when Nef is present could be determined. The lack of co-localization of MHC II with MHC II compartment components such as LAMP-1, Ii, H-2M and H-2O would indicate that Nef affects the trafficking of MHC II in antigen presentation.

In the analysis of Nef function *in vivo*, a Nef transgenic (Tg) mouse was constructed based on the tropism of HIV. Nef was expressed in $CD4^+$ cells including DCs, macrophages and T cells. A defect in immune responses against viral and bacterial pathogens was noted; however, the exact cell population responsible for this deficiency could not be conclusively determined. In order to better assess the contribution of Nef-mediated DC dysfunction to immune impairment, a transgenic mouse with a CD11c promoter driving Nef expression could be constructed. This would allow Nef expression almost exclusively in DCs. Using *in vivo* cross presentation assays previously described in this thesis, the effect on Nef on DC cross presentation could be better assessed to corroborate *in vitro* data.

As mentioned above, Nef is expressed in $CD4^+$ T cells in this transgenic model. In the current Nef Tg model, the affect of Nef on $CD4^+$ T cells and the contribution to immune deficiency could be examined. The ability of Nef Tg mice to develop Th1 and Th2 responses *in vivo* could be assessed. For these studies, an infection model using the protozoan parasite *Leishmania major* could be used. When examining the early immune responses is C57Bl/6 mice, a low parasite dose induces a Th2 response while a high dose induces a Th1 response [488]. By administering differing doses of *L. major* to wild type

and Nef Tg mice and assessing cytokine production, the $CD4^+$ T cell responses can be determined. Similarly, infection of C57Bl/6 mice with varying doses of the intestinal nematode *Trichuris muris* can lead to acute or chronic infection [489]. Following delivery of a high dose for acute infection, a protective Th2 response is generated leading to parasite expulsion. Conversely, following low dose chronic infection, a Th1 immune response dominates [489]. Therefore, use of a *T. muris* infection model would provide further insight into the affect of Nef on $CD4^+$ T cell responses. Parasites are important opportunistic infections affecting HIV-infected individuals in developing countries [490, 491]. Examination of these infections in the Nef Tg model would provide additional evidence that Nef has a direct role in immunodeficiency causing susceptibility to important opportunistic infections.

7.2.2 T cells

7.2.2.1 $Ca_V1.4$

Cues for T cell homeostasis include signals through the TCR receptor and IL7R. Further to this, trafficking of naïve T cells through the T cell zone of secondary lymphoid organs (SLO) is important for T cells to receive these homeostatic signals [172]. The fibroblastic reticular cell (FRC) network in SLOs produce IL-7 and CCR7 ligands (CCL19 and CCL21) [174]. In addition, DCs and stromal cells in FRC networks provide self peptide-MHC complexes. Together, these provide survival signals to the naïve T cell as they move along the network. Here, $Ca_V1.4$-deficient mice were shown to have deficient T cell homeostasis. Therefore, it would be interesting to determine if T cell homing was also impaired. Labelled T cells isolated from wild type and $Ca_V1.4^{-/-}$ mice

could be injected into wild-type mice and tracked for their localization to SLOs [492]. In addition, *in vitro* chemotaxis assays could be performed where wild type and mutant T cells were assessed for their ability to migrate through a transwell plate towards a chemokine gradient [492]. A defect in homing would add to the already impaired ability of naïve $Ca_V1.4$ T cells to survive.

During the analysis of $Ca_V1.4$ protein in murine T cells in this thesis, it was noted that the T cell form was smaller in size that the protein identified in the retinoblastoma cell line. In support of this, the existence of two unique $Ca_V1.4$ spice variants distinct from the retina form have been previously document in human T cells [241]. The splice forms differ at the carboxy-terminus removing a voltage sensor and a 1,4-dihydropyridines (DHP) sensitive site [241]. It has been hypothesized that removal of the voltage sensor may alter the voltage-gating activation of this channel allowing the channel to be activated through an alternate method such as ligation of the TCR [241]. Using RT-PCR methods similar to those used to identify the alternate splice variants in human T cells, the identification of the $Ca_V1.4$ sequence in murine T cells could be performed [241]. Furthermore, upon identification of multiple splice variants, the analysis of the expression patterns in murine $CD4^+$ and $CD8^+$ T cells in various stages of development and activation might provide an explanation for the differential calcium responses noted in this thesis. In addition to $Ca_V1.4$ other Ca_V1 family members (**Table 1.1**) have been shown to be expressed in mouse and human T cells, mRNA analysis of these channels may identify alternative splice variants and expression patterns as well [190]. Following identification of the sequence of the murine $Ca_V1.4$ splice variant(s), overexpression of the individual $Ca_V1.4$ channels in a T cell line could be carried out.

The contribution of each $Ca_V1.4$ channel to T cell function could be assessed using Ca^{2+} flux assays following thapsigargin or TCR ligation and TCR signalling analysis protocols previously described in this thesis. Analysis of the contribution of individual channels to the T cell Ca^{2+} signal will provide insight into the mechanisms of T cell homeostasis, activation and function.

DCs and T cells play important coordinating roles during an immune response to successfully clear an infection. This thesis provides details highlighting the requirement for competent antigen presenting DCs and poised T cells in effective immune responses. DCs are recognized as potent APCs capable of priming primary immune responses [1]. Through interactions with the well-known MHC II chaperone, CD74, MHC I in DCs is able to access internalized exogenous antigen to initiate cross presentation a process essential for the activation of naïve T cells. Naïve peripheral T cells capable of responding to antigen are maintained through continual homeostatic signalling that includes mobilization of the second messenger, Ca^{2+}, provided by plasma membrane channel such as $Ca_V1.4$. These T cells are activated by antigen presenting DCs and gain effector function essential for productive immune responses. Disruption of any of these processes leads to immunodeficiency. For example, HIV has evolved an effective mechanism to evade these immune responses in order to persist in the host. Through analysis of the mechanistics of cross presentation and T cell homeostasis, a better understanding of the basis by which we can manipulate the outcome of immunity for therapeutic intervention including those directed at HIV can be achieved.

REFERENCES

1. Belz, G., A. Mount, and F. Masson, *Dendritic cells in viral infections.* Handb Exp Pharmacol, 2009(188): p. 51-77.
2. Moser, M. and O. Leo, *Key concepts in immunology.* Vaccine, 2010. **28 Suppl 3**: p. C2-13.
3. Stuart, L.M. and R.A. Ezekowitz, *Phagocytosis: elegant complexity.* Immunity, 2005. **22**(5): p. 539-50.
4. Bachmann, M.F., M. Kopf, and B.J. Marsland, *Chemokines: more than just road signs.* Nat Rev Immunol, 2006. **6**(2): p. 159-64.
5. Dempsey, P.W., S.A. Vaidya, and G. Cheng, *The art of war: Innate and adaptive immune responses.* Cell Mol Life Sci, 2003. **60**(12): p. 2604-21.
6. Jung, S., et al., *In vivo depletion of CD11c(+) dendritic cells abrogates priming of CD8(+) T cells by exogenous cell-associated antigens.* Immunity, 2002. **17**(2): p. 211-20.
7. Zammit, D.J., et al., *Dendritic cells maximize the memory CD8 T cell response to infection.* Immunity, 2005. **22**(5): p. 561-70.
8. Belz, G.T., et al., *Bone marrow-derived cells expand memory CD8+ T cells in response to viral infections of the lung and skin.* Eur J Immunol, 2006. **36**(2): p. 327-35.
9. Villadangos, J.A. and P. Schnorrer, *Intrinsic and cooperative antigen-presenting functions of dendritic-cell subsets in vivo.* Nat Rev Immunol, 2007. **7**(7): p. 543-55.
10. Randolph, G.J., V. Angeli, and M.A. Swartz, *Dendritic-cell trafficking to lymph nodes through lymphatic vessels.* Nat Rev Immunol, 2005. **5**(8): p. 617-28.
11. Villadangos, J.A. and W.R. Heath, *Life cycle, migration and antigen presenting functions of spleen and lymph node dendritic cells: limitations of the Langerhans cells paradigm.* Semin Immunol, 2005. **17**(4): p. 262-72.
12. Wilson, N.S. and J.A. Villadangos, *Regulation of antigen presentation and cross-presentation in the dendritic cell network: facts, hypothesis, and immunological implications.* Adv Immunol, 2005. **86**: p. 241-305.
13. Heath, W.R. and F.R. Carbone, *Dendritic cell subsets in primary and secondary T cell responses at body surfaces.* Nat Immunol, 2009. **10**(12): p. 1237-44.
14. Sung, S.S., et al., *A major lung CD103 (alphaE)-beta7 integrin-positive epithelial dendritic cell population expressing Langerin and tight junction proteins.* J Immunol, 2006. **176**(4): p. 2161-72.
15. Naik, S.H., et al., *Intrasplenic steady-state dendritic cell precursors that are distinct from monocytes.* Nat Immunol, 2006. **7**(6): p. 663-71.
16. Wilson, N.S., et al., *Most lymphoid organ dendritic cell types are phenotypically and functionally immature.* Blood, 2003. **102**(6): p. 2187-94.
17. Wilson, N.S., et al., *Systemic activation of dendritic cells by Toll-like receptor ligands or malaria infection impairs cross-presentation and antiviral immunity.* Nat Immunol, 2006. **7**(2): p. 165-72.

18. Sponaas, A.M., et al., *Malaria infection changes the ability of splenic dendritic cell populations to stimulate antigen-specific T cells.* J Exp Med, 2006. **203**(6): p. 1427-33.
19. Reis e Sousa, C., et al., *In vivo microbial stimulation induces rapid CD40 ligand-independent production of interleukin 12 by dendritic cells and their redistribution to T cell areas.* J Exp Med, 1997. **186**(11): p. 1819-29.
20. McIlroy, D., et al., *Investigation of human spleen dendritic cell phenotype and distribution reveals evidence of in vivo activation in a subset of organ donors.* Blood, 2001. **97**(11): p. 3470-7.
21. Leon, B., M. Lopez-Bravo, and C. Ardavin, *Monocyte-derived dendritic cells formed at the infection site control the induction of protective T helper 1 responses against Leishmania.* Immunity, 2007. **26**(4): p. 519-31.
22. Le Borgne, M., et al., *Dendritic cells rapidly recruited into epithelial tissues via CCR6/CCL20 are responsible for CD8+ T cell crosspriming in vivo.* Immunity, 2006. **24**(2): p. 191-201.
23. Krutzik, S.R., et al., *TLR activation triggers the rapid differentiation of monocytes into macrophages and dendritic cells.* Nat Med, 2005. **11**(6): p. 653-60.
24. Shortman, K. and S.H. Naik, *Steady-state and inflammatory dendritic-cell development.* Nat Rev Immunol, 2007. **7**(1): p. 19-30.
25. Tacke, F. and G.J. Randolph, *Migratory fate and differentiation of blood monocyte subsets.* Immunobiology, 2006. **211**(6-8): p. 609-18.
26. Serbina, N.V., et al., *TNF/iNOS-producing dendritic cells mediate innate immune defense against bacterial infection.* Immunity, 2003. **19**(1): p. 59-70.
27. Villadangos, J.A. and L. Young, *Antigen-presentation properties of plasmacytoid dendritic cells.* Immunity, 2008. **29**(3): p. 352-61.
28. Swiecki, M. and M. Colonna, *Unraveling the functions of plasmacytoid dendritic cells during viral infections, autoimmunity, and tolerance.* Immunol Rev, 2010. **234**(1): p. 142-62.
29. Colonna, M., G. Trinchieri, and Y.J. Liu, *Plasmacytoid dendritic cells in immunity.* Nat Immunol, 2004. **5**(12): p. 1219-26.
30. Liu, Y.J., *IPC: professional type 1 interferon-producing cells and plasmacytoid dendritic cell precursors.* Annu Rev Immunol, 2005. **23**: p. 275-306.
31. Bevan, M.J., *Minor H antigens introduced on H-2 different stimulating cells cross-react at the cytotoxic T cell level during in vivo priming.* J Immunol, 1976. **117**(6): p. 2233-8.
32. Bevan, M.J., *Cross-priming for a secondary cytotoxic response to minor H antigens with H-2 congenic cells which do not cross-react in the cytotoxic assay.* J Exp Med, 1976. **143**(5): p. 1283-8.
33. Lizee, G., G. Basha, and W.A. Jefferies, *Tails of wonder: endocytic-sorting motifs key for exogenous antigen presentation.* Trends Immunol, 2005. **26**(3): p. 141-9.
34. Vyas, J.M., A.G. Van der Veen, and H.L. Ploegh, *The known unknowns of antigen processing and presentation.* Nat Rev Immunol, 2008. **8**(8): p. 607-18.
35. Yewdell, J.W. and C.V. Nicchitta, *The DRiP hypothesis decennial: support, controversy, refinement and extension.* Trends Immunol, 2006. **27**(8): p. 368-73.
36. Jensen, P.E., *Recent advances in antigen processing and presentation.* Nat Immunol, 2007. **8**(10): p. 1041-8.

37. Donaldson, J.G. and D.B. Williams, *Intracellular assembly and trafficking of MHC class I molecules.* Traffic, 2009. **10**(12): p. 1745-52.
38. Rocha, N. and J. Neefjes, *MHC class II molecules on the move for successful antigen presentation.* EMBO J, 2008. **27**(1): p. 1-5.
39. Landsverk, O.J., O. Bakke, and T.F. Gregers, *MHC II and the endocytic pathway: regulation by invariant chain.* Scand J Immunol, 2009. **70**(3): p. 184-93.
40. Kurts, C., B.W. Robinson, and P.A. Knolle, *Cross-priming in health and disease.* Nat Rev Immunol, 2010. **10**(6): p. 403-14.
41. Lin, M.L., et al., *The cell biology of cross-presentation and the role of dendritic cell subsets.* Immunol Cell Biol, 2008. **86**(4): p. 353-62.
42. Kovacsovics-Bankowski, M. and K.L. Rock, *A phagosome-to-cytosol pathway for exogenous antigens presented on MHC class I molecules.* Science, 1995. **267**(5195): p. 243-6.
43. Tsai, B., Y. Ye, and T.A. Rapoport, *Retro-translocation of proteins from the endoplasmic reticulum into the cytosol.* Nat Rev Mol Cell Biol, 2002. **3**(4): p. 246-55.
44. Rodriguez, A., et al., *Selective transport of internalized antigens to the cytosol for MHC class I presentation in dendritic cells.* Nat Cell Biol, 1999. **1**(6): p. 362-368.
45. Ackerman, A.L., A. Giodini, and P. Cresswell, *A role for the endoplasmic reticulum protein retrotranslocation machinery during crosspresentation by dendritic cells.* Immunity, 2006. **25**(4): p. 607-17.
46. Imai, J., et al., *Exogenous antigens are processed through the endoplasmic reticulum-associated degradation (ERAD) in cross-presentation by dendritic cells.* Int Immunol, 2005. **17**(1): p. 45-53.
47. Ye, Y., et al., *A membrane protein complex mediates retro-translocation from the ER lumen into the cytosol.* Nature, 2004. **429**(6994): p. 841-7.
48. Lilley, B.N. and H.L. Ploegh, *A membrane protein required for dislocation of misfolded proteins from the ER.* Nature, 2004. **429**(6994): p. 834-40.
49. Norbury, C.C., et al., *Class I MHC presentation of exogenous soluble antigen via macropinocytosis in bone marrow macrophages.* Immunity, 1995. **3**(6): p. 783-91.
50. Touret, N., et al., *Quantitative and dynamic assessment of the contribution of the ER to phagosome formation.* Cell, 2005. **123**(1): p. 157-70.
51. Gagnon, E., et al., *Endoplasmic reticulum-mediated phagocytosis is a mechanism of entry into macrophages.* Cell, 2002. **110**(1): p. 119-31.
52. Guermonprez, P., et al., *ER-phagosome fusion defines an MHC class I cross-presentation compartment in dendritic cells.* Nature, 2003. **425**: p. 397-402.
53. Houde, M., et al., *Phagosomes are competent organelles for antigen cross-presentation.* Nature, 2003. **425**: p. 402-406.
54. Ackerman, A.L., et al., *Early phagosomes in dendritic cells form a cellular compartment sufficient for cross presentation of exogenous antigens.* Proc Natl Acad Sci U S A, 2003. **100**(22): p. 12889-94.
55. Groothuis, T. and J. Neefjes, *The ins and outs of intracellular peptides and antigen presentation by MHC class I molecules.* Curr Top Microbiol Immunol, 2005. **300**: p. 127-48.

56. Rock, K.L. and L. Shen, *Cross-presentation: underlying mechanisms and role in immune surveillance.* Immunol Rev, 2005. **207**: p. 166-83.
57. Shen, L., et al., *Important role of cathepsin S in generating peptides for TAP-independent MHC class I crosspresentation in vivo.* Immunity, 2004. **21**(2): p. 155-65.
58. Saveanu, L., et al., *IRAP identifies an endosomal compartment required for MHC class I cross-presentation.* Science, 2009. **325**(5937): p. 213-7.
59. Lizee, G., et al., *Control of dendritic cell cross-presentation by the major histocompatibibilty complex class I cytoplasmic domain.* Nature Immunology, 2003. **4**(11): p. 1065-1073.
60. Vigna, J.L., K.D. Smith, and C.T. Lutz, *Invariant chain association with MHC class I: preference for HLA class I/beta 2-microglobulin heterodimers, specificity, and influence of the MHC peptide-binding groove.* J Immunol, 1996. **157**(10): p. 4503-10.
61. Sugita, M. and M.B. Brenner, *Association of the invariant chain with major histocompatibility complex class I molecules directs trafficking to endocytic compartments.* J Biol Chem, 1995. **270**(3): p. 1443-8.
62. Pfeifer, J.D., et al., *Phagocytic processing of bacterial antigens for class I MHC presentation to T cells.* Nature, 1993. **361**(6410): p. 359-62.
63. Song, R. and C.V. Harding, *Roles of proteasomes, transporter for antigen presentation (TAP), and beta 2-microglobulin in the processing of bacterial or particulate antigens via an alternate class I MHC processing pathway.* J Immunol, 1996. **156**(11): p. 4182-90.
64. Wick, M.J. and J.D. Pfeifer, *Major histocompatibility complex class I presentation of ovalbumin peptide 257-264 from exogenous sources: protein context influences the degree of TAP-independent presentation.* Eur J Immunol, 1996. **26**(11): p. 2790-9.
65. Basha, G., et al., *MHC class I endosomal and lysosomal trafficking coincides with exogenous antigen loading in dendritic cells.* PLoS One, 2008. **3**(9): p. e3247.
66. Reinicke, A.T., et al., *Dendritic cell cross-priming is essential for immune responses to Listeria monocytogenes.* PLoS One, 2009. **4**(10): p. e7210.
67. Dongre, A.R., et al., *In vivo MHC class II presentation of cytosolic proteins revealed by rapid automated tandem mass spectrometry and functional analyses.* Eur J Immunol, 2001. **31**(5): p. 1485-94.
68. Dengjel, J., et al., *Autophagy promotes MHC class II presentation of peptides from intracellular source proteins.* Proc Natl Acad Sci U S A, 2005. **102**(22): p. 7922-7.
69. Strawbridge, A.B. and J.S. Blum, *Autophagy in MHC class II antigen processing.* Curr Opin Immunol, 2007. **19**(1): p. 87-92.
70. Schmid, D. and C. Munz, *Innate and adaptive immunity through autophagy.* Immunity, 2007. **27**(1): p. 11-21.
71. Crotzer, V.L. and J.S. Blum, *Autophagy and adaptive immunity.* Immunology, 2010. **131**(1): p. 9-17.
72. Brazil, M.I., S. Weiss, and B. Stockinger, *Excessive degradation of intracellular protein in macrophages prevents presentation in the context of major*

histocompatibility complex class II molecules. Eur J Immunol, 1997. **27**(6): p. 1506-14.
73. Dorfel, D., et al., *Processing and presentation of HLA class I and II epitopes by dendritic cells after transfection with in vitro-transcribed MUC1 RNA.* Blood, 2005. **105**(8): p. 3199-205.
74. Nimmerjahn, F., et al., *Major histocompatibility complex class II-restricted presentation of a cytosolic antigen by autophagy.* Eur J Immunol, 2003. **33**(5): p. 1250-9.
75. Paludan, C., et al., *Endogenous MHC class II processing of a viral nuclear antigen after autophagy.* Science, 2005. **307**(5709): p. 593-6.
76. Levine, B. and V. Deretic, *Unveiling the roles of autophagy in innate and adaptive immunity.* Nat Rev Immunol, 2007. **7**(10): p. 767-77.
77. Cooney, R., et al., *NOD2 stimulation induces autophagy in dendritic cells influencing bacterial handling and antigen presentation.* Nat Med, 2010. **16**(1): p. 90-7.
78. Djavaheri-Mergny, M., et al., *NF-kappaB activation represses tumor necrosis factor-alpha-induced autophagy.* J Biol Chem, 2006. **281**(41): p. 30373-82.
79. Scherz-Shouval, R., et al., *Reactive oxygen species are essential for autophagy and specifically regulate the activity of Atg4.* EMBO J, 2007. **26**(7): p. 1749-60.
80. Wilson, N.S., D. El-Sukkari, and J.A. Villadangos, *Dendritic cells constitutively present self antigens in their immature state in vivo and regulate antigen presentation by controlling the rates of MHC class II synthesis and endocytosis.* Blood, 2004. **103**(6): p. 2187-95.
81. Veeraswamy, R.K., et al., *Dendritic cells process and present antigens across a range of maturation states.* J Immunol, 2003. **170**(11): p. 5367-72.
82. Norbury, C.C., et al., *Visualizing priming of virus-specific CD8+ T cells by infected dendritic cells in vivo.* Nat Immunol, 2002. **3**(3): p. 265-71.
83. He, Y., et al., *Skin-derived dendritic cells induce potent CD8(+) T cell immunity in recombinant lentivector-mediated genetic immunization.* Immunity, 2006. **24**(5): p. 643-56.
84. Segura, E. and J.A. Villadangos, *Antigen presentation by dendritic cells in vivo.* Curr Opin Immunol, 2009. **21**(1): p. 105-10.
85. Hildner, K., et al., *Batf3 deficiency reveals a critical role for CD8alpha+ dendritic cells in cytotoxic T cell immunity.* Science, 2008. **322**(5904): p. 1097-100.
86. Amigorena, S. and A. Savina, *Intracellular mechanisms of antigen cross presentation in dendritic cells.* Curr Opin Immunol, 2010. **22**(1): p. 109-17.
87. Schnorrer, P., et al., *The dominant role of CD8+ dendritic cells in cross-presentation is not dictated by antigen capture.* Proc Natl Acad Sci U S A, 2006. **103**(28): p. 10729-34.
88. Pooley, J.L., W.R. Heath, and K. Shortman, *Cutting edge: intravenous soluble antigen is presented to CD4 T cells by CD8- dendritic cells, but cross-presented to CD8 T cells by CD8+ dendritic cells.* J Immunol, 2001. **166**(9): p. 5327-30.
89. Iyoda, T., et al., *The CD8+ dendritic cell subset selectively endocytoses dying cells in culture and in vivo.* J Exp Med, 2002. **195**(10): p. 1289-302.

90. Schulz, O. and C. Reis e Sousa, *Cross-presentation of cell-associated antigens by CD8alpha+ dendritic cells is attributable to their ability to internalize dead cells.* Immunology, 2002. **107**(2): p. 183-9.
91. Dudziak, D., et al., *Differential antigen processing by dendritic cell subsets in vivo.* Science, 2007. **315**(5808): p. 107-11.
92. Savina, A., et al., *The small GTPase Rac2 controls phagosomal alkalinization and antigen crosspresentation selectively in CD8(+) dendritic cells.* Immunity, 2009. **30**(4): p. 544-55.
93. Savina, A., et al., *NOX2 controls phagosomal pH to regulate antigen processing during crosspresentation by dendritic cells.* Cell, 2006. **126**(1): p. 205-18.
94. Burgdorf, S., et al., *Distinct pathways of antigen uptake and intracellular routing in CD4 and CD8 T cell activation.* Science, 2007. **316**(5824): p. 612-6.
95. Lambotin, M., et al., *A look behind closed doors: interaction of persistent viruses with dendritic cells.* Nat Rev Microbiol, 2010. **8**(5): p. 350-60.
96. Cunningham, A.L., et al., *Manipulation of dendritic cell function by viruses.* Curr Opin Microbiol, 2010.
97. Fauci, A.S., *25 years of HIV.* Nature, 2008. **453**(7193): p. 289-90.
98. Levy, J.A., *HIV pathogenesis: 25 years of progress and persistent challenges.* AIDS, 2009. **23**(2): p. 147-60.
99. Duvall, M.G., et al., *Maintenance of HIV-specific CD4+ T cell help distinguishes HIV-2 from HIV-1 infection.* J Immunol, 2006. **176**(11): p. 6973-81.
100. Reeves, J.D. and R.W. Doms, *Human immunodeficiency virus type 2.* J Gen Virol, 2002. **83**(Pt 6): p. 1253-65.
101. *AIDS Epidemic Update*. 2009, United Nations Programme on HIV/AIDS World Health Organization Geneva.
102. Bangham, C.R., *CTL quality and the control of human retroviral infections.* Eur J Immunol, 2009. **39**(7): p. 1700-12.
103. O'Connell, K.A., J.R. Bailey, and J.N. Blankson, *Elucidating the elite: mechanisms of control in HIV-1 infection.* Trends Pharmacol Sci, 2009. **30**(12): p. 631-7.
104. Chakrabarti, L.A. and V. Simon, *Immune mechanisms of HIV control.* Curr Opin Immunol, 2010. **22**(4): p. 488-96.
105. Benito, J.M., M. Lopez, and V. Soriano, *The role of CD8+ T-cell response in HIV infection.* AIDS Rev, 2004. **6**(2): p. 79-88.
106. Borrow, P., et al., *Virus-specific CD8+ cytotoxic T-lymphocyte activity associated with control of viremia in primary human immunodeficiency virus type 1 infection.* J Virol, 1994. **68**(9): p. 6103-10.
107. Koup, R.A., et al., *Temporal association of cellular immune responses with the initial control of viremia in primary human immunodeficiency virus type 1 syndrome.* J Virol, 1994. **68**(7): p. 4650-5.
108. Klein, M.R., et al., *Kinetics of Gag-specific cytotoxic T lymphocyte responses during the clinical course of HIV-1 infection: a longitudinal analysis of rapid progressors and long-term asymptomatics.* J Exp Med, 1995. **181**(4): p. 1365-72.
109. Jin, X., et al., *Dramatic rise in plasma viremia after CD8(+) T cell depletion in simian immunodeficiency virus-infected macaques.* J Exp Med, 1999. **189**(6): p. 991-8.

110. Schmitz, J.E., et al., *Control of viremia in simian immunodeficiency virus infection by CD8+ lymphocytes.* Science, 1999. **283**(5403): p. 857-60.
111. Bevan, M.J., *Antigen presentation to cytotoxic T lymphocytes in vivo.* J Exp Med, 1995. **182**(3): p. 639-41.
112. Appay, V., et al., *Characterization of CD4(+) CTLs ex vivo.* J Immunol, 2002. **168**(11): p. 5954-8.
113. Rosenberg, E.S., et al., *Vigorous HIV-1-specific CD4+ T cell responses associated with control of viremia.* Science, 1997. **278**(5342): p. 1447-50.
114. Kalams, S.A. and B.D. Walker, *The critical need for CD4 help in maintaining effective cytotoxic T lymphocyte responses.* J Exp Med, 1998. **188**(12): p. 2199-204.
115. Migueles, S.A. and M. Connors, *The Role of CD4(+) and CD8(+) T Cells in Controlling HIV Infection.* Curr Infect Dis Rep, 2002. **4**(5): p. 461-467.
116. Kelleher, A.D. and J.J. Zaunders, *Decimated or missing in action: CD4+ T cells as targets and effectors in the pathogenesis of primary HIV infection.* Curr HIV/AIDS Rep, 2006. **3**(1): p. 5-12.
117. Wu, L. and V.N. KewalRamani, *Dendritic-cell interactions with HIV: infection and viral dissemination.* Nat Rev Immunol, 2006. **6**(11): p. 859-68.
118. Wu, L., *Biology of HIV mucosal transmission.* Curr Opin HIV AIDS, 2008. **3**(5): p. 534-40.
119. Cameron, P.U., et al., *Dendritic cells exposed to human immunodeficiency virus type-1 transmit a vigorous cytopathic infection to CD4+ T cells.* Science, 1992. **257**(5068): p. 383-7.
120. Morrow, G., et al., *Current concepts of HIV transmission.* Curr HIV/AIDS Rep, 2007. **4**(1): p. 29-35.
121. McIlroy, D., et al., *Infection frequency of dendritic cells and CD4+ T lymphocytes in spleens of human immunodeficiency virus-positive patients.* J Virol, 1995. **69**(8): p. 4737-45.
122. Smed-Sorensen, A., et al., *Differential susceptibility to human immunodeficiency virus type 1 infection of myeloid and plasmacytoid dendritic cells.* J Virol, 2005. **79**(14): p. 8861-9.
123. de Jong, M.A., et al., *TNF-alpha and TLR agonists increase susceptibility to HIV-1 transmission by human Langerhans cells ex vivo.* J Clin Invest, 2008. **118**(10): p. 3440-52.
124. Coleman, C.M. and L. Wu, *HIV interactions with monocytes and dendritic cells: viral latency and reservoirs.* Retrovirology, 2009. **6**: p. 51.
125. Nair, M.P., et al., *Methamphetamine enhances HIV-1 infectivity in monocyte derived dendritic cells.* J Neuroimmune Pharmacol, 2009. **4**(1): p. 129-39.
126. Duvall, M.G., et al., *Dendritic cells are less susceptible to human immunodeficiency virus type 2 (HIV-2) infection than to HIV-1 infection.* J Virol, 2007. **81**(24): p. 13486-98.
127. Turville, S., et al., *The role of dendritic cell C-type lectin receptors in HIV pathogenesis.* J Leukoc Biol, 2003. **74**(5): p. 710-8.
128. Granelli-Piperno, A., et al., *Dendritic cell-specific intercellular adhesion molecule 3-grabbing nonintegrin/CD209 is abundant on macrophages in the normal*

human lymph node and is not required for dendritic cell stimulation of the mixed leukocyte reaction. J Immunol, 2005. **175**(7): p. 4265-73.
129. de Witte, L., et al., *Langerin is a natural barrier to HIV-1 transmission by Langerhans cells.* Nat Med, 2007. **13**(3): p. 367-71.
130. de Witte, L., et al., *Syndecan-3 is a dendritic cell-specific attachment receptor for HIV-1.* Proc Natl Acad Sci U S A, 2007. **104**(49): p. 19464-9.
131. Wang, J.H., et al., *Functionally distinct transmission of human immunodeficiency virus type 1 mediated by immature and mature dendritic cells.* J Virol, 2007. **81**(17): p. 8933-43.
132. Wang, J.H., C. Kwas, and L. Wu, *Intercellular adhesion molecule 1 (ICAM-1), but not ICAM-2 and -3, is important for dendritic cell-mediated human immunodeficiency virus type 1 transmission.* J Virol, 2009. **83**(9): p. 4195-204.
133. Wiley, R.D. and S. Gummuluru, *Immature dendritic cell-derived exosomes can mediate HIV-1 trans infection.* Proc Natl Acad Sci U S A, 2006. **103**(3): p. 738-43.
134. Izquierdo-Useros, N., et al., *Capture and transfer of HIV-1 particles by mature dendritic cells converges with the exosome-dissemination pathway.* Blood, 2009. **113**(12): p. 2732-41.
135. Sowinski, S., et al., *Membrane nanotubes physically connect T cells over long distances presenting a novel route for HIV-1 transmission.* Nat Cell Biol, 2008. **10**(2): p. 211-9.
136. Quaranta, M.G., et al., *The immunoregulatory effects of HIV-1 Nef on dendritic cells and the pathogenesis of AIDS.* FASEB J, 2006. **20**(13): p. 2198-208.
137. Knight, S.C., *Bone-marrow-derived dendritic cells and the pathogenesis of AIDS.* AIDS, 1996. **10**(8): p. 807-17.
138. Donaghy, H., et al., *Loss of blood CD11c(+) myeloid and CD11c(-) plasmacytoid dendritic cells in patients with HIV-1 infection correlates with HIV-1 RNA virus load.* Blood, 2001. **98**(8): p. 2574-6.
139. Knight, S.C., W. Elsley, and H. Wang, *Mechanisms of loss of functional dendritic cells in HIV-1 infection.* J Leukoc Biol, 1997. **62**(1): p. 78-81.
140. Granelli-Piperno, A., et al., *HIV-1 selectively infects a subset of nonmaturing BDCA1-positive dendritic cells in human blood.* J Immunol, 2006. **176**(2): p. 991-8.
141. Donaghy, H., et al., *Dysfunction and infection of freshly isolated blood myeloid and plasmacytoid dendritic cells in patients infected with HIV-1.* Blood, 2003. **101**(11): p. 4505-11.
142. Granelli-Piperno, A., et al., *HIV-1-infected monocyte-derived dendritic cells do not undergo maturation but can elicit IL-10 production and T cell regulation.* Proc Natl Acad Sci U S A, 2004. **101**(20): p. 7669-74.
143. Lore, K., et al., *Accumulation of DC-SIGN+CD40+ dendritic cells with reduced CD80 and CD86 expression in lymphoid tissue during acute HIV-1 infection.* AIDS, 2002. **16**(5): p. 683-92.
144. Frankel, A.D. and J.A. Young, *HIV-1: fifteen proteins and an RNA.* Annu Rev Biochem, 1998. **67**: p. 1-25.
145. Arien, K.K. and B. Verhasselt, *HIV Nef: role in pathogenesis and viral fitness.* Curr HIV Res, 2008. **6**(3): p. 200-8.

146. Cheng-Mayer, C., et al., *Differential effects of nef on HIV replication: implications for viral pathogenesis in the host.* Science, 1989. **246**(4937): p. 1629-32.
147. Kestler, H.W., 3rd, et al., *Importance of the nef gene for maintenance of high virus loads and for development of AIDS.* Cell, 1991. **65**(4): p. 651-62.
148. Whatmore, A.M., et al., *Repair and evolution of nef in vivo modulates simian immunodeficiency virus virulence.* J Virol, 1995. **69**(8): p. 5117-23.
149. Daniel, M.D., et al., *Protective effects of a live attenuated SIV vaccine with a deletion in the nef gene.* Science, 1992. **258**(5090): p. 1938-41.
150. Whitney, J.B. and R.M. Ruprecht, *Live attenuated HIV vaccines: pitfalls and prospects.* Curr Opin Infect Dis, 2004. **17**(1): p. 17-26.
151. Baba, T.W., et al., *Pathogenicity of live, attenuated SIV after mucosal infection of neonatal macaques.* Science, 1995. **267**(5205): p. 1820-5.
152. Wyand, M.S., et al., *Resistance of neonatal monkeys to live attenuated vaccine strains of simian immunodeficiency virus.* Nat Med, 1997. **3**(1): p. 32-6.
153. Foster, J.L. and J.V. Garcia, *HIV-1 Nef: at the crossroads.* Retrovirology, 2008. **5**: p. 84.
154. Gorry, P.R., et al., *Pathogenicity and immunogenicity of attenuated, nef-deleted HIV-1 strains in vivo.* Retrovirology, 2007. **4**: p. 66.
155. Munch, J., et al., *Efficient class I major histocompatibility complex down-regulation by simian immunodeficiency virus Nef is associated with a strong selective advantage in infected rhesus macaques.* J Virol, 2001. **75**(21): p. 10532-6.
156. Roeth, J.F. and K.L. Collins, *Human immunodeficiency virus type 1 Nef: adapting to intracellular trafficking pathways.* Microbiol Mol Biol Rev, 2006. **70**(2): p. 548-63.
157. Collins, K.L., *How HIV evades CTL recognition.* Curr HIV Res, 2003. **1**(1): p. 31-40.
158. Glushakova, S., et al., *CD4 down-modulation by human immunodeficiency virus type 1 Nef correlates with the efficiency of viral replication and with CD4(+) T-cell depletion in human lymphoid tissue ex vivo.* J Virol, 2001. **75**(21): p. 10113-7.
159. Schwartz, O., et al., *Endocytosis of major histocompatibility complex class I molecules is induced by the HIV-1 Nef protein.* Nat Med, 1996. **2**(3): p. 338-42.
160. Laguette, N., et al., *Human immunodeficiency virus (HIV) type-1, HIV-2 and simian immunodeficiency virus Nef proteins.* Mol Aspects Med, 2010. **31**(5): p. 418-33.
161. Hung, C.H., et al., *HIV-1 Nef assembles a Src family kinase-ZAP-70/Syk-PI3K cascade to downregulate cell-surface MHC-I.* Cell Host Microbe, 2007. **1**(2): p. 121-33.
162. Blagoveshchenskaya, A.D., et al., *HIV-1 Nef downregulates MHC-I by a PACS-1- and PI3K-regulated ARF6 endocytic pathway.* Cell, 2002. **111**(6): p. 853-66.
163. Atkins, K.M., et al., *HIV-1 Nef binds PACS-2 to assemble a multikinase cascade that triggers major histocompatibility complex class I (MHC-I) down-regulation: analysis using short interfering RNA and knock-out mice.* J Biol Chem, 2008. **283**(17): p. 11772-84.

164. Noviello, C.M., S. Benichou, and J.C. Guatelli, *Cooperative binding of the class I major histocompatibility complex cytoplasmic domain and human immunodeficiency virus type 1 Nef to the endosomal AP-1 complex via its mu subunit.* J Virol, 2008. **82**(3): p. 1249-58.
165. Wonderlich, E.R., M. Williams, and K.L. Collins, *The tyrosine binding pocket in the adaptor protein 1 (AP-1) mu1 subunit is necessary for Nef to recruit AP-1 to the major histocompatibility complex class I cytoplasmic tail.* J Biol Chem, 2008. **283**(6): p. 3011-22.
166. Lubben, N.B., et al., *HIV-1 Nef-induced down-regulation of MHC class I requires AP-1 and clathrin but not PACS-1 and is impeded by AP-2.* Mol Biol Cell, 2007. **18**(9): p. 3351-65.
167. Larsen, J.E., et al., *HIV Nef-mediated major histocompatibility complex class I down-modulation is independent of Arf6 activity.* Mol Biol Cell, 2004. **15**(1): p. 323-31.
168. Stumptner-Cuvelette, P., et al., *HIV-1 Nef impairs MHC class II antigen presentation and surface expression.* Proc Natl Acad Sci U S A, 2001. **98**(21): p. 12144-9.
169. Mann, J., et al., *Functional analysis of HIV type 1 Nef reveals a role for PAK2 as a regulator of cell phenotype and function in the murine dendritic cell line, DC2.4.* J Immunol, 2005. **175**(10): p. 6560-9.
170. Chaudhry, A., et al., *HIV-1 Nef promotes endocytosis of cell surface MHC class II molecules via a constitutive pathway.* J Immunol, 2009. **183**(4): p. 2415-24.
171. Stumptner-Cuvelette, P., et al., *Human immunodeficiency virus-1 Nef expression induces intracellular accumulation of multivesicular bodies and major histocompatibility complex class II complexes: potential role of phosphatidylinositol 3-kinase.* Mol Biol Cell, 2003. **14**(12): p. 4857-70.
172. Takada, K. and S.C. Jameson, *Naive T cell homeostasis: from awareness of space to a sense of place.* Nat Rev Immunol, 2009. **9**(12): p. 823-32.
173. Boyman, O., et al., *Homeostatic proliferation and survival of naive and memory T cells.* Eur J Immunol, 2009. **39**(8): p. 2088-94.
174. Surh, C.D. and J. Sprent, *Homeostasis of naive and memory T cells.* Immunity, 2008. **29**(6): p. 848-62.
175. Love, P.E. and S.M. Hayes, *ITAM-mediated signaling by the T-cell antigen receptor.* Cold Spring Harb Perspect Biol, 2010. **2**(6): p. a002485.
176. Smith-Garvin, J.E., G.A. Koretzky, and M.S. Jordan, *T Cell Activation.* Annual Review of Immunology, 2009. **27**: p. 591-619.
177. Alarcon, B. and H.M. van Santen, *Two receptors, two kinases, and T cell lineage determination.* Sci Signal, 2010. **3**(114): p. pe11.
178. Underhill, D.M. and H.S. Goodridge, *The many faces of ITAMs.* Trends Immunol, 2007. **28**(2): p. 66-73.
179. Gascoigne, N.R., *Do T cells need endogenous peptides for activation?* Nat Rev Immunol, 2008. **8**(11): p. 895-900.
180. Salmond, R.J., et al., *T-cell receptor proximal signaling via the Src-family kinases, Lck and Fyn, influences T-cell activation, differentiation, and tolerance.* Immunol Rev, 2009. **228**(1): p. 9-22.

181. Minguet, S., et al., *Full activation of the T cell receptor requires both clustering and conformational changes at CD3.* Immunity, 2007. **26**(1): p. 43-54.
182. Krogsgaard, M., et al., *Agonist/endogenous peptide-MHC heterodimers drive T cell activation and sensitivity.* Nature, 2005. **434**(7030): p. 238-43.
183. Aivazian, D. and L.J. Stern, *Phosphorylation of T cell receptor zeta is regulated by a lipid dependent folding transition.* Nat Struct Biol, 2000. **7**(11): p. 1023-6.
184. Xu, C., et al., *Regulation of T cell receptor activation by dynamic membrane binding of the CD3epsilon cytoplasmic tyrosine-based motif.* Cell, 2008. **135**(4): p. 702-13.
185. Gil, D., et al., *Recruitment of Nck by CD3 epsilon reveals a ligand-induced conformational change essential for T cell receptor signaling and synapse formation.* Cell, 2002. **109**(7): p. 901-12.
186. Szymczak, A.L., et al., *The CD3epsilon proline-rich sequence, and its interaction with Nck, is not required for T cell development and function.* J Immunol, 2005. **175**(1): p. 270-5.
187. Andreotti, A.H., et al., *T-cell signaling regulated by the Tec family kinase, Itk.* Cold Spring Harb Perspect Biol, 2010. **2**(7): p. a002287.
188. Vig, M. and J.P. Kinet, *Calcium signaling in immune cells.* Nat Immunol, 2009. **10**(1): p. 21-7.
189. Oh-hora, M., *Calcium signaling in the development and function of T-lineage cells.* Immunol Rev, 2009. **231**(1): p. 210-24.
190. Kotturi, M.F., S.V. Hunt, and W.A. Jefferies, *Roles of CRAC and Cav-like channels in T cells: more than one gatekeeper?* Trends Pharmacol Sci, 2006. **27**(7): p. 360-7.
191. Feske, S., *Calcium signalling in lymphocyte activation and disease.* Nat Rev Immunol, 2007. **7**(9): p. 690-702.
192. Feske, S., *ORAI1 and STIM1 deficiency in human and mice: roles of store-operated Ca2+ entry in the immune system and beyond.* Immunol Rev, 2009. **231**(1): p. 189-209.
193. Stathopulos, P.B., L. Zheng, and M. Ikura, *Stromal interaction molecule (STIM) 1 and STIM2 calcium sensing regions exhibit distinct unfolding and oligomerization kinetics.* J Biol Chem, 2009. **284**(2): p. 728-32.
194. Park, C.Y., et al., *STIM1 clusters and activates CRAC channels via direct binding of a cytosolic domain to Orai1.* Cell, 2009. **136**(5): p. 876-90.
195. Liou, J., et al., *STIM is a Ca2+ sensor essential for Ca2+-store-depletion-triggered Ca2+ influx.* Curr Biol, 2005. **15**(13): p. 1235-41.
196. Wu, M.M., et al., *Ca2+ store depletion causes STIM1 to accumulate in ER regions closely associated with the plasma membrane.* J Cell Biol, 2006. **174**(6): p. 803-13.
197. Liou, J., et al., *Live-cell imaging reveals sequential oligomerization and local plasma membrane targeting of stromal interaction molecule 1 after Ca2+ store depletion.* Proc Natl Acad Sci U S A, 2007. **104**(22): p. 9301-6.
198. Xu, P., et al., *Aggregation of STIM1 underneath the plasma membrane induces clustering of Orai1.* Biochem Biophys Res Commun, 2006. **350**(4): p. 969-76.

199. Luik, R.M., et al., *The elementary unit of store-operated Ca2+ entry: local activation of CRAC channels by STIM1 at ER-plasma membrane junctions.* J Cell Biol, 2006. **174**(6): p. 815-25.
200. Penna, A., et al., *The CRAC channel consists of a tetramer formed by Stim-induced dimerization of Orai dimers.* Nature, 2008. **456**(7218): p. 116-20.
201. Feske, S., et al., *A mutation in Orai1 causes immune deficiency by abrogating CRAC channel function.* Nature, 2006. **441**(7090): p. 179-85.
202. Feske, S., et al., *A severe defect in CRAC Ca2+ channel activation and altered K+ channel gating in T cells from immunodeficient patients.* J Exp Med, 2005. **202**(5): p. 651-62.
203. Le Deist, F., et al., *A primary T-cell immunodeficiency associated with defective transmembrane calcium influx.* Blood, 1995. **85**(4): p. 1053-62.
204. Partiseti, M., et al., *The calcium current activated by T cell receptor and store depletion in human lymphocytes is absent in a primary immunodeficiency.* J Biol Chem, 1994. **269**(51): p. 32327-35.
205. Feske, S., et al., *Severe combined immunodeficiency due to defective binding of the nuclear factor of activated T cells in T lymphocytes of two male siblings.* Eur J Immunol, 1996. **26**(9): p. 2119-26.
206. Picard, C., et al., *STIM1 mutation associated with a syndrome of immunodeficiency and autoimmunity.* N Engl J Med, 2009. **360**(19): p. 1971-80.
207. Vig, M., et al., *Defective mast cell effector functions in mice lacking the CRACM1 pore subunit of store-operated calcium release-activated calcium channels.* Nat Immunol, 2008. **9**(1): p. 89-96.
208. Stiber, J., et al., *STIM1 signalling controls store-operated calcium entry required for development and contractile function in skeletal muscle.* Nat Cell Biol, 2008. **10**(6): p. 688-97.
209. Gwack, Y., et al., *Hair loss and defective T- and B-cell function in mice lacking ORAI1.* Mol Cell Biol, 2008. **28**(17): p. 5209-22.
210. Varga-Szabo, D., et al., *The calcium sensor STIM1 is an essential mediator of arterial thrombosis and ischemic brain infarction.* J Exp Med, 2008. **205**(7): p. 1583-91.
211. Braun, A., et al., *Orai1 (CRACM1) is the platelet SOC channel and essential for pathological thrombus formation.* Blood, 2009. **113**(9): p. 2056-63.
212. Oh-Hora, M., et al., *Dual functions for the endoplasmic reticulum calcium sensors STIM1 and STIM2 in T cell activation and tolerance.* Nat Immunol, 2008. **9**(4): p. 432-43.
213. Tone, Y., et al., *Smad3 and NFAT cooperate to induce Foxp3 expression through its enhancer.* Nat Immunol, 2008. **9**(2): p. 194-202.
214. Wu, Y., et al., *FOXP3 controls regulatory T cell function through cooperation with NFAT.* Cell, 2006. **126**(2): p. 375-87.
215. Flockerzi, V., *An introduction on TRP channels.* Handb Exp Pharmacol, 2007(179): p. 1-19.
216. Schwarz, E.C., et al., *TRP channels in lymphocytes.* Handb Exp Pharmacol, 2007(179): p. 445-56.
217. Cui, J., et al., *CaT1 contributes to the stores-operated calcium current in Jurkat T-lymphocytes.* J Biol Chem, 2002. **277**(49): p. 47175-83.

218. Bodding, M., U. Wissenbach, and V. Flockerzi, *The recombinant human TRPV6 channel functions as Ca2+ sensor in human embryonic kidney and rat basophilic leukemia cells.* J Biol Chem, 2002. **277**(39): p. 36656-64.
219. Voets, T., et al., *CaT1 and the calcium release-activated calcium channel manifest distinct pore properties.* J Biol Chem, 2001. **276**(51): p. 47767-70.
220. He, L.P., et al., *A functional link between store-operated and TRPC channels revealed by the 3,5-bis(trifluoromethyl)pyrazole derivative, BTP2.* J Biol Chem, 2005. **280**(12): p. 10997-1006.
221. Schwarz, E.C., et al., *TRPV6 potentiates calcium-dependent cell proliferation.* Cell calcium, 2006. **39**(2): p. 163-73.
222. Fanger, C.M., et al., *Characterization of T cell mutants with defects in capacitative calcium entry: genetic evidence for the physiological roles of CRAC channels.* J Cell Biol, 1995. **131**(3): p. 655-67.
223. Philipp, S., et al., *TRPC3 mediates T-cell receptor-dependent calcium entry in human T-lymphocytes.* J Biol Chem, 2003. **278**(29): p. 26629-38.
224. Vazquez, G., et al., *Human Trp3 forms both inositol trisphosphate receptor-dependent and receptor-independent store-operated cation channels in DT40 avian B lymphocytes.* Proc Natl Acad Sci U S A, 2001. **98**(20): p. 11777-82.
225. Hofmann, T., et al., *Direct activation of human TRPC6 and TRPC3 channels by diacylglycerol.* Nature, 1999. **397**(6716): p. 259-63.
226. Perraud, A.L., et al., *ADP-ribose gating of the calcium-permeable LTRPC2 channel revealed by Nudix motif homology.* Nature, 2001. **411**(6837): p. 595-9.
227. Hara, Y., et al., *LTRPC2 Ca2+-permeable channel activated by changes in redox status confers susceptibility to cell death.* Mol Cell, 2002. **9**(1): p. 163-73.
228. Massullo, P., et al., *TRPM channels, calcium and redox sensors during innate immune responses.* Semin Cell Dev Biol, 2006. **17**(6): p. 654-66.
229. Gasser, A., et al., *Activation of T cell calcium influx by the second messenger ADP-ribose.* J Biol Chem, 2006. **281**(5): p. 2489-96.
230. Wehage, E., et al., *Activation of the cation channel long transient receptor potential channel 2 (LTRPC2) by hydrogen peroxide. A splice variant reveals a mode of activation independent of ADP-ribose.* J Biol Chem, 2002. **277**(26): p. 23150-6.
231. Khan, A.A., et al., *IP3 receptor: localization to plasma membrane of T cells and cocapping with the T cell receptor.* Science, 1992. **257**(5071): p. 815-8.
232. Berridge, M.J., *Inositol trisphosphate and calcium signalling.* Nature, 1993. **361**(6410): p. 315-25.
233. Tanimura, A., Y. Tojyo, and R.J. Turner, *Evidence that type I, II, and III inositol 1,4,5-trisphosphate receptors can occur as integral plasma membrane proteins.* J Biol Chem, 2000. **275**(35): p. 27488-93.
234. Zweifach, A. and R.S. Lewis, *Mitogen-regulated Ca2+ current of T lymphocytes is activated by depletion of intracellular Ca2+ stores.* Proc Natl Acad Sci U S A, 1993. **90**(13): p. 6295-9.
235. Patterson, R.L., D. Boehning, and S.H. Snyder, *Inositol 1,4,5-trisphosphate receptors as signal integrators.* Annu Rev Biochem, 2004. **73**: p. 437-65.
236. North, R.A., *Molecular physiology of P2X receptors.* Physiol Rev, 2002. **82**(4): p. 1013-67.

237. Yip, L., et al., *Autocrine regulation of T-cell activation by ATP release and P2X7 receptors.* FASEB J, 2009. **23**(6): p. 1685-93.
238. Solle, M., et al., *Altered cytokine production in mice lacking P2X(7) receptors.* J Biol Chem, 2001. **276**(1): p. 125-32.
239. Buraei, Z. and J. Yang, *The ss subunit of voltage-gated Ca2+ channels.* Physiol Rev, 2010. **90**(4): p. 1461-506.
240. Kotturi, M.F., et al., *Identification and functional characterization of voltage-dependent calcium channels in T lymphocytes.* J Biol Chem, 2003. **278**(47): p. 46949-60.
241. Kotturi, M.F. and W.A. Jefferies, *Molecular characterization of L-type calcium channel splice variants expressed in human T lymphocytes.* Mol Immunol, 2005. **42**(12): p. 1461-74.
242. Savignac, M., et al., *Protein kinase C-mediated calcium entry dependent upon dihydropyridine sensitive channels: a T cell receptor-coupled signaling pathway involved in IL-4 synthesis.* Faseb J, 2001. **15**(9): p. 1577-9.
243. Savignac, M., et al., *Dihydropyridine receptors are selective markers of Th2 cells and can be targeted to prevent Th2-dependent immunopathological disorders.* J Immunol, 2004. **172**(9): p. 5206-12.
244. Stokes, L., J. Gordon, and G. Grafton, *Non-voltage-gated L-type Ca2+ channels in human T cells: pharmacology and molecular characterization of the major alpha pore-forming and auxiliary beta-subunits.* J Biol Chem, 2004. **279**(19): p. 19566-73.
245. Badou, A., et al., *HgCl2-induced interleukin-4 gene expression in T cells involves a protein kinase C-dependent calcium influx through L-type calcium channels.* J Biol Chem, 1997. **272**(51): p. 32411-8.
246. Lacinova, L., *Voltage-dependent calcium channels.* Gen Physiol Biophys, 2005. **24 Suppl 1**: p. 1-78.
247. Fisher, S.E., et al., *Sequence-based exon prediction around the synaptophysin locus reveals a gene-rich area containing novel genes in human proximal Xp.* Genomics, 1997. **45**(2): p. 340-7.
248. Brereton, H.M., et al., *Novel variants of voltage-operated calcium channel alpha 1-subunit transcripts in a rat liver-derived cell line: deletion in the IVS4 voltage sensing region.* Cell Calcium, 1997. **22**(1): p. 39-52.
249. Jha, M.K., et al., *Defective survival of naive CD8+ T lymphocytes in the absence of the beta3 regulatory subunit of voltage-gated calcium channels.* Nat Immunol, 2009. **10**(12): p. 1275-82.
250. Badou, A., et al., *Critical role for the beta regulatory subunits of Cav channels in T lymphocyte function.* Proc Natl Acad Sci U S A, 2006. **103**(42): p. 15529-34.
251. McRory, J.E., et al., *The CACNA1F gene encodes an L-type calcium channel with unique biophysical properties and tissue distribution.* J Neurosci, 2004. **24**(7): p. 1707-18.
252. Gomes, B., et al., *The cGMP/protein kinase G pathway contributes to dihydropyridine-sensitive calcium response and cytokine production in TH2 lymphocytes.* J Biol Chem, 2006. **281**(18): p. 12421-7.
253. Strom, T.M., et al., *An L-type calcium-channel gene mutated in incomplete X-linked congenital stationary night blindness.* Nat Genet, 1998. **19**(3): p. 260-3.

254. Suzuki, Y., T. Inoue, and C. Ra, *L-type Ca2+ channels: a new player in the regulation of Ca2+ signaling, cell activation and cell survival in immune cells.* Mol Immunol, 2010. **47**(4): p. 640-8.
255. Dupuis, G., et al., *Effects of modulators of cytosolic Ca2+ on phytohemagglutin-dependent Ca2+ response and interleukin-2 production in Jurkat cells.* J Leukoc Biol, 1993. **53**(1): p. 66-72.
256. Jurkat-Rott, K. and F. Lehmann-Horn, *The impact of splice isoforms on voltage-gated calcium channel alpha1 subunits.* J Physiol, 2004. **554**(Pt 3): p. 609-19.
257. Bezanilla, F., *Voltage sensor movements.* J Gen Physiol, 2002. **120**(4): p. 465-73.
258. Suzuki, Y., et al., *Ca(v)1.2 L-type Ca2+ channel protects mast cells against activation-induced cell death by preventing mitochondrial integrity disruption.* Molecular Immunology, 2009. **46**(11-12): p. 2370-2380.
259. Savignac, M., B. Mellstrom, and J.R. Naranjo, *Calcium-dependent transcription of cytokine genes in T lymphocytes.* Pflugers Arch, 2007. **454**(4): p. 523-33.
260. Oh-hora, M. and A. Rao, *Calcium signaling in lymphocytes.* Curr Opin Immunol, 2008. **20**(3): p. 250-8.
261. Okamura, H., et al., *Concerted dephosphorylation of the transcription factor NFAT1 induces a conformational switch that regulates transcriptional activity.* Mol Cell, 2000. **6**(3): p. 539-50.
262. Okamura, H., et al., *A conserved docking motif for CK1 binding controls the nuclear localization of NFAT1.* Mol Cell Biol, 2004. **24**(10): p. 4184-95.
263. Gwack, Y., et al., *A genome-wide Drosophila RNAi screen identifies DYRK-family kinases as regulators of NFAT.* Nature, 2006. **441**(7093): p. 646-50.
264. Feske, S., et al., *Gene regulation mediated by calcium signals in T lymphocytes.* Nat Immunol, 2001. **2**(4): p. 316-24.
265. Cristillo, A.D. and B.E. Bierer, *Identification of novel targets of immunosuppressive agents by cDNA-based microarray analysis.* J Biol Chem, 2002. **277**(6): p. 4465-76.
266. Diehn, M., et al., *Genomic expression programs and the integration of the CD28 costimulatory signal in T cell activation.* Proc Natl Acad Sci U S A, 2002. **99**(18): p. 11796-801.
267. Liu, J.O., *Calmodulin-dependent phosphatase, kinases, and transcriptional corepressors involved in T-cell activation.* Immunol Rev, 2009. **228**(1): p. 184-98.
268. Nghiem, P., et al., *Interleukin-2 transcriptional block by multifunctional Ca2+/calmodulin kinase.* Nature, 1994. **371**(6495): p. 347-50.
269. Ho, N., M. Gullberg, and T. Chatila, *Activation protein 1-dependent transcriptional activation of interleukin 2 gene by Ca2+/calmodulin kinase type IV/Gr.* J Exp Med, 1996. **184**(1): p. 101-12.
270. Youn, H.D. and J.O. Liu, *Cabin1 represses MEF2-dependent Nur77 expression and T cell apoptosis by controlling association of histone deacetylases and acetylases with MEF2.* Immunity, 2000. **13**(1): p. 85-94.
271. Jang, H., et al., *Cabin1 represses MEF2 transcriptional activity by association with a methyltransferase, SUV39H1.* J Biol Chem, 2007. **282**(15): p. 11172-9.
272. Youn, H.D., et al., *Apoptosis of T cells mediated by Ca2+-induced release of the transcription factor MEF2.* Science, 1999. **286**(5440): p. 790-3.

273. Youn, H.D., C.M. Grozinger, and J.O. Liu, *Calcium regulates transcriptional repression of myocyte enhancer factor 2 by histone deacetylase 4.* J Biol Chem, 2000. **275**(29): p. 22563-7.
274. Lu, J., et al., *Regulation of skeletal myogenesis by association of the MEF2 transcription factor with class II histone deacetylases.* Mol Cell, 2000. **6**(2): p. 233-44.
275. Feske, S., et al., *Ca2+/calcineurin signalling in cells of the immune system.* Biochem Biophys Res Commun, 2003. **311**(4): p. 1117-32.
276. Mattila, P.S., et al., *The actions of cyclosporin A and FK506 suggest a novel step in the activation of T lymphocytes.* EMBO J, 1990. **9**(13): p. 4425-33.
277. Frantz, B., et al., *Calcineurin acts in synergy with PMA to inactivate I kappa B/MAD3, an inhibitor of NF-kappa B.* EMBO J, 1994. **13**(4): p. 861-70.
278. Steffan, N.M., et al., *Regulation of IkB alpha phosphorylation by PKC- and Ca(2+)-dependent signal transduction pathways.* J Immunol, 1995. **155**(10): p. 4685-91.
279. Trushin, S.A., et al., *Protein kinase C and calcineurin synergize to activate IkappaB kinase and NF-kappaB in T lymphocytes.* J Biol Chem, 1999. **274**(33): p. 22923-31.
280. Kanno, T. and U. Siebenlist, *Activation of nuclear factor-kappaB via T cell receptor requires a Raf kinase and Ca2+ influx. Functional synergy between Raf and calcineurin.* J Immunol, 1996. **157**(12): p. 5277-83.
281. Biswas, G., et al., *Mitochondria to nucleus stress signaling: a distinctive mechanism of NFkappaB/Rel activation through calcineurin-mediated inactivation of IkappaBbeta.* J Cell Biol, 2003. **161**(3): p. 507-19.
282. Huang, Y.H. and K. Sauer, *Lipid signaling in T-cell development and function.* Cold Spring Harb Perspect Biol, 2010. **2**(11): p. a002428.
283. Roose, J.P., et al., *Unusual interplay of two types of Ras activators, RasGRP and SOS, establishes sensitive and robust Ras activation in lymphocytes.* Mol Cell Biol, 2007. **27**(7): p. 2732-45.
284. Genot, E. and D.A. Cantrell, *Ras regulation and function in lymphocytes.* Curr Opin Immunol, 2000. **12**(3): p. 289-94.
285. Cullen, P.J. and P.J. Lockyer, *Integration of calcium and Ras signalling.* Nat Rev Mol Cell Biol, 2002. **3**(5): p. 339-48.
286. Teixeiro, E. and M.A. Daniels, *ERK and cell death: ERK location and T cell selection.* FEBS J, 2010. **277**(1): p. 30-8.
287. Starr, T.K., S.C. Jameson, and K.A. Hogquist, *Positive and negative selection of T cells.* Annu Rev Immunol, 2003. **21**: p. 139-76.
288. Seddon, B. and R. Zamoyska, *TCR signals mediated by Src family kinases are essential for the survival of naive T cells.* J Immunol, 2002. **169**(6): p. 2997-3005.
289. Vivien, L., C. Benoist, and D. Mathis, *T lymphocytes need IL-7 but not IL-4 or IL-6 to survive in vivo.* Int Immunol, 2001. **13**(6): p. 763-8.
290. Kondrack, R.M., et al., *Interleukin 7 regulates the survival and generation of memory CD4 cells.* J Exp Med, 2003. **198**(12): p. 1797-806.
291. Tan, J.T., et al., *IL-7 is critical for homeostatic proliferation and survival of naive T cells.* Proc Natl Acad Sci U S A, 2001. **98**(15): p. 8732-7.

292. Mertsching, E., C. Burdet, and R. Ceredig, *IL-7 transgenic mice: analysis of the role of IL-7 in the differentiation of thymocytes in vivo and in vitro.* Int Immunol, 1995. **7**(3): p. 401-14.
293. Kieper, W.C., et al., *Overexpression of interleukin (IL)-7 leads to IL-15-independent generation of memory phenotype CD8+ T cells.* J Exp Med, 2002. **195**(12): p. 1533-9.
294. Roeth, J.F., et al., *HIV-1 Nef disrupts MHC-I trafficking by recruiting AP-1 to the MHC-I cytoplasmic tail.* J Cell Biol, 2004. **167**(5): p. 903-13.
295. Shen, Z., et al., *Cloned dendritic cells can present exogenous antigens on both MHC class I and class II molecules.* J Immunol, 1997. **158**(6): p. 2723-30.
296. Shastri, N. and F. Gonzalez, *Endogenous generation and presentation of the ovalbumin peptide/Kb complex to T cells.* J Immunol, 1993. **150**(7): p. 2724-36.
297. Ahmad, N. and S. Venkatesan, *Nef protein of HIV-1 is a transcriptional repressor of HIV-1 LTR.* Science, 1988. **241**(4872): p. 1481-5.
298. Neefjes, J.J., et al., *The fate of the three subunits of major histocompatibility complex class I molecules.* Eur J Immunol, 1992. **22**(6): p. 1609-14.
299. Porgador, A., et al., *Localization, quantitation, and in situ detection of specific peptide-MHC class I complexes using a monoclonal antibody.* Immunity, 1997. **6**(6): p. 715-26.
300. Priatel, J.J., et al., *RasGRP1 transmits prodifferentiation TCR signaling that is crucial for CD4 T cell development.* J Immunol, 2006. **177**(3): p. 1470-80.
301. Priatel, J.J., et al., *RasGRP1 transduces low-grade TCR signals which are critical for T cell development, homeostasis, and differentiation.* Immunity, 2002. **17**(5): p. 617-27.
302. David, M.D., et al., *Pure lipopolysaccharide or synthetic lipid A induces activation of p21Ras in primary macrophages through a pathway dependent on Src family kinases and PI3K.* J Immunol, 2005. **175**(12): p. 8236-41.
303. Lelouard, H., et al., *Regulation of translation is required for dendritic cell function and survival during activation.* J Cell Biol, 2007. **179**(7): p. 1427-39.
304. Liu, K.Q., et al., *T cell receptor-initiated calcium release is uncoupled from capacitative calcium entry in Itk-deficient T cells.* J Exp Med, 1998. **187**(10): p. 1721-7.
305. Mansergh, F., et al., *Mutation of the calcium channel gene Cacna1f disrupts calcium signaling, synaptic transmission and cellular organization in mouse retina.* Hum Mol Genet, 2005. **14**(20): p. 3035-46.
306. Sawada, S., et al., *A lineage-specific transcriptional silencer regulates CD4 gene expression during T lymphocyte development.* Cell, 1994. **77**(6): p. 917-29.
307. Rashid, A., H. Auchincloss, Jr., and J. Sharon, *Comparison of GK1.5 and chimeric rat/mouse GK1.5 anti-CD4 antibodies for prolongation of skin allograft survival and suppression of alloantibody production in mice.* J Immunol, 1992. **148**(5): p. 1382-8.
308. Karasuyama, H., A. Kudo, and F. Melchers, *The proteins encoded by the VpreB and lambda 5 pre-B cell-specific genes can associate with each other and with mu heavy chain.* J Exp Med, 1990. **172**(3): p. 969-72.

309. Shen, H., et al., *Recombinant Listeria monocytogenes as a live vaccine vehicle for the induction of protective anti-viral cell-mediated immunity.* Proc Natl Acad Sci U S A, 1995. **92**(9): p. 3987-91.
310. Pope, C., et al., *Organ-specific regulation of the CD8 T cell response to Listeria monocytogenes infection.* J Immunol, 2001. **166**(5): p. 3402-9.
311. Sun, J.C. and M.J. Bevan, *Defective CD8 T cell memory following acute infection without CD4 T cell help.* Science, 2003. **300**(5617): p. 339-42.
312. Priatel, J.J., et al., *Chronic immunodeficiency in mice lacking RasGRP1 results in CD4 T cell immune activation and exhaustion.* J Immunol, 2007. **179**(4): p. 2143-52.
313. Betts, M.R., et al., *Sensitive and viable identification of antigen-specific CD8+ T cells by a flow cytometric assay for degranulation.* J Immunol Methods, 2003. **281**(1-2): p. 65-78.
314. Guagliardi, L.E., et al., *Co-localization of molecules involved in antigen processing and presentation in an early endocytic compartment.* Nature, 1990. **343**(6254): p. 133-9.
315. Chiu, I., D.M. Davis, and J.L. Strominger, *Trafficking of spontaneously endocytosed MHC proteins.* Proc Natl Acad Sci U S A, 1999. **96**(24): p. 13944-9.
316. Reid, P.A. and C. Watts, *Cycling of cell-surface MHC glycoproteins through primaquine-sensitive intracellular compartments.* Nature, 1990. **346**(6285): p. 655-7.
317. Bakke, O. and B. Dobberstein, *MHC class II-associated invariant chain contains a sorting signal for endosomal compartments.* Cell, 1990. **63**(4): p. 707-16.
318. Kleijmeer, M.J., et al., *Antigen loading of MHC class I molecules in the endocytic tract.* Traffic, 2001. **2**(2): p. 124-37.
319. Tourne, S., et al., *Biosynthesis of major histocompatibility complex molecules and generation of T cells in Ii TAP1 double-mutant mice.* Proc Natl Acad Sci U S A, 1996. **93**(4): p. 1464-9.
320. Reber, A.J., et al., *Expression of invariant chain can cause an allele-dependent increase in the surface expression of MHC class I molecules.* Immunogenetics, 2002. **54**(2): p. 74-81.
321. Vitalis, T.Z., et al., *Using the TAP component of the antigen-processing machinery as a molecular adjuvant.* PLoS Pathog, 2005. **1**(4): p. e36.
322. McAdam, A.J., et al., *B7 costimulation is critical for antibody class switching and CD8(+) cytotoxic T-lymphocyte generation in the host response to vesicular stomatitis virus.* J Virol, 2000. **74**(1): p. 203-8.
323. Marzo, A.L., et al., *Fully functional memory CD8 T cells in the absence of CD4 T cells.* J Immunol, 2004. **173**(2): p. 969-75.
324. Imarai, M., et al., *Diversity of T cell receptors specific for the VSV antigenic peptide (N52-59) bound by the H-2Kb class I molecule.* Cell Immunol, 1995. **162**(2): p. 340.
325. den Haan, J.M., S.M. Lehar, and M.J. Bevan, *CD8(+) but not CD8(-) dendritic cells cross-prime cytotoxic T cells in vivo.* J Exp Med, 2000. **192**(12): p. 1685-96.
326. Huang, A.Y., et al., *In vivo cross-priming of MHC class I-restricted antigens requires the TAP transporter.* Immunity, 1996. **4**(4): p. 349-55.

327. Faure-Andre, G., et al., *Regulation of dendritic cell migration by CD74, the MHC class II-associated invariant chain.* Science, 2008. **322**(5908): p. 1705-10.
328. Sallusto, F., et al., *Dendritic cells use macropinocytosis and the mannose receptor to concentrate macromolecules in the major histocompatibility complex class II compartment: downregulation by cytokines and bacterial products.* J Exp Med, 1995. **182**(2): p. 389-400.
329. Brossart, P. and M.J. Bevan, *Presentation of exogenous protein antigens on major histocompatibility complex class I molecules by dendritic cells: pathway of presentation and regulation by cytokines.* Blood, 1997. **90**(4): p. 1594-9.
330. MacAry, P.A., et al., *Mobilization of MHC class I molecules from late endosomes to the cell surface following activation of CD34-derived human Langerhans cells.* Proc Natl Acad Sci U S A, 2001. **98**(7): p. 3982-7.
331. Kornfeld, R. and S. Kornfeld, *Assembly of asparagine-linked oligosaccharides.* Annu Rev Biochem, 1985. **54**: p. 631-64.
332. Rock, K.L., S. Gamble, and L. Rothstein, *Presentation of exogenous antigen with class I major histocompatibility complex molecules.* Science, 1990. **249**(4971): p. 918-21.
333. van Lith, M., M. van Ham, and J. Neefjes, *Stable expression of MHC class I heavy chain/HLA-DO complexes at the plasma membrane.* Eur J Immunol, 2003. **33**(5): p. 1145-51.
334. Nuchtern, J.G., W.E. Biddison, and R.D. Klausner, *Class II MHC molecules can use the endogenous pathway of antigen presentation.* Nature, 1990. **343**(6253): p. 74-6.
335. Malnati, M.S., et al., *Processing pathways for presentation of cytosolic antigen to MHC class II-restricted T cells.* Nature, 1992. **357**(6380): p. 702-4.
336. Cerundolo, V., et al., *Association of the human invariant chain with H-2 Db class I molecules.* Eur J Immunol, 1992. **22**(9): p. 2243-8.
337. Powis, S.J., *CLIP-region mediated interaction of Invariant chain with MHC class I molecules.* FEBS Lett, 2006. **580**(13): p. 3112-6.
338. Sigal, L., et al., *Cytotoxic T-cell immunity to virus-infected non-haematopoietic cells requires presentation of exogenous antigen.* Nature, 1999. **398**(6722): p. 77-80.
339. Sigal, L.J. and K.L. Rock, *Bone marrow-derived antigen-presenting cells are required for the generation of cytotoxic T lymphocyte responses to viruses and use transporter associated with antigen presentation (TAP)-dependent and -independent pathways of antigen presentation.* J Exp Med, 2000. **192**(8): p. 1143-50.
340. Buller, R.M., et al., *Induction of cytotoxic T-cell responses in vivo in the absence of CD4 helper cells.* Nature, 1987. **328**(6125): p. 77-9.
341. Janssen, E.M., et al., *CD4+ T cells are required for secondary expansion and memory in CD8+ T lymphocytes.* Nature, 2003. **421**(6925): p. 852-6.
342. Rock, K.L. and K. Clark, *Analysis of the role of MHC class II presentation in the stimulation of cytotoxic T lymphocytes by antigens targeted into the exogenous antigen-MHC class I presentation pathway.* J Immunol, 1996. **156**(10): p. 3721-6.
343. Mintern, J.D., et al., *Cutting edge: precursor frequency affects the helper dependence of cytotoxic T cells.* J Immunol, 2002. **168**(3): p. 977-80.

344. Machold, R.P. and H.L. Ploegh, *Intermediates in the assembly and degradation of class I major histocompatibility complex (MHC) molecules probed with free heavy chain-specific monoclonal antibodies.* J Exp Med, 1996. **184**(6): p. 2251-9.
345. Luckey, C.J., et al., *Differences in the expression of human class I MHC alleles and their associated peptides in the presence of proteasome inhibitors.* J Immunol, 2001. **167**(3): p. 1212-21.
346. Kruger, T., et al., *Lessons to be learned from primary renal cell carcinomas: novel tumor antigens and HLA ligands for immunotherapy.* Cancer Immunol Immunother, 2005. **54**(9): p. 826-36.
347. Busch, R., et al., *Invariant chain protects class II histocompatibility antigens from binding intact polypeptides in the endoplasmic reticulum.* EMBO J, 1996. **15**(2): p. 418-28.
348. Friedrich, T.C., et al., *Subdominant CD8+ T-cell responses are involved in durable control of AIDS virus replication.* J Virol, 2007. **81**(7): p. 3465-76.
349. Pereyra, F., et al., *Persistent low-level viremia in HIV-1 elite controllers and relationship to immunologic parameters.* J Infect Dis, 2009. **200**(6): p. 984-90.
350. Sajadi, M.M., et al., *Epidemiologic characteristics and natural history of HIV-1 natural viral suppressors.* J Acquir Immune Defic Syndr, 2009. **50**(4): p. 403-8.
351. Streeck, H., et al., *Antigen load and viral sequence diversification determine the functional profile of HIV-1-specific CD8+ T cells.* PLoS Med, 2008. **5**(5): p. e100.
352. Almeida, J.R., et al., *Superior control of HIV-1 replication by CD8+ T cells is reflected by their avidity, polyfunctionality, and clonal turnover.* J Exp Med, 2007. **204**(10): p. 2473-85.
353. Betts, M.R., et al., *HIV nonprogressors preferentially maintain highly functional HIV-specific CD8+ T cells.* Blood, 2006. **107**(12): p. 4781-9.
354. Cohen, G.B., et al., *The selective downregulation of class I major histocompatibility complex proteins by HIV-1 protects HIV-infected cells from NK cells.* Immunity, 1999. **10**(6): p. 661-71.
355. Nou, E., et al., *Effective downregulation of HLA-A*2 and HLA-B*57 by primary human immunodeficiency virus type 1 isolates cultured from elite suppressors.* J Virol, 2009. **83**(13): p. 6941-6.
356. Collins, K.L., et al., *HIV-1 Nef protein protects infected primary cells against killing by cytotoxic T lymphocytes.* Nature, 1998. **391**(6665): p. 397-401.
357. Yang, O.O., et al., *Nef-mediated resistance of human immunodeficiency virus type 1 to antiviral cytotoxic T lymphocytes.* J Virol, 2002. **76**(4): p. 1626-31.
358. Geyer, M., O.T. Fackler, and B.M. Peterlin, *Structure--function relationships in HIV-1 Nef.* EMBO Rep, 2001. **2**(7): p. 580-5.
359. Arold, S.T. and A.S. Baur, *Dynamic Nef and Nef dynamics: how structure could explain the complex activities of this small HIV protein.* Trends Biochem Sci, 2001. **26**(6): p. 356-63.
360. van Kooyk, Y. and T.B. Geijtenbeek, *DC-SIGN: Escape Mechanism for Pathogens.* Nature Reviews Immunology, 2003. **3**: p. 697-709.
361. Chougnet, C.A., et al., *Contribution of prostaglandin E2 to the interleukin-12 defect in HIV-infected patients.* AIDS, 1996. **10**(9): p. 1043-5.

362. Chehimi, J., et al., *Impaired interleukin 12 production in human immunodeficiency virus-infected patients.* J Exp Med, 1994. **179**(4): p. 1361-6.
363. Macatonia, S.E., et al., *Dendritic cell infection, depletion and dysfunction in HIV-infected individuals.* Immunology, 1990. **71**(1): p. 38-45.
364. Knight, S.C., S. Patterson, and S.E. Macatonia, *Stimulatory and suppressive effects of infection of dendritic cells with HIV-1.* Immunol Lett, 1991. **30**(2): p. 213-8.
365. Hanna, Z., et al., *Distinct regulatory elements are required for faithful expression of human CD4 in T cells, macrophages, and dendritic cells of transgenic mice.* Blood, 2001. **98**(7): p. 2275-8.
366. Andrieu, M., et al., *Downregulation of major Histocompatibility Class I on Human Dendritic Cells by HIV Nef Impairs Antigen Presentation to HIV-Specific CD8+ T Lymphocytes.* AIDS Research and Human Retroviruses, 2001. **17**(14): p. 1365-1370.
367. Shinya, E., et al., *Endogenously expressed HIV-1 nef down-regulates antigen-presenting molecules, not only class I MHC but also CD1a, in immature dendritic cells.* Virology, 2004. **326**(1): p. 79-89.
368. Quaranta, M.G., et al., *Immunoregulatory effects of HIV-1 Nef protein.* Biofactors, 2009. **35**(2): p. 169-74.
369. Mellman, I. and R.M. Steinman, *Dendritic cells: specialized and regulated antigen processing machines.* Cell, 2001. **106**(3): p. 255-8.
370. He, T., et al., *Interferon gamma stimulates cellular maturation of dendritic cell line DC2.4 leading to induction of efficient cytotoxic T cell responses and antitumor immunity.* Cell Mol Immunol, 2007. **4**(2): p. 105-11.
371. Obrig, T.G., et al., *The mechanism by which cycloheximide and related glutarimide antibiotics inhibit peptide synthesis on reticulocyte ribosomes.* J Biol Chem, 1971. **246**(1): p. 174-81.
372. Hansen, T.H. and M. Bouvier, *MHC class I antigen presentation: learning from viral evasion strategies.* Nat Rev Immunol, 2009. **9**(7): p. 503-13.
373. Chaudhry, A., et al., *The Nef protein of HIV-1 induces loss of cell surface costimulatory molecules CD80 and CD86 in APCs.* J Immunol, 2005. **175**(7): p. 4566-74.
374. Shen, X., et al., *Direct priming and cross-priming contribute differentially to the induction of CD8+ CTL following exposure to vaccinia virus via different routes.* J Immunol, 2002. **169**(8): p. 4222-9.
375. Akakura, S., et al., *The opsonin MFG-E8 is a ligand for the alphavbeta5 integrin and triggers DOCK180-dependent Rac1 activation for the phagocytosis of apoptotic cells.* Exp Cell Res, 2004. **292**(2): p. 403-16.
376. Chaudhry, A., et al., *A two-pronged mechanism for HIV-1 Nef-mediated endocytosis of immune costimulatory molecules CD80 and CD86.* Cell Host Microbe, 2007. **1**(1): p. 37-49.
377. Chaudhry, A., et al., *HIV-1 Nef induces a Rab11-dependent routing of endocytosed immune costimulatory proteins CD80 and CD86 to the Golgi.* Traffic, 2008. **9**(11): p. 1925-35.

378. Linstedt, A.D. and H.P. Hauri, *Giantin, a novel conserved Golgi membrane protein containing a cytoplasmic domain of at least 350 kDa.* Mol Biol Cell, 1993. **4**(7): p. 679-93.
379. Thomas, G., *Furin at the cutting edge: from protein traffic to embryogenesis and disease.* Nat Rev Mol Cell Biol, 2002. **3**(10): p. 753-66.
380. Le Gall, S., et al., *Nef interacts with the mu subunit of clathrin adaptor complexes and reveals a cryptic sorting signal in MHC I molecules.* Immunity, 1998. **8**(4): p. 483-95.
381. Greenberg, M.E., A.J. Iafrate, and J. Skowronski, *The SH3 domain-binding surface and an acidic motif in HIV-1 Nef regulate trafficking of class I MHC complexes.* Embo J, 1998. **17**(10): p. 2777-89.
382. Piguet, V., et al., *HIV-1 Nef protein binds to the cellular protein PACS-1 to downregulate class I major histocompatibility complexes.* Nat Cell Biol, 2000. **2**(3): p. 163-7.
383. Baugh, L.L., J.V. Garcia, and J.L. Foster, *Functional characterization of the human immunodeficiency virus type 1 Nef acidic domain.* J Virol, 2008. **82**(19): p. 9657-67.
384. Kasper, M.R. and K.L. Collins, *Nef-mediated disruption of HLA-A2 transport to the cell surface in T cells.* J Virol, 2003. **77**(5): p. 3041-9.
385. Kasper, M.R., et al., *HIV-1 Nef disrupts antigen presentation early in the secretory pathway.* J Biol Chem, 2005. **280**(13): p. 12840-8.
386. Wei, B.L., et al., *In vivo analysis of Nef function.* Curr HIV Res, 2003. **1**(1): p. 41-50.
387. Tervo, H.M., C. Goffinet, and O.T. Keppler, *Mouse T-cells restrict replication of human immunodeficiency virus at the level of integration.* Retrovirology, 2008. **5**: p. 58.
388. Chan, D.C. and P.S. Kim, *HIV entry and its inhibition.* Cell, 1998. **93**(5): p. 681-4.
389. Bieniasz, P.D. and B.R. Cullen, *Multiple blocks to human immunodeficiency virus type 1 replication in rodent cells.* J Virol, 2000. **74**(21): p. 9868-77.
390. Mariani, R., et al., *A block to human immunodeficiency virus type 1 assembly in murine cells.* J Virol, 2000. **74**(8): p. 3859-70.
391. Wei, P., et al., *A novel CDK9-associated C-type cyclin interacts directly with HIV-1 Tat and mediates its high-affinity, loop-specific binding to TAR RNA.* Cell, 1998. **92**(4): p. 451-62.
392. Alonso, A., D. Derse, and B.M. Peterlin, *Human chromosome 12 is required for optimal interactions between Tat and TAR of human immunodeficiency virus type 1 in rodent cells.* J Virol, 1992. **66**(7): p. 4617-21.
393. Bieniasz, P.D., et al., *Recruitment of a protein complex containing Tat and cyclin T1 to TAR governs the species specificity of HIV-1 Tat.* EMBO J, 1998. **17**(23): p. 7056-65.
394. Garber, M.E., et al., *The interaction between HIV-1 Tat and human cyclin T1 requires zinc and a critical cysteine residue that is not conserved in the murine CycT1 protein.* Genes Dev, 1998. **12**(22): p. 3512-27.
395. Sun, J., et al., *CD4-specific transgenic expression of human cyclin T1 markedly increases human immunodeficiency virus type 1 (HIV-1) production by CD4+ T*

lymphocytes and myeloid cells in mice transgenic for a provirus encoding a monocyte-tropic HIV-1 isolate. J Virol, 2006. **80**(4): p. 1850-62.
396. Borkow, G., *Mouse models for HIV-1 infection.* IUBMB Life, 2005. **57**(12): p. 819-23.
397. Legrand, N., et al., *Humanized mice for modeling human infectious disease: challenges, progress, and outlook.* Cell Host Microbe, 2009. **6**(1): p. 5-9.
398. D'Souza, M., et al., *Programmed death 1 expression on HIV-specific CD4+ T cells is driven by viral replication and associated with T cell dysfunction.* J Immunol, 2007. **179**(3): p. 1979-87.
399. Trautmann, L., et al., *Upregulation of PD-1 expression on HIV-specific CD8+ T cells leads to reversible immune dysfunction.* Nat Med, 2006. **12**(10): p. 1198-202.
400. El-Far, M., et al., *T-cell exhaustion in HIV infection.* Curr HIV/AIDS Rep, 2008. **5**(1): p. 13-9.
401. Muthumani, K., et al., *Human immunodeficiency virus type 1 Nef induces programmed death 1 expression through a p38 mitogen-activated protein kinase-dependent mechanism.* J Virol, 2008. **82**(23): p. 11536-44.
402. Shin, H. and E.J. Wherry, *CD8 T cell dysfunction during chronic viral infection.* Curr Opin Immunol, 2007. **19**(4): p. 408-15.
403. Wherry, E.J., et al., *Molecular signature of CD8+ T cell exhaustion during chronic viral infection.* Immunity, 2007. **27**(4): p. 670-84.
404. Guss, D.A., *The acquired immune deficiency syndrome: an overview for the emergency physician, Part 1.* J Emerg Med, 1994. **12**(3): p. 375-84.
405. Guss, D.A., *The acquired immune deficiency syndrome: an overview for the emergency physician, Part 2.* J Emerg Med, 1994. **12**(4): p. 491-7.
406. Holmes, C.B., et al., *Review of human immunodeficiency virus type 1-related opportunistic infections in sub-Saharan Africa.* Clin Infect Dis, 2003. **36**(5): p. 652-62.
407. Southwick, F.S. and D.L. Purich, *Intracellular pathogenesis of listeriosis.* N Engl J Med, 1996. **334**(12): p. 770-6.
408. Shedlock, D.J. and H. Shen, *Requirement for CD4 T cell help in generating functional CD8 T cell memory.* Science, 2003. **300**(5617): p. 337-9.
409. Zhang, S., H. Zhang, and J. Zhao, *The role of CD4 T cell help for CD8 CTL activation.* Biochem Biophys Res Commun, 2009. **384**(4): p. 405-8.
410. Kirchhoff, F., et al., *Role of Nef in primate lentiviral immunopathogenesis.* Cell Mol Life Sci, 2008. **65**(17): p. 2621-36.
411. Brady, H.J., et al., *CD4 cell surface downregulation in HIV-1 Nef transgenic mice is a consequence of intracellular sequestration.* EMBO J, 1993. **12**(13): p. 4923-32.
412. Skowronski, J., D. Parks, and R. Mariani, *Altered T cell activation and development in transgenic mice expressing the HIV-1 nef gene.* EMBO J, 1993. **12**(2): p. 703-13.
413. Lindemann, D., et al., *Severe immunodeficiency associated with a human immunodeficiency virus 1 NEF/3'-long terminal repeat transgene.* J Exp Med, 1994. **179**(3): p. 797-807.

414. Hanna, Z., et al., *Nef harbors a major determinant of pathogenicity for an AIDS-like disease induced by HIV-1 in transgenic mice.* Cell, 1998. **95**(2): p. 163-75.
415. Simard, M.C., et al., *Expression of simian immunodeficiency virus nef in immune cells of transgenic mice leads to a severe AIDS-like disease.* J Virol, 2002. **76**(8): p. 3981-95.
416. Bour, S., C. Perrin, and K. Strebel, *Cell surface CD4 inhibits HIV-1 particle release by interfering with Vpu activity.* J Biol Chem, 1999. **274**(47): p. 33800-6.
417. Lama, J., A. Mangasarian, and D. Trono, *Cell-surface expression of CD4 reduces HIV-1 infectivity by blocking Env incorporation in a Nef- and Vpu-inhibitable manner.* Curr Biol, 1999. **9**(12): p. 622-31.
418. Hanna, Z., et al., *Selective expression of human immunodeficiency virus Nef in specific immune cell populations of transgenic mice is associated with distinct AIDS-like phenotypes.* J Virol, 2009. **83**(19): p. 9743-58.
419. Joseph, A.M., M. Kumar, and D. Mitra, *Nef: "necessary and enforcing factor" in HIV infection.* Curr HIV Res, 2005. **3**(1): p. 87-94.
420. Cossarizza, A., *Apoptosis and HIV infection: about molecules and genes.* Curr Pharm Des, 2008. **14**(3): p. 237-44.
421. Rasola, A., et al., *Apoptosis enhancement by the HIV-1 Nef protein.* J Immunol, 2001. **166**(1): p. 81-8.
422. Cosgrove, D., et al., *Mice lacking MHC class II molecules.* Cell, 1991. **66**(5): p. 1051-66.
423. Rahemtulla, A., et al., *Normal development and function of CD8+ cells but markedly decreased helper cell activity in mice lacking CD4.* Nature, 1991. **353**(6340): p. 180-4.
424. Bandera, A., et al., *CD4+ T cell depletion, immune activation and increased production of regulatory T cells in the thymus of HIV-infected individuals.* PLoS One, 2010. **5**(5): p. e10788.
425. Kolenda-Roberts, H.M., et al., *Immunopathogenesis of feline immunodeficiency virus infection in the fetal and neonatal cat.* Front Biosci, 2007. **12**: p. 3668-82.
426. Hazra, R. and C. Mackall, *Thymic function in HIV infection.* Curr HIV/AIDS Rep, 2005. **2**(1): p. 24-8.
427. Correa, R. and M.A. Munoz-Fernandez, *Production of new T cells by thymus in children: effect of HIV infection and antiretroviral therapy.* Pediatr Res, 2002. **52**(2): p. 207-12.
428. Staprans, S.I., et al., *Simian immunodeficiency virus disease course is predicted by the extent of virus replication during primary infection.* J Virol, 1999. **73**(6): p. 4829-39.
429. Sasseville, V.G., et al., *Induction of lymphocyte proliferation and severe gastrointestinal disease in macaques by a nef gene variant SIVmac239.* Am J Pathol, 1996. **149**(1): p. 163-76.
430. Israel, Z.R., et al., *Early pathogenesis of disease caused by SIVsmmPBj14 molecular clone 1.9 in macaques.* AIDS Res Hum Retroviruses, 1993. **9**(3): p. 277-86.
431. Du, Z., et al., *Identification of a nef allele that causes lymphocyte activation and acute disease in macaque monkeys.* Cell, 1995. **82**(4): p. 665-74.

432. Baskin, G.B., et al., *Necropsy findings in rhesus monkeys experimentally infected with cultured simian immunodeficiency virus (SIV)/delta.* Vet Pathol, 1988. **25**(6): p. 456-67.
433. Hirsch, V.M., et al., *Induction of AIDS by simian immunodeficiency virus from an African green monkey: species-specific variation in pathogenicity correlates with the extent of in vivo replication.* J Virol, 1995. **69**(2): p. 955-67.
434. Poudrier, J., et al., *The AIDS-like disease of CD4C/human immunodeficiency virus transgenic mice is associated with accumulation of immature CD11bHi dendritic cells.* J Virol, 2003. **77**(21): p. 11733-44.
435. Grassi, F., et al., *Depletion in blood CD11c-positive dendritic cells from HIV-infected patients.* AIDS, 1999. **13**(7): p. 759-66.
436. Pacanowski, J., et al., *Reduced blood CD123+ (lymphoid) and CD11c+ (myeloid) dendritic cell numbers in primary HIV-1 infection.* Blood, 2001. **98**(10): p. 3016-21.
437. Shortman, K. and W.R. Heath, *The CD8+ dendritic cell subset.* Immunol Rev, 2010. **234**(1): p. 18-31.
438. Ong, E.L., *Common AIDS-associated opportunistic infections.* Clin Med, 2008. **8**(5): p. 539-43.
439. Tsigrelis, C., E. Berbari, and Z. Temesgen, *Viral opportunistic infections in HIV-infected adults.* J Med Liban, 2006. **54**(2): p. 91-6.
440. den Haan, J.M. and M.J. Bevan, *Constitutive versus activation-dependent cross-presentation of immune complexes by CD8(+) and CD8(-) dendritic cells in vivo.* J Exp Med, 2002. **196**(6): p. 817-27.
441. Pron, B., et al., *Dendritic cells are early cellular targets of Listeria monocytogenes after intestinal delivery and are involved in bacterial spread in the host.* Cell Microbiol, 2001. **3**(5): p. 331-40.
442. Lichty, B.D., et al., *Vesicular stomatitis virus: re-inventing the bullet.* Trends Mol Med, 2004. **10**(5): p. 210-6.
443. Cox, M.A. and A.J. Zajac, *Shaping successful and unsuccessful CD8 T cell responses following infection.* J Biomed Biotechnol, 2010. **2010**: p. 159152.
444. Wiesel, M., et al., *Virus-specific CD8 T cells: activation, differentiation and memory formation.* APMIS, 2009. **117**(5-6): p. 356-81.
445. Venzke, S., et al., *Expression of Nef downregulates CXCR4, the major coreceptor of human immunodeficiency virus, from the surfaces of target cells and thereby enhances resistance to superinfection.* J Virol, 2006. **80**(22): p. 11141-52.
446. Michel, N., et al., *The Nef protein of human immunodeficiency virus establishes superinfection immunity by a dual strategy to downregulate cell-surface CCR5 and CD4.* Curr Biol, 2005. **15**(8): p. 714-23.
447. Huang, M.B., et al., *Characterization of Nef-CXCR4 interactions important for apoptosis induction.* J Virol, 2004. **78**(20): p. 11084-96.
448. Simmons, A., V. Aluvihare, and A. McMichael, *Nef triggers a transcriptional program in T cells imitating single-signal T cell activation and inducing HIV virulence mediators.* Immunity, 2001. **14**(6): p. 763-77.
449. Thoulouze, M.I., et al., *Human immunodeficiency virus type-1 infection impairs the formation of the immunological synapse.* Immunity, 2006. **24**(5): p. 547-61.

450. Fackler, O.T., A. Alcover, and O. Schwartz, *Modulation of the immunological synapse: a key to HIV-1 pathogenesis?* Nat Rev Immunol, 2007. **7**(4): p. 310-7.
451. Piguet, V. and Q. Sattentau, *Dangerous liaisons at the virological synapse.* J Clin Invest, 2004. **114**(5): p. 605-10.
452. Sol-Foulon, N., et al., *ZAP-70 kinase regulates HIV cell-to-cell spread and virological synapse formation.* EMBO J, 2007. **26**(2): p. 516-26.
453. Swigut, T., N. Shohdy, and J. Skowronski, *Mechanism for down-regulation of CD28 by Nef.* EMBO J, 2001. **20**(7): p. 1593-604.
454. Weiss, A. and D.R. Littman, *Signal transduction by lymphocyte antigen receptors.* Cell, 1994. **76**(2): p. 263-74.
455. Lifson, J.D., et al., *Containment of simian immunodeficiency virus infection: cellular immune responses and protection from rechallenge following transient postinoculation antiretroviral treatment.* J Virol, 2000. **74**(6): p. 2584-93.
456. Rosenberg, E.S., et al., *Immune control of HIV-1 after early treatment of acute infection.* Nature, 2000. **407**(6803): p. 523-6.
457. Harrer, T., et al., *Strong cytotoxic T cell and weak neutralizing antibody responses in a subset of persons with stable nonprogressing HIV type 1 infection.* AIDS Res Hum Retroviruses, 1996. **12**(7): p. 585-92.
458. Harrer, T., et al., *Cytotoxic T lymphocytes in asymptomatic long-term nonprogressing HIV-1 infection. Breadth and specificity of the response and relation to in vivo viral quasispecies in a person with prolonged infection and low viral load.* J Immunol, 1996. **156**(7): p. 2616-23.
459. Ramsburg, E.A., et al., *Requirement for CD4 T cell help in maintenance of memory CD8 T cell responses is epitope dependent.* J Immunol, 2007. **178**(10): p. 6350-8.
460. Lewandowski, D., et al., *Altered CD4+ T cell phenotype and function determine the susceptibility to mucosal candidiasis in transgenic mice expressing HIV-1.* J Immunol, 2006. **177**(1): p. 479-91.
461. Marquis, M., et al., *CD8+ T cells but not polymorphonuclear leukocytes are required to limit chronic oral carriage of Candida albicans in transgenic mice expressing human immunodeficiency virus type 1.* Infect Immun, 2006. **74**(4): p. 2382-91.
462. Pirofski, L.A. and A. Casadevall, *Rethinking T cell immunity in oropharyngeal candidiasis.* J Exp Med, 2009. **206**(2): p. 269-73.
463. Farah, C.S., et al., *Primary role for CD4(+) T lymphocytes in recovery from oropharyngeal candidiasis.* Infect Immun, 2002. **70**(2): p. 724-31.
464. Gomes, B., et al., *Lymphocyte calcium signaling involves dihydropyridine-sensitive L-type calcium channels: facts and controversies.* Crit Rev Immunol, 2004. **24**(6): p. 425-47.
465. Oh-hora, M. and A. Rao, *The calcium/NFAT pathway: role in development and function of regulatory T cells.* Microbes Infect, 2009. **11**(5): p. 612-9.
466. Catterall, W.A., *Structure and regulation of voltage-gated Ca2+ channels.* Annu Rev Cell Dev Biol, 2000. **16**: p. 521-55.
467. Suzuki, Y., et al., *The high-affinity immunoglobulin E receptor (FcepsilonRI) regulates mitochondrial calcium uptake and a dihydropyridine receptor-mediated*

calcium influx in mast cells: Role of the FcepsilonRIbeta chain immunoreceptor tyrosine-based activation motif. Biochem Pharmacol, 2008. **75**(7): p. 1492-503.
468. Alberola-Ila, J. and G. Hernandez-Hoyos, *The Ras/MAPK cascade and the control of positive selection.* Immunol Rev, 2003. **191**: p. 79-96.
469. Kieper, W.C., et al., *Recent immune status determines the source of antigens that drive homeostatic T cell expansion.* J Immunol, 2005. **174**(6): p. 3158-63.
470. Burgess, D.L., et al., *Mutation of the Ca2+ channel beta subunit gene Cchb4 is associated with ataxia and seizures in the lethargic (lh) mouse.* Cell, 1997. **88**(3): p. 385-92.
471. Grafton, G., et al., *A non-voltage-gated calcium channel with L-type characteristics activated by B cell receptor ligation.* Biochem Pharmacol, 2003. **66**(10): p. 2001-9.
472. Mor, A. and M.R. Philips, *Compartmentalized Ras/MAPK signaling.* Annu Rev Immunol, 2006. **24**: p. 771-800.
473. Boycott, K.M., W.G. Pearce, and N.T. Bech-Hansen, *Clinical variability among patients with incomplete X-linked congenital stationary night blindness and a founder mutation in CACNA1F.* Can J Ophthalmol, 2000. **35**(4): p. 204-13.
474. Nakamura, M., et al., *Novel CACNA1F mutations in Japanese patients with incomplete congenital stationary night blindness.* Invest Ophthalmol Vis Sci, 2001. **42**(7): p. 1610-6.
475. Jalkanen, R., et al., *A novel CACNA1F gene mutation causes Aland Island eye disease.* Invest Ophthalmol Vis Sci, 2007. **48**(6): p. 2498-502.
476. Boycott KM, B.-H.N., Sauvé Y, MacDonald IM *X-Linked Congenital Stationary Night Blindness*. GeneReviews at GeneTests: Medical Genetics Information Resource 2008 16 January 2008 [cited 2009 August 3, 2009]; database online]. Available from: http://www.genetests.org.
477. Surh, C.D. and J. Sprent, *Regulation of mature T cell homeostasis.* Semin Immunol, 2005. **17**(3): p. 183-91.
478. Revy, P., et al., *Functional antigen-independent synapses formed between T cells and dendritic cells.* Nat Immunol, 2001. **2**(10): p. 925-31.
479. Burgdorf, S., et al., *Spatial and mechanistic separation of cross-presentation and endogenous antigen presentation.* Nat Immunol, 2008. **9**(5): p. 558-66.
480. Park, C.Y., A. Shcheglovitov, and R. Dolmetsch, *The CRAC Channel Activator STIM1 Binds and Inhibits L-Type Voltage-Gated Calcium Channels.* Science, 2010. **330**(6000): p. 101-105.
481. Wang, Y., et al., *The Calcium Store Sensor, STIM1, Reciprocally Controls Orai and $Ca_V1.2$ Channels.* Science, 2010. **330**(6000): p. 105-109.
482. Johansson, C. and B.L. Kelsall, *Phenotype and function of intestinal dendritic cells.* Semin Immunol, 2005. **17**(4): p. 284-94.
483. Belz, G.T., et al., *Distinct migrating and nonmigrating dendritic cell populations are involved in MHC class I-restricted antigen presentation after lung infection with virus.* Proc Natl Acad Sci U S A, 2004. **101**(23): p. 8670-5.
484. Datta, S.K., et al., *Vaccination with irradiated Listeria induces protective T cell immunity.* Immunity, 2006. **25**(1): p. 143-52.
485. Lammermann, T., et al., *Rapid leukocyte migration by integrin-independent flowing and squeezing.* Nature, 2008. **453**(7191): p. 51-5.

486. Vascotto, F., et al., *Antigen presentation by B lymphocytes: how receptor signaling directs membrane trafficking.* Curr Opin Immunol, 2007. **19**(1): p. 93-8.
487. Vascotto, F., et al., *The actin-based motor protein myosin II regulates MHC class II trafficking and BCR-driven antigen presentation.* J Cell Biol, 2007. **176**(7): p. 1007-19.
488. Uzonna, J.E., K.L. Joyce, and P. Scott, *Low dose Leishmania major promotes a transient T helper cell type 2 response that is down-regulated by interferon gamma-producing CD8+ T cells.* J Exp Med, 2004. **199**(11): p. 1559-66.
489. Bancroft, A.J., K.J. Else, and R.K. Grencis, *Low-level infection with Trichuris muris significantly affects the polarization of the CD4 response.* Eur J Immunol, 1994. **24**(12): p. 3113-8.
490. Ezra, N., M.T. Ochoa, and N. Craft, *Human immunodeficiency virus and leishmaniasis.* J Glob Infect Dis, 2010. **2**(3): p. 248-57.
491. Wiwanitkit, V., *Intestinal parasite infestation in HIV infected patients.* Curr HIV Res, 2006. **4**(1): p. 87-96.
492. Veerman, K.M., et al., *Interaction of the selectin ligand PSGL-1 with chemokines CCL21 and CCL19 facilitates efficient homing of T cells to secondary lymphoid organs.* Nat Immunol, 2007. **8**(5): p. 532-9.